ANL-82-13

ANL-82-13

CONTROL RODS IN LMFBRS: A PHYSICS ASSESSMENT

MASTER

by

H. F. McFarlane and P. J. Collins

BASE TECHNOLOGY

The facilities of Argonne National Laboratory are owned by the United States Government, under the terms of a contract (W-31-109-Eng-38) among the U. S. Department of Energy, Argonne Universities Association and The University of Chicago, the University employing the staff and operating the Laboratory in accordance with policies and programs formulated, approved and reviewed by the Association.

MEMBERS OF ARGONNE UNIVERSITIES ASSOCIATION

The University of Arizona	The University of Kansas	The Ohio State University
Carnegie-Mellon University	Kansas State University	Ohio University
Case Western Reserve University	Loyola University of Chicago	The Pennsylvania State University
The University of Chicago	Marquette University	Purdue University
University of Cincinnati	The University of Michigan	Saint Louis University
Illinois Institute of Technology	Michigan State University	Southern Illinois University
University of Illinois	University of Minnesota	The University of Texas at Austin
Indiana University	University of Missouri	Washington University
The University of Iowa	Northwestern University	Wayne State University
Iowa State University	University of Notre Dame	The University of Wisconsin-Madison

Printed in the United States of America
Available from
National Technical Information Service
U. S. Department of Commerce
5285 Port Royal Road
Springfield, VA 22161

NTIS price codes

Distribution Category:
LMFBR—Physics: Base
Technology (UC-79d)

ANL-82-13

ANL--82-13

DE83 000935

ARGONNE NATIONAL LABORATORY
9700 South Cass Avenue
Argonne, Illinois 60439

CONTROL RODS IN LMFBRS: A PHYSICS ASSESSMENT

by

H. F. McFarlane and P. J. Collins

Applied Physics Division

August 1982

PREFACE

This document is one of a series of assessments which aim to characterize the state of the art in several areas of fast reactor physics. In this report LMFBR control systems are examined, with emphasis on the ability to calculate system reactivity as changes are made with control rods.

Another document that is part of this assessment series is:

H.F. McFarlane, "The Use of Critical Experiments in CRBR Design: Status and Historical Perspective", ANL-8010, Nov., 1980.

During the last ten years, extensive control rod worth measurements for a wide range of core designs have been made on the ZPPR facility. As a part of this assessment, those experiments have been re-evaluated, and calculations of the results have been put on a consistent basis. Where feasible, the relationship between these results and reactor design has been described. In particular, application of methods that have been tested and calibrated here, together with data from specific mockup experiments, will allow the worth of control systems in future LMFBR plant designs to be determined to a precision of a few percent. To a large extent this approach has already been successfully applied to the design of the Clinch River Breeder Reactor.

Some acronymns and a certain amount of jargon inevitably and unavoidably appear in each of the documents in the physics assessment series. A lexicon is provided to help the reader with some of the terms with which he may not be familiar.

ACKNOWLEDGMENTS

This assessment could not have been done without the efforts of numerous people--those who participated in the measurements, the calculations, and the critical reviews. Stu Carpenter is responsible for developing the measurement techniques that have been employed so successfully at ZPPR. Among those people that conducted the experiments and that are still at ZPPR are Dave Olsen, Dick Kaiser, Ron Goin, and Joe Gasidlo. Clarence Beck and Gary Grasseschi were responsible for many of the calculations. Henry Harper processed some of the more recent data. Steve Brumbach, Noel Corngold, Stu Carpenter, Mike Lineberry, Joe Ross, and Kord Smith have contributed through their incisive critiques of earlier drafts. Thanks also to Herb Henryson II and Jim Lake for providing the review from the designers' perspective. Ruth Ann Andree kept track of the various drafts of this document for two years, incorporated many changes, and did editing as necessary to produce the final version.

The authors gratefully acknowledge the contributions of all these people.

TABLE OF CONTENTS

Table of Contents (con't)

List of Tables

List of Tables (con't)

List of Tables (con't)

List of Tables (con't)

List of Tables (con't)

List of Figures

List of Figures (con't)

List of Figures (con't)

List of Figures (con't)

CONTROL RODS IN LMFBRS: A PHYSICS ASSESSMENT

H.F. McFarlane and P.J. Collins

ABSTRACT

This physics assessment is based on roughly 300 control rod worth measurements in ZPPR from 1972 to 1981. All ZPPR assemblies simulated mixed-oxide LMFBRs, representing sizes of 350, 700, and 900 MWe. Control rod worth measurements included single rods, various combinations of rods, and Ta and Eu rods. Additional measurements studied variations in B_4C enrichment, rod interaction effects, variations in rod geometry, neutron streaming in sodium-filled channels, and axial worth profiles. Analyses were done with design-equivalent methods, using ENDF/B Version IV data. Some computations for the sensitivities to approximations in the methods have been included. Comparisons of these analyses with the experiments have allowed the status of control rod physics in the U.S. to be clearly defined. Procedures now exist by which almost any control rod configuration in an LMFBR design can be predicted confidently to within a few percent. This assessment defines and verifies the steps necessary to achieve such precision. For commercial-size heterogeneous LMFBRs, these steps include analysis of additional experiments that will be required.

I. INTRODUCTION

The purpose of this document is to describe and evaluate the status of control rod physics in LMFBRs. The topics addressed are:

i. the control requirements in present demonstration and commercial-size LMFBR designs,

ii. the effect of other parameters on control system design,

iii. control rod worth measurement techniques,

iv. comparisons of calculated and measured results,

v. sensitivities of the calculations to modeling approximations,

vi. extrapolation from critical experiment results to LMFBR design,

vii. recommendations for calculational methods to be used in predicting control rod worths,

viii. application of critical experiment results to improve those predictions,

ix. determination of the residual uncertainties in the predictions,

x. identification of problems or deficiencies that must be resolved or that should be addressed prior to construction of a U.S. commercial-size LMFBR.

The organization is such that there is a general discussion of control systems at the beginning of the report--how they operate, what the design requirements are, and what the history in operating LMFBRs has been. The main body of the report deals with measurement and analysis of control rod worths in fast critical assemblies, since that work constitutes most of the control rod physics research. These main sections of the report include discussions of the experimental data base, measurement techniques, comparisons of design-method calculations of rod worths, the effect of calculational model improvements, and a summary of the results. The last two sections contain conclusions, recommendations for appropriate modeling in control rod calculations, recommendations for control rod worth bias-factor generation and application to reactor design, and identification of issues that need to be resolved by future research.

All data in this report were generated in the period 1972-1981. For core designs of demonstration and commercial sizes, very little experimental data existed in the U.S. prior to 1972. What did exist was considerable uncertainty about the accuracy of control rod worth predictions. In his 1972 summary paper on fast reactor physics, Avery[1] said of control rod effects,

> "Because of the lack of validated [experimental and calculational] methods and relatively little experimental data, this area represents one of the more pressing needs of the reactor designer."

For the experiments, that situation has been completely reversed during the intervening years. More recently, systematic efforts have addressed the question of calculational validity. Considerable progress has been made, resulting in recommendations for methods and their application. Descriptions of these activities and the results are the subjects of Sections II-V of this report.

A. Design Considerations in the Selection of Control Systems

Reactor control systems are basically mechanical devices that change the power level by making adjustments in the neutron balance. Economics, space, performance criteria, and operational considerations dictate that both the total number of control devices and their effect on the core during normal operations be compatible with design constraints, including safety requirements. In principle, design of a control system begins with selection of the term in the neutron balance equation that can be modified most easily by direct action of the control system. For fast reactors, the most effective term depends on the reactor size, or more specifically, on the relative magnitude of the neutron leakage, absorption, and production terms. Thermal reactors are neutronically much larger, so the choice is more restricted.

In small, leakage-dominated reactors, systems that modify the reflector configurations provide effective control without requiring mechanical perturbations within the core. Such a system was successfully employed in SEFOR[2], a 20 MWt fast reactor, in which movable reflector elements provided over 3% $\Delta k/k$ available reactivity, and satisfied all control requirements. Small reactor designs for space application also typically use reflector control systems.

In larger systems, where neutron leakage and absorption terms are more or less equivalent, movement of fuel subassemblies within the core is more effective than reflector control. Besides having a higher worth per unit volume of material, the fuelled control rods present less difficulty in terms of engineering design. EBR-II[3], an 18.5 MWe LMFBR power plant, uses fuel in the control system of 14 rods with a total worth of about 6% $\Delta k/k$.

For relatively large LMFBRs, neutron losses in the balance equation are dominated by absorption. Hence, the control systems are necessarily limited to in-core mechanisms. Control systems based on movement of fuel or fertile material would require an excessive number of rod drives to meet control requirements, and are therefore impractical. As a result, all designs of larger LMFBRs call for control rods built of materials that are strong neutron absorbers. The worth of such a control subassembly can be several times greater than the worth of a fuel subassembly. For the CRBRP[4], the 350 MWe LMFBR demonstration plant, the two control systems in the present design incorporate a total of 15 highly-enriched B_4C rods, which provide about 13% $\Delta k/k$ in control reactivity.

The following discussion is intended only as a limited overview of LMFBR control rod material. The purpose here is to provide the rationale for the selection of the materials used in the measurements that help form the basis for this report. Only three materials need to be considered: ^{10}B, Ta, and Eu. In the U.S., most studies have been with ^{10}B in the form of natural or enriched B_4C. Tantalum is used in the metallic form, while europium is used in ceramic form as Eu_2O_3 or, more recently in Great Britain, as europium boride (EuB_6).

The principal absorbing reaction in boron carbide is $^{10}B(n,\alpha)^7Li$. Natural boron contains less than 20% ^{10}B and the reaction products, helium and ^7Li, have low absorption cross sections. Consequently, reactivity burnout may be a limiting factor in determining the lifetime of B_4C control rods. To relax this limit, some rod designs call for enriching the B_4C up to 92% in ^{10}B.

Production of the reaction products lithium and helium results in detrimental side effects--swelling, buildup of gas pressure, and a reduction in thermal conductivity. The swelling eventually results in a mechanical interaction between the absorber pellet and the cladding, which may determine limit for the lifetime of the rod. Reduced thermal conductivity is particularly important early in life when heating rates near the rod tip are high and significant thermal stresses are produced. Pellet cracking increases with burnup as the gas pressure builds up. Some designs incorporate venting to release the gas pressure, while some others use plena to capture the gas. Tritium, produced by the secondary reaction $^{10}B(n,2\alpha)^3H$, is also a component of the gas.

Research efforts in improving B_4C rod performance are centered around investigation of the effects of allowing mechanical interaction between the absorber and the cladding. There are several potential advantages that could result from having this option in the rod design. One is a slightly extended lifetime, which is generally considered to be limited by closure of the pin bundle-duct clearance. Swelling may be reduced for highly irradiated absorber pellets because the cracked B_4C could be partially compressed by the cladding. By reducing the pellet-cladding gap in anticipation of mechanical interaction, better heat transfer properties would result, especially for unirradiated pins. Consequently, some concerns about excessive temperatures with highly-enriched B_4C would be reduced. There would also be a longer time between pellet-cladding interaction and pin bundle-duct interaction.

For a tantalum rod, the neutron absorbing reaction is

$$^{181}Ta(n,\gamma)^{182}Ta \xrightarrow[\beta]{115d} {}^{182}W.$$

While this reaction does not lead to a large reduction in absorption cross section, it does produce a high self-heating rate in the tantalum rod. The heat source arises from absorption of the β and γ radiation from the decay of the unstable ^{182}Ta isotope. Irradiated tantalum rods will have to be cooled for about a year after removal from an LMFBR.

Swelling does not limit the useful lifetime of tantalum control rods. The initial swelling due to void formation is eventually reversed by production of tungsten atoms, which occupy less space than the tantalum atoms.

One design problem for tantalum rods is loss of material due to contact with sodium because of the solubility of tantalum in sodium. This requires that the tantalum be coated, and the condition of the coating may determine the rod lifetime. Tantalum contamination of the sodium coolant is reasonably easy to detect.

There has been even less experience with europium-based control rods than with tantalum rods. One advantage to europium is that the neutron-absorbing reactions, $^{151}Eu(n,\gamma)^{152}Eu$ and $^{153}Eu(n,\gamma)^{154}Eu$, result in only a small loss of control rod worth. The higher europium isotopes are also good neutron absorbers, as are their decay products, gadolinium and samarium.

Europia can exist in at least three different crystalline phases, each with slightly different densities and swelling characteristics. In-core heating rates can be high, and the thermal conductivity is low. Depending on which form of europia is chosen, pellet swelling or structural deformation by void swelling may determine rod lifetime.

Studies of EuB_6 as a control material are still in the early stages. By using enriched boron, a high worth seems possible, with reactivity burnout reduced by the presence of europium. Also the initial thermal conductivity is high, but data are not available on irradiation effects. As with B_4C, generation of gases, including tritium, will cause design problems.

For the present, LMFBR designs in the U.S. rely primarily on enriched B_4C control rods. While the resonance absorbers tantalum and europium

have some interesting properties, a high worth per rod can be more easily achieved with enriched B_4C. Also, B_4C rod technologi is considerably advanced relative to the alternatives.

B. Control System Functions and Requirements

Control systems in LMFBRs, as in other types of reactors, have several functions. Generally the functions are separated according to whether they meet safety or operational requirements. Typically, there are two separate control systems to satisfy these functions, although often some part of the operational control system also acts as a redundant safety system.

The operational functions of the control system are based on establishing and maintaining the desired power level and distribution within the core. At the beginning of a fuel cycle, the control system must counteract the excess reactivity that is built into the core to compensate for fuel burnup, fission product accumulation and temperature feedback. The configuration of the inserted rods must be such that the power distribution requirement is met. The control system must be mechanically sensitive to small reactivity changes, yet not induce power oscillations.

Modern LMFBR designs typically have two independent control systems which are capable of performing redundant safety functions. The primary system, which provides the startup and operational functions described above, also serves as a safety system. This requires that the primary system be able to shut the reactor down from full power to a cold subcritical state at any point in the fuel cycle. The secondary system must independently be able to shut down the reactor at any time in the fuel cycle. Generally, the secondary system need not maintain subcriticality for cold core conditions, but there is a stringent requirement on faulted conditions. The CRBRP has the restriction that each shutdown criterion be satisfied under a doubly-faulted condition. In the scenario for the primary system, the maximum worth rod runs out of the reactor core at top speed, then does not scram with the rest of the primary system, and the secondary safety system fails completely. For the secondary system, the worst scenario is the primary rod run-out condition, followed by failure of the primary system to scram, together with failure of any one of the secondary rods to enter the core. While these requirements may appear to be rather bizarre, it must be remembered that for LMFBRs, the only paths to accidents that can result in significant core damage are unprotected transients. Hence, protection against failure to scram is a key safety feature.

Table I.1 summarizes typical limiting requirements for an LMFBR primary control system. The reactivity effects that must be overcome include the full power to cold shutdown temperature defect, the excess reactivity of the core, and the reactivity of the worst faulted condition (e.g. rod run out from a partially inserted position). To the sum of these requirements is added the total uncertainty due each of the effects as well as that due to the uncertainty in the critical position of the rods in the system. Values for each of these effects obviously varies with reactor design and expected fuel cycle, but the values in Table I.1 are sufficiently representative to be illustrative. The primary system then must be able to overcome the reactivity requirement with no help from the secondary system, and with the failure of

TABLE I.1. Typical Reactivity Requirements for an LMFBR Primary Control System

Basis for Requirement	Typical Reactivity, %Δk/k
Cold-to-hot Temperature Defect	1.0
Excess Reactivity	2.5
Faulted Condition	1.0
Reactivity Uncertainty[a]	0.5
Maximum Requirement (sum)	5.0
Primary System Component	
All Rods in System	7.0
Stuck Rod	-1.0
Uncertainty[b]	-1.0
Minimum Available Worth	5.0

[a]Uncertainty on the 3 components and on the critical rod position.

[b]Uncertainty on the worth of scramming the rods from the critical position to fully inserted, plus the uncertainty on the worth of the stuck rod.

the faulted rod. Further, the system worth must be reduced an amount of such that the specified minimum worth can be guaranteed to a prescribed confidence level. In the example table, the minimum worth just equals the maximum requirement. In practice the minimum worth would have to be shown to be larger in order to accommodate any minor changes.

C. Sensitivity of Control Rod Worth to Design Parameters

Design studies for the CRBRP and follow-on LMFBR plants in the U.S. have many common features because of limitations imposed by the development of fuels and other materials. Generally, the fuels have been mixed plutonium-uranium oxides and the control rods have been boron carbide. Variations have been on reactor size, fuel volume fractions, fuel enrichments, number of enrichment zones, distribution of internal blankets in heterogeneous cores, and number, placement, and enrichment of control rods. Each variation in design parameters has an effect on control rod worth, but some parameters are necessarily correlated, so that their effects on control rod design are not completely independent.

The design parameters that most obviously influence control worth are those of the rod itself. One such parameter is the size of the rod. The upper limit of rod size is determined by the size of a hexagonal subassembly in the reactor design. Basically, the worth is increased by increasing the relative cross-sectional area of the absorber pellets within the control subassembly. As noted in the previous section, there are other design constraints that limit this

possibility. Increasing the length of the absorber section to greater than the core height usually adds too little worth to justify the additional cost. Enriching the B_4C in the rod can significantly increase its worth. However, the gain is not one-for-one, as the worth tends to saturate with enrichment. Typically, the increase in rod worth in going from natural to fully enriched B_4C would be less than a factor of two in an LMFBR.

^{10}B absorbs lower energy neutrons more efficiently so that softer neutron spectra tend to increase rod worth. This would favor lower-enrichment cores, e.g., larger homogeneous cores. However, within the range of designs considered, other factors usually override the spectral effects. Increasing core size generally tends to drive the worth of an individual rod down, because the rod affects a smaller fraction of the total neutron population. On the other hand, rod interaction effects* are more important in larger cores. These interactions can greatly enhance the average worth of a rod in a bank. For example, the interaction effect in a 700 MWe size core was +52% for six outer ring rods, while in a smaller 350 MWe core, the equivalent interaction effect was only +22%.

Heterogeneous designs have two significant effects on control rods: reduced worth due to a harder spectrum and greatly enhanced rod interaction effects. In the evolution of the heterogeneous CRBR design, the worth of the secondary control rod bank was increased 30% by slightly rearranging the last row of internal blankets. The maximum interaction effect of 22% measured in the homogeneous core increased to 64% in the equivalent heterogeneous core.

Table I.2 is presented to illustrate the effect of a central control rod on the neutron balance in the largest ZPPR core (ZPPR-10D), a 6100-litre homogeneous assembly with two enrichment zones. Figure I.1 is included to show the flux redistribution when the rod is inserted. For each of the two configurations (with and without the control rod), k_{eff} can be expressed as a sum of components (production, capture, etc.) for each zone of the reactor. In the table, the difference of these balance terms (configuration with rod minus configuration without the rod) is given to show the effect of the rod on overall system reactivity.** Except in the rod itself, the changes are due to the flux redistributions. As shown in Fig. I.1, there is a net shift in flux from the inner core to the outer core. For the reactivity balance, this results in a net loss for the inner core and a net gain for the outer core. Also, there is increased leakage into the radial blanket and out of the radial reflector.

From a design perspective, this illustration demonstrates three things. The first is the almost trivial observation that there is the change in power distribution in the presence of a control rod. Second, with the increased importance of neutrons in the outer core, the worth of inserting a second rod is enhanced for the outer ring and depressed for the inner ring. Finally, the net

*In this report the rod interaction effect is defined as the percentage difference between the worth of a group of rods and the sum of their individual worths with no other rods present.

**The reactivity balance terms have been expressed in units of $ to be consistent with later sections of the report.

Table I.2. Changes in the Neutron Balance by Zone Due to the Insertion of a Central Control Rod in a 900 MWe Size Core

Region	Reactivity Change Due to Rod Insertion[a], $		
	Production	Absorption	Net
Central Rod	---	-1.934	-1.934
Inner Core	-6.600	+5.978	-0.622
Outer Core	+6.374	-4.373	+2.001
Radial Blanket	+0.279	-1.467	-1.188
Axial Blanket	-0.017	+0.375	+0.358
Reflectors	---	-0.207	-0.207
Other			
$\overline{(n,2n)}$			+0.006
Leakage			-0.225
	Total:		-1.811

[a]From rz, 9-group diffusion theory calculation.

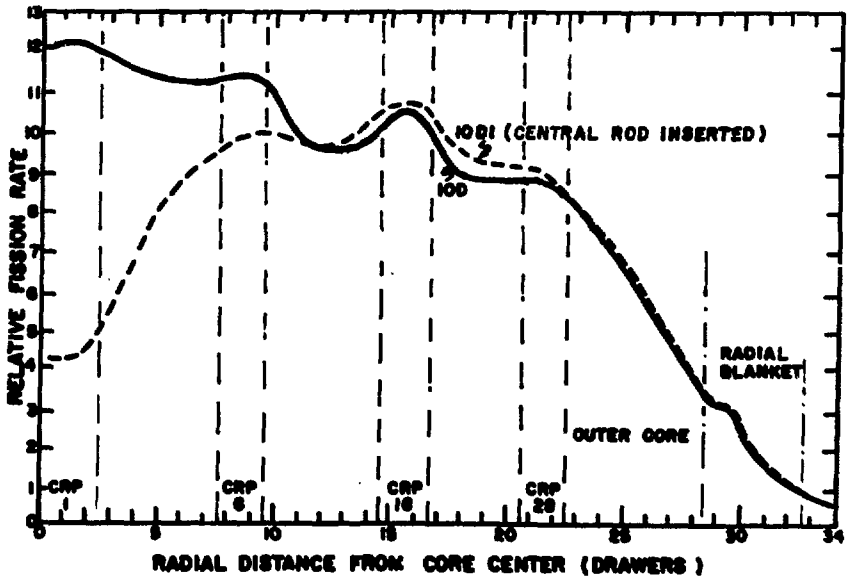

Fig. I.1. Radial Fission Rate per Atom for a 900 MWe size Core with and without a Central Control Rod.

changes in zone reactivities are small relative to the changes in production and absorption. As a result, calculations of outer ring rod worths relative to the central rod worth will be sensitive to core and blanket cross sections.

To illustrate the last point, consider the recent NEACRP* comparisons of a 1250 MWe LMFBR benchmark model,[5] a two-zone homogeneous core. In the model there were no control positions; the core volume was 9950 litres. Cross section sensitivities have been shown to be similar for the NEACRP model and the core discussed above. Calculations of the central rod worth in the benchmark model were among the solutions that were submitted from around the world, representing 15 different cross section sets. Relative to the mean, the calculated worths varied from -12.5% to +32.4%, with a standard deviation of 13%. Only 1-2% of the spread can be attributed to the ^{10}B cross section of the rod. The rest is due to the core material cross sections. Since the same diffusion theory model was used by all contributors, it appears that variations in cross section data sets and processing codes can lead to vastly different predictions of control rod worth in large LMFBRs.

II. CONTROL ROD WORTH MEASUREMENTS

This section describes the types of critical assembly measurements that are useful in control rod design, the relationship between those measurements and rod design parameters, the measurement techniques, the uncertainties associated with the measurements, and the data base selected for this control rod assessment.

A. Critical Experiment Data Relating to Power Reactor Design

Many of the properties of control rods that are of interest in reactor design can be measured in critical experiments. In turn, the measurements form a basis for evaluating various calculational methods and for developing bias factors for design methods.

The following sections describe how the critical experiments have addressed control system design problems. Recent improvements in measurement techniques that have reduced experimental uncertainties to low levels are described. Reference calculations that correspond to conventional design techniques form the basis for most comparisons. Refined calculational methods that are beyond the scope of normal design practices are used to examine some discrepancies and to determine the effects of modeling approximations.

Most physics parameters associated with control rod design have been measured in the ZPPR critical experiments, and for many parameters an extensive data base has been compiled. Control rod worths can be examined as a function of core size, fuel enrichment, core heterogeneity rod size, rod enrichment, insertion depth, rod heterogeneity, and rod material.

The fundamental data include the worths of simulated rod banks in a variety of cores. Most measured rod configurations have been representative

*Nuclear Energy Agency Committee for Reactor Physics.

of conditions expected at some time in the operating cycle, although measurements have also represented highly-unlikely faulted conditions. The rods used in the measurements have had worths that are typical of those in the reactor design, though the rod heterogenity and B_4C enrichment often have not been representative. The measured rod worth is defined to be the difference between the reactivities of a subcritical configuration with rods inserted and a near-critical reference configuration.

Some critical configurations are built that include control rods that are fully or partially inserted. Criticality adjustment is made by increasing the effective enrichment of the core or by adding fuel drawers to the outer boundary. Such measurements provide benchmarks for criticality predictions with and without inserted control material, and inherently tie control worth to fuel worth.

The worth of rod banks and especially the effects of faulted conditions are dependent on the rod interactions. These interactions are measured in the critical experiments by determining the worth of each representative individual rod with no other rods inserted, and then determining the worth of multiple rod patterns. The rod interaction effect here is the historical one, and is defined as the percentage difference between the bank worth and the sum of the individual rod worths with no other rods present. Alternative definitions are often used; some designers prefer to define the worth of an individual rod as its average value in a bank.

Most current LMFBR rod designs call for ^{10}B-enriched B_4C, but the ZPPR facility inventory contains primarily natural B_4C. Therefore, additional critical experiments are required to determine enrichment effects. The enrichment studies ideally determine rod worth as a function of enrichment for a fixed geometry. Enrichments vary from natural (~20% ^{10}B) to fully enriched (~92% ^{10}B). The absorber density is sometimes varied by interspersing steel and/or sodium. Typically, a simple relationship exists between the worth per unit ^{10}B mass and the mass per unit length of perimeter of the cross section that encircles the absorber.[6]

The use of highly-enriched B_4C rods in LMFBR core designs causes problems in the design of the rods themselves. Most of these problems are related to the steep gradients in the capture rates between the surface and the interior of the rods. Alpha and gamma heating of the surface pellets can be severe relative to the rod average. Designs must provide for adequate cooling, especially for the rod tip. Measurements of the power distribution in the rod are provided by critical experiments. As discussed in Section I of this report, the rod lifetime will probably be determined by the swelling characteristics of the pellet. Since swelling is a function of the total number of captures, knowledge of the capture rate is important in estimating rod lifetime. The critical experiment data also provide information on how much reactivity is burned out during the rod lifetime.

Critical experiment studies of the worth of the alternative control materials Ta and Eu have also been done. One motivation for the interest in alternative materials is to have a secondary control system that is physically different from the primary system. Another is to remove reactivity

burnout as a limiting factor in effective control rod lifetime. The resonance absorbers, especially europium, hold some promise of the latter.

When withdrawn from the core, control rods leave channels of sodium and stainless steel that provide streaming paths for core neutrons. Ordinary design codes do not accurately compute the neutron leakage in these channels. Part of the misprediction of the early Phenix critical loading was attributed to improperly biasing the calculated reactivity of these channels in the design.[7] Such reactivity effects are studied in benchmark critical assemblies by replacing simulated fuel subassemblies with sodium and stainless-steel channels. In the critical assemblies, these channels are called control rod positions, or CRPs. It is important that they be represented in the critical experiments from which design factors are produced.

The reactivity of control rods as a function of axial insertion into the core is of interest to nuclear designers because partial insertion is the normal operating condition for the primary control bank. Three dimensional power-distribution predictions are based on calculations with partial rod insertions. Knowledge of the effects of deviations from the nominal insertion depth is essential in determining the uncertainties in other design parameters.

B. Measurement Techniques

There have been two principal goals in the development and selection of measurement techniques for the determination of control rod worth. First, the measured worth should correspond closely to what is calculated in the design process. Second, experimental uncertainties should not be a limit in the achievement of desired design uncertainty levels. How both of these goals have been achieved in the U.S. program is the subject of this section.

The control rods (CRs) described in this report are non-movable control subassemblies that are simulated by 4-9 ZPPR drawers in a rectangular or square group. Generally, the absorber section of the rod is simulated by plates of absorber and diluents stacked in the drawers. Changes in rod configurations are made by shutting down and reloading the reactor. Holes left by withdrawn rods are filled with drawers of sodium and stainless steel (CRPs). The experimental control rods are not to be confused with the operational safety and shim rods of the critical facility. For ZPPR, the latter are narrow blades (1/4 x 2 x 28 in.) of fully-enriched B_4C. The operational rods enter the core from both ends, with the 30 in. stroke allowing the tips to reach the reactor midplane. During the measurements, all such operational rods are removed from the core.*

At the NEACRP specialists meeting in 1976, Carpenter[8] reviewed the reactivity measurement techniques that have been used at the U.S. fast critical facilities. At that time, the modified source multiplication (MSM) technique[9] was identified as the reference method for control rod measurements in plutonium-fuelled assemblies. The method has the advantage of being applicable to the wide range of subcritical states (-0.5$ to -50$) that are encountered in experimental control rod studies. ZPPR plutonium contains

*Prior to 1977, one or two operational rods were partially inserted in ZPPR to balance the system reactivity.

about 11% ^{240}Pu, so that for a typical assembly, spontaneous fission of this isotope provides a source of more than 10^8 neutrons per second.[10] Since this source is distributed uniformly with the fuel, flux distributions are predominately fundamental mode, even for far-subcritical states.

The calculational method in the design process for control rods is described in Section III. Basically it consists of two eigenvalue calculations, one for the reference configuration and the other for the subcritical configuration with the rods inserted. The worth of the rods is defined in terms of the difference between the two fundamental mode eigenvalues.

$$\text{Rod worth} \equiv \frac{\Delta k}{k_1 \, k_2},$$

where $\frac{1}{k_n}$ is the fundamental mode eigenvalue for the n^{th} reactor configuration.

Ideally, the experiments should measure the equivalent quantities, but that is impossible. What can be measured are specific reaction rates in and around the assembly. These are related to the fundamental mode eigenvalues through the MSM prescription that is described below. With the control rods inserted and the reactor in a subcritical state, the neutrons are in a source-driven distribution which deviates from that of the fundamental mode. In the MSM technique, the neutron flux fission distribution is sampled and converted to the fundamental mode reactivity by forming the product of several measured and calculated ratios.[8] In principle, all the ratios could be determined by measurements. In practice, it has been demonstrated for a few cases that the two approaches give consistent results, and further, that the calculated ratios are relatively insensitive to deficiencies in the calculations.

Using Carpenter's notation, the expression used in simple applications of the MSM technique is:

$$\rho_2 = \rho_1 \cdot \frac{\varepsilon_2}{\varepsilon_1} \cdot \frac{S_{e2}}{S_{e1}} \cdot \frac{R_1}{R_2} \cdot \frac{\beta_{e1}}{\beta_{e2}}, \qquad (1)$$

where ρ is the subcritical reactivity in units of dollars, R is the count rate of the detector that is used to sample the neutron flux, ε is the detector efficiency (in this case the ratio of R to the total production rate by fission), β_e is the effective delayed neutron fraction, and S_e is the effective worth of the source neutrons. Subscripts 1 and 2 refer to the two different states of the reactor, the reference (1) and the rodded configuration (2).

$$\rho = \frac{\Delta k}{k\beta} \qquad (2)$$

$$\varepsilon = \frac{\int \sigma_d \, \phi_d \, dE}{\langle F\phi \rangle} \qquad (3)$$

$$S_e = \frac{\langle \phi^*, \, S \rangle \cdot \langle F\phi \rangle}{\langle \phi^*, \, F\phi \rangle} \qquad (4)$$

Here σ_d is the detector cross section, ϕ_d is the neutron flux at the detector, and F is the fission production operator. S is the distributed

external (^{240}Pu spontaneous fission) source that is input for the calculation of the real flux, ϕ. ϕ^* is the fundamental-mode adjoint flux for the specific reactor configuration.

The next several paragraphs are a brief description of the measurement technique as it is now applied at ZPPR. Included are the step-by-step procedures and identification of when and how each term in the expression for ρ_2 is obtained.

The first step in the MSM procedure is to establish the slightly subcritical reference configuration. This is done by removing fuel from the critical assembly until a configuration is obtained that is 10-30¢ subcritical with all operational rods withdrawn. Historically, this subcritical condition was achieved by partial insertion of the operational rods. However, improvements in the precision of the MSM technique coincided with construction of the first heterogeneous cores, which had the prominent characteristic of large rod interactions. In those measurements, it was found that the operational rods could affect the worth of a control rod by up to 12%. Besides eliminating this problem, establishing a subcritical reference configuration of slightly reduced mass incurs some additional experimental benefits, while being at worst a slight nuisance in setting up calculations for a whole program. The subcriticality range of -10¢ to -30¢ is important for three reasons. The first is that the neutron flux is sufficiently low that the experimental detectors do not require significant corrections for dead-time losses (i.e., the measured signal is proportional to the flux). The second is that the system is close enough to critical to assure the validity of a kinetics technique for determining the reactivity of the reference configuration. Third, the neutron flux is essentially in a fundamental mode distribution, so that it is the fundamental mode reactivity that is determined.

With the subcritical reference configuration established, data are recorded from the detectors. These data are converted to count rates to form the quantity R_1 in the MSM expression. (Each of the n experimental detectors has its own R_1 value, so that there are n separate, but correlated, measurements. Presently, n=64.) Immediately after these data are recorded, several operational rods are scrammed into the core. The initial reactivity of the system (ρ_1 in the MSM expression) is determined from analysis of the power history following the rod drop. The product $\rho_1 \cdot R_1$ calibrates the MSM method.

The best estimate of the uncertainty in determining ρ_1 is that it is less than one percent when contributions from all known sources are considered. The largest contribution to the uncertainty comes from the relative fractions in the different delayed neutron groups, and is about 0.6% for a typical -15¢ condition. These relative fractions, generally called the a_i set, are determined in a separate experiment for each critical assembly, and are compared with calculated values. Detector efficiency changes during the rod drop are also experimentally determined, thus eliminating one systemmatic error. Each of these experimental procedures has been thoroughly tested and validated. The scrammed rods are completely withdrawn, not to be re-inserted during any of the subsequent rod worth measurements. The statistical uncertainty in R_1 can be reduced to an arbitrarily low

level by accumulating a sufficiently large count. Therefore, the uncertainty in the calibration term for the MSM technique is due only to ρ_1.

The next step in the procedure is to replace the control rod positions with control rods. Physically, this involves replacing drawers whose composition is sodium and stainless steel with drawers whose composition is neutron absorbing material, stainless steel, and possibly sodium. For a typical fully-inserted rod, the extent of the absorber is just through the core, with the sodium/stainless steel composition in both axial blankets.

With the rods in place and the configuration in a second subcritical state, data from the detectors are again recorded. For each detector, there is an R_2, the count rate in the configuration with the unknown reactivity. At this point the reactivity of that configuration (ρ_2) and the rod worth ($\rho_2-\rho_1$) can be determined with reasonable accuracy for many cases of interest. The remaining three terms in the MSM expression $\left(\frac{\varepsilon_2}{\varepsilon_1}, \frac{S_{e_2}}{S_{e_1}}, \frac{\beta_{e_1}}{\beta_{e_2}}\right)$ are ratios which are either inherently within a few percent of unity or, in the case of $\varepsilon_2/\varepsilon_1$, can be forced to unity by careful placement of the detector.

The ratio β_{e1}/β_{e2} is generally assumed to be exactly 1.0 and dropped from the expression. There are two reasons for this. First, several numerical studies, thought to contain some extreme examples, have found deviations from unity of no more than 0.7%.* The second reason is more pragmatic. The same ratio would also apply to the calculated rod worth, but in practice is never computed. In comparing calculated and measured worths, results are usually displayed as ratios of the two, so that this small correction term would disappear anyway.

The ratios $\varepsilon_2/\varepsilon_1$ and S_{e2}/S_{e1} require four base calculations plus computation of several integrals shown in Eqs. (3) and (4). The base calculations include the eigenvalue calculations for the real and adjoint fluxes in the reference state, an eigenvalue calculation of the adjoint flux in the second state, and a source-driven calculation of the real flux in the second state. A source-driven calculation of the real flux is not required for the reference state since that flux distribution would be essentially identical to the fundamental mode distribution obtained from the eigenvalue calculation.

The term $\varepsilon_2/\varepsilon_1$ is the quotient of two ratios that are determined from some integrals involving fission cross sections and the neutron fluxes (Eq. 3). The numerator of each ε is the integral over energy of the product of the appropriate cross section for the detector and the neutron flux at the location of the detector. The denominator is the total neutron production by fission, i.e., the space and energy integral of the product of the number of neutrons per fission (ν), the fission cross section, and the neutron flux over the whole reactor. Since the flux distribution appears in both the numerator and denominator of the appropriate ε, the ratio $\varepsilon_2/\varepsilon_1$ is not thought to be overly sensitive to deficiencies in the real flux calculations. For rod worth measurements, 10% deviations of $\varepsilon_2/\varepsilon_1$

*See Chapter III of this report.

from unity are common, and deviations of 50% are observed for some cases of interest. It is thought that misprediction of these deviations is no larger than observed mispredictions of fission rates, typically no more than 5% in the core, nor more than 10% in the blankets. Nevertheless, a single detector, with a large correction for relative efficiency, could contribute an uncertainty of several percent to an MSM measurement if it were used alone.

As the MSM technique is applied at ZPPR, the spatial fission distribution is mapped by multiple ^{235}U fission chambers throughout the core and blankets. Results from each detector can be treated as separate, but correlated, measurements of the same reactivity state. A complex data reduction technique folds the data together in such a way that the residual uncertainty from the $\varepsilon_2/\varepsilon_1$ calculations is reduced to an insignificant level. Qualitatively this can be seen because the weighted sum of the multiple detectors (presently 64) is representative of the total fission integral for each respective state. In the MSM expression, $(R_1/\varepsilon_1)/(R_2/\varepsilon_2)$ is just the ratio of powers for the two states, so that if the reactor power distribution is well characterized by the measurement, there can be little residual error introduced through calculations.

The third ratio in the MSM expression that involves calculations is S_{e2}/S_{e1}. The effective source worth (S_e) is the product of the adjoint-weighted source integral and the total calculated fission integral, divided by the perturbation denominator (see Eq. 4). In the plutonium-fuelled assemblies of interest here, the source is due to the spontaneous fission of ^{240}Pu. Since the source is distributed uniformly with the fuel, its effective worth is not greatly changed by flux redistributions brought about by changes in control patterns. Furthermore, all integrals are over the whole reactor, which reduces the sensitivity to local perturbations. Typical S_{e2}/S_{e1} ratios deviate from unity by no more than a few percent for rod measurements; deviations of 10% are rare and are representative only of unusual configurations. If it is assumed that deviations from unity can be calculated with an accuracy of 10% or better, the contribution of the source term to the uncertainty in the subcriticality of the second state (the rodded configuration) is less than one percent. While this assumption has not been rigorously tested, the available evidence is strongly supportive. Several measurements of source importance have been made in near-critical configurations, and detector responses to point sources in far subcritical configurations have also been made. Comparisons with calculations have shown that the spatial dependence of source importance was well-predicted in those cases. Chi-squared tests of special sets of calculated and measured data also indicate that random component of uncertainty is not underpredicted.

Utilization of a large number of detectors also enables $\varepsilon_2/\varepsilon_1$ to be determined experimentally. Each fission chamber is assigned an appropriate and unique part of the reactor volume. The sum of the product of the fission rates and the fissile masses in each volume element is then a good approximation of a quantity proportional to the total fission integral, with the constant of proportionality being essentially independent of changes in control rod patterns. ε_2/e_1 can be determined for each detector by computing the ratio of the detector count rate and the sum for state 2 divided by the

equivalent ratio for the reference state. At ZPPR, such experimental determinations of efficiency ratios, together with calculations of the ratios, are now routine procedure.

In principle, the source ratio also can be determined experimentally by measuring a quantity whose spatial distribution is proportional to that of the fundamental mode adjoint flux (for each of the two states). This measured distribution can then be used as a Green's function in integrating the distributed source over the core volume. Near critical this can be done directly by moving a point source throughout the core and measuring its relative importance as a function of position.[8] This is not a practical approach since such a measurement is difficult and the time required is substantial. Another approach, using an approximate spatial distribution in place of the adjoint flux for both configurations, has been successfully used at ZPPR. The approximate distribution is that of the ^{235}U fission rate, determined from the 64 distributed chambers. While this may seem to be an odd approximation, calculations have shown good agreement in terms of spatial distribution. The most important tests of using this approximate technique have been in measuring reactivity changes between steps in an approach to critical where changes in the effective source worth ratio are quite large. The largest deviations from calculated values have been only a few percent, easily within the expected accuracy of the calculations. Confidence in the approximate technique has reached a point at ZPPR where it is now routinely applied in order to obtain preliminary experimental reactivities. Since the requisite calculations sometimes lag a few months behind the measurements, the preliminary data are often utilized for diagnosing problems, for planning future experiments, and for comparisons with predicted values.

Having generated the reactivity normalization and all the necessary ratios, the subcritical reactivity of the second state, ρ_2, can be obtained from the MSM expression (Eq. 1). The worth of the rod configuration is then the difference in the two reactivities, $\rho_2-\rho_1$, after they are adjusted to the same experimental conditions (average reactor temperature, ^{241}Pu decay date, etc.). Contributions to the uncertainty in the measured worth of the rod configuration are about 1% for reactivity normalization, less than 1% for the source ratio, 0.1-0.2% for the product of the efficiency ratio and the count rate for the collective system of 64 detectors, and less than 1% for the ratio of effective delayed neutron fractions. (The latter disappears when comparisons with calculations are expressed as ratios.) There is an additional uncertainty of about 0.005$ for normalization of experimental conditions, but this contributes less than 0.5% even for a single rod, and is negligible for banks of rods. Statistically combining the uncertainty contributions, a measured control worth has an uncertainty of less than 2% when expressed in units of dollars of reactivity.

For assemblies prior to ZPPR-9,* the total rod worth uncertainty is somewhat higher because fewer than 64 detectors were used, and there was a slight difference in the application of the MSM technique. For assemblies 7 and 8, there were 12 independent fission chambers, which raises the uncertainty in $(R_1/\varepsilon_1)/(R_2/\varepsilon_2)$ to the 0.2-0.3% range, but leaves the overall value at about 2%. In ZPPR-6 there were also 12 detectors, but a cruder statistical

*See Section II.C of this report.

evaluation was used, and the reference configurations had partially-inserted shim rods. For that assembly, the total uncertainties are in the 2-3% range. Assemblies prior to ZPPR-6 effectively used a single detector, making the uncertainty in $(R_1/\varepsilon_1)/(R_2/\varepsilon_2)$ as high as 3% and the overall uncertainty correspondingly higher.

When measured worths are compared with calculated values, an additional uncertainty of significant magnitude is introduced. To convert back and forth between units of k_{eff} and dollars requires application of the scale factor β_{eff}. For mixed plutonium-uranium systems, the uncertainty in β_{eff} is about 4%. However, it is not necessary to carry this scale factor uncertainty over into the design uncertainties.*

The modern value of 2% uncertainty easily allows design target accuracies to be met if bias factors are developed from an EMC. Unforeseen uncertainties from engineering considerations or poor design calculations could push the design uncertainties outside of the target limits, but at least the physics measurements will not provide an inherent barrier.

C. Critical Experiment Data Base

The critical experiment data base has been chosen from ZPPR assemblies 3 through 11. These assemblies represent a reasonable range of core designs in terms of size, heterogeneity, and volume fractions, as well as most of the control rod worth measurements that have been a part of the U.S. LMFBR program. A large majority of the measurements have been calculated with ENDF/B-IV cross sections. Furthermore, by limiting the data base to ZPPR, experimental techniques and calculational methods are reasonably consistent throughout. In general, there is not sufficient information available about results from foreign programs either to include them or to calculate them consistently.

Most of the experimental results (worths of fully-inserted control rods) are presented Section III.B along with comparisons with reference calculations. These reference calculations, as described in Section III.A, correspond to current design practices. In addition, some assemblies were built that were critical with rods inserted. Comparisons of C/E values for k_{eff} of equivalent critical assemblies with and without inserted rods provide the potential for an examination of rod worths relative to fuel enrichment.

The data base also contains about information several special topics. Among these are determination of rod-insertion worth curves; studies of the effects of B_4C enrichment, rod interactions, rod-geometry variations, and neutron streaming in empty control channels; comparisons of calculations by different organizations; and studies of such modeling refinements as increasing the number of energy groups, decreasing the mesh spacing, and including transport effects. Results of these special studies are contained in Section IV.

The data base is summarized in Table II.1. ZPPR assemblies are grouped according to size and heterogeneity. Although not all of the special studies are represented in each group, there is generally good representation.

*See Section V.B.

TABLE II.1. Critical Experiment Data Base for Control Rod Worths

ZPPR Assembly	Reference C/E's*	Interaction Effects	Enrichment & Geometry Effects	Alternative Materials	Axial Profiles	Neutron Streaming in CRPs	Improved Methods	k_{eff} Bias
350 MWe Homogeneous								
3/1B	✓	✓		[a]				
4/1	✓					✓	✓	
4/2	✓							✓
4/3	✓							✓
4/4	✓							
6/CEOC**	[b]		b		✓			
6/CBOC**	[b]		a		✓			
350 MWe Heterogeneous								
7B	✓	✓	✓			✓	✓	
7C	✓					✓	✓	
7G	✓	✓						[c]
8F	✓							
11A	✓				✓			✓
11B	✓	✓	✓		✓			
11C	✓							
11D	✓							✓
11E	✓							
11F	✓		✓					
700 MWe Homogeneous								
9	✓	✓	✓	✓		✓	✓	
10A	✓		✓	✓			✓	
10B	✓						✓	[d]
900 MWe Homogeneous								
10C	✓					[a]	✓	
10D	✓							[e]

[a] Data taken, but not reduced to consistent form.

[b] GE calculations only.

[c] Critical version built as 7H.

[d] Including step-by-step approach to critical in going from ZPPR-10A to -10B.

[e] Critical with central CR--10D/1, critical with ring of six rods--10D/2.

*C/E: Ratio of calculated to measured result; calculation/experiment.
**CEOC: Clean end-of-cycle core; CBOC: Clean beginning-of-cycle core.

Appendix A contains interface views of the relevant ZPPR assemblies. Control rod numbering schemes are identified on the interfaces. Cross-sectional views of the control rod designs are also contained in Appendix A, as are the homogenized number densities for the rods. Data that do not conveniently fit into any particular topic or are somehow inconsistent are contained in Appendix B.

D. Data from Operating Power Reactors

Although the data base for this report is limited to critical experiments in the ZPPR critical facility, where conditions can be carefully controlled and reactivities can be precisely measured, some information from operating fast reactors is available and can be summarized here:

i. Fermi:[11] Rod worth predictions were based directly on ZPR-3 experiments. Operational rod worths were overpredicted by 8.5% and the worth of the safety rods was overpredicted by 15%. The overpredictions can be attributed to mismatches between the critical assembly and the power reactor that included volume, enrichment, geometry, and composition.

ii. SEFOR:[2] The measured worth of the reflector control system was 10$ compared with a predicted range of 11 ± 2$ based on analysis of ZPR-3 experiments.

iii. EBR-II:[3] Three types of fuelled control rods were used in EBR-II. Worth predictions were based on methods that were verified with the EBR-II mockup in ZPR-3. Normal rods had a worth of 0.345% Δk compared to a 0.340% Δk predicted value; rods with B_4C followers were worth 0.57% Δk compared to the predicted value of 0.55% Δk; and the safety rods were worth 1.2% Δk compared to a predicted value of 1.3% Δk.

iv. Phenix:[7,12] Single rod worths were overpredicted by 6 ± 5% and the worth of a gang of six rods agreed to within 1.4 ± 5% of the predicted value. However, the worth of the sodium-filled control channels was felt to be partially responsible for the underprediction of the initial critical mass, which just fell within the limits of uncertainty assigned to the predicted value. Section IV.D contains a discussion of the effects of such channels.

v. BN-350:[13] Methods were developed on the critical facility BFS-15. The worth of B_4C control rods was underpredicted by 5% and the worth of fuelled rods was overpredicted by 20-25%.

vi. PFR:[14] A 10% uncertainty on rod bank worth was based on analysis of measurements in the ZEBRA critical facility. The as-measured value agreed within 2%, although the uncertainty on the measurement was 6%. Some significant deviations from predicted worths were noted for individual rods, but this was believed to be due to an asymmetric loading that was not considered in the calculations.

vii. FFTF:[15] Bias factors for FFTF rod worths were developed in critical experiments on ZPR-9. Early results indicate that the measured rod worths agreed with the biased design prediction with the uncertainties in the FFTF measurements.

These results from small operating fast reactors indicate that acceptable predictions of rod worths in LMFBRs can be achieved through the careful application of bias factors produced from analysis of critical experiments. The goal now is reduction of the uncertainty range and application of appropriate bias factor methods and data for large LMFBRs.

III. ANALYSIS OF THE CRITICAL EXPERIMENT DATA BASE FOR CONTROL ROD WORTHS

This section describes the calculational methods that have been used in analyzing the control rod worth experiments. Emphasis is on the simplest method which corresponds closely to current LMFBR design practice. Results calculated using this reference method are compared with the measured worths from each ZPPR assembly in the data base. The ANL results are compared with those of General Electric - Advanced Reactor Systems Department (GE) and Westinghouse - Advanced Reactors Division (W-ARD) for the same data base. The effects of improved calculational methods are then demonstrated for a few selected measurements from several assemblies. Finally, results of control rod analyses are compared with those for small perturbation samples of absorber materials.

A. The Reference Calculational Method

A consistent calculational method and ENDF/B Version IV cross sections have been used to calculate ZPPR control rod worths. The reference method is similar to those used in the CRBRP project, and has the following characteristics:

(i) diffusion theory

(ii) xy geometry

(iii) 9-group cross sections

(iv) group and region dependent absorption terms (bucklings) to treat axial leakage

(v) 1 or 4 mesh spaces per ZPPR matrix position

(vi) worth defined as $W(\$) = \frac{k_2 - k_1}{k_1 k_2 \beta_{eff}}$,

where the subscripts 1 and 2 refer to the reference configuration and the rodded configuration, respectively; β_{eff} is calculated for the reference condition.

A summary of the calculational procedure that is used at ZPPR is shown in Fig. III.1. The general relationship between the control rod worth calculations and calculations of other reactor parameters can be seen in the figure. A more detailed view of the control rod worth calculation is provided in Fig. III.2.

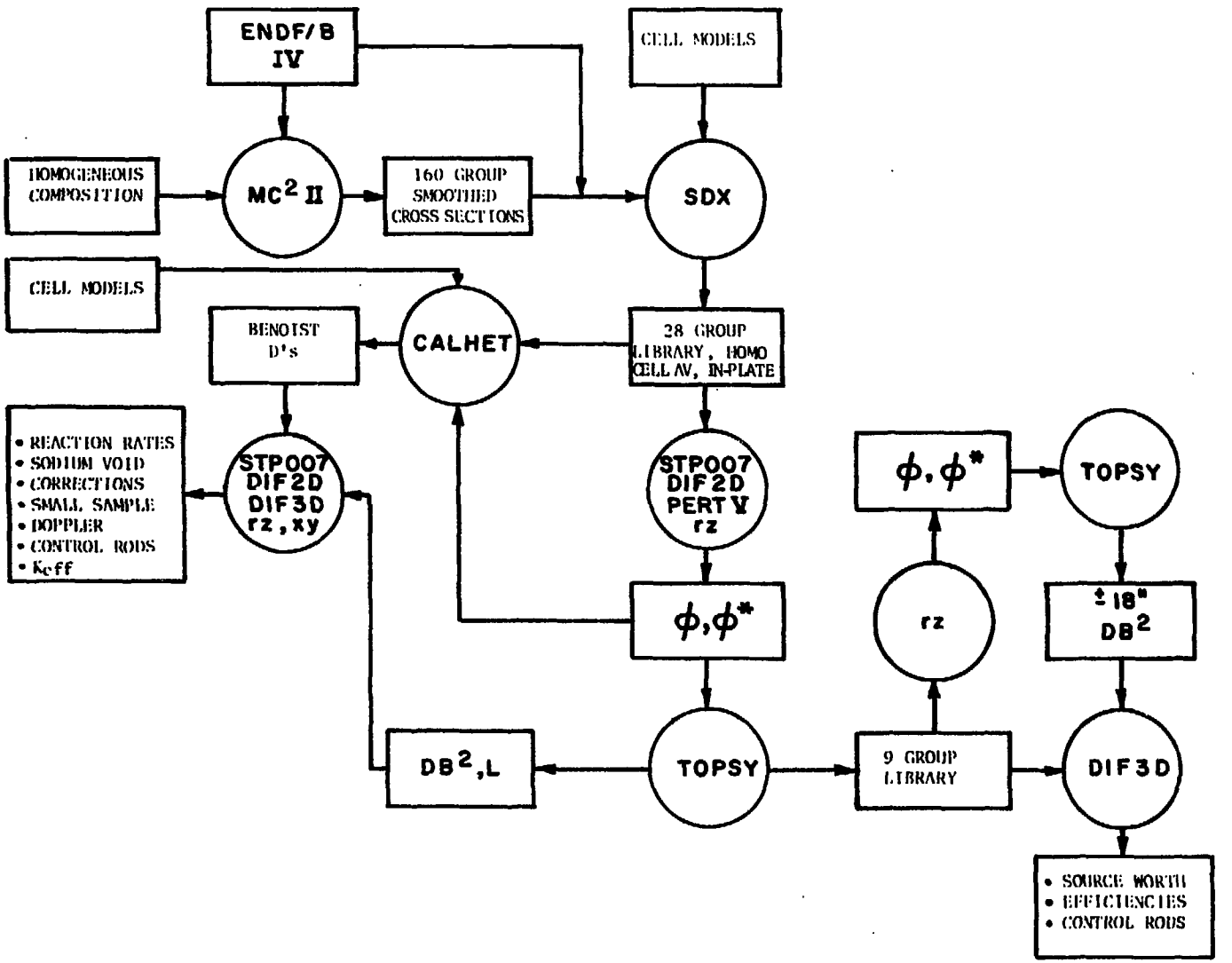

Fig. III.1. Flow Diagram for Calculations.

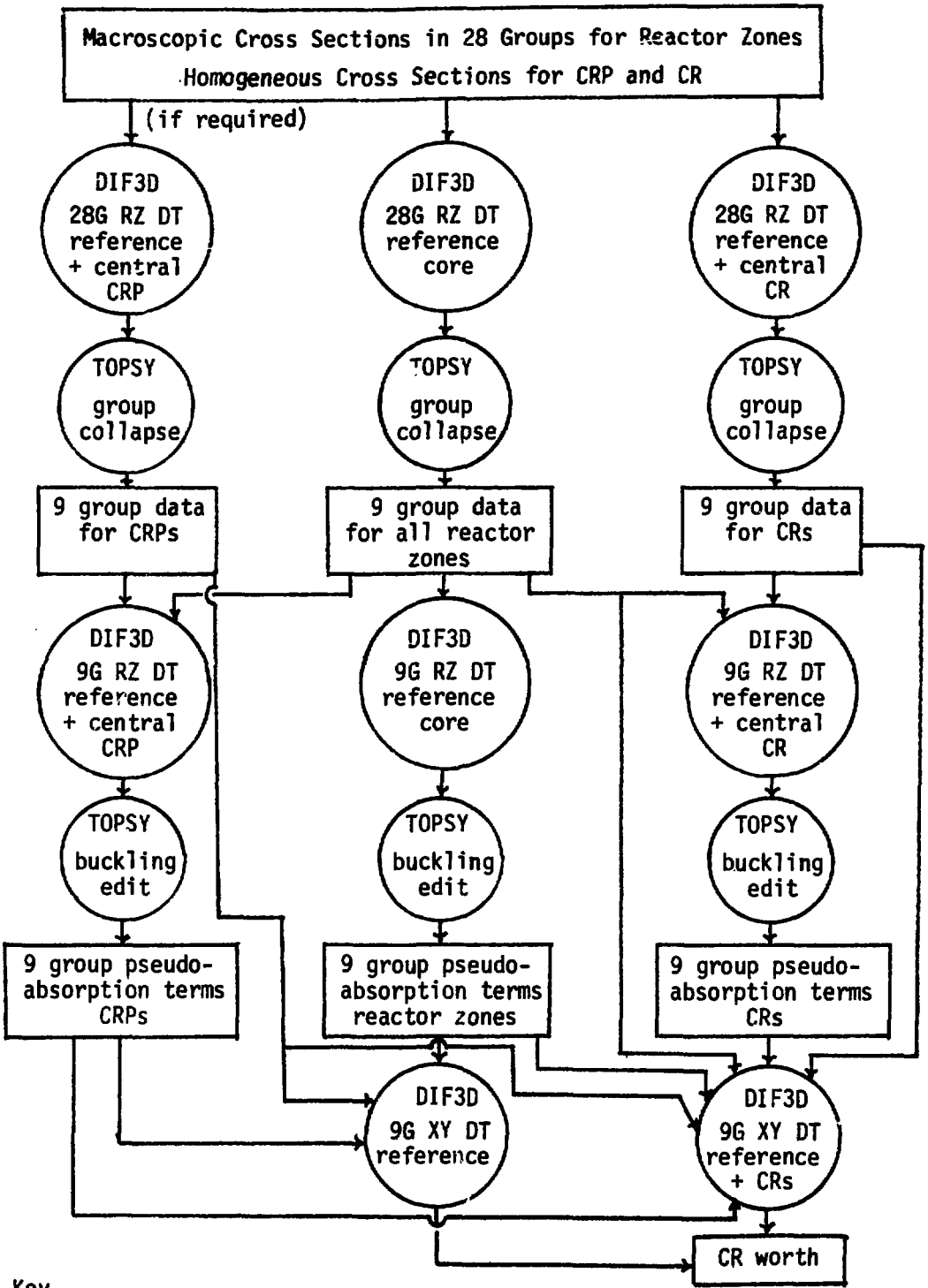

Key

28G = 28 groups
RZ,XY = geometry
DT = diffusion theory

Fig. III.2. Flow Diagram for Control Rod Calculations.

Preparation of the 9-group cross sections and leakage terms involves several steps which are summarized below:

1. Group Condensation

Group structures for the 28- and 9-group sets are shown in Table III.1.

a. Group condensation involves an rz calculation in 28 groups for the reference core. CRPs (or CRs if required) in this model are represented as annular rings. The macroscopic cross sections are collapsed to nine groups for each zone in this model--usually inner core, outer core, radial blanket, axial blanket, etc., for conventional (homogeneous) cores; and central blanket, fuel ring 1, blanket ring 1, fuel ring 2, etc., for heterogeneous cores. Collapsed group cross sections for CRP rings are not used.

b. For conventional cores, the reference configuration usually contains a central CRP, and if so, nine group CRP cross sections are also obtained. If there is no central CRP, a second 28-group rz calculation with a central CRP is made specifically to obtain these cross sections.

c. To obtain 9-group cross sections for a control rod, an rz calculation is made with the rod at the center, regardless of what material is there in the actual assembly.

Fuel and blanket cross sections are taken from case (a) even when the control rod is inserted. It can be demonstrated that the group collapse can be made more accurately if macroscopic cross sections were used from case (c) when the central rod is inserted. However, it is not clear that these cross sections are more appropriate for cases with off-center rods. Cross sections for all CRPs and CRs are taken from the central position.

It should be noted that, as far as possible, the energy structure of the nine-group cross sections was chosen to be consistent with that used by W-ARD. The reason for this was to improve the consistency of comparisons in a cooperative analysis program. The lowest group is a thermal group, and has negligible impact on core calculations. Thus, control rod worths are effectively calculated with eight groups.

2. Buckling Generation

Buckling generation follows a similar procedure to that for group collapse, except that 9-group rather than 28-group rz calculations are made for the same two or three configurations. As in the group collapse, bucklings for core and blanket zones are generated using models a, b, or c as appropriate for the reference configuration. Bucklings for all CRPs and rods, including off-center positions, are generated from models b and c, respectively.* The bucklings are generated with a module of the

*The procedure changed for analysis of the ZPPR-11 heterogeneous core. Group collapse and buckling generation for CRPs and CRs were done in the central zone with a 50/50 mixture of blanket and fuel material. It is felt that this mixture is more typical of the average of material surrounding the actual rod positions.

TABLE III.1. Energy Structure of the 28- and 9-Group Macroscopic Cross Section Sets[a]

Energy Boundary	28-Group Number	9-Group Number[b]
14.191 MeV[c]		
6.065	1	
3.679	2	
2.231	3	1
1.353	4	
820.9 keV	5	2
497.9	6	
302.0	7	
183.2	8	3
111.1	9	
67.38	10	
40.87	11	4
24.79	12	
15.03	13	
9.119	14	5
5.531	15	
3.355	16	
2.035	17	6
1.234	18	
748.5 eV	19	
454.0	20	7
275.4	21	
167.0	22	
101.3	23	
61.44	24	
37.27	25	
22.60	26	
5.044	27	8
Thermal	28	9

[a]The MC^2-II library used 2082 groups with a lethargy width of 1/120. The SDX intermediate library had 160 groups with a lethargy width of 1/10.

[b]The 9-group boundaries are the same as used by W-ARD except for the lower energy of group 8(0.6826 eV).

[c]Analysis for assemblies earlier than ZPPR-9 used an upper energy of 10 MeV.

TOPSY* system which calculates a DB^2 that will preserve the axial neutron leakage from each radial zone for every group. The DB^2 terms are stored in the cross section library as pseudo-isotopes having only an absorption cross section and are added to the zone macroscopic cross sections for the calculations in xy geometry.

*Auxiliary modular system used in ZPPR analysis.

The buckling terms used in control rod calculations are designed to preserve the neutron balance over the full height of the core.* In contrast, for calculations of reaction rates near the midplane, bucklings are generated at the midplane itself in order to produce a more appropriate spectrum.

Several approximations in the reference calculational method introduce errors of several percent each. As an example, Table III.2 shows corrections derived for the worths of sodium/steel CRPs relative to fuel as well as for worths of natural B_4C rods and 80% enriched B_4C rods relative to CRPs. These data, taken from Ref. 16, describe results from the control rod experiments for the mock-up of the Monju reactor on ZEBRA. The size of this assembly was similar to those in the ZPPR-2 to ZPPR-6 series. The central rod worths were about 2.5$ for natural and 4.6$ for enriched rods. The reference calculational method was essentially the same as that used for ZPPR analysis, but used cross sections derived from FGL5 data.

Similar results are found for the ZPPR calculations and are shown, for some cases, in Section III.C. Increases in computer capacity and development of the DIF3D code have enabled diffusion theory calculations to be made in full xyz geometry. These eliminate the buckling approximation and also the approximation of using macroscopic cross sections derived for central rods at other positions in the core. The results in Section III.C show that the model approximations have different effects for central rods and for the the outer ring rods.

B. Comparisons of Calculations and Experiments

This section reports the results of the fully-inserted rod worth measurements and calculations for the standard rod design in each of the assemblies in the data base. Reference calculations are not quite consistent for all measurements. The main inconsistency is a factor of four difference in mesh area. The effect of this difference is up to 8% in the direction of increasing C/E as the mesh is made finer. The actual mesh spacing used is noted in the appropriate tables, and corrections are reported in Section III.C. Delayed neutron yields and emission spectra for the β_{eff} calculations were based on ENDF/B-V data, while all cross sections were based on ENDF/B-IV.

Table III.3 summarizes results for each assembly in terms of the mean and the standard deviation for the distribution of C/E values. Table III.4 shows results for characteristic rod positions as well as enrichment data for the cores. Results of individual measurements in each assembly are presented in Tables III.5-III.24. Several observations that are useful in understanding the tables are described in the paragraphs below. Additional discussion relating to application of these results is contained in Section V.B.

The largest observable effect was for reactor heterogeneity. All results tended to be lower (by as much as 10%) when internal blankets were present. Even when these assemblies were made more homogeneous by adding

*An exception is ZPPR-7C in which only the neutron balance for the central 2/3 of the core was preserved, corresponding to the part of the internal blankets that was spiked with plutonium.

plutonium to the internal blankets, the average C/E values remained low. However, the addition of plutonium did flatten the radial C/E distribution.

When control rods were present in the reference critical configuration, there was an effect on average C/E values relative to the assemblies with no control rods in the reference configuration, i.e., clean end-of-cycle cores. In the larger cores $\overline{C/E}$ increased by 3.6% when the rods were present, while in the smaller homogeneous cores, any changes were statistically insignificant. In ZPPR-4 a 1.5% decrease was noted, but the C/E distributions had standard deviations of 2-4%. In ZPPR-6 an increase of 1.7% was observed when rods were present in the critical reference configuration. This was similar in magnitude to the 1.2% standard deviation for the C/E distributions. ZPPR-4/3 and ZPPR-4/4 are effectively larger cores, but their C/E distributions are characteristic of the smaller ZPPR-4/2 and ZPPR-4/1, respectively.

The effect of plutonium to simulate equilibrium conditions in the blankets has been studied in the smaller assemblies. In ZPPR-4, the effect of over 350 kg of plutonium in the radial blanket amounted to less than a 1% decrement on the mean C/E for control rods, which was well within the uncertainties. In that case the core enrichment changed from 0.142 to 0.138. When plutonium was added to the internal blankets of ZPPR-7, the core enrichment dropped from 0.254 to 0.212. The change in mean C/E for control worth from ZPPR-7B to ZPPR-7C was -2%, which is smaller than the standard deviation for the C/E distribution. However, there was a definite shift of -7.3% in C/E for the outer ring control rods.

The calculations for ZPPR-6 that are included in the tables for this section were done by the General Electric Company.[18] Their results have been scaled to make them consistent (in β_{eff}) with the other calculations. The GE methods were similar to those used on the other 350 MWe size cores (including use of ENDF/B-IV cross sections), except that only one mesh per drawer was used. The normalization to the four-mesh-per-drawer results required an increment of 5% in the calculated results. Comparisons of General Electric, Westinghouse, and Argonne calculations are discussed in Section III.D.

TABLE III.2. Typical Percentage Corrections for Modeling Approximations in the Reference Calculational Method[a]

Correction	Sodium/Steel CRP Relative to Fuel	Natural B_4C Rod Relative to CRP	80% enriched B_4C Rod Relative to CRP	Estimated Uncertainty
Group collapse	-1.8	-1.8	-1.8	0.5
Mesh size in xy diffusion theory	+1.1	+1.9	+2.9	1.0
Use of zone and group dependent bucklings	-2.7	-2.9	-3.4	0.7
(Use of constant buckling)[c]	(-12.1)	(+7.4)	(+3.7)	0.5
Transport (S_4) in xy plane	-2.9	-5.3	-6.6	0.5
Transport (S_4) in z-dimension	-6.5	+1.7[b]	+0.6[b]	0.5
Mesh size in transport calculations	0.0	0.0	-0.5	1.0
S_n order[d]	+2.6	+2.6	+2.6	2.0

[a]Results taken from Ref. 16.

[b]Note that these results are dominated by corrections for the CRP, corrections for rods relative to fuel are negative.

[c]Alternative method to using group and region dependent bucklings.

[d]More recent results, Ref. 17, indicate smaller corrections (about 0.5%) with reduced uncertainty.

TABLE III.3. Summary of Reference Results for Control Rod Worths C/Es in ZPPR Assemblies

ZPPR Assembly	Size, MWe	Rods in Reference	Internal Blankets	Blanket Plutonium	No. C/Es	Mesh Size, MPD[a]	Mean C/E	σ(C/E)[b]
3/1B	350	No	No	No	21	4	1.114	0.015
4/1	350	No	No	No	10	4	1.110	0.019
4/2	350	Yes	No	No	5	4	1.095	0.038
4/3	350	Yes	No	Yes	5	4	1.092	0.027
4/4	350	No	No	Yes	8	4	1.107	0.018
6/CEOC	350	No	No	No	9	1	1.043	0.012
6/CBOC	350	Yes	No	No	10	1	1.060	0.011
7B	350	No	Yes	No	18	4	1.034	0.043
7C	350	No	Yes	Yes	10	4	1.014	0.015
7G	350	No	Yes	No	32	4	1.050	0.026
8F	350	No	Yes	No	6	4	1.053	0.018
9	700	No[c]	No	No	22	1	0.988[c]	0.016
10A	700	No	No	No	19	1	1.047	0.013
10B	700	Yes	No	No	6	1	1.083	0.004
10C	900	No	No	No	5	1	1.047	0.020
10D	900	No	No	No	9	1	1.058	0.033
11A	350	Yes	Yes	No	4	1	0.955	0.041
11B	350	No	Yes	No	34	1	0.981	0.027
11C	350	No	Yes	Yes	9	1	0.979	0.019
11D	350	Yes	Yes	Yes	2	1	0.961	0.026
11F	350	No	Yes	No	3	1	0.970	0.024

[a]MPD: mesh per drawer in calculation.

[b]In some cases considerably smaller deviations are obtained when the results are grouped by radial position. See individual tables.

[c]Also no control positions, but rod worths are relative to configuration with CRPs added. With corrections for CPR reactivity, the mean C/E is 1.044 ± 0.024.

TABLE III.4. Variation of Control Rod Worth Predictions with Selected Core Design Parameters

ZPPR Assembly	Size, MWE	Inner Core Enrichment[a]	Enrichment Ratio Outer/Inner Core Zones	Ratio of Calculated[b] to Measured Worth		
				Central Rod	Inner Ring	Outer Ring
3/1B	350	0.142	1.48	1.140	1.143	1.131
4/1	350	0.142	1.44	1.106	1.082	---
4/2	350	0.150	1.40	---	1.080	1.152
4/3	350	0.146	1.42	---	1.066	1.120
4/4	350	0.138	1.46	1.092	1.101	---
7B	350	0.254[c]	SEC[d]	---	0.983	1.098
7C	350	0.212[c]	SEC	---	0.990	1.025
7G	350	0.254[c]	SEC	---	0.996	1.091
8F	350	0.254[c]	SEC	---	---	1.080
11B	350	0.254	SEC	---	0.977	1.085
9	700	0.097	1.47	1.097[e]	1.072[e]	1.115[e]
10A	700	0.104	1.43	1.066	1.079	1.107
10B	700	0.123	1.36	---	1.122	1.151
10C	900	0.104	1.27	1.067	1.078	1.111
10D	900	0.103	1.36	1.07[e]	1.080	1.150

[a]Ratio of fissile plutonium to total heavy metal.

[b]Diffusion theory in xy geometry, 9-energy groups, ENDF/B-IV data, 4 mesh spaces per ZPPR matrix position.

[c]Heterogeneous cores. When internal blankets are included in the average, enrichments are typically 0.14.

[d]Single enrichment core.

[e]Approximate correction of +6% for extrapolation from 1 to 4 mesh spaces.

TABLE III.5. Control Rod Worth Results from ZPPR-3/1B

Positions[a] with Rods Inserted	Designs[b]	Worth,[c] $	C/E[d]
Central			
1	A	- 2.13±0.02	1.140
1	I	- 4.14±0.06	1.120
		$\overline{C/E}$ = 1.130 ± 0.014	
Inner Ring			
2	H	- 2.02±0.02	1.130
2,5	H	- 4.26±0.06	1.127
2,4,6	H	- 6.51±0.08	1.143
		$\overline{C/E}$ = 1.133 ± 0.009	
Outer Ring			
8	I	- 1.94±0.02	1.095
10	I	- 2.07±0.02	1.106
9	J	- 1.95±0.03	1.096
17	J	- 2.16±0.03	1.105
8;9	I;J	- 3.42±0.05	1.093
8,14	I	- 4.24±0.06	1.109
8,10,12,14,16,18	I	-14.88±0.21	1.133
8-19	I;J	-28.96±0.55	1.131
		$\overline{C/E}$ = 1.109 ± 0.016	
Mixed Rings			
2;8	I;I	- 3.58±0.05	1.112
2;9	H;J	- 3.66±0.05	1.110
2;8;9	H;I;J	- 4.85±0.07	1.099
2,4,6;10,14,18	H;I	-14.33±0.16	1.121
2,4,6;8,10,12,14,16,18	H;I	-22.65±0.23	1.119
2-7;8,10,12,14,16,18	H;I	-30.12±0.39	1.099
2,4,6;10,14,18;9,11,13,15, 17,19	H;I;J	-28.99±0.29	1.110
2-19	H;I;J	-44.76±0.48	1.110
		$\overline{C/E}$ = 1.110 ± 0.008	
		TOTAL $\overline{C/E}$ = 1.114 ± 0.015	

[a]See Fig. VII.1 for position identification.

[b]See Figs. VII.18 and VII.19. Rods identified for B_4C mass: A = 4.58 kg, H = 5.62 kg, I = 13.10 kg, and J = 8.57 kg. See Table VII.1 for compositions.

[c]Statistical uncertainty only; additional systematic uncertainty of 2% for reactivity normalization.

[d]9-group, diffusion theory calculations in xy geometry with 4 mesh spaces per drawer. β_{eff} = 0.3217% Δk.

TABLE III.6. Control Rod Worth Results from ZPPR-4/1

Positions[a] with Rods Inserted	Designs[b]	Worth,[c] $	C/E[d]
Central			
1	N	- 3.53±0.04	1.106
1	M	- 4.82±0.07	1.121
1	A	- 2.32±0.01	1.098
1	I	- 4.39±0.06	1.116
		$\overline{C/E}$ = 1.110 ± 0.010	
Inner Ring			
2,4,5,7	M	-16.88±0.14	1.082
Mixed Rings			
1,8,10,12,14,16,18	N	-13.51±0.14	1.127
1,9,11,13,15,17,19	N	-16.95±0.19	1.100
1,8-19	N	-26.41±0.26	1.130
2,4,5,7;1,8,10,12,19,16,18	M;N	-33.92±0.51	1.082
2,4,5,7;1,3,6,8-19	M;N	-50.41±1.56	1.137
		$\overline{C/E}$ = 1.115 ± 0.023	
		TOTAL $\overline{C/E}$ = 1.110 ± 0.019	

[a]See Fig. VII.2 for position identification.

[b]See Figs. VII.18-20. Rods identified by B_4C mass: A = 4.58 kg, N = 8.67 kg, I = 13.10 kg, and M = 15.80 kg. See Tables VII.1 and VII.2 for compositions.

[c]Statistical uncertainties only; additional systematic uncertainty of 2% for reactivity normalization.

[d]9-group, diffusion theory calculations in xy geometry with 4 mesh spaces per drawer. β_{eff} = 0.3257% Δk.

TABLE III.7. Control Rod Worth Results from ZPPR-4/2

Positions[a] with Rods Inserted	Designs[b]	Worth,[c] $	C/E[d]
Inner Ring			
3,6	N	- 5.86±0.09	1.055
2,4,5,7	M	-16.30±0.29	1.077
3,6;2,4,5,7	N;M	-21.56±0.58	1.080
		$\overline{C/E}$ = 1.071 ± 0.014	
Outer Ring			
8,10,12,14,16,18	N	- 8.76±0.10	1.152
Mixed Rings			
3,6,8,10,12,14,16,18; 2,4,5,7	N;M	-32.99±0.83	1.111
		TOTAL $\overline{C/E}$ = 1.095 ± 0.038	

[a]See Fig. VII.2 for position identification. Type N rods in 1,9,11,13,15,17, and 19 in the reference configuration.

[b]See Fig. VII.20. Rods identified by B_4C mass: N = 8.67 kg and M = 15.80 kg. See Table VII.2 for compositions.

[c]Statistical uncertainties only; additional systematic uncertainty of 2% for reactivity normalization.

[d]9-group, diffusion theory calculation in xy geometry with 4 mesh spaces per drawer. β_{eff} = 0.3194% Δk.

TABLE III.8. Control Rod Worth Results from ZPPR-4/3

Positions[a] with Rods Inserted	Designs[b]	Worth,[c] $	C/E[d]
Inner Ring			
3,6	N	- 5.27±0.08	1.058
2,4,5,7	M	-13.15±0.21	1.107
3,6;2,4,5,7	N;M	-18.00±0.45	1.066
		$\overline{C/E}$ = 1.077 ± 0.026	
Outer Ring			
8,10,12,14,16,18	I	-14.88±0.21	1.133
Mixed Rings			
3,6,8,10,12,14,16,18;	N;M	-29.60±0.74	1.105
		TOTAL $\overline{C/E}$ = 1.091 ± 0.027	

[a]See Fig. VII.2 for position identification. Type N rods in 1,9,11,13,15,17, and 19 of the reference configuration.

[b]See Fig. VII.29. Rods identified for B_4C mass: A = 4.58 kg, H = 5.62 kg, I = 13.10 kg, and J = 8.57 kg. See Table VII.2 for compositions.

[c]Statistical uncertainty only; additional systematic uncertainty of 2% for reactivity normalization.

[d]9-group, diffusion theory calculations in xy geometry with 4 mesh spaces per drawer. β_{eff} = 0.3210% Δk.

TABLE III.9. Control Rod Worth Results from ZPPR-4/4

Positions[a] with Rods Inserted	Designs[b]	Worth,[c] $	C/E[d]
Central			
1	N	- 3.02±0.03	1.101
Inner Ring			
2,4,5,7	M	-14.23±0.23	1.101
Mixed Rings			
1,8,10,12,14,16,18	N	-13.91±0.15	1.090
1,9,11,13,15,17,19	N	-16.13±0.23	1.097
1,8-19	N	-27.01±0.38	1.097
1;9,11,13,15,17.19	N;M	-21.86±0.50	1.103
2,4,5,7; 1,9,11,13,15,17,19	M;N	-28.74±0.66	1.124
2,4,5,7; 1,3,6;8-19	M;N	-44.57±1.34	1.144
		$\overline{C/E}$ = 1.109 ± 0.020	
		TOTAL $\overline{C/E}$ = 1.107 ± 0.018	

[a]See Fig. VII.2 for position identification.

[b]See Fig. VII.20. Rods identified for B_4C mass: N = 8.67 kg, M = 15.80 kg. See Table VII.2 for compositions.

[c]Statistical uncertainties only; additional correlated uncertainty of 2% for reactivity normalization.

[d]9-group, diffusion theory calculations in xy geometry with 4 mesh spaces per drawer. β_{eff} = 0.3275% Δk.

TABLE III.10. Control Rod Worth Results from the ZPPR-6 Clean Beginning-of-Cycle Core

Positions[a] with Rods Inserted	Designs[b]	Worth,[c]$	C/E[d]
Inner Ring			
4,5,7	M	-11.1±0.06	1.06
4,5,7,(-1)[e]	M	- 7.9±0.04	1.06
2,4,5,7,(-1)	M	-12.4±0.06	1.05
2,4,5,7,(-1)	M	-15.3±0.08	1.05
		$\overline{C/E}$ = 1.055 ± 0.006	
Outer Ring			
8,10,12,14,16,18	N	- 9.5±0.06	1.05
8,10,12,14,16,18,(-1)	N	- 4.4±0.03	1.08
		$\overline{C/E}$ = 1.065±0.021	
Mixed Rings			
6,8,10,12,14,16,18,(-1)	N	- 7.8±0.04	1.06
3,6,8,10,12,14,16,18,(-1)	N	-11.5±0.06	1.07
3,6,8,10,12,14,16,18	N	-15.8±0.08	1.07
3,6,8,10,12,14,16,18; 2,4,5,7	N;M	-33.3±0.20	1.05
		$\overline{C/E}$ = 1.063 ± 0.010	
		TOTAL $\overline{C/E}$ = 1.060 ± 0.011	

[a]See Fig. VII.4 for position identification. Type N rods in positions 1,9,11,13,15,17,19 of reference.

[b]See Fig. VII.20. Rods identified by B_4C mass: N = 8.67 kg, M = 15.80 kg. See Table VII.2 for compositions.

[c]Statistical uncertainties only; additional systematic uncertainty of 2% for reactivity normalization.

[d]GE calculations using 9-groups diffusion theory, xy geometry, and one mesh space per drawer[18]; β_{eff} = 0.3096% Δk (ZPPR-3/3 value).

[e]CR-1 removed from reference.

TABLE III.11. Control Rod Worth Results from the ZPPR-6 Clean End-of-Cycle Core

Positions[a] with Rods Inserted	Designs[b]	Worth,[c]$	C/E[d]
Central			
1	N	- 2.26±0.01	1.04
Inner Ring			
4,5,7	M	-11.16±0.07	1.05
2,4,5,7	M	-16.56±0.08	1.03
		$\overline{C/E}$ = 1.04 ± 0.014	
Outer Ring			
9,11,13,15,17,19	N	-12.24±0.06	1.06
8-19	N	-21.69±0.15	1.05
		$\overline{C/E}$ = 1.055 ± 0.007	
Mixed Rings			
1,9,11,13,15,17,19	N	-16.17±0.08	1.05
1,8-19	N	-26.58±0.13	1.05
1,3,6,8-19	N	-33.39±0.20	1.04
1,3,6,8-19;2,4,5,7	N;M	-51.20±0.36	1.02
		$\overline{C/E}$ = 1.04 ± 0.014	
		TOTAL $\overline{C/E}$ = 1.043 ± 0.012	

[a]See Fig. VII.4 for position identification.

[b]See Fig. VII.20. Rods identified by B_4C mass: N = 8.67 kg and M = 15.80 kg. See Table VII.22 for compositions.

[c]Statistical uncertainties only; additional systematic uncertainty of 2% for reactivity normalization.

[d]GE calculations using 9-group diffusion theory, xy geometry, and one mesh space per drawer.[18] β_{eff} = 0.3257% Δk (ZPPR-4/1 value).

TABLE III.12. Control Rod Worth Results from ZPPR-7B

Positions[a] with Rods[b] Inserted	Worth,[c] $	C/E[d]	C/E[e]
Inner Ring			
3	- 2.57±0.01	0.992	0.923
5	- 2.31±0.01	0.986	0.917
2-7	-14.01±0.08	0.983	0.911
	$\overline{C/E}$ =	0.987 ± 0.005	0.917 ± 0.006
Outer Ring			
10	- 2.45±0.01	1.070	1.022
14	- 1.67±0.01	1.045	0.999
8,10,12,14,16,18	-17.86±0.09	1.098	1.020
9,11,13,15,17,19[f]	-14.26±0.10	1.022[g]	0.930[g]
	$\overline{C/E}$ =	1.071 ± 0.027	1.014 ± 0.013
Mixed Rings			
2,4,6,8,10,12,14,16,18	-27.59±0.14	1.064	---
2-8,10,12,14,16,18	-34.97±0.17	1.037	0.960
	$\overline{C/E}$ =	1.051 ±	1.019
TOTAL $\overline{C/E}$ = 1.034 ± 0.043 and 0.965 ± 0.049			

[a]See Fig. VII.5 for position identification.

[b]See Fig. VII.24 for the natural and enriched B_4C rod designs for ZPPR-7. The natural rods used here were fully-packed B_4C and contained 2.89 kg of ^{10}B. See Table VII.4 for compositions.

[c]Statistical uncertainties only; additional systematic re- uncertainty of 2% for reactivity normalization.

[d]9-group diffusion theory calculations in xy geometry with 4 mesh spaces per drawer. β_{eff} = 0.3380% Δk.

[e]9-group calculation with one mesh per drawer for comparison with later cores and to show the mesh effect.

[f]CRPs added to outer ring hex flats.

[g]Not included in average. When corrected for CRP worth misprediction, C/E's are 1.058 and 0.967, respectively.

TABLE III.13. Control Rod Worth Results from ZPPR-7C

Positions[a] with Rods[b] Inserted	Worth,[c] $	C/E[d]	C/E[e]
Inner Ring			
3	- 3.55±0.01	1.010	0.942
5	- 3.41±0.02	1.013	0.944
2-7	-22.12±0.09	0.990	0.922
	$\overline{C/E}$ =	1.004 ± 0.013	0.936 ± 0.012
Outer Ring			
10	- 2.04±0.01	1.029	0.966
14	- 1.72±0.01	1.027	0.970
8,10,12,14,16,18	-14.35±0.07	1.025	1.950
9,11,13,15,17,19[f]	-16.52±0.13	1.013[g]	0.928[g]
	$\overline{C/E}$ =	1.027 ± 0.002	0.962 ± 0.011
Mixed Rings			
2,4,6,8,10,12,14,16,18	-28.82±0.14	1.024	0.942
2-8,10,12,14,16,18	-42.25±0.21	0.997	0.920
2,4,6,8-19[f]	-49.38±0.44	0.985[h]	0.904[h]
	$\overline{C/E}$ =	1.011 ± 0.019	0.931 ± 0.016
TOTAL $\overline{C/E}$ = 1.014		0.945 and ± 0.965	± 0.018

[a]See Fig. VII.5 for position identification.

[b]See Fig. VII.24 for the natural and enriched B_4C rod designs for ZPPR-7. The natural rods used here were fully-packed B_4C and contained 2.89 kg of ^{10}B. See Table VII.4 for compositions.

[c]Statistical uncertainties only; additional systematic uncertainty of 2% for reactivity normalization.

[d]9-group diffusion theory calculations in xy geometry with 4 mesh spaces per drawer. β_{eff} = 0.3384% Δk.

[e]9-group calculation with one mesh per drawer for comparison with later cores and to show the mesh effect.

[f]Worth relative to configuration with 6 CRPs added on outer ring flats.

[g]Not included in average. When corrected for CRP worth misprediction, C/Es are 1.067 and 0.982, respectively.

[h]Not included in average.

TABLE III.14. Control Rod Worth Results from ZPPR-7G

Positions[a] with Rods Inserted	Worth,[b] $	C/E[c]	Δ β_{eff}, %[d]
Inner Ring			
4	- 1.52±0.009	0.997	---
6	- 1.67±0.014	0.994	-0.090
4,6	- 3.26±0.019	0.992	---
2,4,6	- 4.96±0.024	0.996	-0.267[e]
	$\overline{C/E}$ = 0.995 ± 0.002		
Outer Ring Hex Corners			
10	- 1.96±0.019	1.088	0.090
12	- 1.59±0.011	1.062	---
14	- 1.59±0.010	1.062	---
16	- 2.03±0.022	1.071	0.090
8,10	- 3.22±0.041	1.060	---
10,16	- 5.39±0.019	1.082	---
8,10,12	- 4.71±0.077	1.053	0.150
10,12,16	- 7.26±0.057	1.077	---
8,10,12,14	- 6.93±0.120	1.066	---
8,10,12,14,18	-10.44±0.163	1.068	0.329
8,10,12,14,16,18	-17.08±0.095	1.091	0.688[f]
	$\overline{C/E}$ = 1.071 ± 0.012		
Outer Ring Hex Flats			
11	- 1.53±0.012	1.044	---
13	- 1.35±0.007	1.028	---
15	- 1.53±0.012	1.044	---
9,11,13,15,17,19	-11.57±0.014	1.042	-0.090
	$\overline{C/E}$ = 1.039 ± 0.008		
Outer Ring Mixed			
15,16	- 2.86±0.031	1.032	---
8,10-15,17-19	-20.22±0.433	1.039	---
8-15,18,19	-16.22±0.398	1.044	---
8-19	-28.83±0.261	1.055	0.479
	$\overline{C/E}$ = 1.043 ± 0.010		
Outer Ring and Inner Ring Mixed			
4,8,10,12,14,18	-11.23±0.193	1.058	---
6,8,10,12,14,18	-13.78±0.193	1.064	0.180
4,6,8,10,12,14,18	-14.67±0.260	1.050	---
2,4,6,8,10,12,14,18	-15.48±0.296	1.037	-0.030
4,8,10,12,14,16,18	-18.75±0.094	1.084	---
6,8,10,12,14,16,18	-19.05±0.114	1.075	0.569
4,6,8,10,12,14,16,18	-20.73±0.200	1.070	---

TABLE III.14. Control Rod Worth Results from ZPPR-7G (cont'd)

Positions[a] with Rods Inserted	Worth,[b] $	C/E[c]	Δ β_{eff}, %[d]
2,4,6,8,10,12,14,16,18	-22.53±0.217	1.045	0.269
2,4,6,8-19	-33.08±0.367	1.037	0.090
		$\overline{C/E}$ = 1.059 ± 0.016	
		TOTAL $\overline{C/E}$ = 1.050 ± 0.026	

[a]See Fig. VII.7 for position identification. Normal ZPPR-7 rods. See Table VII.4 and Fig. VII.23.

[b]Statistical uncertainties only; additional 1% correlated uncertainty for reactivity normalization.

[c]9-group, diffusion theory calculations in xy geometry with 4 mesh spaces per drawer. β_{eff} = 0.3324% Δk, ZPPR-11B calculation.

[d]Calculated change in β_{eff} relative to the reference configuration.

[e]Minimum β_{eff} value, 0.27% lower than reference.

[f]Maximum β_{eff} value, 0.69% higher than reference.

TABLE III.15. Control Rod Worth Results from ZPPR-8A

Positions[a] with Rods Inserted	Worth,[b] $	C/E[c]
Inner Ring		
3	- 2.80 ± 0.03	1.014
4	- 2.54 ± 0.02	1.013
5	- 2.54 ± 0.02	1.010
6	- 2.80 ± 0.04	1.010
7	- 2.55 ± 0.03	1.008
2,4,6	- 8.88 ± 0.09	1.010
5,6,7	- 7.04 ± 0.07	0.995
2-7	-15.85 ± 0.10	1.000
	$\overline{C/E}$ = 1.008 ± 0.007	

[a]Very similar to the ZPPR-7B core, just slightly smaller. Position numbers are the same. See Fig. VII.8. Normal ZPPR-7 rod described in Fig. VII.24 and Table VII.4.

[b]Statistical uncertainties only ; Additional 1% systematic uncertainty for reactivity normalization.

[c]9-group, diffusion theory calculations in xy geometry with 4 mesh spaces per drawer. β_{eff} = 0.3382% Δk.

TABLE III.16. Control Rod Worth Results from ZPPR-8F

Positions[a] with Rods Inserted	Worth,[b] $	C/E[c]
Outer Ring		
8,10,12,14,18	-10.73 ± 0.15	1.058
8,10,12,14,16,18	-17.68 ± 0.15	1.080
9,11,13,17,19	-11.20 ± 0.13	1.036
9,11,13,15,17,19	-15.19 ± 0.10	1.051
8-14,17-19	-18.45 ± 0.43	1.031
8-19	-33.40 ± 0.45	1.063
	$\overline{C/E}$ = 1.053 ± 0.018	

[a]See Fig. VII.9 for position identification. ZPPR-7 natural B_4C rods. Rods described in Table VII.4 and Fig. VII.24.

[b]Statistical uncertinties only; additional 1% correlated uncertainty for reactivity normalization.

[c]9-group, diffusion theory calculations in xy geometry with 4 mesh spaces per drawer. β_{eff} = 0.3324% Δk, ZPPR-11B calculation.

TABLE III.17. Control Rod Worth Results from ZPPR-9

Positions[a] with Rods Inserted	Relative to Core Material		Relative to CRPs		
	Worth[b], $	C/E[c]	Worth, $	C/E[d]	C/E[e]
1	- 3.32±0.01	1.027	- 2.77	0.992	1.033
B	- 3.68±0.01		- 2.63	0.977	---
A,B	- 6.00±0.02	1.020	- 4.95	0.974	1.024
4	- 3.40±0.01		- 2.40	0.989	---
4,7	- 6.53±0.02	1.019	- 5.52	0.977	1.022
D	- 2.82±0.02		- 1.92	1.004	---
C,D	- 5.57±0.02	1.033	- 4.67	0.991	1.039
13	- 1.73±0.01	1.052	- 1.37	1.004	---
13,19	- 4.38±0.03	1.044	- 3.62	0.993	1.053
F	- 2.03±0.01		- 0.90	0.980	---
E,F	- 3.11±0.02	1.050	- 1.99	0.980	1.078
H	- 1.38±0.01		- 0.55	0.974	---
G,H	- 2.01±0.01	1.047	- 1.17	0.970	1.081
Inner Ring					
4	- 5.46±0.06	1.117	- 2.39	0.965	---
5	- 5.43±0.06	1.120	- 2.36	0.971	---
2-7	-16.77±0.18	1.011	-13.70	0.963	1.014
1-7	-17.28±0.20	1.011	---	---	---
Outer Ring					
13	- 4.41±0.06	1.175	- 1.68	1.021	---
15	- 4.33±0.06	1.174	- 1.60	1.010	---
9,17,19	- 7.37±0.13	1.101	- 4.64	1.002	---
9,13,17	- 9.43±0.12	1.070	- 6.62	1.003	---
9,11,15,17,19	-13.63±0.25	1.046	-10.91	0.990	---
9,11,13,15,17,19	-17.60±0.25	1.043	-14.87	1.002	1.050
1,9,11,13,15,17, 19	-24.61±0.27	1.032	---	---	---
	TOTAL C/E =	1.032 ±0.015		0.988 ±0.016	1.044 ±0.024

[a]For the first 13 entries, pairs of CRPs were added to ZPPR-9, except for position 1 and position 13, when only 1 CRP was added. For the next three entries, six CRPs were present prior to CR insertions. CR-1 and CRP-1 were added relative to six inserted rods, to account for entry 17. For entries 18-23, six CRPs were present prior to any CR insertions. For the last entry, CRP-1 and CR-1 were added relative to six rods inserted. See Fig. VII.10, VII.11.

[b]Statistical uncertainties only; additional 1% correlated reactivity normalization uncertainty--relative uncertainties are on the order of tenths of a percent.

[c]For these positions C/E's only for cases with no residual CRPs in core, to avoid biasing results because of large CRP reactivity mispredictions (C/E's for CRPs ~1.25). Nine-group, diffusion theory calculations in xy geometry with 1 mesh per drawer. Rods were 3x3 matrix positions, fully-packed natural B_4C. See Fig. VII.25 and Table VII.5. β_{eff} = 0.3436% Δk.

[d]Three calculations: reference, core with CRPs added and core with CRs added. Difference between last two taken as calculated rod worth.

[e]Calculated rod worth taken as difference between calculated worth of CRs relative to fuel and experimental worths of CRPs. This avoids the large error (~25%) introduced by calculation of CRP reactivity and puts the results on a similar basis to those for cores with CRPs in the reference. See IV.D.

TABLE III.18. Control Rod Worth Results from ZPPR-10A

Positions[a] with Rods Inserted	Worth,[b] $	C/E[c]
Central		
1	- 2.61 ± 0.01	1.019
Inner Ring		
2,4-7	-10.81 ± 0.02	1.032
2-7	-13.25 ± 0.05	1.035
	$\overline{C/E}$ = 1.035 ± 0.002	
Outer Ring		
9,11,13,15,17	- 9.29 ± 0.06	1.059
8,12,14,16,18	- 7.15 ± 0.05	1.065
9,11,13,15,17,19	-12.29 ± 0.04	1.059
8,10,12,14,16,18	-9.54 ± 0.05	1.066
8,9,11-19	-18.93 ± 0.21	1.056
8,11-19	-14.58 ± 0.23	1.057
8,10-19	-18.79 ± 0.19	1.059
8-19	-21.09 ± 0.23	1.055
	$\overline{C/E}$ = 1.060 ± 0.004	
Mixed Rings		
1-7	-14.20 ± 0.05	1.029
2-8,12,14,16,18	-22.61 ± 0.11	1.041
2,4-8,10,12,14, 16,18	-23.79 ± 0.03	1.046
2-8,10,12,14,16, 18	-27.34 ± 0.10	1.043
2-7,9,11,13,15,17	-22.89 ± 0.07	1.040
2-7,9,11,13,15, 17,19	-28.27 ± 0.15	1.036
1,9,11,13,15,17, 19	-16.27 ± 0.15	1.048
1,8,10,12,14,16, 18	-13.63 ± 0.03	1.054
	$\overline{C/E}$ = 1.042 ± 0.008	
	TOTAL $\overline{C/E}$ = 1.047 ± 0.013	

[a]See Fig. VII.12 for position identification. All rods composed of 50% natural B_4C and 50% stainless-steel-canned sodium. See Fig. VII.25 for representative drawer and Table VII.6 for composition.

[b]Statistical uncertainties only; additional 1% systematic uncertainty for reactivity.

[c]9-group, diffusion theory calculations in xy geometry with one mesh space per drawer. β_{eff} = 0.3393% Δk.

TABLE III.19. Control Rod Worth Results from ZPPR-10B

Positions[a] with Rods Inserted	Worth,[b] $	C/E[c]
Inner Ring		
3	- 1.82 ± 0.01	1.078
2,4-7	- 9.36 ± 0.04	1.085
2-7	-11.41 ± 0.04	1.079
	$\overline{C/E}$ = 1.081 ± 0.003	
Outer Ring		
10	- 1.[illegible] ± 0.02	1.083
8,12,14,16,18	- 7.73 ± 0.08	1.087
8,10,12,14,16,18	-10.98 ± 0.07	1.085
	$\overline{C/E}$ = 1.085 ± 0.002	
	TOTAL $\overline{C/E}$ = 1.083 ± 0.004	

[a]See Fig. VII.12 for position identification. Seven rods inserted in critical 10B reference configuration (1,9,11,13,15,17,19). ZPPR-10 rod design. See Fig. VII.25 and Table VII.6.

[b]Statistical uncertainties only, additional 1% systematic uncertainty for reactivity normalization.

[c]9-group, diffusion theory calculations in xy geometry with one mesh space per drawer. β_{eff} = 0.3309% Δk.

TABLE III.20. Control Rod Worth Results from ZPPR-10C

Positions[a] with Rods Inserted	Worth,[b] $	C/E[c]
Central		
1	- 2.46 ± 0.02	1.020
Inner Ring		
2-7	-12.40 ± 0.08	1.034
Outer Ring		
8,10,12,14,16,18	- 5.87 ± 0.05	1.070
9,11,13,15,17,19	- 8.44 ± 0.05	1.057
8-19	-13.48 ± 0.20	1.055
	$\overline{C/E}$ = 1.061 ± 0.008	
	TOTAL $\overline{C/E}$ = 1.047 ± 0.020	

[a]See Fig. VII.13 for position identification. All rods are normal ZPPR-10 design. See Fig. VII.25 and Table VII.6.

[b]Statistical uncertainties only; additional 1% systematic uncertainty for reactivity normalization.

[c]9-group, diffusion theory calculations in xy geometry with one mesh space per drawer. β_{eff} = 0.3406% Δk.

TABLE III.21. Control Rod Worth Results from ZPPR-10D

Positions[a] with Rods Inserted	Worth,[b] $	C/E[c]
Central	- 1.96 ± 0.01	1.009
Ring 1	- 7.33 ± 0.01	1.021
Ring 2 Corners	- 8.24 ± 0.02	1.062
Ring 3 Corners	- 5.24 ± 0.02	1.110
Ring 3	-11.98 ± 0.09	1.097
Ring 1 + Ring 2	-19.87 ± 0.02	1.035
Ring 2 Corners + Ring 3	-20.49 ± 0.12	1.061
Ring 1 + Ring 2 Corners + Ring 3 Corners	-22.93 ± 0.07	1.059
Ring 1 + Ring 3	-24.88 ± 0.08	1.066
	TOTAL $\overline{C/E}$ = 1.058 ± 0.033	

[a]See Fig. VII.14 for position identification. Normal ZPPR-10 composition but only 2x3 matrix positions except for CRP-1. Normal ZPPR-10 rod composition. See Fig. VII.25 and Table VII.6.

[b]Statistical uncertainties only; additional 1% systematic uncertainty for reactivity normalization.

[c]9-group, diffusion theory calculations in xy geometry with one mesh space per drawer. β_{eff} = 0.3394% Δk.

TABLE III.22. Control Rod Worth Results from ZPPR-11A

Positions[a] with Rods Inserted	Measured Worth,[b] $	C/E[c]
Inner Ring		
2,4,6	- 3.96 ± 0.006	0.894
Outer Ring		
9,11,13,15,17,19	-12.87 ± 0.017	0.975
8,10,12,14,16,18[d]	- 8.21 ± 0.016	0.986
	$\overline{C/E}$ = 0.981 ± 0.008	
Mixed Rings		
2,4,6,8-19	-24.19 ± 0.046	0.964
	TOTAL $\overline{C/E}$ = 0.955 ± 0.041	

[a]See Fig. VII.17 for position identification. All rods are normal ZPPR-11 design. See Fig. VII.24 and Table VII.8. Rods 8,10,12,14,16,18 are half inserted in the critical reference configuration.

[b]Relative to configuration with half inserted rods; statistical uncertainties only; additional 1% uncertainty for reactivity normalization.

[c]9-group, diffusion theory calculations in xyz geometry with one mesh space per drawer. β_{eff} = 0.33385% Δk.

[d]From half to full insertion.

TABLE III.23. Control Rod Worth Results from ZPPR-11B

Positions[a] with Rods Inserted	Measured Worth,[b] $	C/E[c]
Inner Ring		
6	- 1.10 ± 0.01	0.889
2,4,6	- 3.34 ± 0.01	0.883
	$\overline{C/E}$ = 0.886 ± 0.004	
Outer Ring Hex Flats		
9,11,13,15,17,19	-12.42 ± 0.07	0.967
9,11,13,17,19	- 9.35 ± 0.05	0.968
11,13,15,17,19	- 9.35 ± 0.05	0.969
15	- 1.50 ± 0.01	0.975
	$\overline{C/E}$ = 0.970 ± 0.004	
Outer Ring Hex Corners		
16	- 1.74 ± 0.01	1.007
10	- 1.72 ± 0.01	1.008
8,10	- 2.96 ± 0.03	1.003
10,16	- 4.50 ± 0.01	1.007
14,16	- 3.01 ± 0.03	0.991
8,14	- 4.08 ± 0.03	0.990
12,18	- 4.08 ± 0.03	0.990
10,14,18	- 7.00 ± 0.01	1.001
8,10,18	- 4.33 ± 0.07	1.008
8,12,16	- 7.16 ± 0.01	0.989
12,14,16	- 4.44 ± 0.07	0.989
12,14,16,18	- 6.88 ± 0.11	0.992
8,12,14,18	- 8.60 ± 0.04	0.988
8,10,12,18	- 6.82 ± 0.11	0.998
8,10,14,16	- 9.66 ± 0.02	0.998
8,10,12,14,18	-10.55 ± 0.12	0.993
8,12,14,16,18	-10.68 ± 0.12	0.989
8,10,12,14,16,18	-16.28 ± 0.03	0.989
	$\overline{C/E}$ = 0.996 ± 0.008	
Outer Ring, Flats & Corners		
8-19	-28.18 ± 0.02	0.979
8-14,16-19	-25.19 ± 0.08	0.976
8,10-19	-25.13 ± 0.08	0.978
8,11-19	-16.86 ± 0.33	0.982
8,10-15,17-19	-20.88 ± 0.14	0.983
8-14,17-19	-16.69 ± 0.33	0.987
8,9,11-14,16-19	-21.02 ± 0.18	0.980
	$\overline{C/E}$ = 0.981 ± 0.004	

TABLE III.23. Control Rod Worth Results from ZPPR-11B (con't)

Positions[a] with Rods Inserted	Measured Worth,[b] $	C/E[c]
Mixed Rings		
2,4,6;8,10,12,14, 18	-13.83 ± 0.17	0.971
2,4,6;8,10,12,14, 16,18	-19.70 ± 0.03	0.968
2,4,6;8-19	-30.65 ± 0.10	0.962
	$\overline{C/E}$ = 0.967 ± 0.005	
	TOTAL $\overline{C/E}$ = 0.981 ± 0.027	

[a]See Fig. VII.16 for position identification. Normal ZPPR-11 rods; see Fig. VII.24 and Table VII.8.

[b]Statistical uncertainties only; additional 1% systematic uncertainty for normalization.

[c]9 group, diffusion theory calculation in xy geometry with 1 mesh space per drawer. β_{eff} = 0.3324% Δk.

TABLE III.24. Control Rod Worth Results from ZPPR-11C

Positions[a] with Rods Inserted	Measured Worth,[b] $	C/E[c]
Inner Ring		
6	- 1.94 ± 0.002	0.944
2,4,6	- 6.27 ± 0.012	0.935
	$\overline{C/E}$ = 0.940 ± 0.006	
Outer Ring		
10	- 1.83 ± 0.004	0.994
8,12,14,16,18	-11.83 ± 0.126	0.991
8,10,12,14,16,18	-16.19 ± 0.016	0.991
8-19	-31.88 ± 0.081	0.986
9,11,13,15,17,19	-15.36 ± 0.076	0.982
	$\overline{C/E}$ = 0.989 ± 0.005	
Mixed Rings		
2,4,6;8,10,12,14, 16,18	-23.76 ± 0.071	0.971
2,4,6;8-19	-39.16 ± 0.176	0.968
	$\overline{C/E}$ = 0.970 ± 0.002	
	TOTAL $\overline{C/E}$ = 0.974 ± 0.019	

[a] See Fig. VII.17 for position identification. Normal ZPPR-11 rods; see Fig. VII.24 and Table VII.8.

[b] Statistical uncertainties only; additional 1.2% systematic uncertainty for normalization.

[c] 9 group, diffusion theory calculation in xy geometry with 1 mesh space per drawer. β_{eff} = 0.3435% Δk.

C. Corrections for Approximations in the Reference Method

There are several calculational improvements that change the C/E ratios for control worths by more than the experimental uncertainties. Some results of a British* study[16] on the sensitivity calculated control rod worths to methods approximations were presented in Table III.2. Sensitivities for the ANL calculations are expected to be similar. The approximations that have been investigated include mesh spacing, diffusion theory, bucklings to simulate the z-dimension, number of energy groups and neutron streaming. The mesh effect can be significant, as was seen in the reference calculations, where corrections of up to 9% were observed for a change in mesh area from 30.5 cm^2 to 7.6 cm^2 (see e.g. Table III.12). Similarly, the use of an S_4 transport calculation using the smaller mesh size can reduce the calculated values by several percent relative to the fine-mesh diffusion-theory result. Full xyz calculations--rather than xy calculations with group-and-region-dependent bucklings--have been shown to have a few percent effect in some cases. For B_4C rods, the correction for the few-group approximation is usually small. Experimental evidence suggests that corrections for rod heterogeneity are not large (<1.5%) if the B_4C is spread across the whole rod. The bunching effect in a power reactor rod is large (5-15%) and must be considered in application of critical experiment results. At ZPPR, this effect has been studied experimentally and with diffusion theory calculations for a central rod in rz geometry. (See Section IV.B.) The subject of control rod homogenization is treated separately in Section IV.C. Corrections for neutron streaming in sodium plates that are aligned in the y and z dimensions throughout the core contribute about 2% to the adjusted value. Axial streaming effects in the CRPs can be a several-percent effect for multiple rods. This effect has been investigated using transport theory calculations in rz geometry for a central position. Because of the significance of this correction to k_{eff} calculations, it is also treated separately in Section IV.E.

Systematic study of the effects of methods approximations at ZPPR has not progressed beyond the early stages. Nevertheless, results are presented in Tables III.25 - III.28 for each representative reactor type. After the corrections have been applied, the full range of C/E's is from 0.98 to 1.12. There is still need for further studies before the residual discrepancies can be ascribed to the basic nuclear data. Some inconsistencies are obvious in the tables in that not all approximations are treated for every case. Other inconsistencies that have to be resolved include discrepancies between results obtained with different codes (e.g., DOT and the DIF3D transport option). The effect of improved cross section generation methods, both for the core and the rods, has been neglected altogether.

As a result of application of the modeling corrections, some improvement in the consistency of C/E values has obviously been made. For central control rods (Tables III.25 and III.27) corrected C/E's are 1.046 and 1.071 for the small and the large homogeneous cores, respectively. However, no correction has been applied for neutron streaming in ZPPR plates for the

*One of the authors (P.J. Collins) participated in that study and notes that although different data libraries were used, the calculational methods were similar.

ZPPR-4 rod. Based on other calculations, the correction could be as much as +2%,* which would raise the ZPPR-4 C/E value to 1.068. The ZPPR-4 and -10A results would then agree within the uncertainties, having been intially discrepant by more than 4%.** Improvements in the radial distributions of C/E's are also evident. In ZPPR-7B, the inner and outer ring worth C/E's had an initial discrepancy of 10%, which was reduced to 5% when the corrections were applied.

*The streaming correction is tricky to estimate, and this approximate value may not be close, even though the cells in ZPPR-4 are not much different from those in assemblies where the correction has been calculated.

**When adjustments are made for consistent mesh spacing.

TABLE III.25. The Effect of Selected Calculational Improvements on C/E for the Central Rod Worth in ZPPR-4/1

Measured Worth, $	-3.53
Reference C/E[a]	1.106 ± 0.015
Modeling Improvement	**Corrections, %**
Transport (S_4) in xy	-4.4 ± 1.0
xyz geometry	-2.5 ± 0.5
28 group	-1.0 ± 0.5
Rod heterogeneity	0 ± 1.0
Axial CRP transport[b]	+2.5 ± 0.5
Total	-5.4 ± 1.3
Corrected C/E	1.046 ± 0.020

[a]9 group, diffusion theory calculation in xy geometry with 4 mesh spaces per ZPPR drawer.

[b]Streaming in axial direction that is not treated in xy geometry.

TABLE III.26. The Effect of Selected Calculational Improvements on Control Rod C/E Values in ZPPR-7B and -7C

	7B		7C		
	6 Inner Ring Rods	6 Outer Ring Rods	6 Inner Ring Rods	6 Outer Ring Rods	Uncertainty %
Measured Worth, $	14.01	17.86	22.12	14.35	
Reference C/E:[a]	0.983	1.098	0.990	1.025	2.0
Modeling Improvement	Correction, %				
28 groups	+0.9	-2.5	-0.7	-1.6	0.5
Transport (S_4) in xy	-4.6	-3.2	-3.2	-1.8	0.5
Directional diffusion	+2.6	-0.1	+1.3	+0.4	0.5
Axial CRP transport[b]	+4.3	+3.0	+2.8	+4.0	
xyz geometry	-1.0	-1.0	-1.0	-1.0	0.5
Total	+2.2	-3.8	-0.8	0.0	1.5
Corrected C/E	1.005	1.056	0.982	1.025	2.5

[a]9 group, diffusion theory calculation in xy geometry with 4 mesh spaces per ZPPR drawer.

[b]Estimated from results for a single rod.

TABLE III.27. The Effect of Selected Calculational Improvements on Control Rod C/E Values in ZPPR-10A

	Central Rod	Six Inner Ring Rods	Six Outer Ring Rods
Measured Worth, $	2.61	13.25	9.54
Reference model[a] C/E:	1.019	1.035	1.056
Modeling Improvement	Correction, %		
Mesh[b]	+4.6	+4.3	3.8
Transport (S_4) in xy	-3.6	-4.6	-1.9
Directional diffusion	+1.9	+2.9	+0.3
Axial CRP transport	+1.6	+1.6	+0.9
Groups, geometry, and Method[c]	+0.6	+0.2	-1.0
Total	+5.1	+4.4	+2.1
Corrected C/E	1.071	1.081	1.078

[a]9 group diffusion theory calculation in xy geometry with one mesh per ZPPR drawer.

[b]4 mesh spaces per ZPPR drawer.

[c]Comparison of 28-group xyz calculation with reference result (a).

TABLE III.28. The Effect of Selected Calculational Improvements on Control Rod C/E Values in ZPPR-10D

	6 Ring 1 Rods	12 Ring 3 Rods	6 Ring 1 + 12 Ring 3 Rods
Measured worth, $	7.33	11.98	24.88
Reference C/E[a]	1.021	1.097	1.066
Modeling Improvement	Corrections, %		
Mesh[b]	+5.8	+4.8	+5.5
Transport (S_4) in xy	-5.4	-2.7	-3.3
Direction diffusion	+2.0	+0.2	+0.6
Axial CRP transport	+2.4	+0.4	+1.8
xyz geometry	-0.8	-0.3	NC
Groups	NC[c]	NC	NC
Total	+4.0	+2.4	+4.6
Corrected C/E	1.062	1.123	1.115

[a] 9 group, diffusion theory calculation in xyz geometry with 1 mesh per ZPPR drawer.

[b] 4 mesh spaces per ZPPR drawer.

[c] No correction calculated.

D. Comparisons of ANL, GE, and W-ARD Calculations

All of the 350 MWe size assemblies in the data base were a part of the CRBRP program on ZPPR. In order to generate and verify bias factors for use in the evolving CRBR design, many experiments were also calculated by the General Electric Company and the Westinghouse Advanced Reactors Division. A comparison of the three calculational methods and a few of the results are presented in this section.

All ANL calculations in this report used ENDF/B-IV data. GE used Version IV data for the later assemblies, and made comparisons between results obtained using Versions III and IV for selected cases in ZPPR-4 and -7.[19] Those comparisons are presented in Table III.29. Changes in data processing methods were also implemented with the Version IV calculations so that differences do not reflect only those between the data libraries. However, differences in calculated rod worths are generally less than 2%.

The calculational method used for control rod worths by GE and W-ARD is similar to that used by ANL as described in Section III.A. Differences are in the codes used to process ENDF/B libraries, ZPPR cell calculation codes, and methods used to collapse the data to macroscopic 9-group cross sections. The three methods are compared in Table III.30. The GE and W-ARD paths are quite similar, using 50 intermediate energy groups, Bondarenko shielding-factor similar, using 50 intermediate energy groups, Bondarenko shielding-factor method, elastic removal corrections and S_N cell calculations. One-dimensional models are used for group collapse instead of the 28-group rz models used by ANL.

TABLE III.29. Comparison of Control Rod Worths using ENDF/B-III at ENDF/B-IV Data in Calculations by General Electric Company

Assembly	Rods	Difference in Rod Worth (Version IV-Version III)[a], %
ZPPR-4/1	Mean for 5 Rod Groups	+2.2
ZPPR-4/2	Mean for 5 Rod Groups	+1.1
ZPPR-7B	6 Inner Ring Rods	+0.5
	6 Outer Ring Rods	-2.4
	6 Inner + 6 Outer Ring Rods	-1.2%
ZPPR-7C	6 Inner Ring Rods	-1.4%
	6 Outer Ring Rods	-2.2%
	6 Inner + 6 Outer Ring Rods	-2.0%

[a]Some change in processing methods also.

Table III.31 compares ANL and GE results for ZPPR-4. ANL results are taken from Tables III.6 and III.B.7, but adjusted by -5% to compare with the coarse-mesh values used by GE.[19] The original GE results have been adjusted to compare with the latest evaluation of experiments used by ANL and also adjusted to β_{eff} values calculated with ENDF/B-V delayed neutron data. Also included in the table are summaries of the ZPPR-6 results to compare with those in ZPPR-4. The agreement between ANL and GE calculations for ZPPR-4 control rods is within 1.5%.

Table III.32 compares the analyses of rod bank worths in ZPPR-11. All calculations used ENDF/B-IV and a fine mesh (four mesh spaces per drawer). The W-ARD[20] results have been adjusted to the ANL b_{eff} values for the comparison. The rod worths differ by as much as 5% among the three analyses and are related to differences in calculated radial flux distributions. These differences arise from methods used to process the basic data for each zone in the reactor. The results emphasize the need for consistent analysis of the critical experiments and the power reactor for proper application of bias factors. This is more important in heterogeneous designs because of the higher sensitivity to methods and data approximation.

E. Boron Perturbation Sample Worths

A seemingly obvious question is how the control rod worth C/E's compare with those for small perturbation measurements using absorber samples. Unlike control rods, the small samples exert only a minimal perturbation on the gross reactor flux. Such experiments traditionally have been analyzed by first-order perturbation (FOP) theory, and the corrections that are required for modeling approximations were thought to be smaller than those described in Section III.C. However, perturbation experiments have been the source of a consistent discrepancy in the U.S. program.[21] C/E's for the perturbation reactivity smal plutonium samples have ranged from 1.13 to

TABLE III.30. Comparison of Calculational Methods used by ANL, GE, and W-ARD

Step	ANL	GE	W-ARD
ENDF/B library processing	ETOE/MC^2-II to 160 groups	MINX to 50 groups GMUG library	MINX to 50 groups
ZPPR cell heterogeneity	SDX/MC^2-II in 160 groups Resonance shielding by equivalence theory.	TDOWN in 50 groups Bondarenko-equivalence theory Elastic removal correction	SPHINX in 50 groups Bondarenko equivalence theory Elastic removal correction
	Integral transport Assembly-dependent cell model[b] Single B^2 Collapse to 28 groups	S_N transport[a] Assembly-dependent cell model[b] Energy and region DB^2	ANISN transport (S_{16})[a] Assembly-dependent cell model[b] Energy and region DB^2
Group collapse to 9 groups	DIF3D 28 group rz models	50-group 1-dimensional diffusion theory	SPHINX 50 group 1-dimensional diffusion theory
Buckling generation	9-group rz diffusion theory DB^2 to match leakage at core/axial blanket interface	9-group rz diffusion theory DB^2 to match leakage at core/axial blanket interface	9-group rz diffusion theory DB^2 to match leakage at core/blanket interface
Reference method	9-group xy diffusion theory	9-group xy diffusion theory	9-group xy diffusion theory

[a]Using special angular quadrature.

[b]There were some differences in the cell models among the three organizations and for different assembly types.

TABLE III.31. Comparisons of ANL and GE Results[a] for ZPPR-4 and GE Results for ZPPR-6 and ZPPR-4

Assembly	ANL/GE Analysis	Number of Calculations	RMS Deviation, %	Mean C/E
ZPPR-6				
CBOC	GE	10	1.1	1.060
CEOC	GE	9	1.1	1.043
ZPPR-4				
Phase 2 (CBOC)	GE	5	2.3	1.039
Phase 1 (CEOC)	GE	6	1.7	1.044
ZPPR-4				
Phase 2 (CBOC)	ANL	5	3.7	1.044
Phase 1 (CEOC)	ANL	6	2.5	1.059

[a]Calculations with Version-IV data, adjusted for Version-V β_{eff} values.

TABLE III.32. Comparison of ANL, GE, and W-ARD Results for Control Rod Worths in ZPPR-11

Assembly	Control Rod Configuration	C/E[a] Values ANL	GE	W-ARD[b]
ZPPR-11B	3 Inner Ring	0.978	0.986	1.028
	6 Outer Ring Flats	1.058	1.048	1.076
	6 Outer Ring Corners	1.073	1.045	1.073
ZPPR-11C	3 Inner Ring	---	1.029	1.014
	6 Outer Ring Flats	---	1.059	1.060
	6 Outer Ring Corners	---	1.046	1.064

[a]All calculations used 9-group xy diffusion theory with four mesh points per ZPPR drawer, ENDF/B-IV data.

[b]W-ARD calculations use β_{eff} values of 0.3426% Δk (11B) and 0.3540% Δk (11C). Results in the table are adjusted to the ANL values of 0.3324% Δk (11B) and 0.3435% Δk (11C).

1.19 when calculations are based on ENDF/B Version-IV data. C/E values for ^{10}B typically have been 5-15% lower.*

Major developments in the analysis of small sample worth measurements within the last two years have, however, completely revised traditional U.S. thinking on small sample worth C/E's. The principal breakthrough was Smith's correction[22] for intracell adjoint flux heterogeneity, a major source of error in the traditional FOP analysis of perturbation samples. Subsequent tests on ZPR-6 and ZPR-9[23] have verified both the need for and the magnitude of such corrections. The geometry of the historical measurements generally is too complex for direct calculation of the effect, but reasonable estimates are that 5% reductions in Pu worth and a net 0% change in B worth can be expected.

The small sample measurements and analyses will be discussed in detail in a separate assessment document, but publication is not expected for some time. For completeness, a selection of results obtained for the different reactor types is included here to compare with the control rod analysis.

Table III.33 compares C/E values for perturbation samples of ^{10}B and ^{239}Pu with those for control rods in the small homogeneous cores, small heterogeneous cores and the large homogeneous cores. Because of the relatively large modeling corrections for control rods, adjusted results were taken from Tables III.25-III.27. For ZPPR-8A, modeling corrections were taken from Table III.26 since 7B and 8A were essentially identical assemblies. Corrections for mesh, transport, and neutron streaming effects were generated for the ZPPR-9 rod, but the correction of +0.6% for group collapse and three-dimensional effects was taken from the ZPPR-10A results in Table III.27.

The C/E results for control rods and boron samples are consistent within 6%. For the smaller cores, the small sample results are higher than for the rods, with the reverse being true for the larger cores. However the differences are within the uncertainties in the calculations.

Although no results are presented here, it is worth noting that in the heterogeneous cores and the large cores, the small sample distributions show higher C/E values in the outer regions of the core than near the center. This trend is consistent with the higher C/E values for control rod worths in the outer ring positions.

IV. CONTROL ROD EFFECTS THAT INFLUENCE CORE AND ROD DESIGN

The last section described the results of measurements and calculations of the worth of fully-inserted control rods in a variety of ZPPR assemblies. That information provides most of what is required to bias LMFBR control rod design calculations. However, some additional information is either necessary or useful in producing accurate design values. For example, in its actual design geometry with an effectively reduced volume, a control rod's

*In Europe, use of adjusted data sets and much higher delayed neutron yields for ^{238}U fission result in C/E values close to unity for perturbation measurements.

TABLE III.33. Comparison of Small Sample and Control Rod C/E Results

Assembly	^{10}B Sample	Control Rod[a]	^{239}Pu Sample[b]
ZPPR-4/1	1.08[c]	1.05[c]	1.11[c]
ZPPR-7A	1.05[d]	--	1.10[d]
ZPPR-7B	--	1.01[e]	--
ZPPR-8A	1.09[d]	1.03[e]	1.14[d]
ZPPR-9	1.05[c]	1.09[c]	1.08[c]
ZPPR-10A	1.05[c]	1.07[c]	1.09[c]

[a]C/E corrected for most modeling approximations.

[b]C/E reduced by 5% to account for adjoint heterogeneity.

[c]At or near core center.

[d]In first fuel ring.

[e]Inner ring of rods.

worth can be reduced by 5-15% relative to the normal critical experiment mockup rod. Other effects that need consideration are rod interactions, the influence of boron enrichment on bias factors, the influence of CRP modeling on k_{eff} and rod worth predictions, the variation of worth with insertion depth, worths of the alternative absorbers, and k_{eff} predictions with rods inserted in a critical configuration. This section addresses each of these topics and describes the data base and the status of the capability to calculate the effects.

A. Rod Interactions

One of the important considerations in core layout and control system design is the the worth of a rod as a function of the insertion pattern of other rods. This relationship is generally referred to as the rod interaction effect, although definitions vary for assigning a numerical value to the effect. Here the interaction effect is defined* as the percentage change in worth of rods when measured as a group, relative to the sum of their individual worths.

Measured and calculated rod interaction effects are presented for ZPPR assemblies 3/1B, 7B, 7C, 7G, and 9 in Tables IV.1 - IV.4. This range of assemblies includes a small homogeneous core, heterogeneous cores with and without plutonium in the internal blankets, and one of the larger homogeneous cores. In all cases, reference calculations agreed with the measurements to within a few percent. Interaction effects were considerably larger in the heterogeneous cores and in the larger homogeneous cores than in the smaller homogeneous cores. This result is consistent with differences among eigenvalue spectra for the assemlbies. Interactions were considerably

*Rod Interaction $\equiv \frac{\text{(Rod group worth) - (Sum of single rod worths)}}{\text{(Sum of single rod worths)}} \times 100\%$

TABLE IV.1. Control Rod Interactions in ZPPR-3/1B

Rod Group[a]	Interaction, %	
	Measured[b]	Calculated
2,5	+ 5.4	+ 5.1
2,8	- 9.7	- 9.8
2,9	- 7.7	- 7.9
8,9	-12.2	-12.3
8,14	+ 8.4	+10.5
2,4,6	+ 4.8	+ 5.9
2,8,9	-18.1	-18.7
2,4,6;10,14,18	+16.6	+17.2
8,10,12,14,16,18	+22.5	+25.9
2-7;10,14,18	+11.2	+10.4
2,4,6,8,10,12,14,16,18	+23.4	+24.2
2-7;8,10,12,14,16,18	+22.6	+20.6
8-19	+19.4	+22.7
2-19	+22.0	+22.0

[a]See Table III.5 for descriptions and worths.

[b]Uncertainties can be estimated from the measured results in Table III.5.

TABLE IV.2. Control Rod Interactions in ZPPR-7B and -7C

Rod Group[a]	Interaction, %			
	Measured[b]		Calculated	
	7B	7C	7B	7C
Inner Ring	- 2.6	+ 6.7	- 3.0	+ 4.3
Outer Ring	+54.2	+30.9	+60.4	+30.6

[a]See Tables III.12 and III.13 for descriptions and worths.

[b]Uncertainties can be estimated from the measured results in Tables III.12 and III.13.

TABLE IV.3. Control Rod Interactions in ZPPR-7G

Rod Group[a]	Interaction, % Measured[b]	Calculated
Outer Ring		
15,16	-19.7	-21.7
8,10	- 9.3	-10.7
10,16	+35.3	+35.4
8,10,12	- 9.1	-10.0
10,12,16	+29.3	+30.4
8,10,12,14	+ 2.3	+ 2.6
8,10,12,14,18	+24.9	+25.5
8,10,12,14,16,18	+64.5	+68.5
9,11,13,15,17,19	+31.3	+31.5
8-15,18,19	+ 1.1	+ 2.9
8,10-15,17-19	+29.2	+27.7
8-19	+50.2	+50.4
Inner Ring		
4,6	+ 2.2	+ 2.3
2,4,6	+ 5.2	+ 5.3

[a]Refer to Table III.14 for descriptions and worths.

[b]Uncertainties can be estimated from measured results in Table III.14.

TABLE IV.4. Control Rod Interactions in ZPPR-9

Rod Group[a]	Interaction, % Measured[b]	Calculated[c]
A,B	- 5.7	- 6.2
4,7	+15.2	+13.6
C,D	+21.5	+20.4
13,19	+19.4	+17.7
13 (4-pin),19[d]	+10.3	+10.0
13 (4-pin), 19 (4-pin)	+ 7.5	+ 7.0
E,F	+10.0	+10.6
G,H	+ 6.6	+ 5.9
2-7	- 3.9	- 4.3
9,17,19	- 5.0	- 6.0
9,13,17	+35.7	+34.2
9,11,15,17,19	+35.0	+32.1
9,11,13,15,17,19	+52.4	+50.6

[a]Refer to Table III.17 for descriptions and worths.

[b]Uncertainties can be estimated from the measured values in Table III.17.

[c]Values calculated relative to CRPs are used here.

[d]Factor of 10 reduction in ^{10}B content; factor of 2.6 reduction in worth; for rod design, see Fig. VII.25, and Table VII.5 for compositions.

changed by inserting plutonium into the internal blankets of the heterogeneous core. As can be seen in Table IV.2 for example, the outer ring rod interaction dropped from 54% to 31%, while the sign changed from negative to positive for the smaller inner ring rod interaction.[24]

Many two-rod interactions were studied in ZPPR-9.[25] In Fig. IV.1 the results of these studies are plotted as a function of rod separation across the core. Some limited results suggested that the rod interaction effect was proportional to the single rod worth, so the normalized value is also plotted on the same figure. This could have some application for estimating interactions for different rod designs, or in power reactor operation, where it is often easier to measure the worth of a single rod than the worth of a bank of rods.

Since one reactivity fault that has been considered in LMFBR safety studies is the uncontrolled withdrawal of a rod from the primary operating bank, the change worth of a single rod under different core conditions has been of interest. In Table IV.5 the change in worth of rods as other rods are inserted is shown for several examples in ZPPR-7G. Reference calculational methods were successful in predicting the effect, even though in some cases the change in worth was more than 100%. Similar results from other assemblies can be derived from Tables III.5 and III.17, for example.

TABLE IV.5. Variations in Rod Worths with Insertions of Other Rods in ZPPR-7G

Rods Inserted	Reference Rod Pattern	Worth, $		% Change[b]
		Measured[a]	Calculated	
1 Outer ring corner	None	- 2.03	- 2.17	---
"	1 adjacent flat	- 1.33	- 1.35	- 34.5
"	1 opposite corner	- 3.40	- 3.71	67.5
"	2 opposite corners	- 4.04	- 4.41	99.0
"	5 corners	- 6.65	- 7.50	227.9
"	5 corners + inner ring	- 7.04	- 7.90	246.8
2 Adjacent outer ring	None	- 2.86	- 2.95	---
"	10 outer ring	-12.61	-13.50	340.9
3 Inner ring	None	- 4.96	- 4.94	---
"	5 outer ring corners	- 5.05	- 4.91	1.8
"	6 outer ring corners	- 5.42	- 5.32	9.3

[a]See Table III.14 for descriptions and data on relative uncertainties.

[b]Measured change in magnitude relative to value with no other rods inserted.

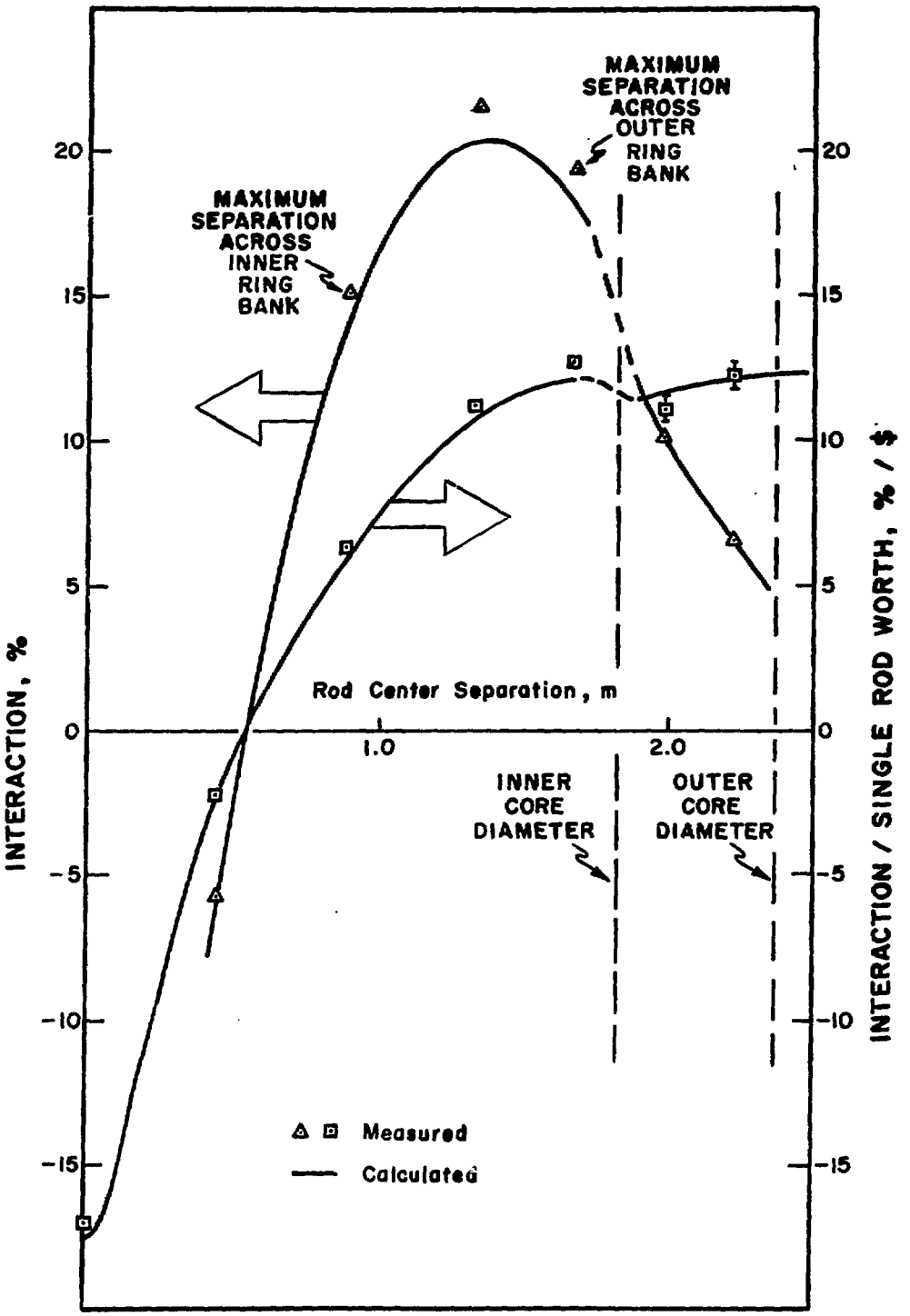

TWO-ROD INTERACTIONS AS A FUNCTION OF SEPARATION IN ZPPR-9

Fig. IV.1

B. The Effects of Rod Geometry and Boron Enrichment

The measurements that were described in Section III do not address two of the significant issues that must be confronted by designers: exact rod geometry and ^{10}B-enrichment of B_4C. Special experiments are done to measure these effects in ZPPR. Since the effects are often coupled in one set of measurements, they are combined in a single section here. The effects of boron enrichment and cross-sectional geometry on rod worths were studied in ZPPR-6, -10A, and -11. Worths of enriched rods were also measured in ZPPR-7B and -7C.

The absorber bundle in power-reactor designs usually covers an appreciably smaller area than a subassembly hexagon, whereas in the critical assembly, absorbers usually fill the entire mockup control position. Many designs call for enriched B_4C, which is not available in large quantities at ZPPR. Rod worths are made approximately correct by increasing the density of natural B_4C at the expense of steel and sodium. Calculations of the special enrichment and geometry experiments in single rods then provide a basis for extrapolating from the normal ZPPR experiments to the reactor design. Section IV.C contains a more detailed discussion of the calculational problems.

The enriched rods used in the ZPPR-6 experiments are described in Table IV.6. Results of the measurements are found in Table IV.7 and in Fig. IV.2. Substantial variations in worth, from -1.6\$ to -4.4\$, were found as the ^{10}B mass was increased from 1.2 kg to 5.6 kg. The more homogeneous pin rod was worth slightly more than the equivalent plate rod. The effect of bunching the absorber plates to form a smaller volume was about -10%. Comparisons with GE calculations, based on a model similar to that of the reference method described in Section III.A, are included in Table IV.7 and in Fig. IV.1. It is seen that for large changes in worth, heterogeneity, and enrichment, the calculations produced C/E's that varied at most by 6%.

Comparisons of worths and C/E's for the normal and enriched ZPPR-7 rods are presented in Table IV.8. Some differences in C/E for equivalent measurements are evident. However, these differences may be partially explained by differences in heterogeneity (see Fig. VII.24) rather than just by enrichment alone. Calculations were done with the ANL reference method.

More extensive enrichment/geometry studies were done in ZPPR-10A.[26] There, natural and fully-enriched B_4C pins were arranged in a variety of shapes within the 3x3 central control position. The geometries are shown in Fig. IV.3. Diffusion theory calculations in rz geometry were done in a two-region model. For the compact rod designs, the absorber was concentrated in the inner region of the model. For the diffuse rod designs, the B_4C was spread over both regions of the model. No attempts were made to model the explicit xy geometry of the rod. Results are summarized in Table IV.9. Going from natural (20% ^{10}B) to 92% enriched B_4C increased the worth from about 1.6\$ to -2.7\$. Spreading the enriched B_4C over the whole 3x3 region increased the worth further to 3.1\$. The overall spread in C/E, including the value for the normal plate rod was about 2%, indicating that the effect can be accurately computed. This is in contrast to results from some foreign LMFBR programs, as discussed in Section IV.C. Finally, a curve similar to

TABLE IV.6. Isotopic and Elemental Mass Summary for ZPPR-6 B_4C Control Worth Enrichment and Geometry Study

Rod Type	Mass of Material in Rod, kg			
	^{10}B	^{11}B	Total Boron	Carbon
Matched Plate[a]	1.270	5.664	6.933	1.992
Pin[b]	1.140	5.134	6.274	1.696
ALSS[c]	4.065	0.379	4.444	1.280
M[d]	2.266	10.102	12.368	3.507
N[d] (normal)	1.248	5.564	6.812	1.925
N[e] (50% enriched)	2.769	2.666	5.435	1.570
N (75% enriched)	4.378	1.356	5.711	1.740
N (90% enriched)	5.638	0.519	6.157	1.856

[a]Designed to Match Pin Rod Composition. See Fig. VII.23.

[b]Standard ZPPR calandria filled with 16 B_4C pins.

[c]See Figs. VII.21 and VII.22 for ALSS rod design.

[d]See Fig. VII.20 for M and N designs.

[e]90%-enriched B_4C progressively substituted for natural B_4C in enriched type-N designs.

TABLE IV.7. Results of ZPPR-6 B_4C Control Worth Enrichment and Geometry Studies

Rod Type[a]	Position[b]	Worth[c], $	C/E[d]
Pin	13	1.61	1.04
Plate	13	1.57	1.06
Bunched ALSS	5	3.61	1.07
ALSS	5	4.01	1.03
M	5	3.57	1.01
N	5	2.62	1.05
N (50% enriched)	5	3.46	1.06
N (75% enriched)	5	4.10	1.03
N (90% enriched)	5	4.40	1.05

[a]See Table IV.6 for rod description.

[b] See Fig. VII.4 for position identification.

[c]Relative uncertainties are less than 1%. There is an additional correlated uncertainty of 2% for reactivity normalization.

[d]GE calculations: 9-group, xy diffusion theory, 1 mesh space per drawer; β_{eff} = 0.3257% Δk (ZPPR-4/1 value).

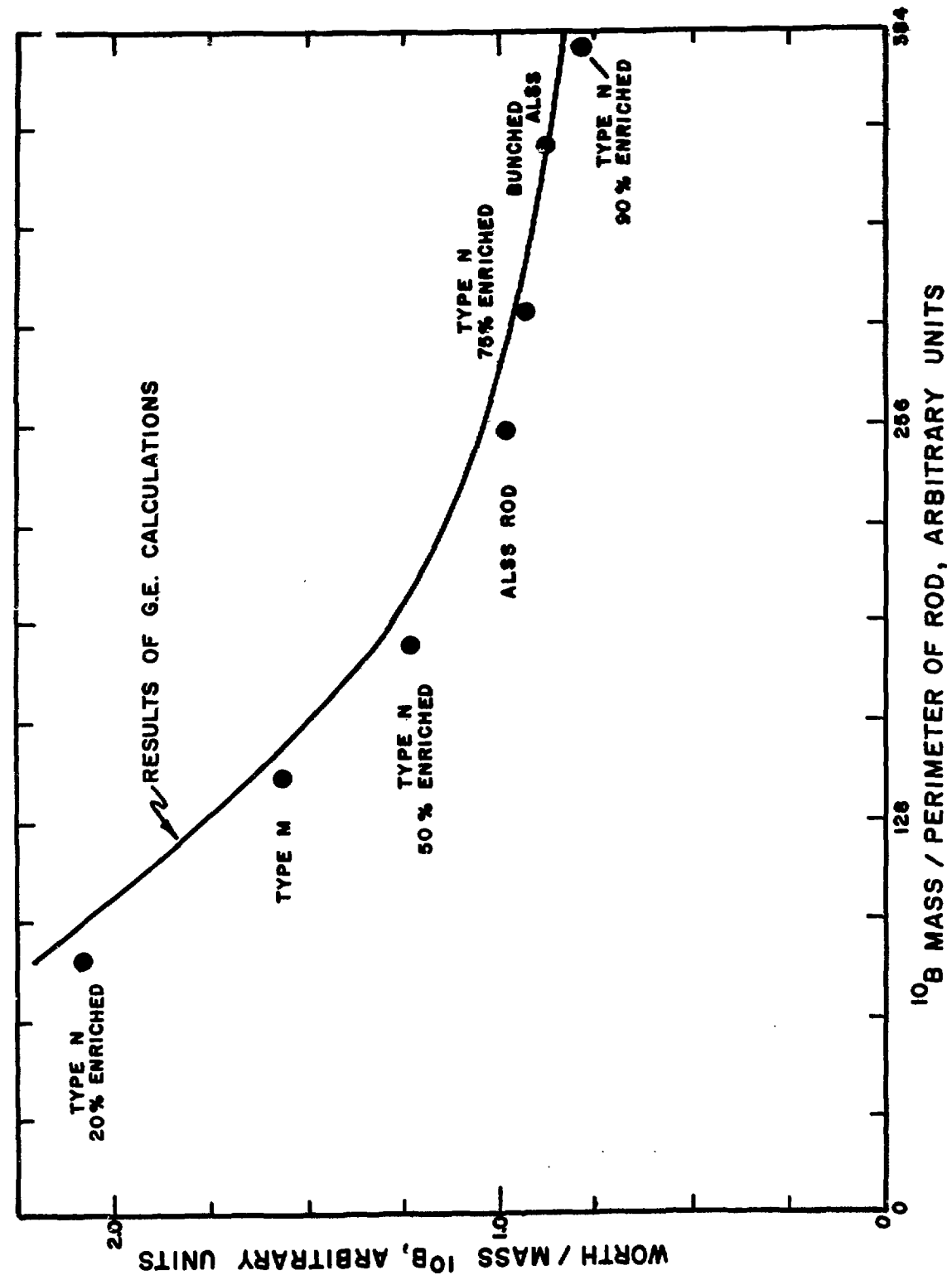

Fig. IV.2. Normalized Worth Curve for Central Control Rods in ZPPR-6.

TABLE IV.8. Results of Control Worth Enrichment Studies in ZPPR-7

Phase	Position[a]	Worth[b], $		C/E[d]	
		Enriched[c]	Normal[c]	Enriched	Normal
7B	3	2.73	2.57	1.011	0.992
7B	10	2.62	2.45	1.066	1.070
7C	3	3.85	3.55	1.020	1.010
7C	10	2.18	2.04	1.053	1.029
7G	10	2.16	1.96	1.094	1.088

[a]See Figs. VII.5 and VII.7 for position identification.

[b]See Tables III.11-III.13 for uncertainties.

[c]See Fig. VII.23 for the natural and enriched B_4C rod designs for ZPPR-7. The natural rods were fully-packed B_4C and contained 2.89 kg of ^{10}B. The enriched rods were B_4C and sodium, and contained 4.76 kg ^{10}B. Compositions are found in Table VII.4.

[d]9-group, diffusion theory calculations in xy geometry with 4 mesh spaces per drawer.

TABLE IV.9. Results of ZPPR-10A Rod Geometry and Enrichment Studies

Cross-Sectional Geometry[a]	Material	Enrichment	^{10}B Mass, kg	Measured Worth[b],$	C/E[c]
Circular	B_4C	Natural	1.58	-1.659	1.060
Hex #2	B_4C	Natural	1.58	-1.654	1.063
Rectangular	B_4C	Natural	1.58	-1.670	1.053
Rectangular	B_4C	92%	7.82	-2.712	1.043
Hex #1	B_4C	92%	7.82	-2.692	1.051
Hex #2	B_4C	92%	7.82	-2.689	1.052
Circular	B_4C	92%	7.82	-2.680	1.055
Secondary	B_4C	92%	7.82	-2.705	1.045
Square	B_4C	92%	7.82	-3.086	1.048
Rectangular	B_4C	92%	3.91	-2.139	1.066
Plates	B_4C	Natural	3.64	-2.608	1.079

[a]See Fig. IV.2 for details. Compositions are found in Tables VII.6 and VII.7.

[b]The total uncertainty in a measured value is 1%, but for purposes of comparing measurements, the uncorrelated part of the uncertainty is only about 0.1%.

[c]Exact geometries were not considered in the calculations so that the same calculation was used for the first three rods, a second calculation for the next five rods, and separate calculations for each of the last three rods. The calculations were done with diffusion theory in rz geometry with 28 energy groups. The control rod was modeled in two regions.

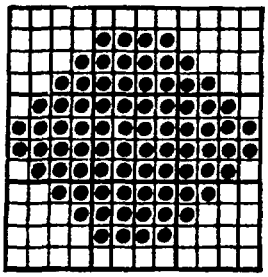

Hexagonal #1
80 Pin
Enriched B_4C

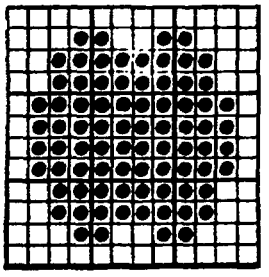

Secondary Design
80 Pin
Enriched B_4C

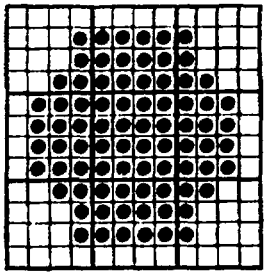

Hexagonal #2
80 Pin
Enriched and
Natural B_4C

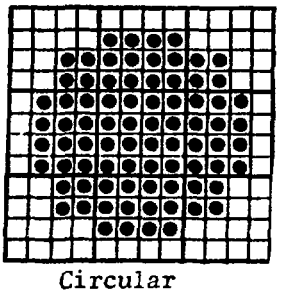

Circular
80 Pin
Enriched and
Natural B_4C

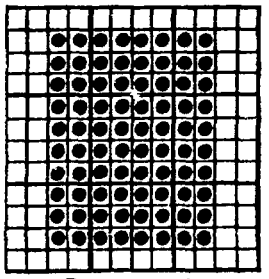

Rectangular
80 Pin
Enriched and
Natural B_4C

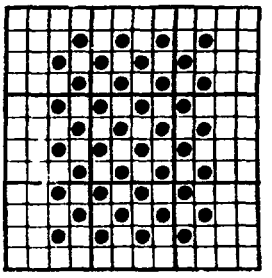

Rectangular
40 Pin
Enriched B_4C

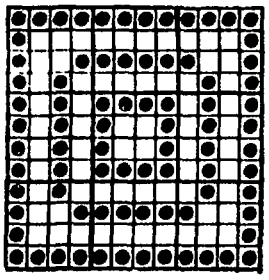

Square
80 Pin
Enriched B_4C

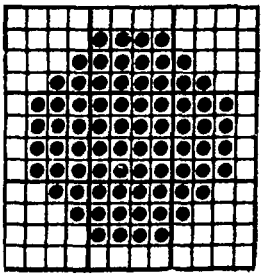

Octagonal
76 Ta Pins

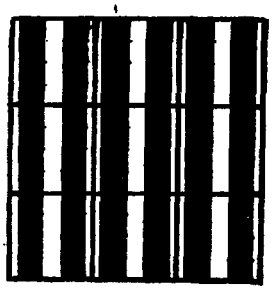

ZPPR-10 Rod Design
Alternating Plates
of Natural B_4C (Black)
and Na (White)

ABSORBER SURROUNDED BY Na

STEEL SURROUNDED BY Na

Fig. IV.3. Cross-sectional Views of Rod Designs Used in ZPPR-10A to Study Geometry and Enrichment Effects.

the one for the ZPPR-6 results is presented in Fig. IV.4. In both cases, the results fall on a smooth curve when the normalized worth is plotted against the ^{10}B mass per unit length of perimeter, which is consistent with 38 years of reactor physics experience.[6]

The worths of pin-type control rods were studied in ZPPR-11, the engineering mock-up critical assembly for the CRBRP. The pin rods were compared with the reference plate rods in characteristic inner and outer ring positions to test methods of calculating rod bunching factors which are applied to the power reactor rods. The rod designs are shown in Fig. IV.5. The rod which best approximated the CRBRP control rods in disposition of boron and steel contained 52 enriched boron carbide pins arranged in an octagonal pattern. The other rod designs were used to provide additional data for study of calculation methods. Measurements were made both in ZPPR-11B and in -11F. Both assemblies represented the CRBR BOC1 core, but they had significantly different radial power shapes. Analysis of the pin rod experiments followed methods that had been used in design calculations. The worths were first calculated using atomic densities averaged over the four matrix positions and then adjusted by bunching factors. The bunching factors were defined as the ratios of worths of the rods calculated in representative cross-sectional area to worths calculated with the absorber homogeneously spread across the subassembly. In the design method these were estimated from calculations in cylindrical geometry with the rods at the reactor center surrounded by a mixture of fuel and blanket materials. Because of discrepancies encountered in the analyses of the rods in ZPPR-11B, some special measurements were made within the central blanket zone of 11F to provide data in a configuration more amenable to calculational modeling. Rods containing 64 pins were also studied in ZPPR-11F. The pin-rod compositions are given in Table VII.8 of Appendix A.

A number of calculations of rod bunching factors were made. In cylindrical geometry these ranged from rz diffusion models with 28 groups to S_{16} transport models in r geometry with 9 groups and a fine mesh spacing. The bunching factors are given in Table IV.10. The reference 52-pin enriched-boron rod showed little sensitivity to the models, and the bunching factor varied by only 0.5%. However, the bunching factor for the 32-pin rod was lower by 2% when the calculations used transport rather than diffusion theory.

The measured rod worths and calculations are given in Table IV.11. Results for the plate-type rods are shown for comparison. The following trends are noted:

i. C/E results for the pin rods are significantly higher than for the reference plate rods.*

ii. The comparison of pin and plate rods is different between the inner and outer ring positions. In ZPPR-11B the standard rod (52-pin enriched) has higher C/Es by 6% in the inner ring, and by 3% in the outer ring. (It is interesting that the experimental ratios of

*Note that the ZPPR-11 control rod drawers were completely filled with B_4C plates rather them with alternate B_4C and sodium plates as in ZPPR-10.

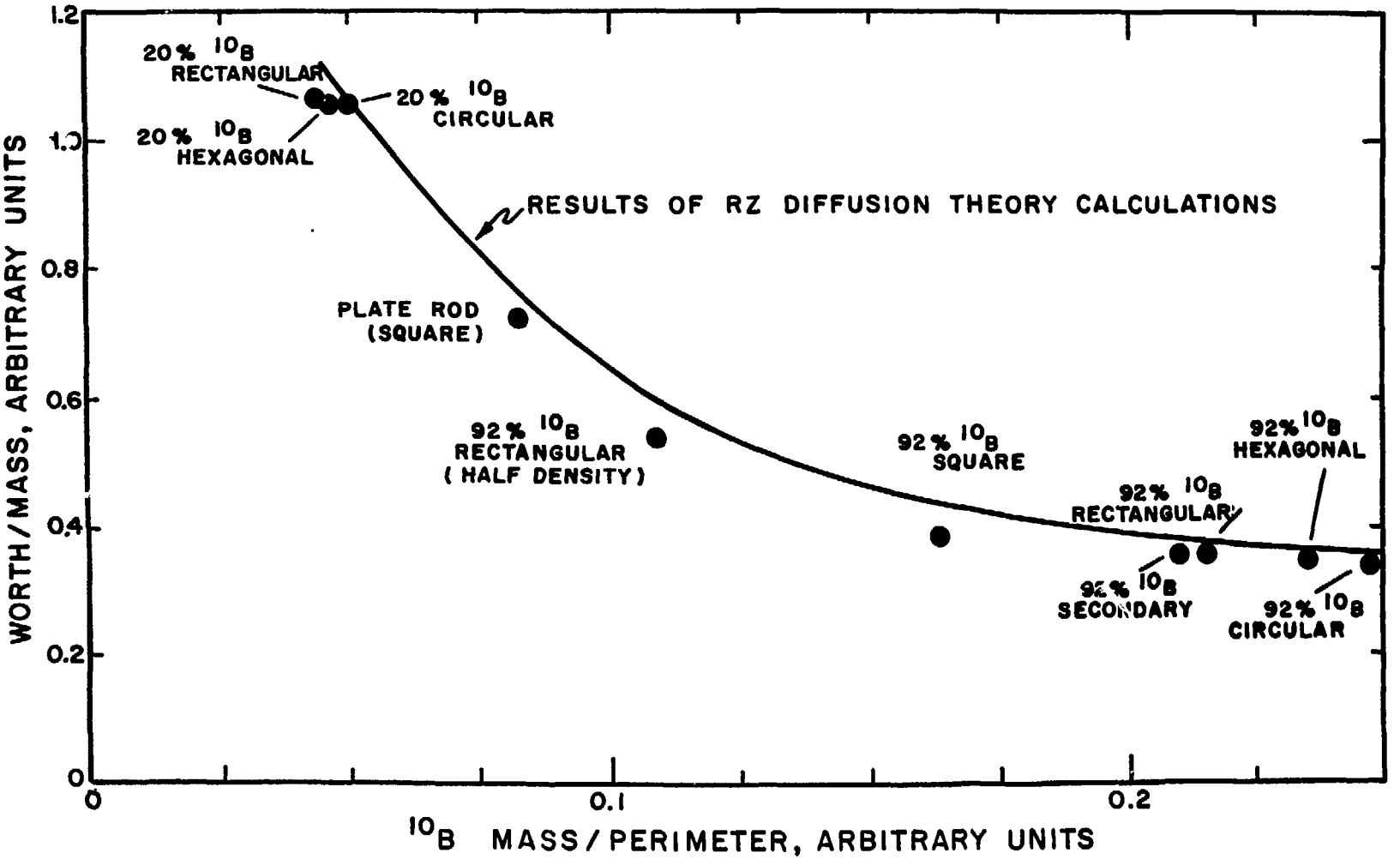

Fig. IV.4. Normalized Worth Curve for Central Control Rods in ZPPR-10.

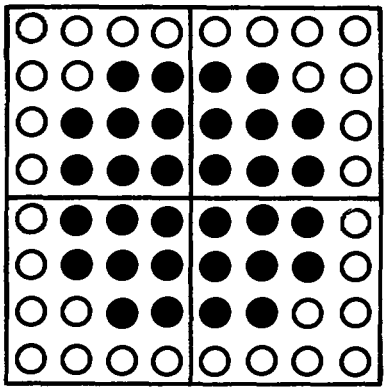

Bunched 32 pin Rod

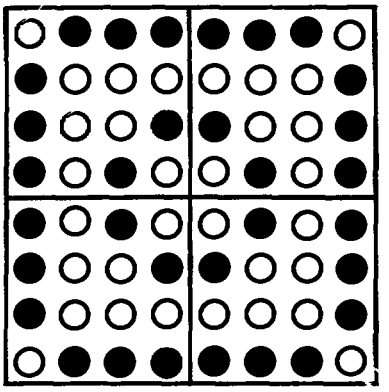

Spread 32 Pin Rod

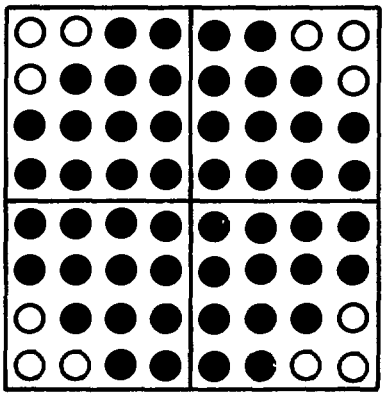

52 Pin Rod

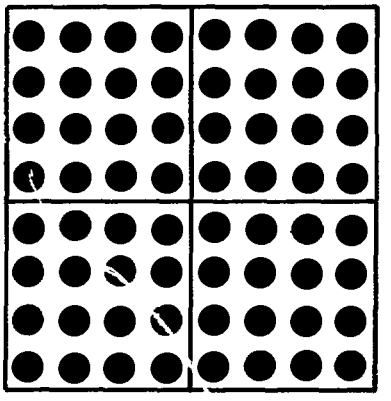

64 Pin Rod

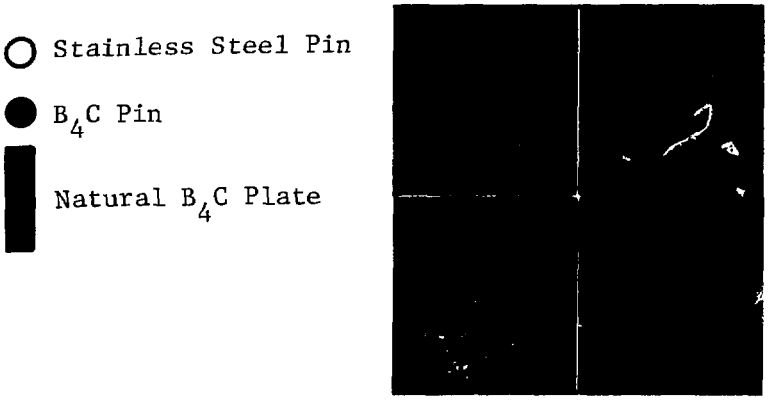

Fig. IV.5. ZPPR--11 Rod Designs for Geometry and Enrichment Studies.

TABLE IV.10. Calculated Bunching Factors for ZPPR-11 Pin Control Rods[a]

Model[b]	rz Mesh, mm	52 Pin Natural B_4C Rod	52 Pin Enriched B_4C Rod	32 Pin Enriched B_4C Rod
28G rz DT	53 x 23	0.983	0.969	0.913
9G rz DT	53 x 23	0.982	0.969	0.912
9G rz S_4	67 x 23	- -	0.963	- -
9G r DT	67	0.981	0.968	0.911
9G r S_4	67	0.977	0.963	0.893
9G r S_{16}	134	0.977	0.964	0.896

[a]Bunching factor is the worth of the control rod calculated with the two-region model divided by the worth calculated with the homogeneous model.

[b]28G = 28 groups, 9G = 9 groups, rz or r = geometry, DT = diffusion theory, Sn = transport theory.

TABLE IV.11. Pin-type Control Rod Worths in ZPPR-11B and -11F

Assembly	Rod	Position	Measured Worth, $[a]	Bunching Factor[b]	C/E[c]	C/E (PIN) / C/E (PLATE)
11B	Plate	6	1.096	---	0.892	---
		15	1.502	---	0.974	---
		16	1.746	---	1.004	---
11B	52-pin enriched B_4C	6	1.071	0.964	0.948	1.063
		15	1.518	0.964	0.999	1.026
		16	1.751	0.964	1.032	1.028
11B	52-pin natural B_4C	6	0.611	0.977	0.924	1.036
		15	0.896	0.977	0.982	1.008
		16	1.095	0.977	1.004	1.000
11B	32-pin enriched B_4C	6	0.834	0.896	0.950	1.065
		15	1.211	0.896	1.000	1.027
		16	1.446	0.896	1.012	1.008
11B	32-pin spread	6	0.935	1.000	0.945	1.059
		15	1.337	1.000	1.010	1.037
		16	1.572	1.000	1.039	1.035
11F	Plate	6	1.365	---	0.891	---
		16	1.693	---	0.985	---
11F	52-pin enriched B_4C	6	1.344	0.964	0.941	1.056
		16	1.678	0.964	1.019	1.035
11F	64-pin enriched B_4C	6	1.500	1.000	0.930	1.044
		16	1.836	1.000	1.015	1.030
11F	Plate	Central	1.039	---	0.853	---
	52-pin enriched B_4C	Central	1.010	0.959	0.906	1.062
	32-pin enriched B_4C	Central	0.767	0.880	0.905	1.061
	32-pin spread	Central	0.875	1.000	0.902	1.057
	64-pin enriched B_4C	Central	1.143	1.000	0.893	1.047
	64-pin natural B_4C	Central	0.649	1.000	0.895	1.049

[a]Relative uncertainties between the pin rods within a series are 0.2¢ to 0.3¢. Total uncertainties, including reactivity calibration, are about 1.1%. In 11B the plate and pin rods were measured in separate series so that the total uncertainties of 1.1% apply. In 11F they were measured in the same series, and the relative uncertainties should be used in the comparison.

[b]Bunching factors from the S_{16} transport calculation.

[c]Calculations used β_{eff} = 0.3324% for 11B and 0.3351% for 11F.

worths for the bunched and spread 32-pin designs also differ by 3% between these positions.) The same trend is obtained in ZPPR-11F, but with somewhat more consistent results between the inner and outer positions.

iii. The C/E values for the special measurements in the central blanket are similar to those for the inner ring position (CRP-6).

iv. C/E values for the enriched boron rods in 11B are 2% to 3% higher than for the natural boron rods. However, the two 64-pin rods at the center of 11F yielded consistent C/E results.

The different comparisons betwen pin and plate rods in the inner and outer rings may be due to the local environments and flux gradients. Additional studies of pin-rod bunching factors for ZPPR-11B were made in xy geometry. In these calculations, the control rods were modeled with 16 mesh points per drawer so that each mesh region represented 1/16th of a calandria containing a boron or steel pin. The two adjacent matrix positions contained four meshes, and one mesh per drawer was used over the remainder of the reactor. Diffusion theory calculations were made for control rod positions 6 and 16.

The bunching factors calculated in xy geometry are higher in the outer rod position than in the inner position and improve the consistency between pin and plate-rod results. The comparison with experiment is shown in Table IV.12. The bunching factors from xy diffusion calculations were adjusted by the ratio of transport to diffusion worths from the cylindrical models in Table IV.10. These results show some improvement, but a difference of 2% remains when comparing pin and plate rods in the inner and outer ring positions. It is possible that further improvement would be obtained by using fine mesh transport calculations in xy geometry.

Control rod experiments made in the PRE-RACINE program on Masurca[27] have been analyzed with ENDF/B-IV data. In the measurements, critical radii were determined for cores with central rods of natural B_4C with two cross section areas, and for rods with 47% and 90% enriched B_4C. The data were supplied to ANL in the form of equivalent homogeneous cylindrical models which were derived from the experimental dimensions by calculations with the CARNAVAL-IV set. The experimental and calculated core radius increments are compared in Table IV.13. As in the ZPPR-10 studies, little difference is found in the ability to calculate the enriched rods compared with the natural B_4C rods. The spread of results with CARNAVAL-IV data is somewhat greater.

C. Control Rod Homogenization

Power reactor calculations normally use hexagonal geometry with a mesh of six triangles per hexagon. The control rod fine structure cannot be modeled explicitly in the reactor calculations, and cross sections must be homogenized over the rod area. The principal effect to be taken into account (as shown, for example, in the ZPPR-10A pin measurements, Section IV.B) is the bunching of the absorber pins around the center of the subassembly. This typically reduces the worth by 5% to 15% compared with the normal ZPPR rods

TABLE IV.12. The Effect of Bunching Factors from xy Calculations on ZPPR-11B Pin Rod C/E's

Rod	CRP-6 Bunching[a] Factor	CRP-6 C/E	CRP-16 Bunching[a] Factor	CRP-16 C/E
52 pin enriched B_4C	0.957	0.941	0.973	1.042
52 pin natural B_4C	0.972	0.919	0.980	1.007
32 pin enriched B_4C	0.886	0.939	0.919	1.038
32 pin spread	1.000	0.945	1.000	1.039
Relative to plate rod:		C/E (PIN) ÷ C/E (PLATE)		
52 pin enriched B_4C		1.055		1.038
52 pin natural B_4C		1.030		1.003
32 pin enriched B_4C		1.053		1.034
32 pin spread		1.059		1.035

[a]The factors calculated by xy diffusion theory have been adjusted by transport/diffusion ratios of 0.996 for the 52-pin enriched and natural rods, and by 0.984 for the 32-pin bunched rod.

TABLE IV.13. Rod Size and Enrichment Variations in MASURCA

Rod	Cross-Section Area cm^2	Increase in Core Radius, cm: Experiment[a]	Increase in Core Radius, cm: Calculation	C/E: ENDF/IV	C/E: CARNAVAL[b]
Natural B_4C	112	8.56	8.93	1.043	1.06
Natural B_4C	98	7.87	8.20	1.042	1.06
47% enriched B_4C	98	10.47	10.89	1.040	1.09
90% enriched B_4C	98	11.74	12.09	1.030	1.10

[a]Experiment corrected to homogeneous core, the experimental critical radius for the reference.

[b]From Ref. 27.

in which the absorber is distributed more uniformly over the control rod region. The effect can be treated to an accuracy of a few percent by a simple two-region rod model in treated to an accuracy of a few percent by a simple two-region rod model in which the inner region contains boron, steel and sodium and the outer region contains the steel and sodium representing the structure and guide tube. Such a model was used, in cylindrical geometry, for the analysis of central rod worths in ZPPR-10A. A further refinement is to model the actual absorber pins. Calculations in Great Britain for the Monju mock-up rods[1/] in ZEBRA used collision probability methods and gave corrections of -1.5% for natural boron rods, and -3.0% for 80% enriched boron rods, compared with the cylindrical model.

Power reactor calculations commonly use simple volume-weighted cross sections for control rod channels. For rod worth estimates, the absorber bunching effect may be included in the bias factors that are applied to the design calculations. However, one reason for modifying the homogenization treatment is to improve calculations of reaction rates in the vicinity of the rods. Reaction rates around pin control rods were studied experimentally in the ZPPR-11 program.

Recently, Rowlands et al.[28] have reported results for different methods of homogenizing fast reactor control rods. The reference for the study was a two-region cylindrical rod surrounded by a fuel region, and was calculated in one-dimensional transport theory. Results were compared for three homogenization methods: volume averaging, flux averaging, and "perturbation theory equivalence." In the latter method, group dependent factors are applied to the flux averaged capture and moderation cross sections to preserve the group reactivity effect of capture plus moderation. The weighting involves the adjoint calculated for the homogenized model, and an iterative procedure is necessary. Table IV.14, taken from Ref. 28, compares differences between the reference transport solution and each of the three methods. In addition to the rod worth, results are given for the absorption in the control rod per fission in the fuel region, and for the dip in fission rate at the surface of the rod. The volume averaging method is in error by 13% for the worth--in agreement with experiments of bunched versus distributed pin rods in ZPPR-10A. Results for flux averaging show some improvement, but are inadequate, while the perturbation equivalence method yields an accurate prediction of the worth. The 4% error in predicting the dip in the fission rate by this latter method is nevertheless significant (note that this translates to a smaller error of only 0.4% in the total fission rate in this case).

The perturbation theory equivalence homogenization method was also applied to the analyses of natural and enriched boron control rods in the Monju mock-up program. The reference calculations for these rod worths used xy diffusion theory with flux averaging of the cross sections. These results, in agreement with others (e.g., Ref. 29), showed C/E's for enriched rods that were as much as 10% higher than those for the natural boron rods. These results, shown in Table IV.15, suggest that the method of homogenization is responsible for variation of C/E values with enrichment. This conclusion is consistent with the ZPPR-10A pin rod studies where a two-region model was used in the analysis and no significant C/E variation was observed.

TABLE IV.14. Percentage Errors Due to Different Control Rod Homogenization Methods[a]

Homogenization Method	Difference Relative to Reference Result, %		
	Rod Worth	Rod Absorptions	Fission Rate[b] Dip
Volume Averaging	12.8	12.3	21
Flux Averaging	4.0	3.6	10
Perturbation Theory Equivalence	-0.1	-0.5	3.7

[a]Data taken from Rowlands.[28] The reference calculation was a two-region cylindrical model using transport theory.

[b]The fission rate dip is the difference between fission rates at the surface of the rod and in the asymptotic region.

TABLE IV.15. Predictions of Boron Enrichment Effects for the Monju Mock-Up Rods

Rod Type	C/E[a]	
	Flux-Averaging Method	Perturbation-Equivalance Method
Natural boron	1.04	0.98
30% enriched boron	1.07	0.99
80% enriched boron	1.14	1.02
90% enriched boron	1.13	1.00
Tantalum	1.10	1.04

[a]The reference method used xy diffusion theory and flux-averaging homogenization. The perturbation-equivalance values were obtained from these by correction factors calculated from "supercell model". These results are taken from Ref. 28.

D. Alternative Control Materials

Tantalum and europium oxide have been investigated as alternatives to B_4C for use in control rods at ZPPR. These studies have been limited to a few measurements, partly because of insufficient materials and partly because of lack of strong interest. There was a sizable study during the FFTF program on ZPR-9[30], but those data are not included in the base that was chosen for this report. Results from ZPPR-3/1B are contained in Appendix VII.B, since no calculations were available.

Results from two assemblies, ZPPR-9 and ZPPR-10A, are reported here. In ZPPR-9, plate rods of tantalum and Eu_2O_3 were inserted in a 2x2 matrix position at the core center and compared with the worth of a B_4C rod in the same position. The results in Table IV.16 show that both rods were worth less than the B_4C rod, although no attempt was made to preserve either representative or constant volume fractions. The C/E results are presented for general interest, but the cross section treatment for the resonance absorbers* may not provide adequate self shielding for the tantalum and europia rods. In ZPPR-10A, a rod composed of tantalum pins was included in the pin-rod study. The results in Table IV.16 compare its worth to that of an enriched B_4C rod with about the same geometry. The design of both rods is shown in Fig. IV.2. A natural B_4C pin rod of the equivalent geometry had a worth of -1.65$, compared to the -2.14$ tantalum rod and 2.69$ for the enriched B_4C rod.

To date the worth measurements of alternative control materials have not turned up any major surprises. The paucity of data reflects the historical level of interest in these materials. Calculational experience with ZPPR results is not sufficient to warrant any hard conclusions. For assemblies with typical LMFBR spectra, the enriched B_4C rods clearly have an advantage in worth per unit volume.

E. Neutron Streaming in Sodium/Steel Control Rod Positions

As in LMFBRs, control positions in the ZPPR critical assemblies consist of sodium and stainless steel. These diluent channels cause complications in reactor analysis. The first difficulty results from axial neutron streaming along the channels, and is serious because it is not well-treated in the reference-method calculations. A second problem, which results partially from the streaming effect, is that the worth of diluents relative to fuel is not well predicted. The latter results in a discrepancy between k_{eff} calculations of critical configurations with and without CRPs (e.g., 7A vs. 7B and 9 vs. 10A).

The effect of replacing core material with CRPs was investigated in ZPPR-9. CRPs were substituted for fuel in several radial positions; three different sizes were used at the central position. From one to six CRPs were put in for individual measurements. Results of these measurements and the accompanying calculations are presented in Table IV.17. The substitution worths were typically overpredicted by more than 20%. The two lower values were in the outer-core positions where the fuel enrichments were higher and

*Actually generated for small perturbation samples.

TABLE IV.16. Results of Alternate Material Control Worth Studies in ZPPR

ZPPR Assembly[a]	Principal Absorber	Absorber Mass, kg	Worth[e], $	C/E[f]
9	^{10}B[b]	3.17	1.89	1.033
9	Eu[c]	21.09	1.16	1.074
9	Ta	174.12	1.41	1.063
10A	^{10}B[d]	7.82	2.69	1.052
10A	Ta	82.50	2.14	1.096

[a]All measurements in central position. ZPPR-9 had 2x2 (4 drawer) CRP-1 for these measurements. See Figs. VII.25 and IV.2 for descriptions of rods. Compositions are found in Tables VII.5 and VII.6.

[b]Natural B_4C, included for comparison.

[c]In the form of Eu_2O_3.

[d]92%-enriched B_4C in a similar pin geometry to that of the Ta pins, included for comparison.

[e]Relative uncertainties within an assembly about 0.3%.

[f]9-group, diffusion theory calculations, xy geometry for ZPPR-9 and rz for ZPPR-10A. C/E's corrected for the CRP worth bias in ZPPR-9. (See Section IV.E.)

TABLE IV.17. Results of Diluent/Fuels Interchange Reactivity Measurements in ZPPR-9

CRPs Replacing Fuel, Positions[a]	Interchange Worth, $	C/E[b]
1	-0.557 ± 0.006	1.205
1 (2x3)[c]	-0.390 ± 0.006	1.200
1 (2x2)[d]	-0.267 ± 0.005	1.198
1 (stainless steel)[e]	-0.777 ± 0.010	1.226
10	-0.367 ± 0.006	1.252
13	-0.358 ± 0.006	1.284
A,B	-1.054 ± 0.012	1.235
4,7	-1.007 ± 0.012	1.249
C,D	-0.901 ± 0.011	1.248
13,19	-0.755 ± 0.009	1.287
E,F[f]	-1.121 ± 0.014	1.174
G,H[f]	-0.833 ± 0.014	1.157
2-7	-3.07 ± 0.03	1.234
9,11,13,15,17,19	-2.73 ± 0.03	1.270
		$\overline{C/E}$ = 1.230 ± 0.039

[a]Refer to Fig. VII.11 for position identification.

[b]9-group, diffusion theory calculations in xy geometry with 1 mesh space per drawer. β_{eff} = 0.3436% Δk.

[c]6 matrix positions rather than 9.

[d]4 matrix positions rather than 9.

[e]Type 304 stainless steel rather than sodium.

[f]Outer core fuel replaced--higher enrichment than in previous substitutions.

radial streaming effects may be more important. A limited number of similar measurements was made in ZPPR-7B, -7C, and -8F. Results and reference-method calculations of these measurements are shown in Table IV.18. Measurements were also made in ZPPR-11, but they have not been calculated.

Diffusion theory calculations are known to mispredict leakage in sodium-filled control rod positions. As described in Section III.A, the reference calculational method for control rod worths uses diffusion theory in xy geometry with zone- and group-dependent buckling treatment for axial leakage. The bucklings are generated from an rz model with a central CRP. Diffusion theory errors therefore are carried over from the rz to the xy model in the axial bucklings. Corrections for diffusion theory mispredictions of CRP worth have been applied to calculations of control rod worths in several cores. Representative results were presented in Section III.C, while some additional results are described below.

Calculations were made for a central CRP in ZPPR-4/1 using transport (S_4) and diffusion theory in rz geometry. The transport result for the worth of the CRP relative to fuel, -0.32% Δk, was 10% less than the diffusion theory result. This discrepancy is consistent with studies of the Monju CRPs made in ZEBRA.[16] Comparisons of results using other calculational models indicate that about 70% of this CRP transport correction is due to the axial dimension. Therefore, transport calculations of rod worths in xy geometry, as applied in Section III.C, will account for only about 30% of the total correction.

In ZPPR-4/1, the worths of four central rods were compared with B_4C loadings varying from 4.6 kg to 15.8 kg with reactivity worths from -2.3$ to -4.8$. As seen in Table III.6, the reference calculational method gives higher C/E values for the larger rod worths. On the other hand, the CRP transport correction is independent of the control rod inserted, and thus gives a higher percentage correction to the rods with lower worth. The corrected calculations (Table IV.19) yield C/E values that are exceptionally consistent and no bias with increasing B_4C mass is apparent. However, other approximations in the calculations vary with rod worth, and could reduce the C/E consistency shown here. Corrections have been derived for two approximations. For the N and M rods, transport corrections have been calculated to be -5.5% and -6.6%, respectively. For these same rods, heterogeneity corrections are estimated to be -1.5% and -0.1%, due to the plate structure of the rods. These latter corrections were obtained by one-dimensional transport calculations. Other approximations may vary by up to 1% among the different rods. Corrections for the type N rod at the center of ZPPR-4/1 are summarized in Table III.25.

Transport corrections for control rod positions have been applied to the worths of rod groups in ZPPR-7G. The reference calculations gave C/E values that were systematically somewhat higher for rod patterns with strong positive interactions. Such interactions increase the average worth per rod, and therefore reduce the percentage correction for CRP transport effects. For off-center rod positions, it is difficult to derive an accurate correction, since the rz model is not directly applicable. However, for the heterogeneous core, the radial power distributions were relatively flat. Thus, it was assumed that the correction of +0.03% Δk per CRP, derived for ZPPR-4/1, would

TABLE IV.18. Results of CRP/Fuel Interchange Reactivity Measurements in ZPPR-7 and 8

ZPPR Assembly	No. of CRPs Added	Positions	Interchange Worth, $	C/E[a]
7B	6	Outer Ring Flats	-5.44 ± 0.14	1.10 ± 0.03
7C	6	Outer Ring Flats	-4.70 ± 0.12	1.19 ± 0.03
8F[b]	1	Adj. to CR-16[c]	-0.78 ± 0.17	1.36 ± 0.29
8F	3	Adj. to CR-8,12,16	-2.04 ± 0.20	1.19 ± 0.11
8F	6	Adj. to CR-8, 10, 12,14,16,18	-5.28 ± 0.28	0.99 ± 0.05

[a]9-group, diffusion theory calculations in xy geometry with 4 mesh spaces per drawer. β_{eff} = 0.3380% Δk (7B), 0.3384% Δk (7C), and 0.3324% Δk (8F).

[b]All measurements in ZPPR-8F relative to six outer ring corner rods inserted to make reference configuration 17.68$ subcritical.

[c]In ZPPR-8F, the positions of the added CRPs are just outside and adjacent to the indicated control rod positions.

TABLE IV.19. The Effect of CRP Reactivity Corrections on Central Control Rod Worth Calculations in ZPPR-4/1

Rod Type[a]	B_4C, Mass, kg	Worth[b], $	Reference Calculation[b], C/E	CRP Transport Correction, %	Adjusted C/E
A	4.58	-2.32 ± 0.02	1.098	+3.8	1.139
N	8.67	-3.53 ± 0.05	1.106	+2.5	1.134
I	13.10	-4.39 ± 0.11	1.116	+2.0	1.138
M	15.80	-4.82 ± 0.10	1.121	+1.8	1.141

[a]Refer to Figs. VII.18, VII.19, and VII.9 and Tables VII.1 and VII.2.

[b]Refer to Table III.6.

be applicable for all CRPs in 7G. The correction ot k_{eff} for the reference core with 15 CRPs was thus 0.45% Δk*. Corrections for different rod patterns vary with the number of rods, and the percentage corrections vary with the average rod worth and hence with the interaction effect.

C/E results for the outer ring corner rods in ZPPR-7G are given in Table IV.20. The CRP transport corrections are smallest where the average rod worth is the highest, i.e., for high positive interactions. The standard deviation of the C/E distributions was reduced from 1.3% to 0.8% by application of the CRP corrections. Several other approximations in the calculation model may lead to different corrections for the worths of these rod banks, resulting in a different C/E spread. For example, the equivalent rod banks in ZPPR-11B, calculated with a coarse-mesh model, have an initial standards deviation of only 0.8%. It appears that corrections for CRP streaming would make the spread of C/E's larger.

Misprediction of CRP reactivity had the largest effect on calculated control rod worths in ZPPR-9, the core with no positions in the reference configurations. In order to obtain the rod worths relative to CRPs, core material had to be replaced by CRPs and then by control rods. The calculations were done in a similar manner, determining the worth of CRPs as well as CRs perturbing the reference configuration. The difference between the two results was then the calculated worth of the CRs relative to the CRPs. But, as was shown in Table IV.17, the worths of the CRPs were overpredicted by 20-30%. Since the worth of the CRPs was about 25% of the worth of control rods (both relative to the reference fuel configuration), a 6% error was introduced into the calculated worth of the rods relative to CRPs. In ZPPR-10A, a core of the same size that was critical with 19 CRPs in the reference configuration, the corrections for neutron streaming in the CRPs were only about 1% (see Table III.27). Therefore, the relative C/E's for ZPPR-9 and -10A control rod worths should differ by about 5%. From Tables III.17 and III.18, it can be seen that the range of differences between C/E's for comparable rod patterns in ZPPR-9 and -10A was actually 3-7%.

Since some corrections for the diffusion theory mispredictions in ZPPR-9 could be derived from the experiments, they were applied in Table III.17 to the extent possible. The corrected results show improved agreement with the ZPPR-10A results. Ratios of ZPPR-9 to ZPPR-10A C/E's for the central rod, the inner ring, and the outer ring of rods were 1.033/1.019, 1.014/1.035, and 1.050/1.048, respectively.

The magnitude of the errors introduced by mispredictions of neutron streaming in CRPs is such that some practical means should be developed for proper accounting of the streaming effect in the reference calculations. In the current circumstances, it is essential that the CRPs be present in the reference engineering mockup critical configurations if they are to be used to help bias design calculations. Reaction rate distributions, criticality, and control rod worths will all be affected.

*The correction, based on the ZPPR-4 calculations, is 10% of the CRP worth (0.1 x 0.3% Δk = 0.03% Δk) times the number of CRPs without rods inserted (from 9 to 15 in this 7G example).

TABLE IV.20. ZPPR-7G Outer Ring Corner Control Rod Worth Calculations with CRP Streaming Corrections

Rod Group[a]	Av. Worth per Rod, $	Reference Diffusion Calculated C/E	CRP Transport Correction, %	Adjusted C/E
8,10,12	1.57	1.053	+4.9	1.105
12	1.59	1.062	+4.7	1.112
14	1.59	1.062	+4.7	1.112
8,10	1.61	1.060	+4.7	1.110
8,10,12,14	1.73	1.066	+4.4	1.113
10	1.96	1.088	+3.6	1.127
16	2.03	1.071	+3.4	1.107
8,10,12,14,18	2.08	1.068	+3.6	1.106
10 (enriched rod)	2.16	1.094	+3.1	1.128
10,12,16	2.42	1.077	+2.9	1.108
10,16	2.70	1.082	+2.4	1.109
8,10,12,14,16,18	2.85	1.091	+2.5	1.118
Mean		1.073 ± 0.013		1.113 ± 0.008

[a]Refer to Table III.14.

F. Critical Configurations with Inserted Control Rods

An alternative way to measure control worths is to add fuel to the configuration with inserted rods until it is returned to critical. The fuel can be added at the reactor boundary or distributed throughout the assembly, effectively changing the enrichment. Several assemblies have been built at ZPPR that had critical configurations with and without control rods inserted, although the intent was not to measure rod worths.

Table IV.21 is a summary of the k_{eff} C/E's for 21 ZPPR assemblies that were critical with different numbers of CRPs and control rods. Unfortunately, the reference calculations were not consistent, so that only a few comparisons can be made. The best comparisons are among calculations that were corrected as much as possible for modeling approximations. Some assemblies show essentially no discrepancy between k_{eff} calculated with and without control rods present. The sources of the discrepancies that are present are speculative at this time. Among other things, they include different calculational biases for fuel, CRPs, and rod worths, and neglect of boundary effects between drawer types in cross section preparation.

In the conversion from ZPPR-10A to ZPPR-10B, the step-by-step reactivity was measured as the control rods and additional fuel was loaded. In Table IV.22, the measured and calculated worth of each fuel addition step are compared. The average C/E for fuel addition was 1.11, whereas the C/E for the seven control rods was 1.05 using the same calculational method. Effectively, these measurements are a means of comparing measured and calculated k_{eff} for the system at several levels of subcriticality. The C/E for k_{eff} increased from 0.982 to 0.986 as fuel is added.

TABLE IV.21. Preliminary Comparisons of k_{eff} Calculations for ZPPR Assemblies Which were Critical with Different Control Rod Characteristics

ZPPR Assembly	Characteristic	Experimental k_{eff} Corrected to 293K	Reference Calculation k_{eff}	Corrected Calculation[f]
4/1	19 CRPs	1.0009	0.9823[i]	0.9823
4/2	7 CRs	1.0008	0.9827[e]	
4/4	19 CRPs Pu in RB	1.0010	0.9840[d]	
4/3	7 CRs Pu in RB	1.0010	0.9842[d]	
5A	19 CRPs	1.0011	0.9801[c]	
5B	7 CRs	1.0009	0.9840[c]	
6 CEOC	19 CRPs	1.0015	0.9842[e]	
6 EEOC[g]	7 CRs one-third in.	1.0017	0.9854[e]	
6 EBOC[h]	7 CRs two-third in.	1.0010	0.9853[e]	
6 CBOC	7 CRs	1.0015	0.9870[e]	
7A	No CRPs and CRs	1.0005	0.9801[i]	0.9822
7B	12 CRPs	1.0008	0.9808[i]	0.9837
7C	12 CRPs, Pu in IBs	1.0016	0.9864[i]	0.9851
7G	15 CRPs	1.0008	0.9808[a]	
7H	6 CRs half in.	1.0012	0.9849[b]	
9	No CRPs or CRs	1.0011	0.9827[c]	0.9842
10A	19 CRPs	1.0010	0.9800[c]	0.9856
10B	7 CRs	1.0004	0.9826[c]	0.9867
10D	31 CRPs	1.0005	0.9783[c]	0.9831
10D/1	1 CR	1.0003	0.9801[c]	0.9852
10D/2	6 CRs	1.0007	0.9809[c]	0.9852
11A	6 CRs half in.	1.0011	0.9784[b]	
11B	15 CRPs	1.007	0.9764[b]	
11C	15 CRPs, Pu in blkts.	1.006	0.9787[b]	
11D	6 CRs one-third in Pu in blkts.	1.0013	0.9813[b]	

[a]28 group, diffusion theory, xy geometry with 1 mesh per drawer.

[b]9 group, diffusion theory, xyz geometry with 1 mesh per drawer in xy plane.

[c]Same as (b) but with 28 groups and modified to account for plate streaming.

[d]Same as (a) but with 9 groups and 4 meshes per drawer.

[e]GE calculations, otherwise same as (b).

[f]Corrected for some modeling approximations, but not consistently.

[g]Expected end of cycle.

[h]Expected beginning of cycle.

[i]28 group, diffusion theory, xy geometry with 4 mesh spaces per drawer.

TABLE IV.22. Worth of Fuel in the ZPPR-10B Approach to Critical

No. of Spikes Added	Worth per Spike[a], $ Measured	Calculated[b]	C/E
64	0.0815	0.0901	1.106
68	0.0833	0.0924	1.110
32	0.0767	0.0863	1.125
16	0.0794	0.0873	1.099
16	0.0785	0.0883	1.124
4	0.0555	0.0656	1.182
200		$\overline{C/E}$ = 1.113 ± 0.002	

[a]One column of fuel (~70% U, 28% Pu, 2% Mo) replacing one column of U_3O_8. Fissile Pu mass = 1.1 kg.

[b]9-group, diffusion theory calculations in xy geometry with one mesh space per drawer.

The significance of these measurements is that in reactor design, control rod worth is balanced against fuel worth. In that sense, the k_{eff} comparisons may be more useful than the static measurements of rod worth alone. However, the full interpretation of the fuel-addition experiments requires considerable additional effort, and will require inclusion and analysis of experiments that are beyond the range of this document.

One approach to making consistent comparisons among C/E's for different assemblies is to use bias factors to adjust k_{eff} for differences in CRPs, CRs, and core enrichment. The bias factors for each effect must be developed from separate experiments that are calculated with consistent methods. For example, CRP worth has been biased from Table IV.17, CR worth from Table III.18, and fuel enrichment from Table IV.22. Applying these biases to the calculated k_{eff}'s of ZPPR-9, -10A, and -10B yields substantial improvement C/E consistency, as shown in Table IV.23. The maximum difference of 0.4% was reduced to 0.13%. There is good agreement between the adjusted C/E's for ZPPR-9 and -10A, with the original discrepancy being reduced by an order of magnitude. The ZPPR-10B value is not in such good agreement. However, the adjustment for CRP reactivity used here is fairly uncertain, primarily due to CRP interaction with the inserted control rods.

G. Axial Worth Profiles

One of the parameters of interest in LMFBR design is the change in worth of rods as a function of position relative to the reactor core. These axial worth profiles together with rod drive speeds provide reactivity insertion rates that are used in automatic control system design and in analysis of some accident scenarios.

TABLE IV.23. Comparisons of k_{eff} C/E's for ZPPR-9, -10A, and -10B

	ZPPR-9	ZPPR-10A	ZPPR-10B
Reference C/E for k_{eff}[a]	0.9863	0.9826	0.9866
CRP bias[b]	---	+0.0073	+0.0042
Pu bias[c]	---	-0.0032	-0.0080
CR bias[d]	---	---	+0.0026
Adjusted C/E	0.9863	0.9867	0.9854

[a]9-group, xy, single-mesh diffusion calculation. Experimental k_{eff} on the order of 0.999 for all assemblies.

[b]Developed from CRP reactivity experiments and calculations in ZPPR-9.

[c]Developed from measurements and calculations of fuel spike worth in the ZPPR-10A to -10B conversion.

[d]Developed from a ZPPR-10A measurement and calculation.

Limited measurements of axial worth profiles have been obtained in some ZPPR assemblies. Generally these have agreed with integrated small ^{10}B-sample worth traverses and with calibrated curves for the ZPPR operational rods*. Results for partially-inserted rod banks and complete axial profiles for single CR drawers (1/4 of total CR) are available from the ZPPR-6 program. No ANL calculations are available for comparisons.

Measured results from ZPPR-6 are presented in Fig. IV.5. The normalized bank worths are consistent with the full axial profile. The axial profile that was measured relative to a bank of seven rods two-thirds inserted in the critical EBOC** configuration differed slightly from the profile in the CBOC** core. The difference is consistent with redistribution of the flux towards the bottom of the core.

More extensive measurements were made in the ZPPR-11 EMC program for the heterogeneous core. They included the worth of an entire single control rod withdrawn in steps relative to a bank of six rods in the expected beginning-of-cycle core (11A), a six-point measurement of the whole-bank worth in the clean beginning-of-cycle core (11B), and a complete axial worth profile for a single CR drawer. The data were expected to be of interest because of the large interaction effect (60%) for the operating rod bank.

Results from analysis of the single rod and the rod bank measurements are given in Tables IV.24 and IV.25, respectively. When calculated in xyz geometry, the relative rod worth as a function of axial insertion is predicted to within about 2%. Thus, the large rod interaction effects do not seem to have a significant impact on the accuracy of predicting the axial worth profile.

TABLE IV.24. Measured Axial Worth Profile for CR-10 in ZPPR-11A

Position Relative to Parked Position, in.	Measured Worth[a],$	C/E[b]
0	0	---
2	-0.11	1.000
6	-0.56	0.982
12	-1.59	0.996
18	-2.81	0.992
24	-3.78	0.991
36	-4.50	0.989

[a]Relative to the other 5 outer ring corner rods (5R7C) fully inserted and all other rods parked at top of core; uncertainties on the order of 2%.

[b]9-group, diffusion theory calculations in xyz geometry with one mesh space per ZPPR drawer; β_{eff} = 0.0033385.

TABLE IV. 25. Measured and Calculated Axial Worth Profile for the 6R7C Control Rod Bank in ZPPR-11B

Position Relative to Parked Position, in.	Measured Worth[a],$	C/E[b]
0	0	---
3	0.50	0.930
6	1.36	0.998
12	4.12	0.997
18	7.94	1.004
24	11.98	0.998
36	15.81	0.994

[a]The six outer-ring, corner-position control rods were moved as a bank of rods; the other nine control rods remained parked at the top of the core; uncertainties on the order of 2%.

[b]9-group diffusion theory in xyz geometry with 1 mesh space per ZPPR drawer; β_{eff} = 0.003324.

V. CONCLUSIONS AND RECOMMENDATIONS

For LMFBR designs that are studied in critical experiments, there is a high probability that the estimated accuracy of biased control rod worth predictions will meet any reasonable design criteria. While significant progress has been made in calculational capability, application of current methods without supporting integral experiments is unlikely to result in acceptably of small design uncertainties. Rod worth measurements in plutonium-fueled critical assemblies have been eliminated as a major source of design uncertainty. This situation is the result of accomplishments over the last ten years.

The significance of these accomplishments is put into perspective by re-examination of Avery's summary of the status of fast reactor physics in 1972.[1] Concerning control rods, he said,

> "Although there is some data available from previous critical experiments, the data are generally fragmentary. Appropriate experimental and calculational tools have not been validated."

Updating the status of fast reactor physics at the 1980 meeting on Advances in Reactor Physics and Shielding in Sun Valley, LeSage[21] remarked on the magnitude of the improved situation.

> "Since then, literally hundreds of control rod worth measurements have been included in the ZPPR programs. Calculational methods for application to reactor design have been validated through analysis of the experiments. For designs that have been studied in the ZPPR experiments, uncertainties in control worth C/Es have been reduced to less than 5%. The component of these uncertainties due to current measurements is only about 2%."

Based on this progress, recommendations for analysis and application of critical experiments can be made with reasonable confidence. The recommended measurement technique for control rod worths in critical assemblies was discussed in Section II.B. Recommendations for critical experiment analysis, design calculations, and bias factors generation are discussed below.

A. Recommended Methods and Models

Adequate reactor modeling for calculation of control worths is somewhat dependent on the application. Reference methods (two-dimensional, few group diffusion theory) were shown to do a credible job for a wide range of experiments. However, corrections for several approximations (mesh, transport, neutron streaming, etc.) were shown to be larger than the experimental uncertainties. In general, it should be adequate to rely on the reference methods, with corrections calculated for a few key cases. A discussion of the issues to be considered in selection of methods and models is contained below.

1. Critical Experiment Analysis

There are three main tasks in analyzing control rod worth experiments in critical assemblies. They are:

i. Production of ratios that are needed in reducing the experimental data, i.e. detector efficiency ratios ($\varepsilon_2/\varepsilon_1$) and effective source worth ratios (S_2/S_1).

ii. Rod worth calculations that are homologous with power reactor design methods, yet take into account any special features of the critical facility. These methods are used to generate the basic results and design bias factors.

iii. Application of calculated corrections for approximations in the reference method. These calculations are done with more powerful methods, with each correction assumed to be independent of the others (usually). Application of these corrections is necessary to gain a deeper understanding of the results, to assure the reliability of bias factors, and ultimately to test the basic nuclear data libraries.

In order to facilitate the generation of bias factors, the reference analysis method should follow as closely as possible the method used for power reactor calculations. If differences are required, additional method biases may be necessary for the design calculations. For example, consistency has been achieved in the CRBRP program by the design organization (W-ARD) applying their methods and codes to both the ZPPR experiments and the CRBRP design. An additional factor, also verified in ZPPR experiments, is applied to account for the rod bunching effect.

Unique features of the EMC assembly must be included in the ZPPR model in order to avoid introducing an error in the LMFBR design through application of the bias factor. This implies adequate treatment of plate-cell heterogeneity in cross section processing, considerations of directional neutron streaming because of aligned sodium plates, and perturbations due to ZPPR operational rods when they are present.

At ANL, the reference (or design-equivalent) method is used for both the experimental support calculations and the rod worth calculations. As described in Section III.A, the method incorporates the following characterisitcs:

i. diffusion theory
ii. few energy groups
iii. coarse mesh spacing
iv. xy geometry
v. cross sections generated in asymptotic spectra
vi. group collapse in rz geometry
vii. bucklings from single rod and CRP in rz geometry
viii. no special treatment for heterogeneity of the plate-type rods.

With this method, quite consistent results are obtained for a wide range of cases. For example, the dispersion in the average results among all homogeneous cores was only 1.3% when corrections were applied for mesh inconsistency. Nevertheless, some caution is in order. Typical C/E values from heterogeneous cores were several percent lower than average values for homogeneous cores. Furthermore, there was a strong dependence of C/E values

on radial position for both large homogeneous cores and for 350 MWe size heterogeneous cores. Detailed statistical analyses and variations in C/E distributions and in bias factors are discussed further in Appendix VII.C

Since it is known that the many approximations in the reference method introduce errors of several percent, it is important to assess the magnitude of these errors for several special cases. Such cases should include banks of rods that are designed to operate as a group and a representative rod group from each control ring. These cases cover the most important design values as well as the spatial dependence of the modeling corrections.

The two largest corrections for calculated rod worths are usually for mesh spacing and transport effects. However, these are compensating corrections when mesh-centered finite difference codes are used. The coarse mesh that describes ZPPR geometry is the area of one matrix tube (about 55 x 55 mm). Since transport corrections should be generated with a finer mesh spacing, four mesh spaces per matrix position have been used for the S_n calculations in xy geometry. Diffusion theory calculations are run with the same mesh spacing for comparison and to generate the mesh correction. The extent that the mesh and transport effects compensate depends on the rod location and the general characteristics of the core. Several examples calculated with S_4 angular quadrature were presented in Section III.C. Some additional studies have shown that extrapolation to finer mesh spacing and higher angular quadrature change the correction by less than 1% for at least a few cases of interest.

Corrections for group condensation and buckling approximation may be estimated for central rods in rz geometry. However, a better approach is to compare xyz calculations with the reference method. This also takes into account the approximation inherent in applying cross sections and bucklings for a single central rod to off-center rod banks.

Producing reasonable corrections for neutron streaming in CRPs is more difficult. Studies of this effect have been emphasized more overseas than in the U.S. program. If the CRP compositions are representative of the power reactor, the errors should be carried over properly in the bias factors. The effects appear not only in the reactivity difference due to replacing the CRP by a CR, but also in the flux distributions. The latter can result in different C/E ratios for inner and outer ring rod worths. Comparisons with experiment indicate that S_4 transport calculations are adequate for handling the streaming effect in a central CRP, so that such calculations can provide an additional basis for validating methods of deriving effective diffusion coefficients and bucklings.

Small corrections for rod heterogeneity may be required to account for the plate structure of the control rods in the critical experiments. Such corrections would require either two-dimensional transport calculations with a fine mesh and angular quadrature to represent the plate structure, or implementation of two-dimensional collision probability codes. However, for many experiments (e.g., ZPPR-7 and ZPPR-9), rods constructed of fully packed drawers of B_4C have been used. The composition of these rods is

reasonably homogeneous. When C/E results for these rods and the half-sodium, half-B_4C rods in ZPPR-10 were compared, effects of less than 2% were indicated by C/E differences.

Directional diffusion coefficients may be used to correct flux distributions for the effect of neutron streaming in the sodium plates of critical assemblies. These flux corrections in turn modify the rod worths. Directional diffusion coefficients generated by the Benoist method routinely have been applied to studies of reaction rate distributions and sodium-void reactivities. For control rod worths, calculated corrections for this effect are no larger than 3%. The recommendation for future ZPPR analysis is to include directional diffusion coefficients in the reference method.

Application of modeling corrections does not completely resolve all C/E discrepancies. When different assemblies are considered, residual discrepancies of greater than 10% are noted. For C/E results from the same assembly, spatial discrepancies of up to 6% are observed in some cases, whereas in other cases no spatial discrepancy exists. Corrected C/E values do not scatter about 1.0 but rather tend to average about 1.1. Although considerable speculation exists as to the source of this systematic discrepancy between calculations and experiments, no conclusive explanation has been put forth. In the U.S. program, the corrections are too sparse and too inconsistent for hard conclusions to be warranted.

2. Reactor Design Analysis

The reference method for analysis of the critical experiments closely resembles current design practices. In fact, the methods for critical experimental analysis should closely correlate with design methods in order to facilitate bias-factor generation. There are several differences between the methods:

i. Hex-planar geometry is generally used in design methods; xy geometry is used in critical experiment analysis.

ii. The design calculations have to account for the reduced area that the absorber actually occupies (as described in Section IV.C.).

iii. Cell heterogeneity treatment is considerably different in the power reactor (pin geometry) relative to the critical experiment (plate geometry).

iv. Design calculations use hot-temperature cross sections instead of the room-temperature cross sections used for the critical experiments.

As reactor design nears completion, it is important to apply calculational methods for which bias factors can be easily produced. In general this means maximizing the correlation between critical experiment analysis and design analysis. This close correlation allows systematic errors from modeling and cross-sections to be biased out of the design calculations.

As with the critical experiments, it is useful to make corrections for modeling approximations in a limited number of cases. Corrections from the critical experiment calculations do not carry over directly to the design calculations because of the different sensitivities of the two models. For example, the extrapolation to infinitesimal mesh spacing from the triangular geometry is expected to be different from the extrapolation in xy geometry. If that is the case, corrections must be applied for these different sensitivities in order to produce appropriate bias factors. For the final design, a few calculations in hex-z geometry probably will be useful for configurations with partially inserted rod banks. These calculations should be biased from calculations in xyz geometry of critical experiments with similar configurations.

B. Bias Factor Generation and Use in Reactor Design

When an appropriate engineering mockup critical experiment is available, bias-factor generation and application to LMFBR design can be reasonably straightforward for control rod worths. If similar methods are used for both the critical experiment analysis and the nuclear design analysis, bias factors which essentially are E/C ratios from the critical experiments, are applied to the design calculation. Calculated adjustments are made for rod geometry (~5-15%, tested in special experiments), enrichment effects (generally 1-2%, depending on whether different C/E ratios are observed for enriched rods), mesh effect (can be several percent, depending on differences between the two models), and approximations that have different sensitivites for the two models (finite mesh spacing could be an example). The bias factors may also be different for different rings of rods. Spatially-dependent bias factors were used in the FFTF and may also be appropriate for heterogeneous and/or large reactors.

The next step is to assign an uncertainty to the predicted rod worth in the LMFBR design. Here experimental uncertainties, modeling approximation uncertainties, and C/E dispersions can be considered. Reasonably small uncertainties can be assigned if the design is sufficiently correlated with the EMC experiments. However, in a case where there is a large extrapolation from the critical experiment to the reactor design, uncertainties increase accordingly. For example, given the greater than 10% spread in C/E values for the best available calculations of results from several assemblies, confidence in extrapolating to a new reactor type or size is diminished. In addition, there is a 4-5% uncertainty in the scaling factor (β_{eff}) that relates calculations and experiments. For close matches of composition and geometry between the two reactors, errors in the two β_{eff} values are correlated and are therefore mostly removed through the use of a bias factor. The latter assumes use of comparable methods and cross section sets. Finally, results of the NEACRP comparisons for a large homogeneous reactor[5] show 30% discrepancies among calculations of the worth of a central control rod. Since the model was well defined, the differences should be due to processing codes and different cross section data for core materials. Boron cross section differences could only explain differences on the order of 2%.

Table V.1 contains a summary of the differences and similarities between an LMFBR design and the ZPPR critical assembly. The differences have to be considered in the generation and application in bias factors and predicted

TABLE V.1. A Summary of Features of LMFBRs and Critical Assemblies That Are Significant in Bias Factor Generation and Uncertainty Estimates

Feature	LMFBR	ZPPR	Comments
Geometry			
· Subassembly (SA)	Hexagonal	Rectangular (2 x2, 2x3, or 3 x3)	Representation constrained by matrix
· Control rod position	SA	Simulated SA	Correct number and locations
· Control rod	Absorber surrounded by sodium and structure of hex tubes	Absorber spread across whole rod	Homogenization problem for LMFBR rod
· Reactor	Layout determined by hex SA's	Layout constrained by matrix	Similar
Materials	Pins, SA cans, and sodium	Plates, drawers and matrix	Basic heterogeneity difference
· Fuel	Mixed oxide, at BOC uniform enrichment and isotopics	Alloy and oxide, fixed isotopics, enrichment adjusted thru complex plate cells	Good match for CRBRP and FFTF
· Diluents	Stainless steel, Na, and oxygen	Matched average composition	Differences in neutron streaming
· Blankets	UO_2	U, U_3O_8	Well matched
· Fission products	Vary with burnup	Not simulated	Significant extrapolation issue
· Control rod absorber	Enriched B_4C, centered in SA; nominal composition	Natural B_4C spread across CR; known composition	Special geometry and enrichment experiments
· CRP	Stainless steel, sodium	Matched composition	Errors should be correlated

TABLE V.1. A Summary of Features of LMFBRs and Critical Assemblies That Are Significant in Bias Factor Generation and Uncertainty Estimates (con't)

Feature	LMFBR	ZPPR	Comments
Calculations	Design predictions	Experiment analysis	Similar by intent
· Basic method	Few group, coarse mesh, 2-dimension diffusion theory	Same	Same processing codes should be used
· Representative geometry	hex-z	xyz	Triangular mesh vs. square mesh
· Geometry of calculation	hex	xy	rz group collapse and buckling generation
· Additional methods biases			CR homogenization, mesh sensitivity, streaming, heterogenity, etc.
· Cross section library	ENDF/B-IV	ENDF/B-IV	Must be the same
Operational Parameters			Additional extrapolation issues
· Temperature	Variable and distributed	300 K, nearly uniform	Handled in cross sections, increases uncertainty in rod worth
· β_{eff}	Composition and geometry dependent	Same	With good match, reactivity scale uncertainties mostly eliminated

uncertainties for design methods. The similarities allow some potential errors to be ignored because of direct correlations between the two reactors. Most of the issues that are raised in this comparison were addressed in Sections III and IV of this report. The action required to resolve some of the issues is dependent on the specific reactor design.

VI. PROBLEMS AND FUTURE WORK

As a result of this assessment, several deficiencies in the control rod worth experimental data base and in the analysis of those data have been identified. Some of those deficiencies are discussed below, with the expectation that the specified problem areas will be addressed in the future.

A. Data Base

Although an extensive experimental data base has been compiled in the last 10 years, there are some omissions that should be addressed eventually. Measurement of control rod worths in large heterogeneous cores is of the most interest because heterogeneous cores are the reference concept for eventual commercial-size LMFBRs in the U.S. Since large rod interactions were confirmed for both large homogeneous cores and 350 MWe size heterogeneous cores, it is known that larger heterogeneous cores will display some significant interaction effects and associated gross flux tilts. More data on the effect of internal blankets on rod worth are also necessary in confirming acceptable core layouts.

If future designs deviate significantly from the present expected systems of 32-42 v/o mixed-oxide, additional experiments will be required. For example, mixed-carbide or metal-alloy core designs would require investigations of control worth in addition to other parameters. Development of cores with longer fuel cycles would require some significant changes from current rod designs because of constraints on rod lifetimes. Besides rod worth measurements, detailed measurements of internal heating and capture rates may be necessary for advanced rod designs.

Some of the obvious holes in the data base will be filled in the next two years as a part of the ZPPR-13 and -14 programs. Those data will be the first rod worth measurements in 700 MWe size heterogeneous cores, and will include data on rod size effects as well as the effects of blanket arrangement.

Although some data on rod-tip heating are available from ZPPR-11, additional information will be necessary for larger cores with different rod designs. Excessive heating rates in highly-enriched B_4C rods are expected to be a design concern, at least until sufficient burnup and operational data are obtained.

The data base for materials other than B_4C is sparse. If interest revives in tantalum or europium-based rods, additional data, including multiple rod worths, will be required. Also, analysis of the existing resonance-absorber data has been done only with crudely prepared cross sections. Better resonance self-shielding treatment could help clarify the present situation.

An obvious deficiency in the large homogeneous core program was the inability to measure the worth of the larger multiple rod groups. In ZPPR-10D, only 18 of the 31 CRPs could be filled with control rods at one time. Additional material will be required in order to expand the measurement capability. Also, different spatially-varying C/E ratios were obtained in the same core size as the number of CRPs was expanded from 19 in ZPPR-10C to 31 in ZPPR-10D. This was accompanied by an incremental misprediction of the radial power distribution. Since most large core designs call for a significant number of CRPs, measurement of their effect on core parameters will be required. Intepretation of such measurements will require a significant and innovative analysis effort.

B. Calculational Methods

The reference method described in Section III proved to be adequate for most of the control rod worth analysis. It is apparent that by using design-equivalent methods and good EMC data, bias factors can be produced that lead to design predictions of rod worths that should have acceptably small uncertainties.

Application of corrections for approximations in the reference calculations has improved the consistency of the C/E data base. Some residual discrepancies still persist, and the tendency is for the corrected values to cluster around 1.1 rather than 1.0. Although this result is generally consistent with results from other reactivity experiments, the evidence strongly indicates that not all effects are being properly calculated. Among the residual discrepancies, the most significant is the difference between C/E values from heterogeneous and homogeneous cores. The radial distribution of most parameters is poorly predicted in heterogeneous cores. Further investigation of improved cross section generation methods is needed for core and blanket materials.

For the present collection of model-corrected rod worth calculations, there are several inconsistencies that need to be resolved. They are:

i. Methods inconsistencies.

   Different codes have been used to generate some of the corrections. For example, transport corrections have been calculated with DOT, TWOTRAN, and DIF3D. Comparisons of results from different codes used for a single case have shown results that are inconsistent by a few tenths of a percent of the total correction. For consistency, all transport corrections should be regenerated with DIF3D.

ii. Methods application.

   Corrections have been calculated as a percentage adjustment to the reference values. Applications of the corrections have not always proceeded in the same order, and at times some corrections have been combined. It has been assumed that the effects are separable, but this needs to be tested.

iii. Estimated values.

A few corrections have been estimated from values produced for other assemblies.

iv. Incomplete corrections.

The corrected C/E values in Section III.C do not contain all necessary corrections for each case. As an example, coupling between core and blanket sections has not been accounted for in the heterogeneous core calculations for control rod worths.

Besides resolving these inconsistencies, there is some developmental and verification work that needs to be done. Such work includes:

i. Methods for treating neutron streaming in CRPs.

Axial neutron streaming in CRPs has been shown to contribute significantly to misprediction of k_{eff}, control rod worths and power distributions. At present, only rudimentary corrections have been made in ZPPR analysis. These use either reactivity corrections calculated for a central CRP and scaled to off-center positions, or a CRP buckling correction factor that is generated for the center position and applied to all CRPs in the xy model. Development of a method that is generally applicable in xyz geometry is needed. Currently, it is expected that this will be accomplished by defining special directional diffusion coefficients for use in CRPs. At least two methods are possible. One is to use the transport solution directly to define the diffusion coefficients as, for example, in the response matrix formulation.[31] An alternative method, which is easier in application, is to derive approximate formulae for calculating diffusion coefficients.[32,33,34] These are tested over a range of material composition and sizes against reference transport solutions. Rowlands[28] quotes an accuracy of 3% using these methods for the reactivity effect of replacing fuel by a CR channel in the CDFR.

ii. Verification of correction methods.

The corrections for approximations in the standard method of analysis have been gleaned from results obtained over a number of years. For a selected number of cases, detailed re-evaluations using the modern code capabilities are required. Documented verification is needed to show that the effects of extrapolation to an infinite number of groups, mesh spaces, and angles is either not significant or can be estimated with confidence.

iii. Homogenization of control rod regions.

Methods of generating homogeneous cross section data for use in control rod regions of an LMFBR need to be investigated. The measurements in ZPPR-10A and ZPPR-11 using both natural and enriched boron

provide data for testing different approaches. Attention should also be given to calculation of reaction rates in the vicinity of detailed pin-geometry mockups of actual rod designs. Such data are now available from ZPPR-11.

Finally, the analysis goals include resolution of inconsistent C/E values for control rod worths in different cores and at different radial positions. Based on uncertainties in the measurements, the range of C/E values should be only a few percent for fully corrected calculations. If the mean values for fully corrected C/E's do not fluctuate about 1.0 as now seems likely, an understanding of the reason for the discrepancy should be gained. Failure to achieve consistent C/E's near 1.0 could result from errors in the basic nuclear data. Cross section sensitivity studies[35] have shown that some of the radial C/E discrepancy can be removed by reasonable adjustments to the ^{238}U capture cross section. However, much greater confidence in the calculational methods must be attained before there can be any significant contribution to cross section evaluation based on control rod worth measurements.

Ultimately, the control rod worth results will have to be understood in the context of a broader physics assessment of LMFBR physics parameters. Consider the following examples:

i. Radial discrepancies in reaction rates correlate with those for control rod worths.

ii. Measurements of β_{eff} in Pu/U-fuelled critical assemblies consistently yield results that are several percent higher than the calculations. Although the uncertainties in an individual measurement is too large to verify the misprediction of β_{eff}, values closer to the experimental ones would make the C/E's closer to 1.0.

iii. Using the same methods, C/E's for the worth of significant changes in fuel enrichment are 6% higher than C/E's for control rod worths. Separate physics assessments are in progress in several of these areas--reaction rates, β_{eff}, and perturbation samples.

In summary, the status of control rod worth measurements and their analyses has been well defined. Specific analyses needed for further understanding some persistent discrepancies and for investigating heretofore neglected effects have been identified. Together with data obtained from analysis of suggested additional measurements, the basis for improved understanding of the effects of control rods in LMFBRs should be established. Further, the capability for accurate prediction of control rod worths in the first U.S. commercial-size LMFBR plant can be confidently anticipated to follow from these studies.

REFERENCES

1. R. Avery, "Review of FBR Physics," *Proc. of the Natl. Topical Mtg. on New Developments in Reactor Physics and Shielding*, CONF-720901, Book 2, Kiamesha Lake, NY, pp. 771-788 (1972).

2. A.B. Reynolds and S.L. Stewart, "Application of the SEFOR Critical Experiments at ZPR-3 to SEFOR," *Proc. of the Intl. Conf. on Fast Critical Experiments and Their Analysis*, ANL-7320, p. 569 (1966).

3. W.B. Lowenstein, "The Utilization of Critical Assemblies for Fast Reactor Design," *ibid*, p. 543.

4. J.M. Lake, "Fuel Enrichment Requirements for the Clinch River Breeder Reactor," *Proc. of the Conf. on 1980 Advances in Reactor Physics and Shielding*, Sun Valley, Idaho, Sept. 14-19, 1980, American Nuclear Society, LaGrange Park, IL, pp. 480-493 (1980).

5. L.G. LeSage, et al., *Proc. of the NEACRP/IAEA Specialsts Mtg. on the Int. Comparison Calc. of a Large Sodium-Cooled Fast Breeder Reactor*, Argonne National Laboratory, 7-9 Feb 1978, ANL-80-78, NEA-CRP-L-243, p. 64 (1978).

6. J.A. Wheeler, *Principles of Nuclear Power*, N-2292, Chap. 22, (June 1944).

7. P. Hammer, "Control Rod Studies in the CEA Fast Reactor Physics Program," *Proc. of the Intl. Conf. on Advanced Reactors: Physics, Design and Economics*, Atlanta 1974, p. 267 (1975).

8. S.G. Carpenter, "Measurements of Control Rod Worths Using ZPPR," *Proc. of the Specialists Mtg. Control Rod Meas. Tech: Reactivity Worth and Power Dist.*, Cadarache, France, 1976, NEACRP-U-75.

9. R.E. Kaiser, "Evaluation of Detector-Efficiency and Source-Worth Corrections for Subcritical Reactivity Measurements in a Fast Critical Assembly," *Nucl. Tech.*, *25*, p. 138 (1975).

10. K.H. Beckurts and K. Wirtz, *Neutron Physics*, Springer-Verlag, New York, p. 34 (1964).

11. M.L. Bach and R.E. Mueller, "Physics Measurements in the Fermi Reactor," *Proc. of the Intl. Conf. on Physics of Fast Reactor Operation and Design*, London, June 1969, pp. 299-305.

12. P.P. Clauzon, et al., "Experimental Physics Results at the Startup of Phenix," *Proc. of the Intl. Conf. on Fast Reactor Power Stations*, London 1974.

13. V.V. Orlov, et al., "Comparison of Calculated Basic Physical Characteristics of the BN-350 Reactor with Their Measured Values," *ibid.*

14. D.C.G. Smith and R.C. Wheeler, "Reactor Physics Measurements of Some Key Parameters of the PFR," *ibid.*

15. R.B. Rothrock, "Analysis of Initial FTR Zero-Power Physics Test," *Trans. Am. Nuc. Soc.*, *41*, p. 574 (1982).

16. A.M. Broomfield, et al., "The MOZART Control Rod Experiments and Their Interpretation," *Int. Symp. on Physics of Fast Reactors*, Tokyo, Japan, 1973, p. 312.

17. J.L. Rowlands, et al., "The Development and Validation of Control Rod Calculation Methods," *Int. Symp. on Fast Reactor Physics*, Aix-en-Provence, France, 24-28 September 1979, IAEA-SM-244/36, p. 83, IAEA (1980).

18. Y.S. Lu (GE), private communication.

19. S.L. Stewart (GE), private communcation.

20. R.V. Rittenberger and J.A. Lake (W-ARD), private communication.

21. L.G. LeSage, "Status of Fast Reactor Physics," *Proc. of the Conf on 1980 Advances in Reactor Physics and Shielding*, Sun Valley, Idaho, Sept. 14-19, 1980, American Nuclear Society, LaGrange Park, IL, pp. 51-69 (1980).

22. K.S. Smith, "The Effects of Intracell Adjoint Flux Heterogeneity on First-Order Perturbation Reactivity Calculations," *Nucl. Sci. and Eng.*, *81*, pp. 451-458 (1982).

23. R.H. Schaefer and R.G. Bucher, "Calculated and Measured Reactivities in U9," to be presented at the ANS Topical Meeting on Advances in Reactor Physics and Core Thermal Hydraulics, Sept. 22-24, 1982, Kiamesha Lake, NY.

24. P.J. Collins, et al., "A Comparison Between Physics Parameters in Conventional and Heterogeneous LMFBR's Using Results from ZPPR," *Proc. of the Intl. Mtg. on Advances in Reactor Physics*, Gatlinburg, Tennessee, CONF-78041, p. 207 (1978).

25. H.F. McFarlane and P.J. Collins, "Measurements of Control Rod Interactions in ZPPR-9," *Trans. Am. Nuclear. Soc.*, *33*, pp. 832-833 (1979).

26. P.J. Collins, et al., "Experimental Studies of Control Rod Geometry and Enrichment Effects in ZPPR-10A," *Trans. Am. Nucl. Soc.*, *34*, pp. 751-752 (1980).

27. Y.H. Bouget, et al., "Etude experimentale des barres de commande pour les reacteurs de puissance a neutrons rapides dans Masurca," *op cit* (Ref. 17).

28. J.R. Rowlands, et al., *op cit* (Ref. 17).

29. U. von Mollendorff and F. Helm, "SNEAK-11: Mockup Critical Studies of a Small Sodium-Cooled Fast Reactor," *op cit*, (Ref. 21) Sun Valley 1980, p. 510.

30. R.B. Pond, et al., "Europium Oxide Measurements in the Engineering Mockup Critical Assembly of the Fast Test Reactor," *op cit*, (Ref. 7) Atlanta 1974, p. 305.

31. D.J. Malloy, "Response Matrix Directional Diffusion Coefficients for Application within Large Cavities," *op cit*, (Ref. 21) Sun Valley 1980, p. 816.

32. J.L. Rowlands and C. Eaton, "The Effective Axial Diffusion Coefficient for a Low-Density Channel," *Nucl. Sci. Eng.*, *76*, pp. 263-281 (1980).

33. T. Yoshida, "Improved Treatment of the Neutron Streaming Through Control Rod Followers in a Sodium-Cooled Fast Reactor," *Nucl. Sci. Eng. 72*, p. 361 (1979).

34. E.A. Fischer, "Neutron Streaming in Fast Reactor Slab Lattices, and in Cylindrical Channels," submitted for publication in *Nuclear Sci. Eng.*

35. M.J. Lineberry et al., "Physics Studies of a Heterogeneous Liquid-Metal Fast Breeder Reactor," *Nucl. Tech.*, *44*, p. 37 (June 1979).

VII. APPENDICES

APPENDIX A: Descriptions of Critical Configurations and Control Rods

This appendix contains tables and figures that describe the control rods that were used in the control worth measurements in ZPPR assemblies 3-11. The homogeneous atom densities of the rods are found in Tables VII.1 through VII.8, while the interface view of the rods, or of a representative drawer, are found in Figs. VII.18 through VII.27. The interface views of assemblies 3-11, Figs. VII.1 through VII.17, identify the numbering scheme for the rods.

TABLE VII.1. Composition of Control Rods Used in ZPPR-3

	Average Composition, 10^{22} atoms/cm^3			
Material	Design A	Design H	Design I	Design J
	CRP-1	CRPs 2-7	Even Outer	Odd Outer
^{10}B	0.3329	0.4047	0.9520	0.6232
^{11}B	1.3516	1.6411	3.8607	2.5275
C	0.4401	0.5271	1.2240	0.8046
Na	1.2899	1.2899	0.6020	0.8456
Fe	1.1254	0.9827	0.0280	1.1827
Cr	0.3215	0.2808	0.2911	0.3354
Ni	0.1471	0.1287	0.1320	0.1521
Mn	0.0274	0.0234	0.0252	0.0294
Si	0.0173	0.0160	0.0214	0.0208
Cu	0.0030	0.0030	0.0028	0.0028
Co	0.0004	0.0004	0.0004	0.0004
Mo	0.0021	0.0021	0.0020	0.0020
O	---	0.0033	0.0097	0.0054
Al	0.0004	0.0004	0.0003	0.0003
P	0.0006	0.0005	0.0006	0.0008
S	0.0002	0.0002	0.0002	0.0002
LIP[a]	---	0.0024	0.0025	0.0008
HIP[b]	---	0.0009	0.0010	0.0004

[a]LIP = Light Impurities, A < 23.

[b]HIP = Heavy Impurities, A > 23.

TABLE VII.2. Composition of Control Rods Used in ZPPR Assemblies 4, 5, and 6

Material	Average Composition, 10^{22} atoms/cm^3	
	Design N	Design M
^{10}B	0.6390	1.1642
^{11}B	2.5913	4.7210
C	0.8287	1.5051
Na	0.7901	0.3791
Fe	1.2152	0.8625
Cr	0.3447	0.2443
Ni	0.1568	0.1107
Mn	0.0301	0.0207
Si	0.0211	0.0189
Cu	0.0029	0.0028
Mo	0.0020	0.0020
O	0.0049	0.0088
Al	0.0003	0.0003
LIP[a]	0.0023	0.0039
HIP[b]	0.0009	0.0016

[a]LIP = Light Impurities, A < 23.

[b]HIP = Heavy Impurities, A ≥ 23.

TABLE VII.3. Composition of Control Pin and Matched Plate Control Rods Used in ZPPR-6

Material	Average Composition, 10^{22} atoms/cm^3	
	Pin Rod	Plate Rod
^{10}B	0.5872	0.5883
^{11}B	2.4052	2.3865
C	0.7313	0.7732
Na	0.8886	0.8480
Fe	0.8771	1.0822
Cr	0.2523	0.3077
Ni	0.1144	0.1413
Mn	0.1950	0.0266
Si	0.0123	0.0174
Cu	0.0018	0.0029
Mo	0.0014	0.0018
Al	0.0003	0.0004

TABLE VII.4. Composition of Control Rods Used in ZPPR Assemblies 7 and 8

	Average Composition, 10^{22} atoms/cm^3			
	ZPPR-7 to ZPPR-7E		ZPPR-7F to ZPPR-7H, and ZPPR-8	
Material	Natural[b]	Enriched	Natural[b]	Enriched
^{11}B	6.0576	0.2228	6.3502	5.1796
^{10}B	1.4861	2.4500	1.5580	2.8349
C	1.9344	0.6679	2.0277	2.0190
Fe	0.7052	1.7806	0.7281	0.7262
Cr	0.1981	0.4126	0.2003	0.1999
Ni	0.0877	0.1877	0.0852	0.0860
Si	0.0180	0.0227	0.0208	0.0202
Mn	0.0174	0.0372	0.0175	0.0175
O	0.0109	0.4762	0.0095	0.0134
Na	0.0000	0.6023	0.0000	0.0000
N	0.0005	0.0249	0.0002	0.0224
Al	0.0008	0.0004	0.0008	0.0001
Cu	0.0025	0.0028	0.0030	0.0039
Mo	0.0018	0.0018	0.0015	0.0015
LIP[d]	0.0034	0.0113	0.0032	0.0151
HIP[e]	0.0013	0.0010	0.0012	0.0023

[a]Matrix dimensions changed between 7E and 7F.

[b]Reference rod for most measurements.

[c]LIP = Light Impurities A < 23.

[d]HIP = Heavy Impurities A > 23.

TABLE VII.5. Composition of Control Rods Used in ZPPR-9

	ZPPR-9 Control Rod		ZPPR-10 Control Rod
	Absorber Section	Absorber Section	50/50 B_4C/Na Absorber Section
Number of drawers	9	4 or 6	9
Axial length, mm	1018	1018	1018
Material	Average Composition, 10^{22} atoms/cm^3		
Be	--	--	--
^{10}B	1.53792	1.54346	0.78588
^{11}B	6.23701	6.25966	3.18704
C	1.98950	1.99907	1.02010
N	--	--	--
O	0.01002	0.00959	0.00459
Na	--	--	0.88833
Mg	--	--	--
Al	0.00008	0.00008	0.00045
Si	0.02020	0.01980	0.02089
P	0.00040	0.00040	0.00050
S	0.00012	0.00012	0.00012
Cl	--	--	0.00003
Ca	--	--	0.00020
Cr	0.20365	0.20354	0.27793
Mn	0.01774	0.01774	0.02328
Fe	0.74010	0.74027	0.99181
Co	0.00038	0.00038	0.00049
Ni	0.08696	0.08691	0.12502
Cu	0.00299	0.00299	0.00339
Mo	0.00150	0.00150	0.00154
Ta	--	--	--
^{151}Eu	--	--	--
^{153}Eu	--	--	--
LIP[a]	0.00328	0.00380	0.00163
HIP[b]	0.00129	0.00149	0.00069

[a]LIP = Light Impurities, A < 23.

[b]HIP = Heavy Impuriuties, A > 23.

TABLE VII.5. Composition of Control Rods Used in ZPPR-9 (con't)

	Tantalum Rod	Europium Oxide Rod	Pin Rod for Interaction Experiment		Stainless Steel Subassembly
	Absorber Section	Absorber Section	Absorber Section	Axial Section	
Number of drawers	4	4	9	9	9
Axial length, mm	1018	916	914	458	1831
Material	Average Composition, 10^{22} atoms/cm^3				
Be	--	--	0.00043	0.00043	--
^{10}B	--	--	0.15360	--	--
^{11}B	--	--	0.62919	--	--
C	0.00289	0.01440	0.21245	0.02428	0.02146
N	--	--	--	0.00168	--
O	--	1.11918	--	--	--
Na	--	0.88719	0.92977	0.92977	--
Mg	--	--	0.00036	--	--
Al	--	0.00222	0.00031	0.00029	--
Si	0.01108	0.02046	0.01413	0.01944	0.08642
P	0.00040	0.00050	0.00213	0.00243	0.00534
S	0.00012	0.00012	0.00103	0.00128	0.00252
Cl	--	0.00003	--	--	--
Ca	--	0.00020	--	--	--
Cr	0.18169	0.35443	0.25543	0.41435	1.50656
Mn	0.01610	0.03003	0.03752	0.04514	0.15265
Fe	0.65195	1.24887	3.24082	3.81783	5.31836
Co	0.00038	0.00049	0.00062	0.00133	--
Ni	0.07571	0.16312	0.11247	0.17486	0.66722
Cu	0.00289	0.00387	0.00226	0.00362	0.00171
Mo	0.00145	0.00150	0.00102	0.00117	0.00082
Ta	4.66322	--	--	--	--
^{151}Eu	--	0.35986	--	--	--
^{153}Eu	--	0.38784	--	--	--
LIP	--	0.00022	--	--	--
HIP	--	0.00015	--	--	--

TABLE VII.6. Composition of Control Rods Used in ZPPR-10

	ZPPR-10 Control Rod	Control Rod Position		80-pin Enriched Boron	80-pin Natural Boron	40-pin Enriched Boron	76-pin Tantalum
	Absorber Section	Axial Section	Core Section	Absorber Section	Absorber Section	Absorber Section	Absorber Section
Number of drawers	9	9	9	9	9	9	9
Axial length, mm	1018	406	1018	1016	1016	1016	914.4
Material	Average Composition, 10^{22} atoms/cm^3						
Be	- - -	- - -	- - -	0.00043	0.00043	0.00043	0.00043
^{10}B	0.78588	- - -	- - -	1.68742	0.34134	0.84371	- - -
^{11}B	3.18704	- - -	- - -	0.14696	1.39820	0.07348	- - -
C	1.02010	0.00411	0.00372	0.48005	0.43042	0.25059	0.01473
N	- - -	- - -	- - -	0.00352	0.00298	0.00325	- - -
O	0.00459	0.00013	0.00013	0.00160	- - -	0.00080	- - -
Na	0.88833	1.81993	1.85969	0.92977	0.92977	0.92977	0.92977
Mg	- - -	- - -	- - -	- - -	0.00080	- - -	- - -
Al	0.00045	0.00059	0.00056	0.00037	0.00033	0.00033	0.00029
Si	0.02089	0.01848	0.01810	0.02347	0.02343	0.02341	0.01409
P	0.00050	0.00055	0.00055	0.00095	0.00095	0.00159	0.00150
S	0.00012	0.00012	0.00012	0.00065	0.00065	0.00095	0.00072
Cl	0.00003	0.00006	0.00006	- - -	- - -	- - -	- - -
Ca	0.00020	0.00042	0.00043	0.00019	- - -	0.00010	- - -
Ti	- - -	- - -	- - -	- - -	0.00001	- - -	- - -
Cr	0.27793	0.30024	0.29408	0.53369	0.53369	0.53369	0.25543
Mn	0.02328	0.02499	0.02450	0.03268	0.03272	0.03935	0.03083
Fe	0.99181	1.07154	1.04233	1.91123	1.91308	2.77816	2.37281
Co	0.00049	0.00056	0.00055	0.00189	0.00189	0.00189	0.00062
Ni	0.12502	0.13618	0.13328	0.22172	0.22167	0.22169	0.11247
Cu	0.00339	0.00356	0.00349	0.00461	0.00462	0.00461	0.00226
Mo	0.00154	0.00155	0.00152	0.00126	0.00126	0.00126	0.00102
Ta	- - -	- - -	- - -	- - -	- - -	- - -	1.09351
LIP[a]	0.00163	0.00033	0.00032	- - -	- - -	- - -	- - -
HIP[b]	0.00069	0.00021	0.00021	- - -	- - -	- - -	- - -

[a]LIP = Light Impurities, A < 23.

[b]HIP = Heavy Impurities, A > 23.

TABLE VII.6. Composition of Control Rods Used in ZPPR-10 (con't)

	80-pin Rods	40-pin Rods	Tantalum Rods	All Rods	All Rods
	Axial Section (A)	Axial Section (A)	Axial Section (A)	Axial Section (B)	Axial Section (C)
Number of drawers	9	9	9	9	9
Axial length, mm	101.6	101.6	152.4	304.8	127
Material	Average Composition, 10^{22} atoms/cm^3				
Be	0.00043	0.00043	0.00043	- - -	- - -
^{10}B	- - -	- - -	- - -	- - -	- - -
^{11}B	- - -	- - -	- - -	- - -	- - -
C	0.01223	0.01669	0.01982	0.00315	0.05988
N	0.00670	0.00484	0.00354	- - -	- - -
O	- - -	- - -	- - -	0.00013	- - -
Na	0.92977	0.92977	0.92977	1.85366	- - -
Mg	- - -	- - -	- - -	- - -	- - -
Al	0.00029	0.00029	0.00029	0.00058	- - -
Si	0.03503	0.02926	0.02521	0.01522	0.00814
P	0.00163	0.00193	0.00213	0.00051	0.00228
S	0.00120	0.00123	0.00125	0.00010	0.00321
Cl	- - -	- - -	- - -	0.00006	- - -
Ca	- - -	- - -	- - -	0.00043	- - -
Ti	- - -	- - -	- - -	- - -	- - -
Cr	0.88340	0.70969	0.58810	0.26389	0.15086
Mn	0.04935	0.04779	0.04670	0.02113	0.06413
Fe	3.18296	3.41814	3.58281	0.93570	7.62342
Co	0.00347	0.00268	0.00213	0.00017	- - -
Ni	0.35894	0.29076	0.24305	0.11903	0.06122
Cu	0.00759	0.00612	0.00509	0.00250	0.00188
Mo	0.00159	0.00143	0.00132	0.00101	0.00094
Ta	- - -	- - -	- - -	- - -	- - -
LIP	- - -	- - -	- - -	0.00032	- - -
HIP	- - -	- - -	- - -	0.00021	- - -

TABLE VII.7. Two-region Models for Pin Control Rods in ZPPR-10A

	80-pin Enriched Boron	80-pin Natural Boron	40-pin Enriched Boron	All Boron Rods	Tantalum Rod	
	Inner Region	Inner Region	Inner Region	Outer Region	Inner Region	Outer Region
Outer radius, mm	69.695	69.695	69.695	93.506	67.931	93.506
Axial length, mm	1016	1016	1016	1016	914.4	914.4
Material	Average Composition, 10^{22} atoms/cm^3					
Be	0.00043	0.00043	0.00043	0.00043	0.00043	0.00043
^{10}B	3.03736	0.61441	1.51868	- - -	- - -	- - -
^{11}B	0.26453	2.51676	0.13226	- - -	- - -	- - -
C	0.85434	0.76500	0.44131	0.01219	0.00261	0.02828
N	0.00098	- - -	0.00049	0.00670	- - -	- - -
O	0.00288	- - -	0.00144	- - -	- - -	- - -
Na	0.92977	0.92977	0.92977	0.92977	0.92977	0.92977
Mg	- - -	0.00143	- - -	- - -	- - -	- - -
Al	0.00043	0.00036	0.00035	0.00030	0.00029	0.00029
Si	0.01433	0.01426	0.01422	0.03490	0.01409	0.01409
P	0.00042	0.00042	0.00156	0.00162	0.00042	0.00270
S	0.00021	0.00021	0.00075	0.00119	0.00021	0.00130
Cl	- - -	- - -	- - -	- - -	- - -	- - -
Ca	0.00034	- - -	0.00017	- - -	- - -	- - -
Ti	- - -	0.00001	- - -	- - -	- - -	- - -
Cr	0.25569	0.25569	0.25569	0.88119	0.25543	0.25543
Mn	0.01950	0.01958	0.03151	0.04916	0.01948	0.04352
Fe	0.90020	0.90353	2.46067	3.17502	0.89881	4.02022
Co	0.00062	0.00063	0.00062	0.00347	0.00062	0.00062
Ni	0.11265	0.11257	0.11261	0.35805	0.11247	0.11247
Cu	0.00226	0.00227	0.00226	0.00755	0.00226	0.00226
Mo	0.00102	0.00102	0.00102	0.00156	0.00102	0.00102
Ta	- - -	- - -	- - -	- - -	2.07191	- - -
LIP[a]	- - -	- - -	- - -	- - -	- - -	- - -
HIP[b]	- - -	- - -	- - -	- - -	- - -	- - -

[a]LIP = Light Impurities, A < 23.

[b]HIP = Heavy Impurities, A > 23.

TABLE VII.8. Homogenized Composition of Pin Control Rods Used in ZPPR-11

Material	Average Composition, 10^{22} atoms/cm^3						
	Standard Pin Control Rod With Natural B_4C	Standard Pin Control Rod With Enriched B_4C	"Bunched" and "Spread" Pin Control Rod With Enriched B_4C	Standard Calandria Filled With Stainless Steel Pins	Standard Calandria Filled With Enriched B_4C Pins	Standard Calandria Filled With Natural B_4C Pins	Natural B_4C Plate Rod[a]
Be	0.0004310	0.0004310	0.0004310	0.0004310	0.0004310	0.0004310	- - -
^{10}B	0.4989941	2.4667807	1.5180189	- - -	3.0360378	0.6141466	1.56442
^{11}B	2.0439724	0.2148315	0.1322040	- - -	0.2644080	2.5156584	6.34458
C	0.6235568	0.6961178	0.4330609	0.0121700	0.8539518	0.7646461	2.02636
N	0.0012562	0.0020493	0.0038379	0.0066998	0.0009761	- - -	0.00015
O	- - -	0.0023354	0.0014372	- - -	0.0028744	- - -	0.00954
Na	0.9293738	0.9293738	0.9293738	0.9293738	0.9293738	0.9293738	- - -
Al	0.0003465	0.0004026	0.0003594	0.0002903	0.0004285	0.0003594	0.00012
Si	0.0180960	0.0181499	0.0245783	0.0348638	0.0142928	0.0142265	0.02077
P	0.0006425	0.0006425	0.0010166	0.0016152	0.0004180	0.0004180	0.00040
S	0.0003905	0.0003905	0.0007015	0.0011990	0.0002039	0.0002039	0.00012
Ti	0.0000105	0.0002772	0.0001706	- - -	- - -	0.0000130	- - -
Cr	0.3724343	0.3724343	0.5678217	0.8804415	0.2552019	0.2552019	0.29605
Mn	0.0250500	0.0249857	0.0342475	0.0490664	0.0194286	0.0195078	0.01857
Fe	1.3273498	1.3246464	2.0352228	3.1721451	0.8983006	0.9016279	0.77816
Co	0.0011666	0.0011580	0.0020500	0.0034771	0.0006228	0.0006334	0.00038
Ni	0.1584530	0.1585218	0.2351730	0.3578151	0.1125310	0.1124463	0.09263
Cu	0.0032402	0.0032322	0.0048856	0.0075311	0.0022402	0.0022500	0.00304
Mo	0.0011111	0.0011111	0.0012838	0.0015602	0.0010074	0.0010074	0.00152
Mg	0.0011634	- - -	- - -	- - -	- - -	0.0014319	- - -
Ca	- - -	- - -	- - -	- - -	0.0003411	- - -	- - -

[a]Normal ZPPR-11 rod used in most measurements.

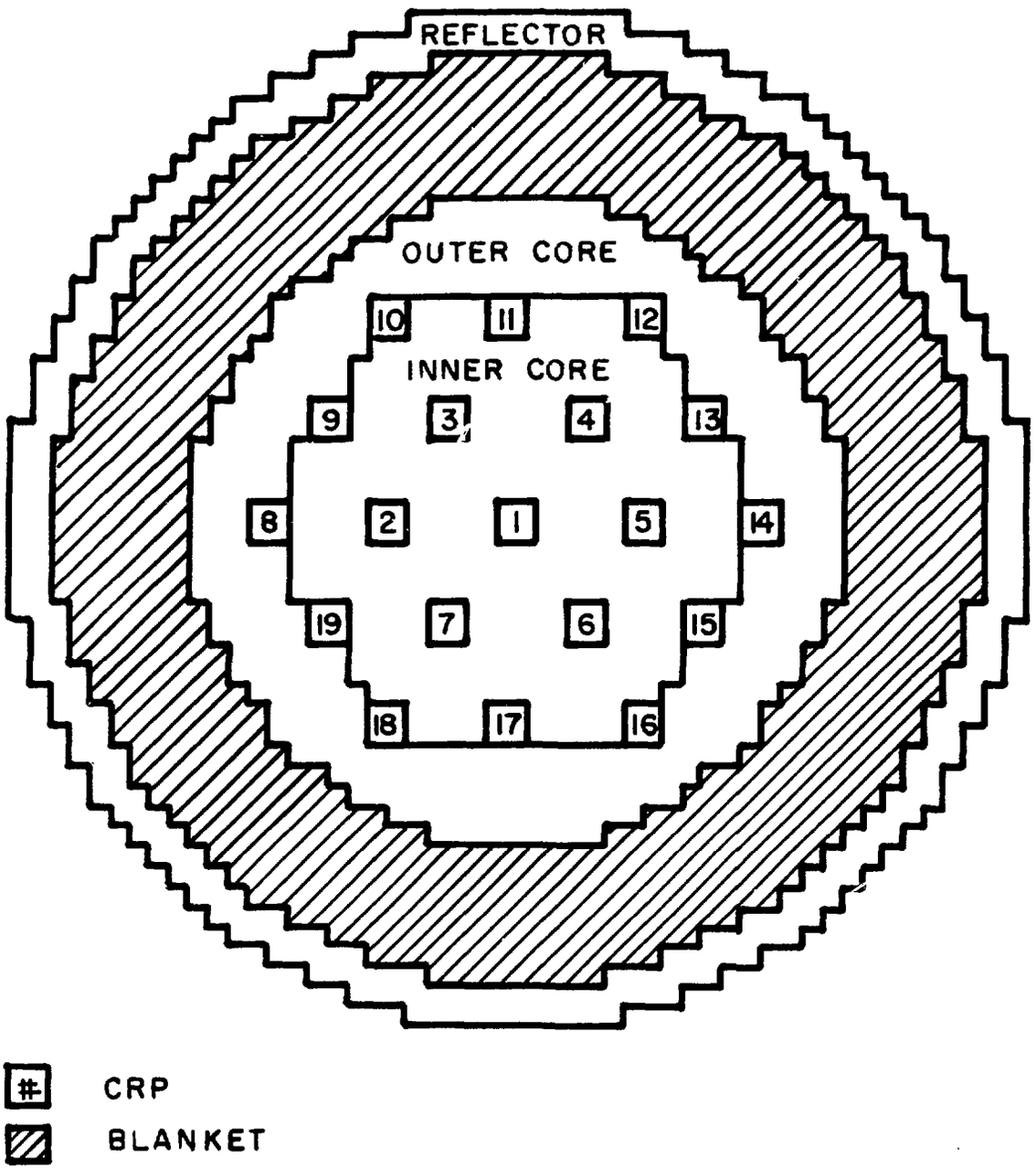

ZPPR-3/ 1B, 2, 3

Fig. VII.1

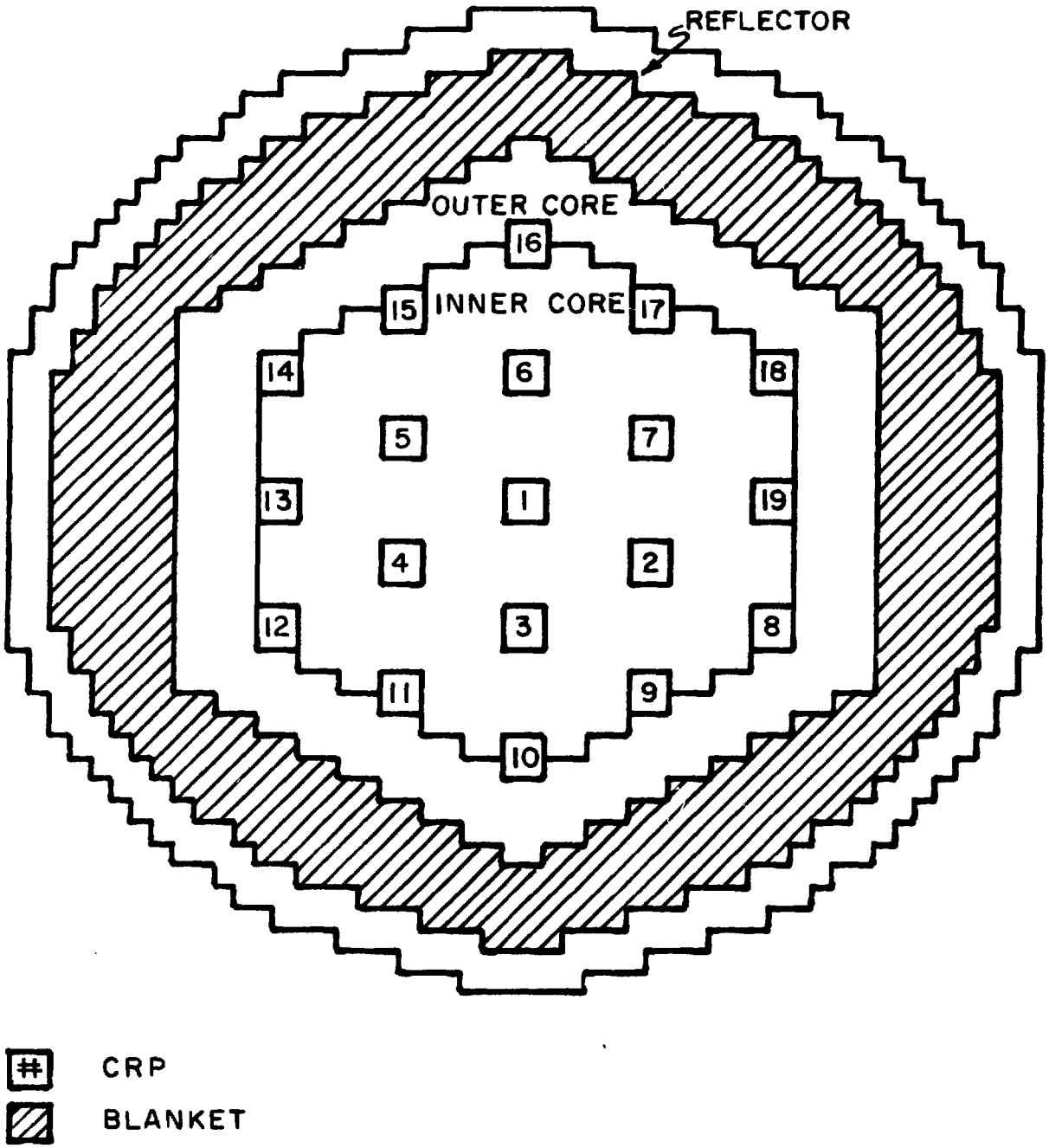

ZPPR – 4, PHASES 1, 2, 3, & 4

Fig. VII.2

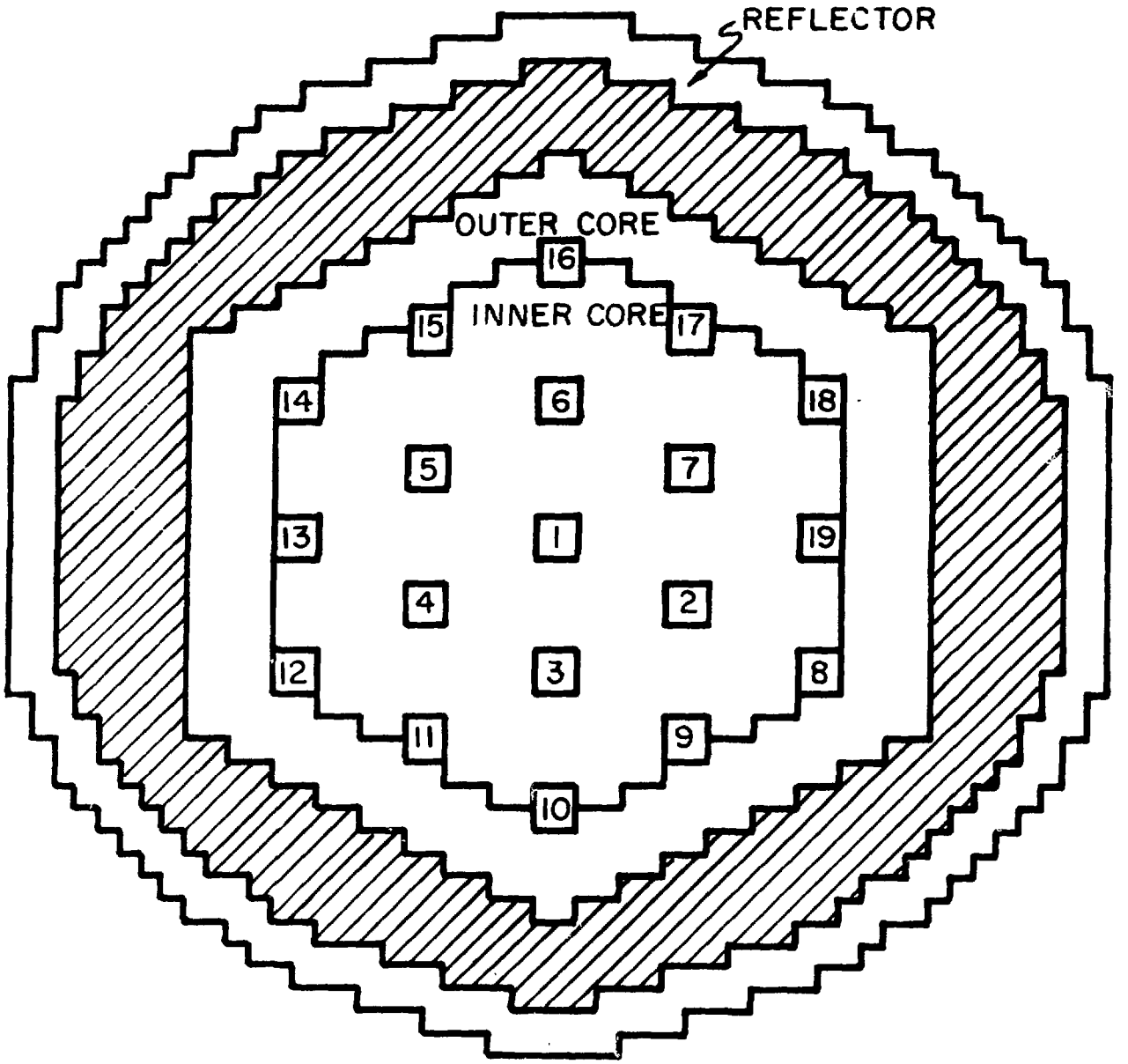

ZPPR-5A & 5B

Fig. VII.3

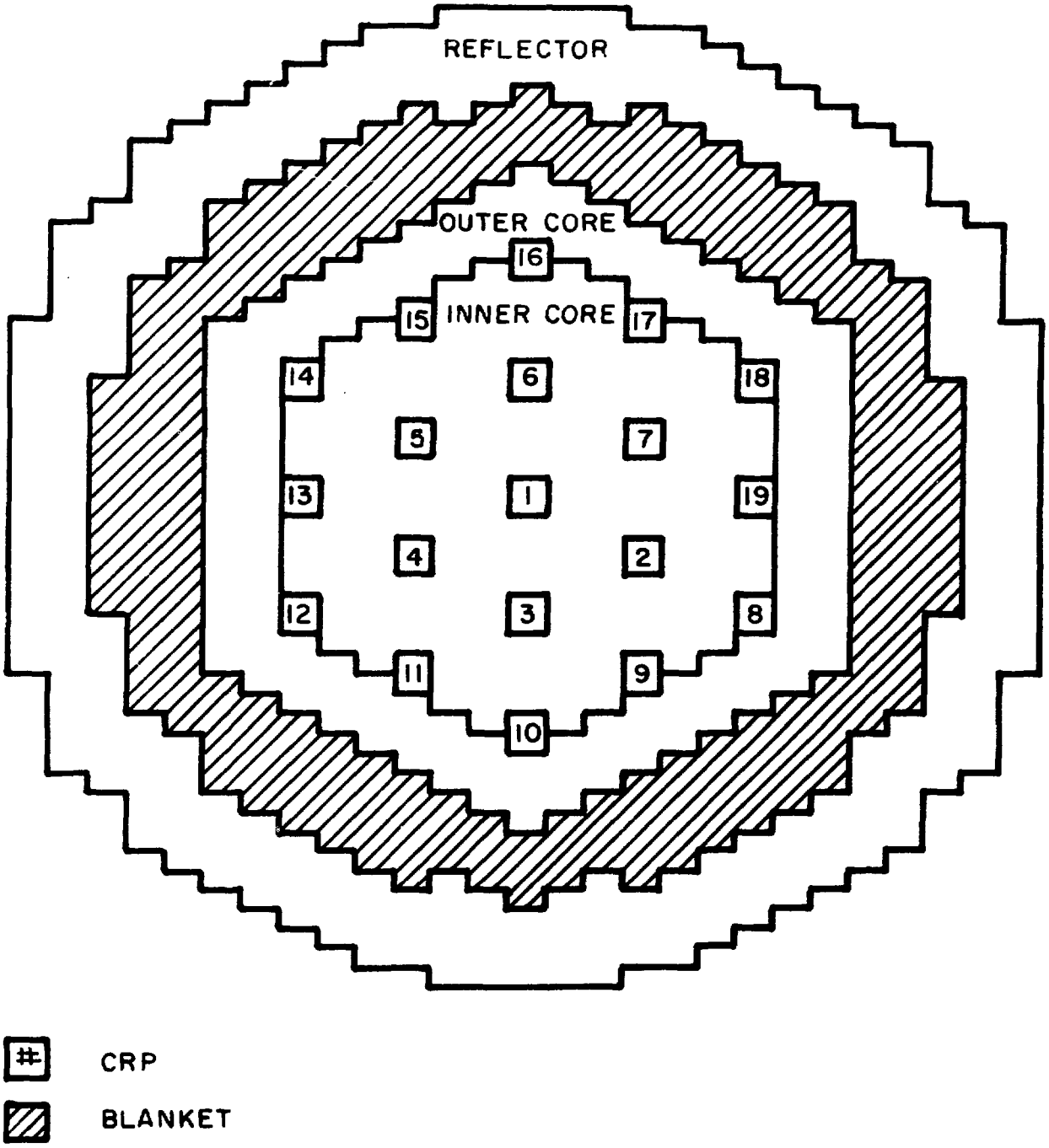
REFLECTOR
OUTER CORE
INNER CORE
16
15
17
14
6
18
5
7
13
1
19
4
2
12
3
8
11
9
10
CRP
BLANKET
ZPPR - 6

Fig. VII.4

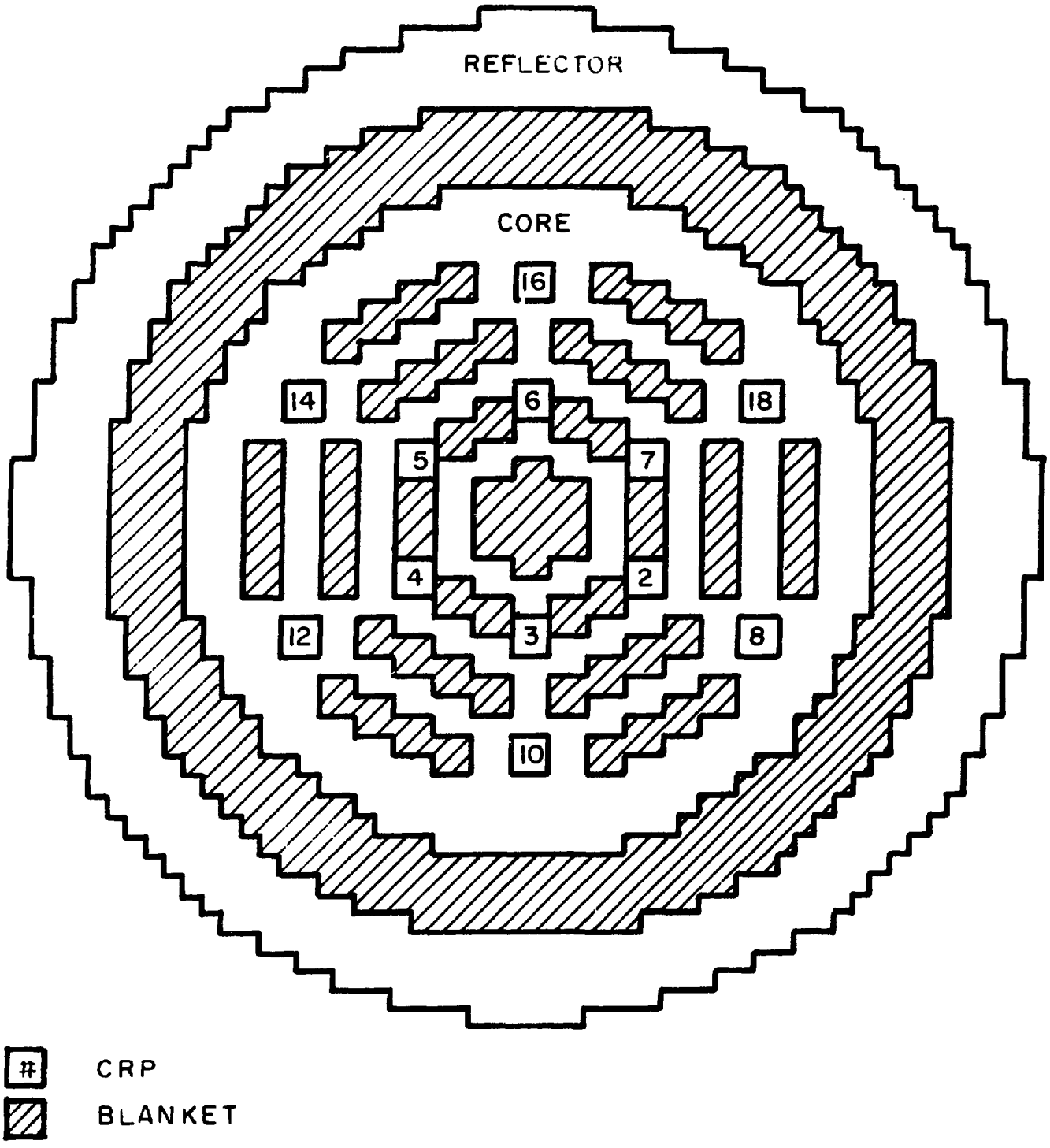

ZPPR - 7B, 7C

Fig. VII.5

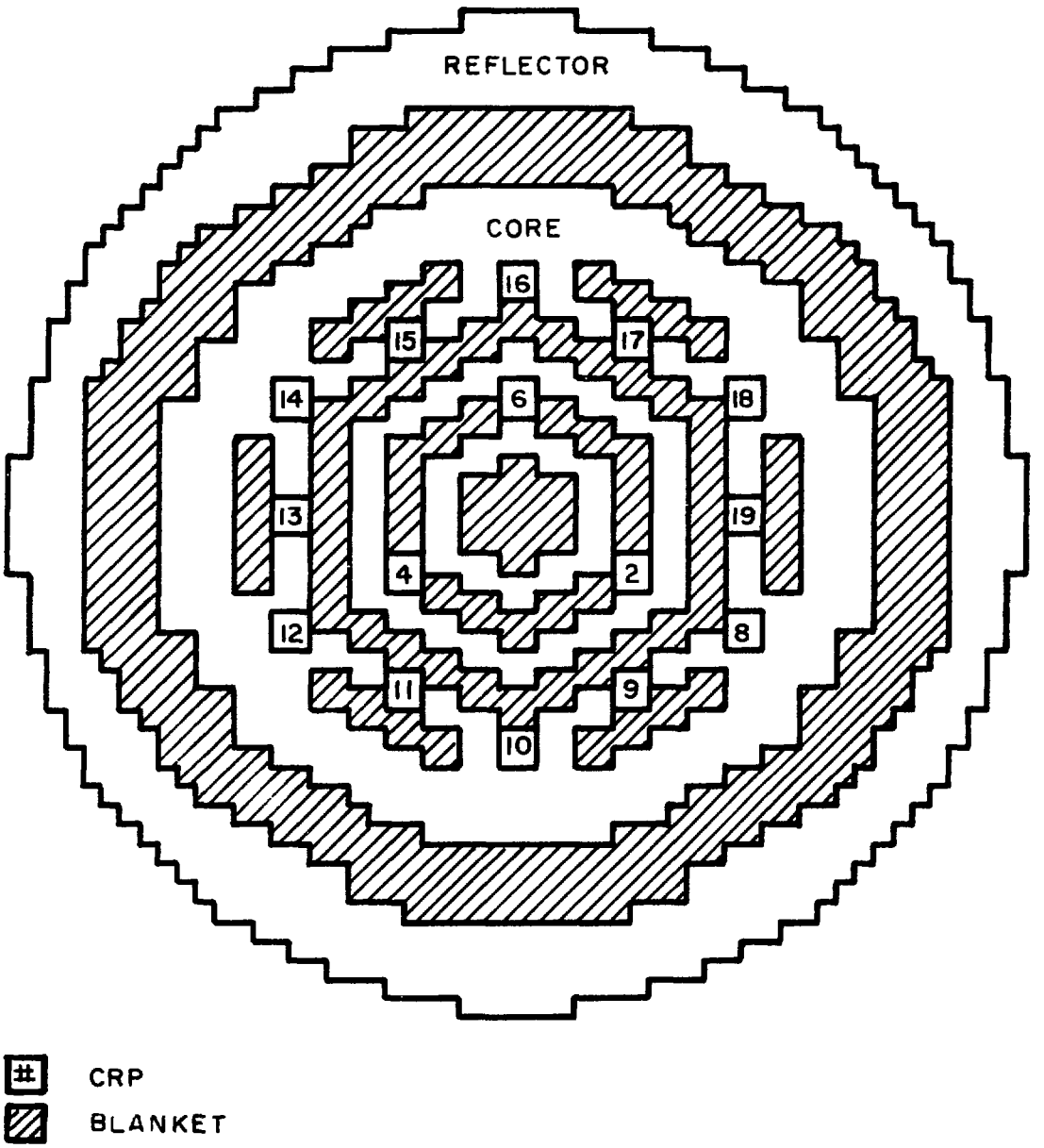

ZPPR - 7D & 7E

Fig. VII.6

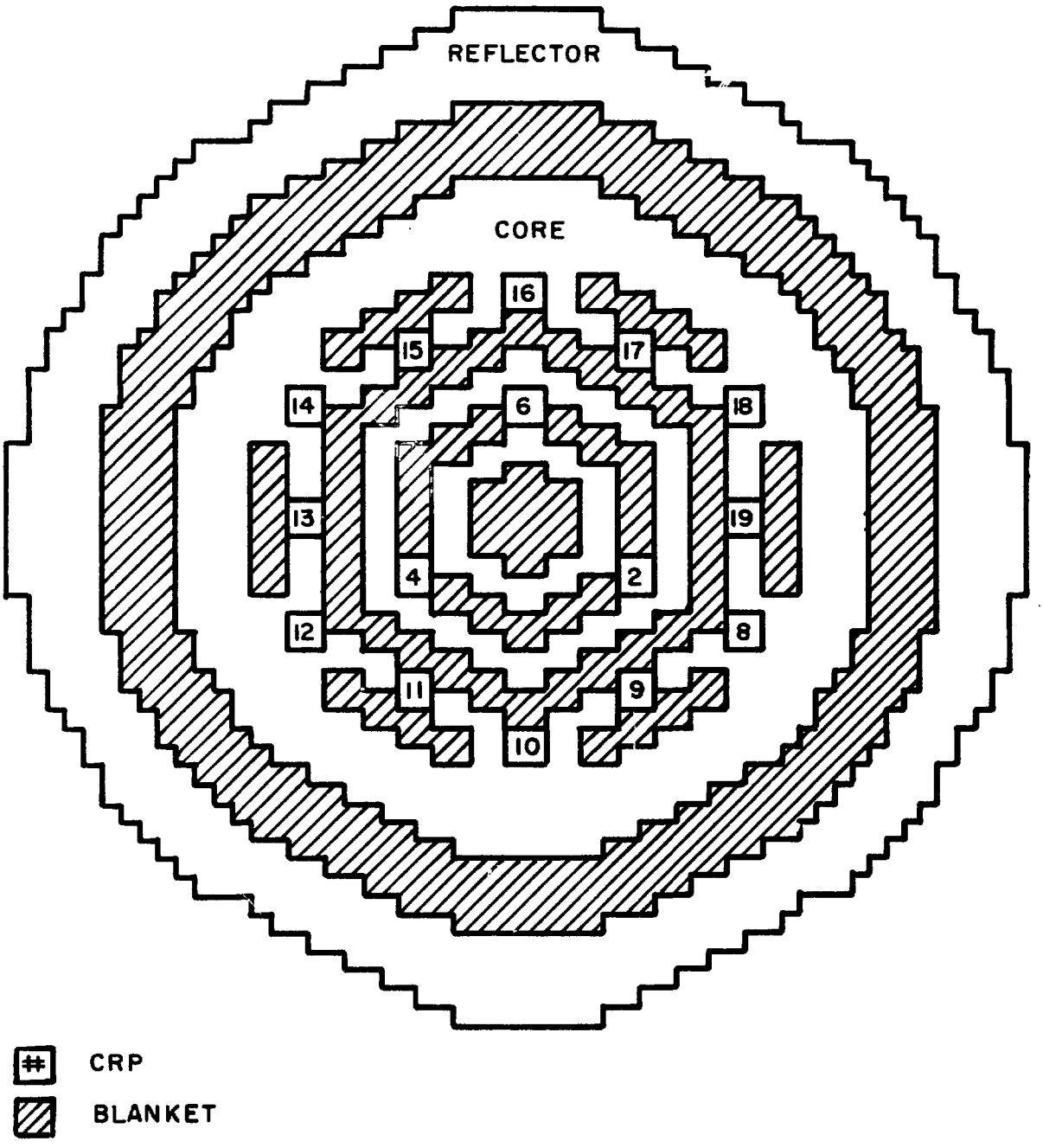

ZPPR – 7G

Fig. VII.7

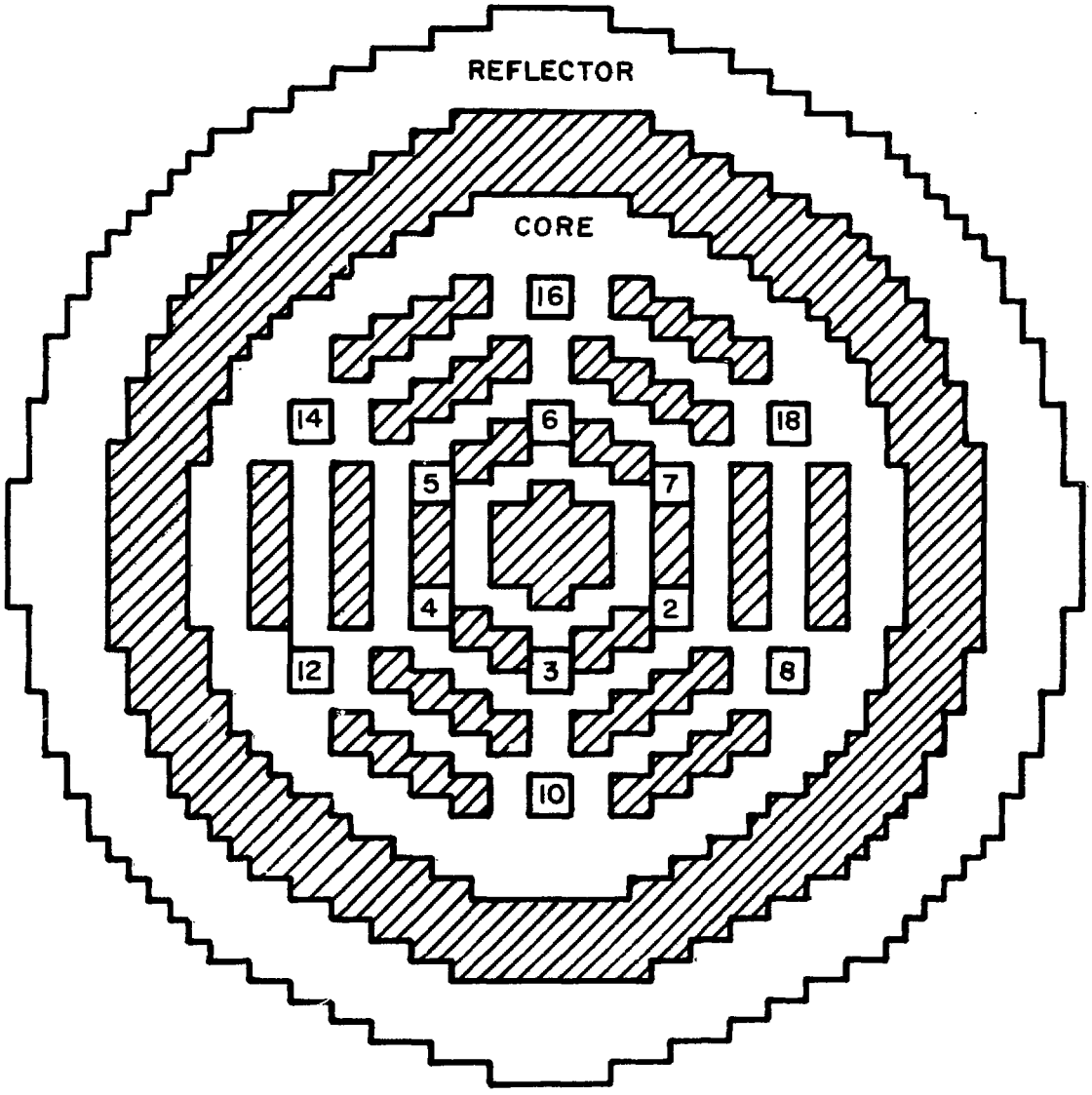

ZPPR — 7F, 8A, 8B, 8C, 8D, & 8E

Fig. VII.8

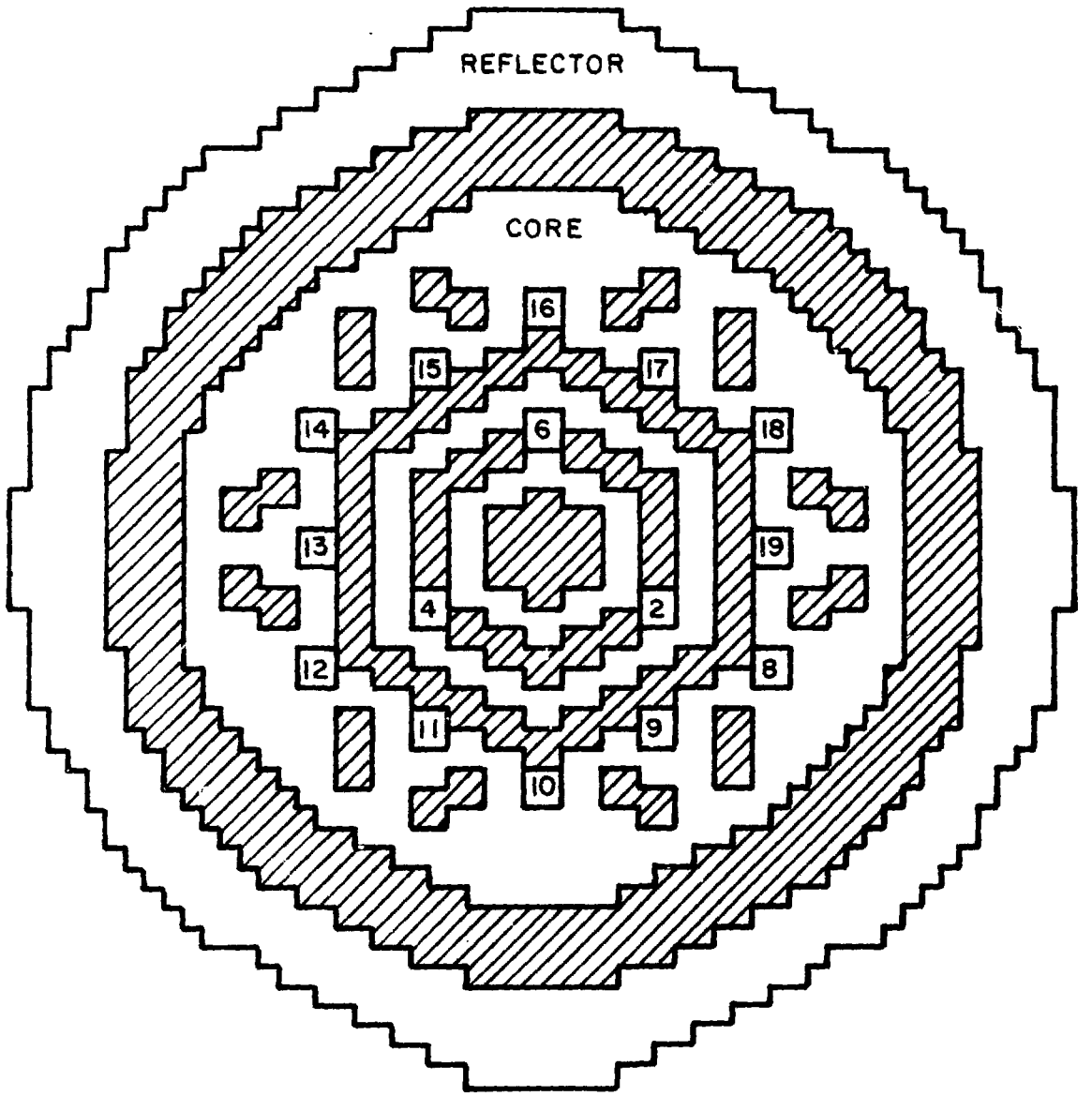

ZPPR – 8 F

Fig. VII.9

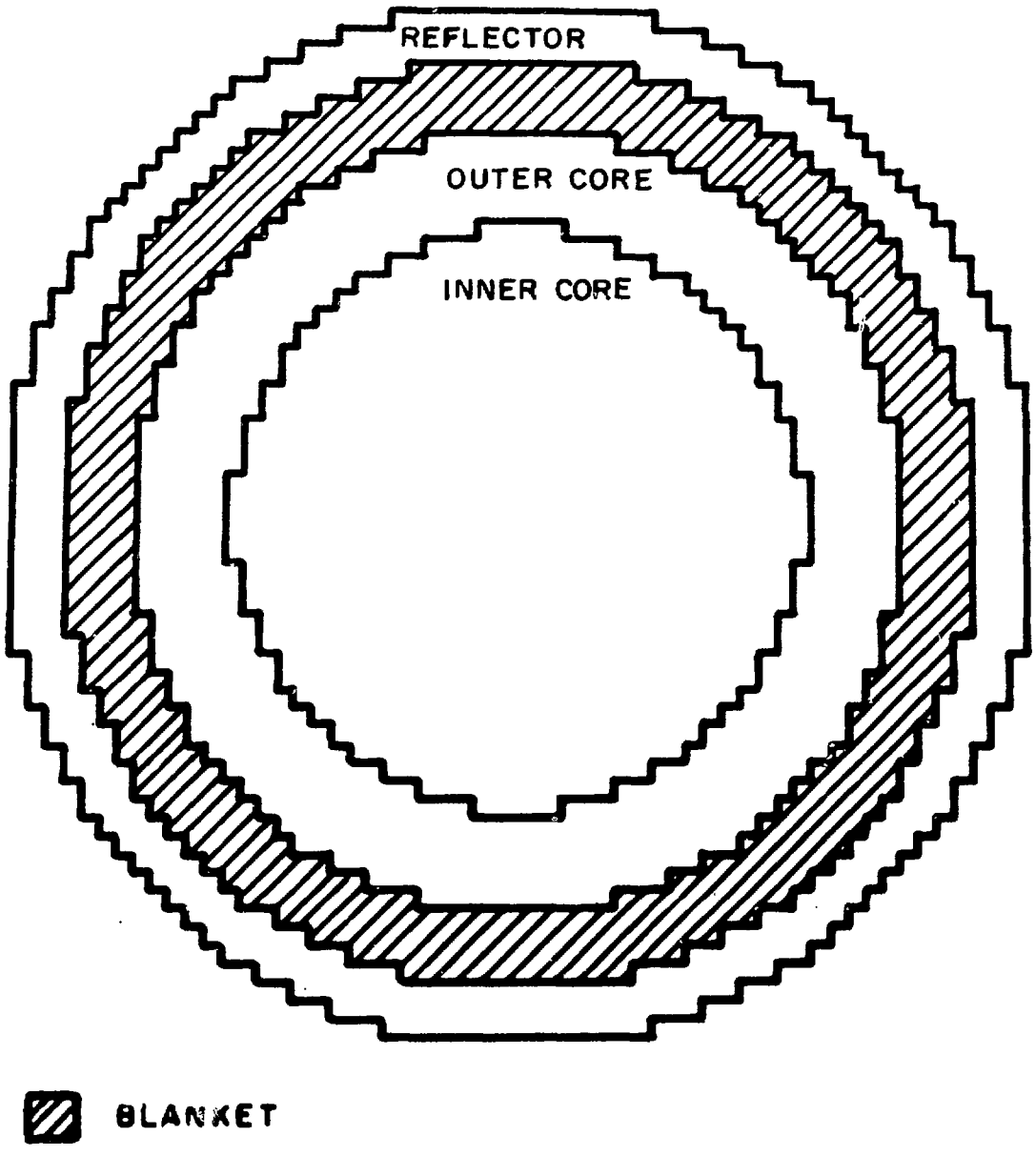

ZPPR – 9

Fig. VII.10

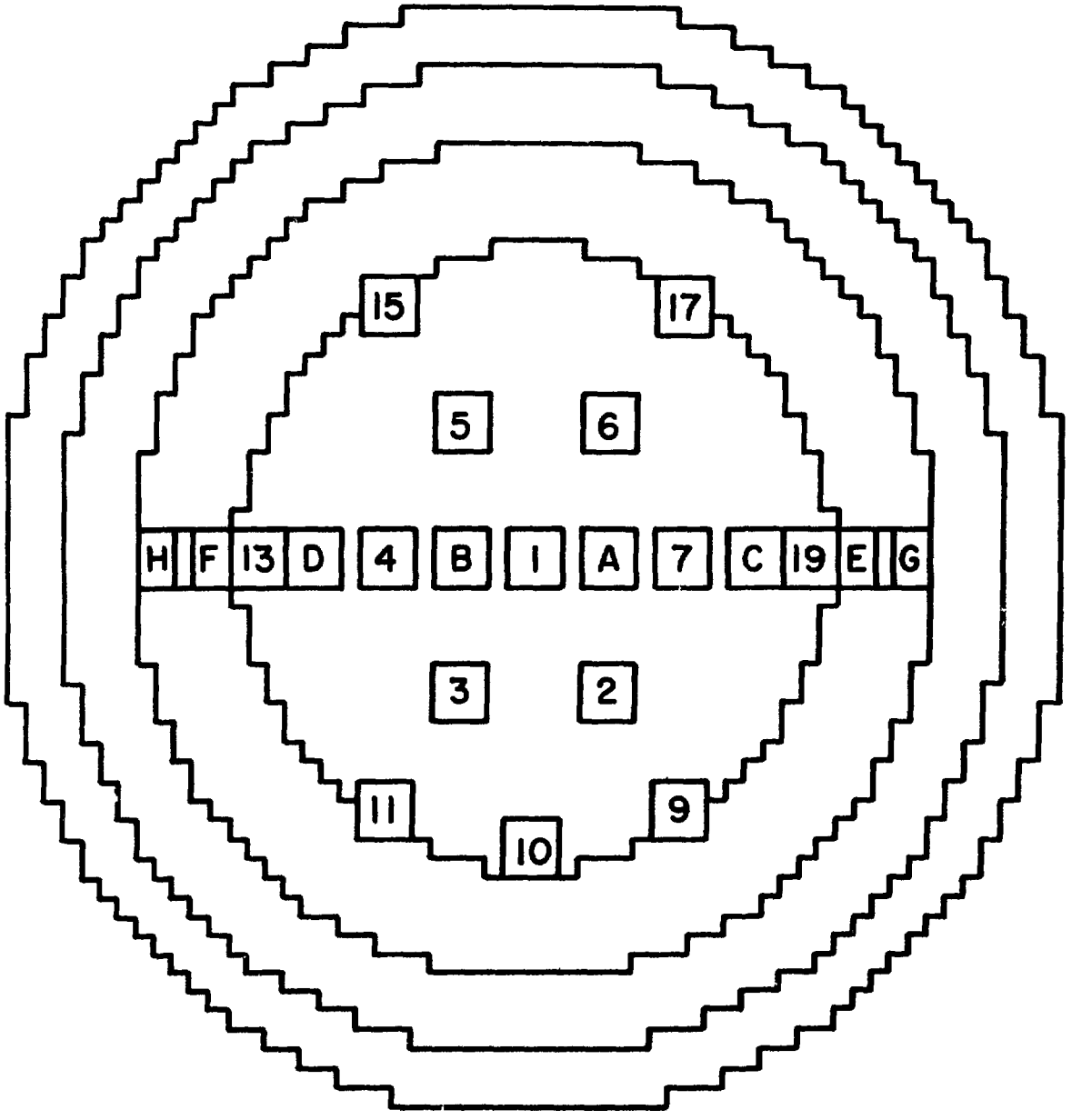

ZPPR – 9 WITH EXPERIMENTAL CONTROL RODS

Fig. VII.11

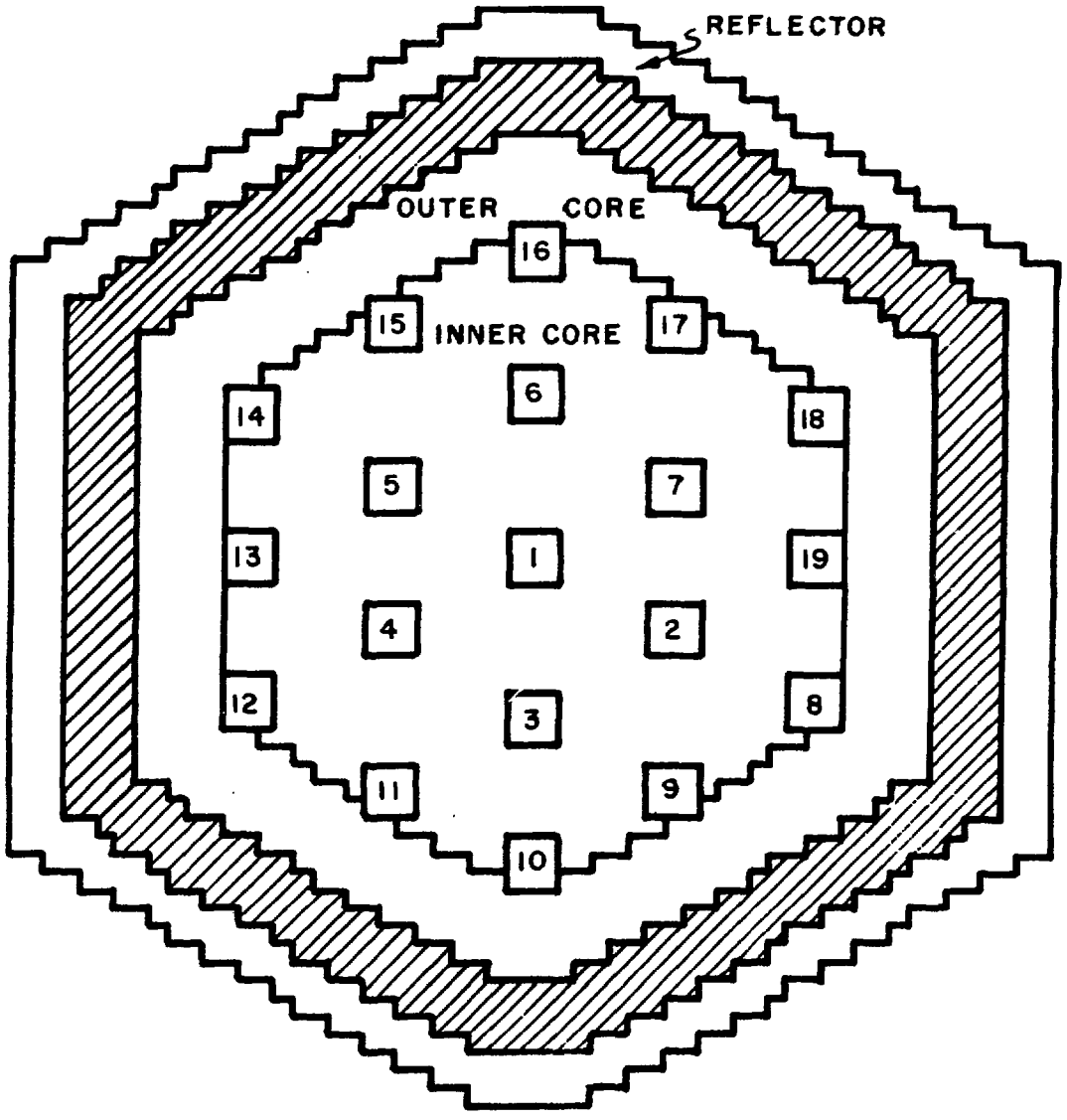

ZPPR-10A & 10B

Fig. VII.12

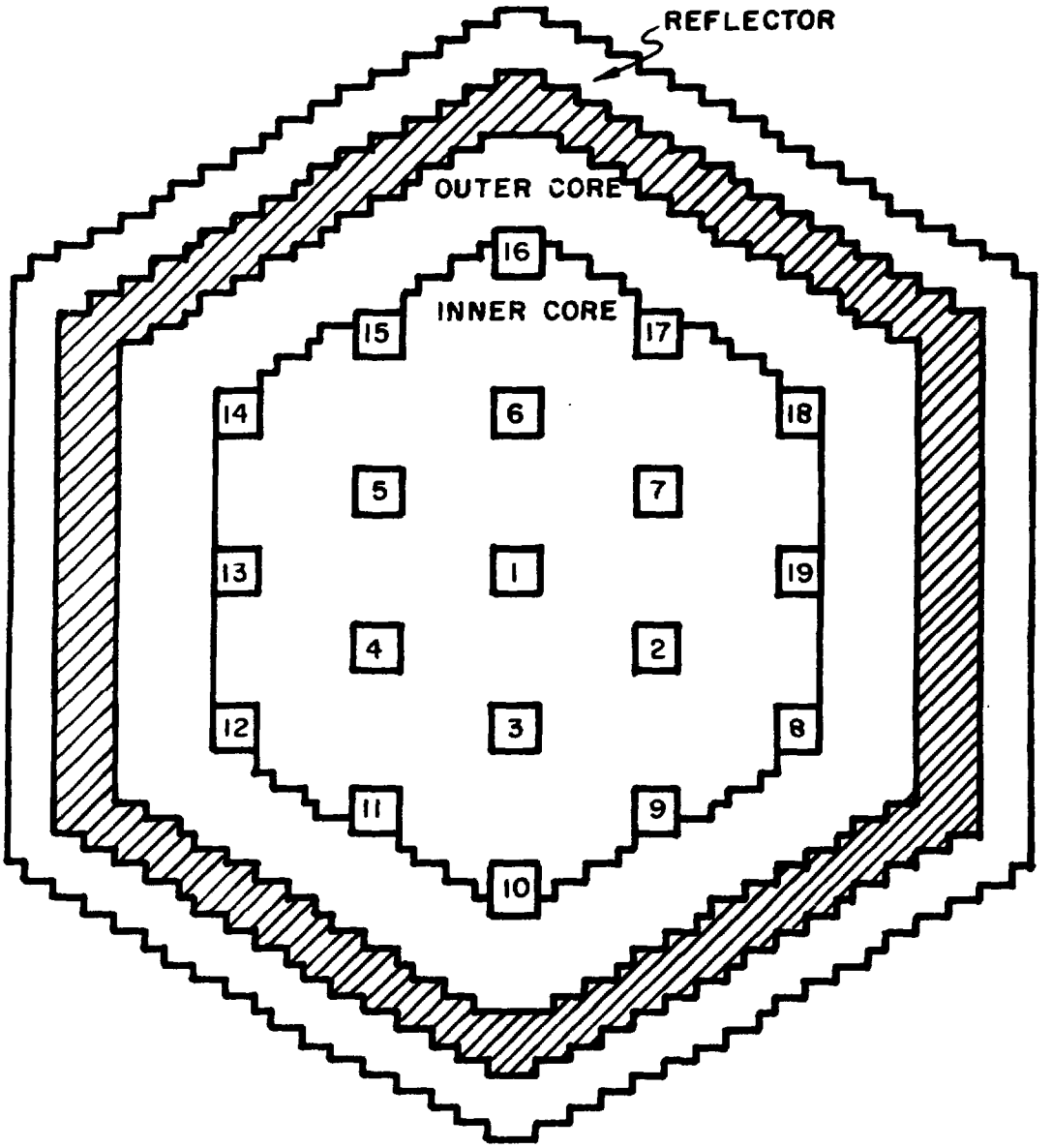

ZPPR-10C

Fig. VII.13

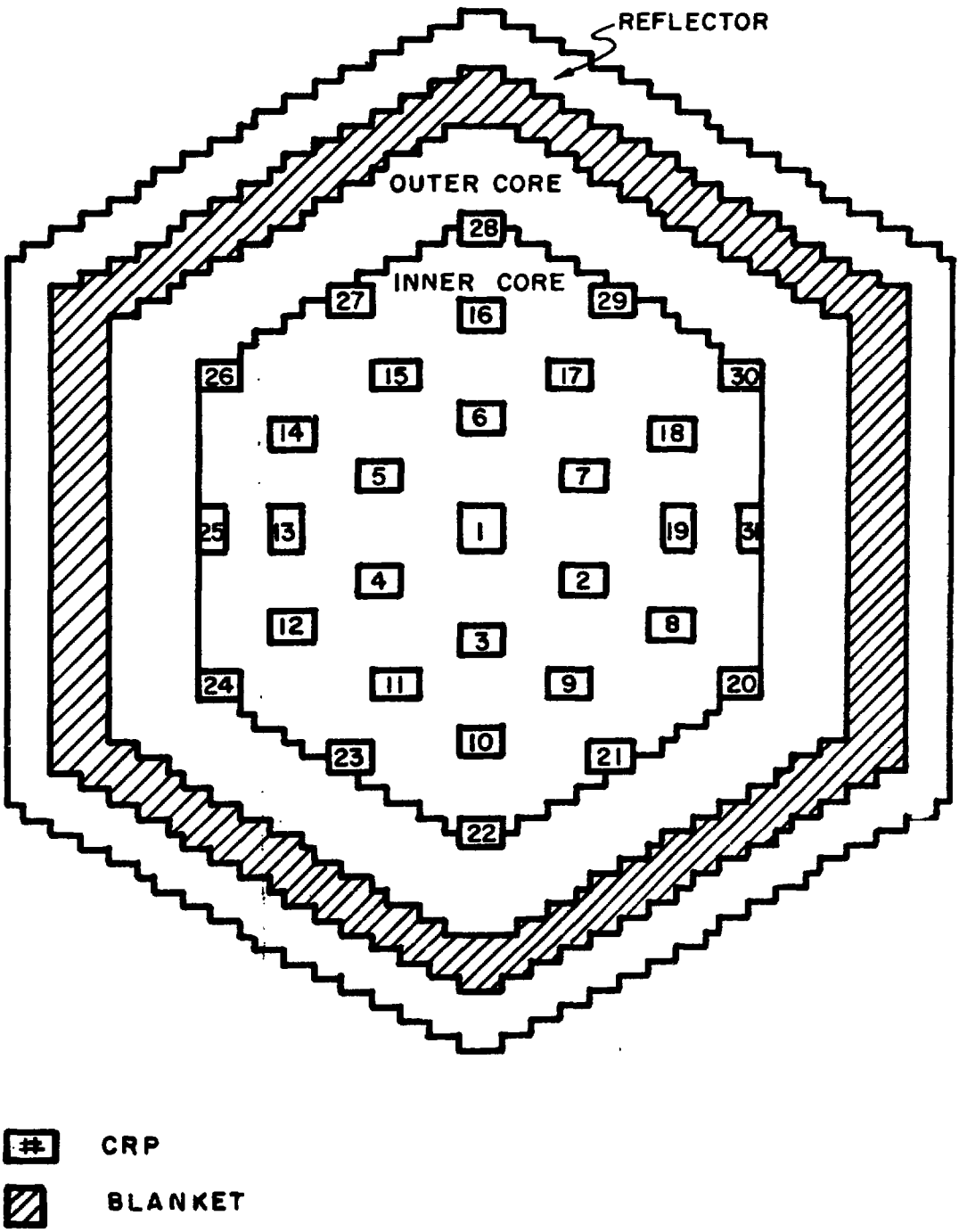
REFLECTOR
OUTER CORE
INNER CORE
28
27
29
16
26
15
17
30
6
14
18
5
7
25
13
1
19
4
2
12
8
3
24
11
9
20
10
23
21
22
#
CRP
BLANKET
ZPPR-10D

Fig. VII.14

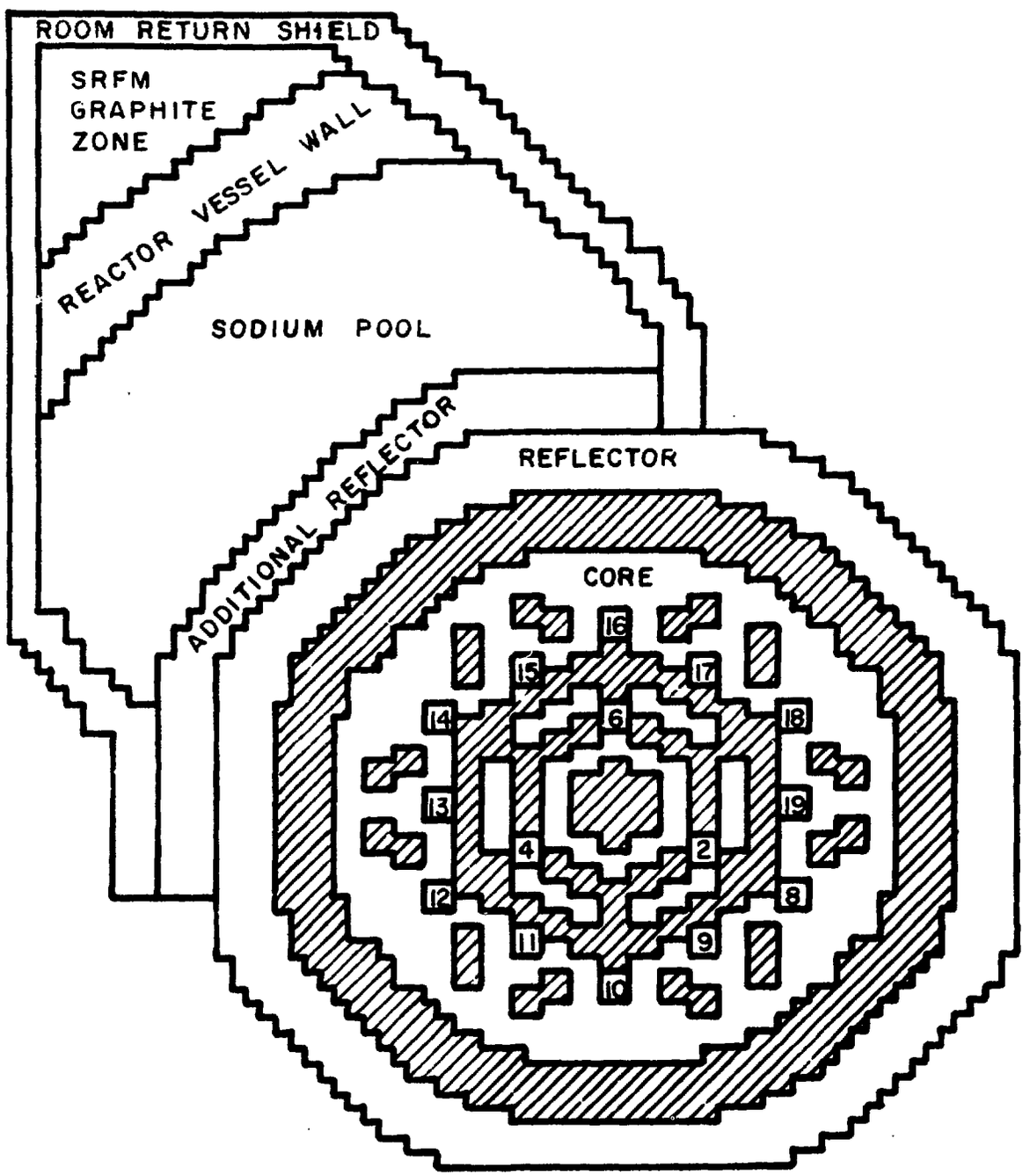

ZPPR 11A & 11F

Fig. VII.15

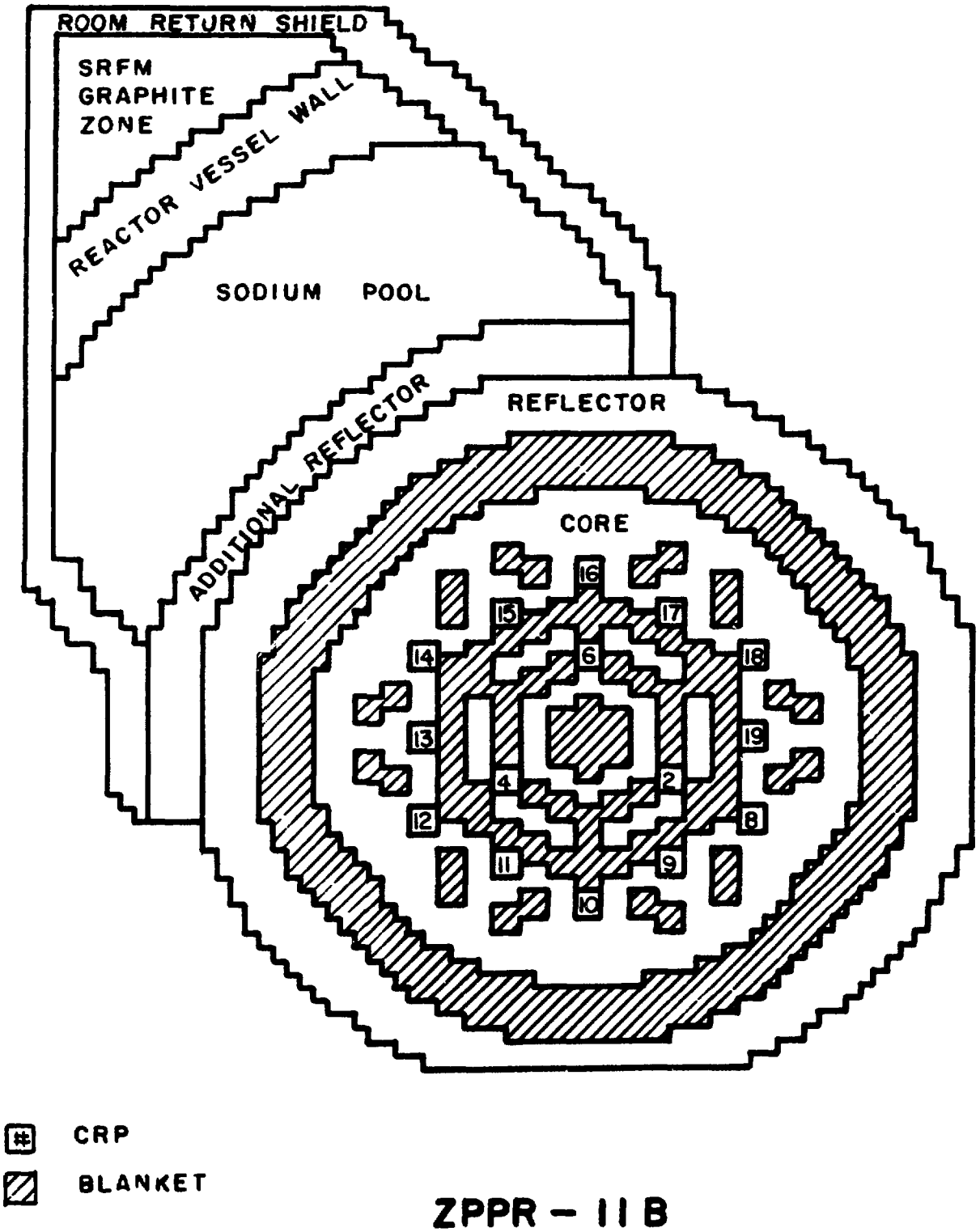
ROOM RETURN SHIELD
SRFM
GRAPHITE
ZONE
REACTOR VESSEL WALL
SODIUM POOL
ADDITIONAL REFLECTOR
REFLECTOR
CORE
16
15
17
14
6
18
13
19
4
2
12
8
11
9
10
CRP
BLANKET
ZPPR - 11 B

Fig. VII.16

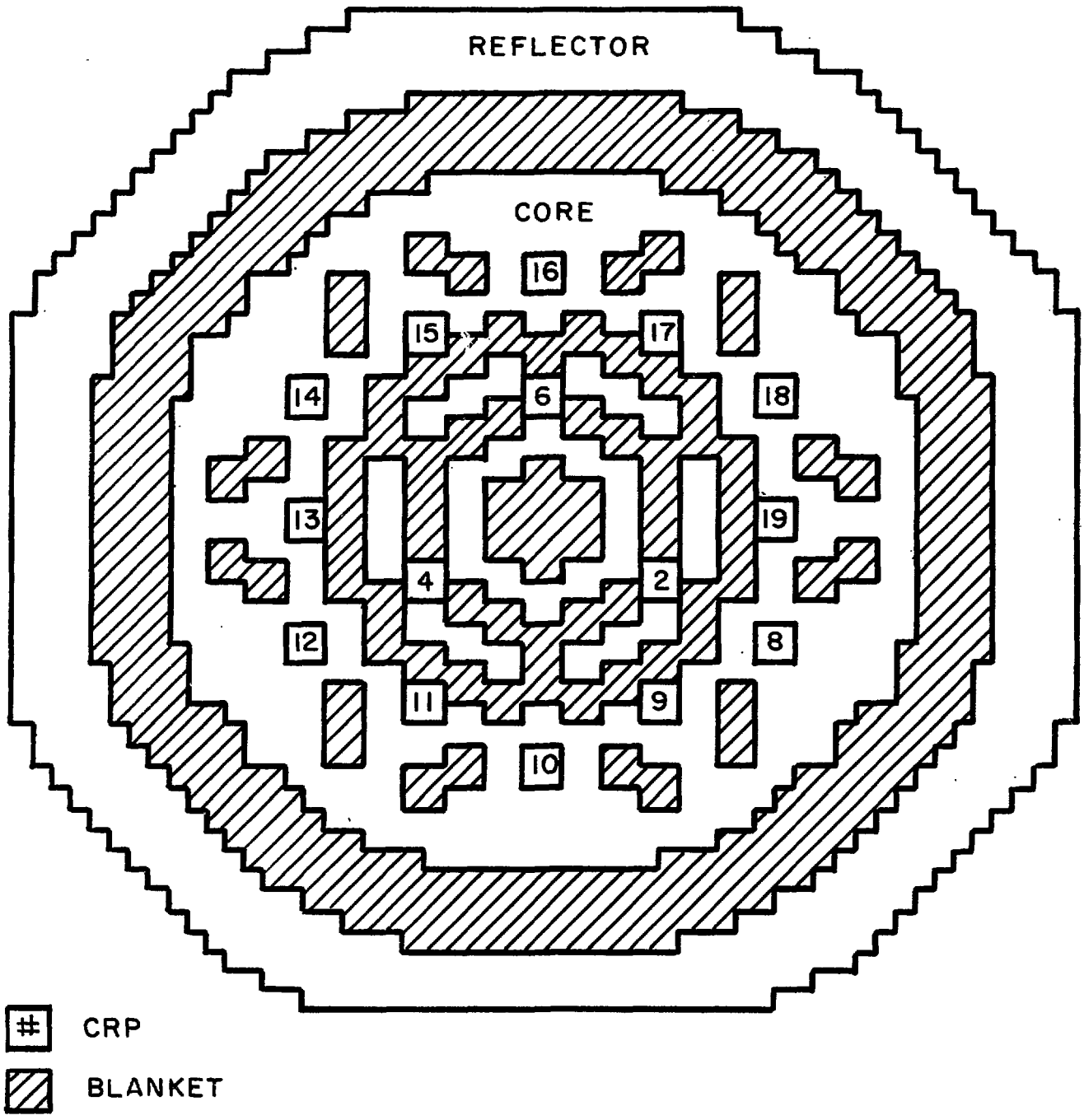

ZPPR IIC, IID, & IIE

Fig. VII.17

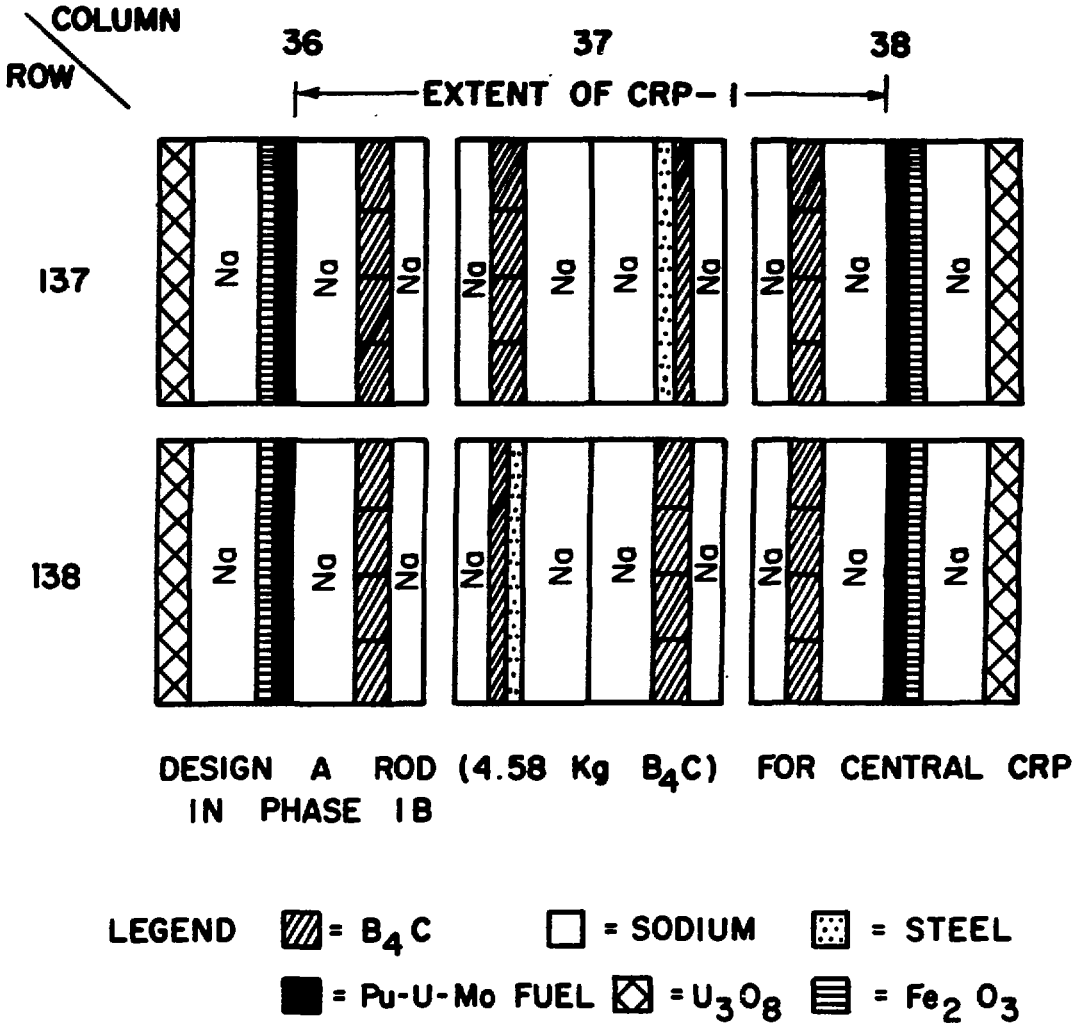

Fig. VII.18. Type A Control Rod Design Used in ZPPR-3/1B.

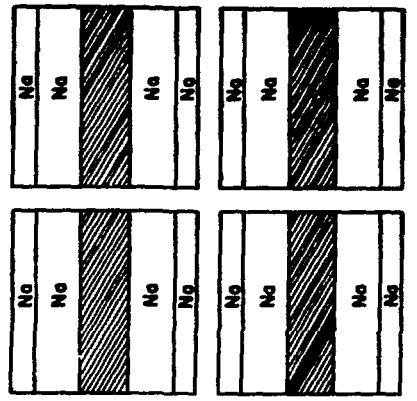

DESIGN H (5.62 Kg B_4C)
FOR CRP NOS.
2,3,4,5,6, &7.

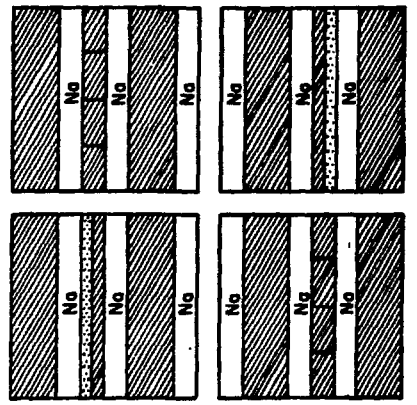

DESIGN I (13.16 Kg B_4C)
FOR CRP NOS.
8, 10, 12, 14, 16, & 18.

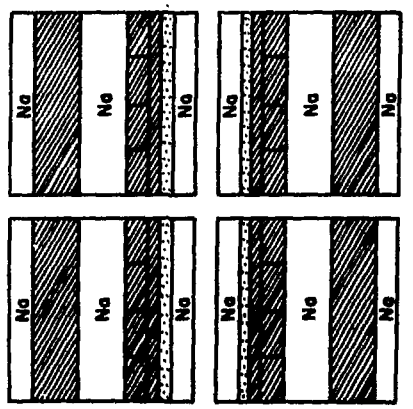

DESIGN J (8.60 Kg B_4C)
FOR CRP NOS.
9, 11, 13, 15, 17, & 19

LEGEND = B_4C = SODIUM = STEEL

Fig. VII.19. Type H,I,J Control Rod Designs Used in ZPPR-3/1B.

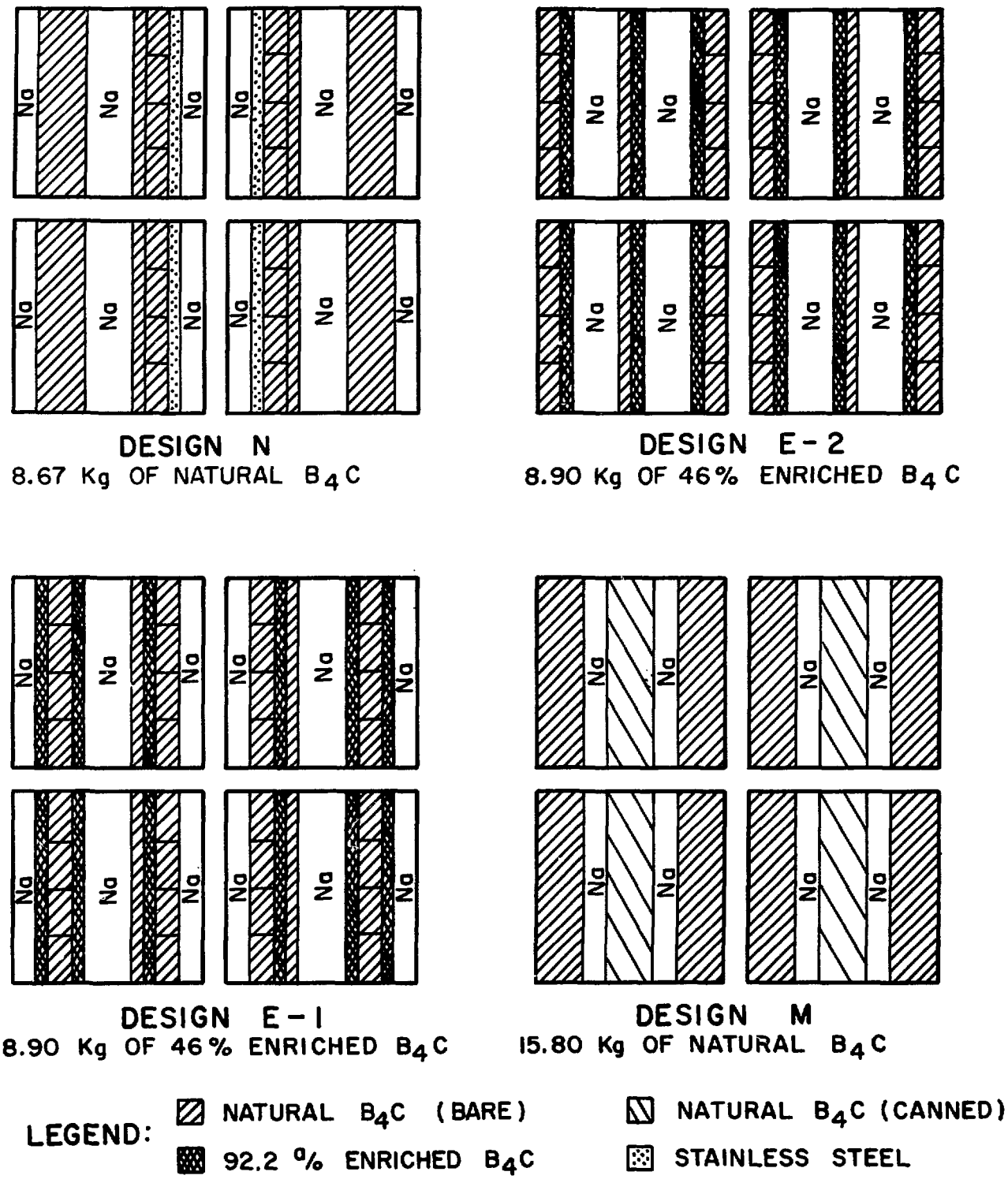

Fig. VII.20. Control Rod Designs Used in ZPPR-4.

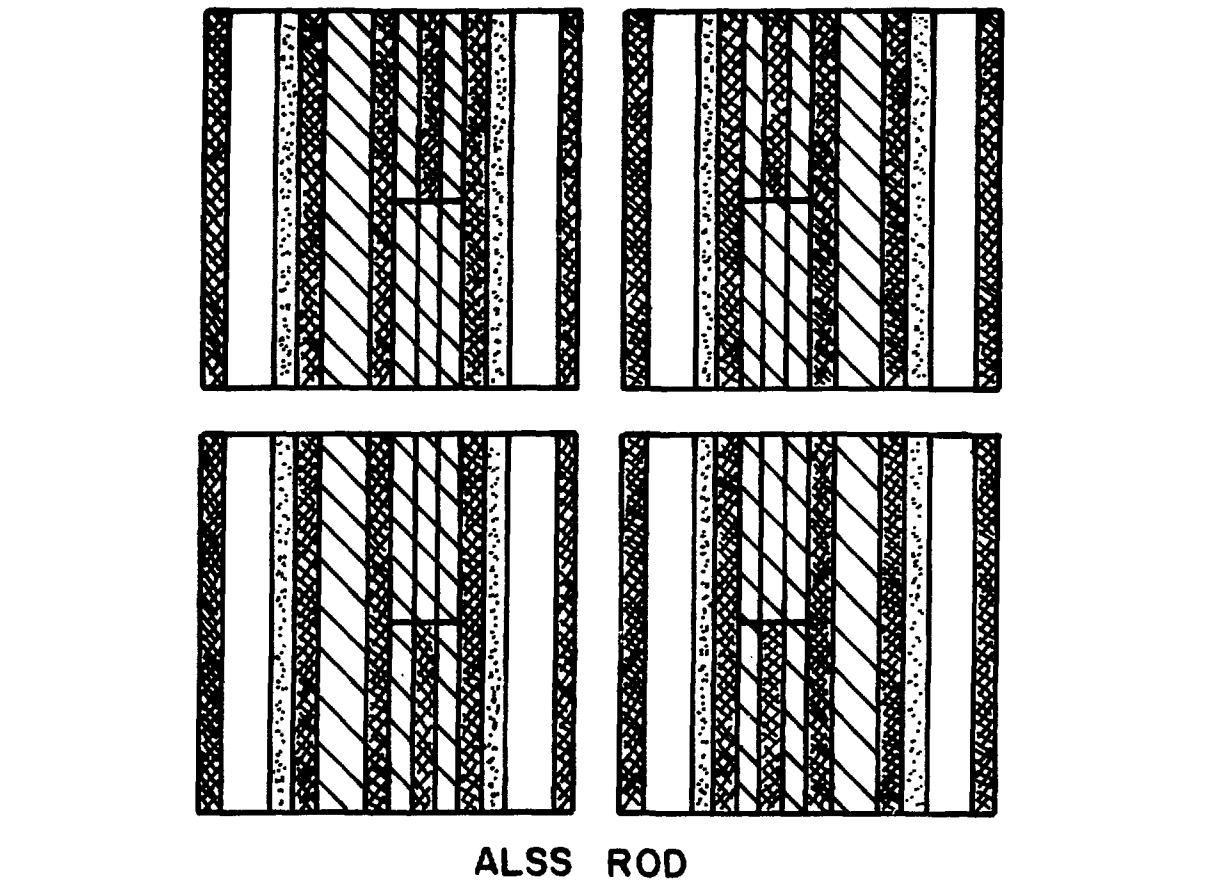

Fig. VII.21. Normal ALSS Control Rod Design
Used in ZPPR-6.

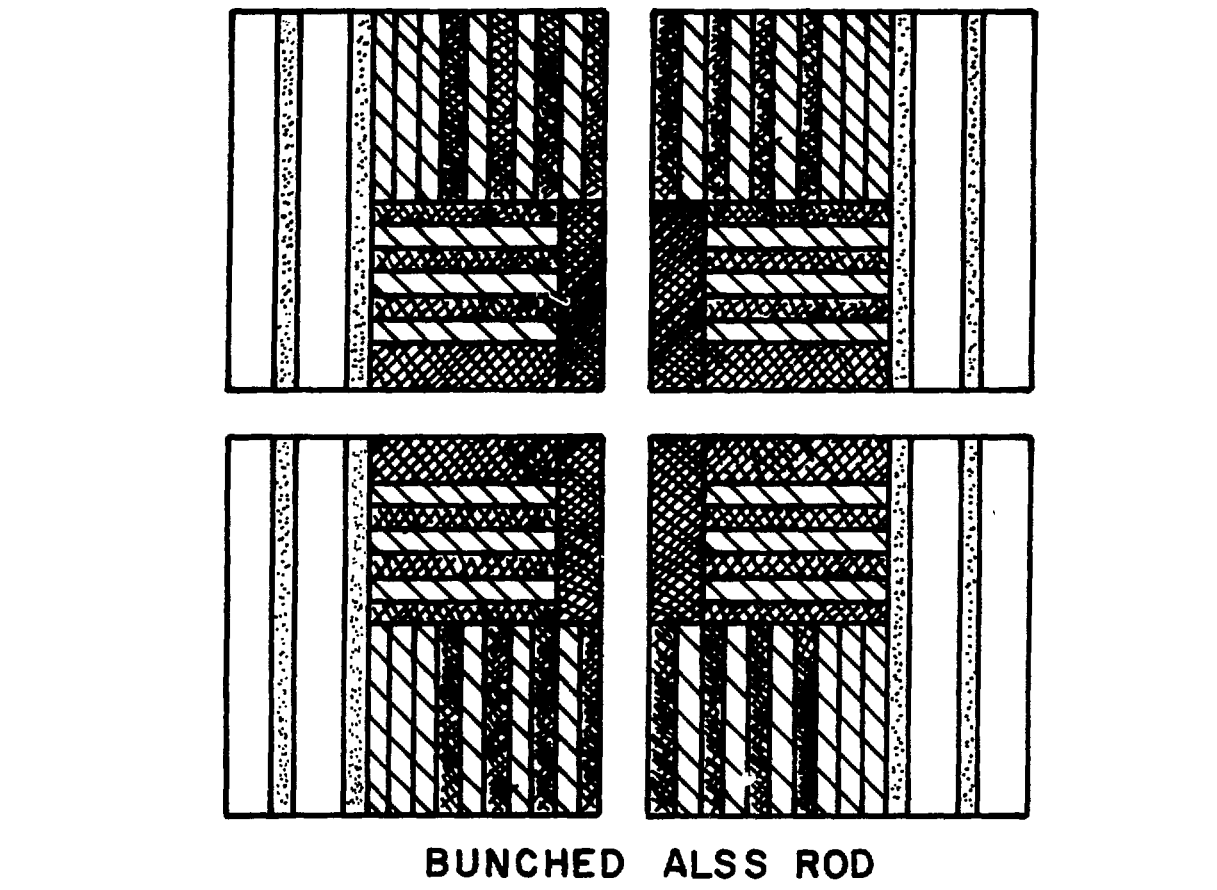

Fig. VII.22. Bunched ALSS Control Rod Design Used in ZPPR-6.

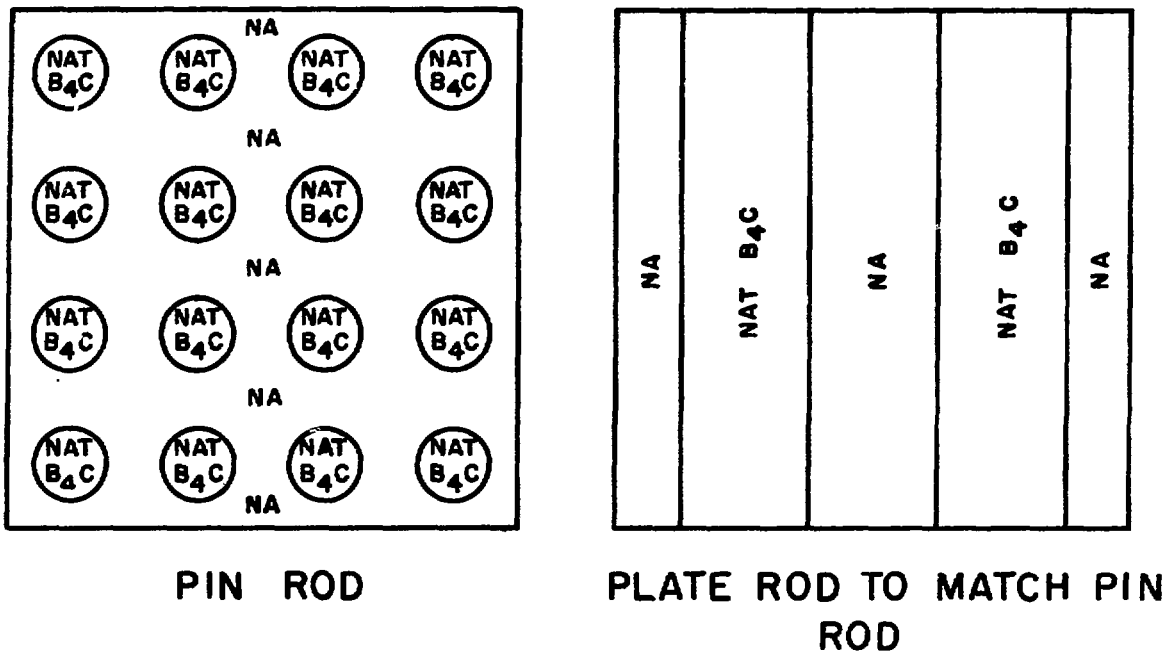

Fig. VII.23. Matched Composition Used Rods in ZPPR-6.

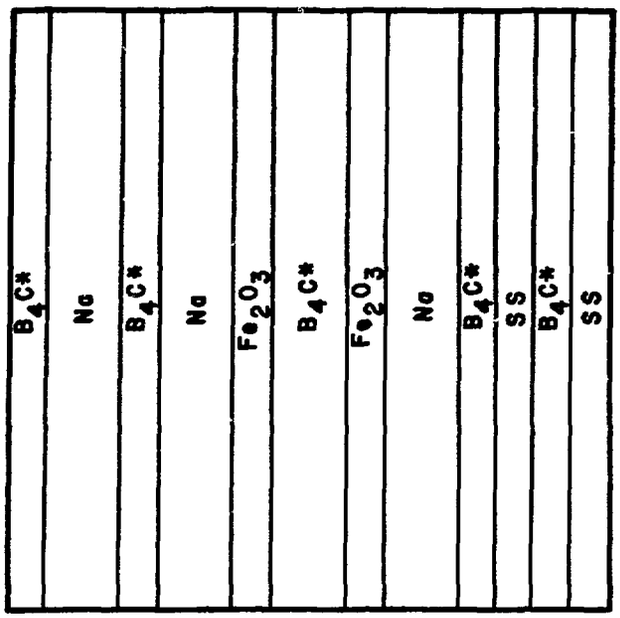

Enriched Control Rod Drawer Used
in ZPPR-7.

*92.2% enriched in ^{10}B.

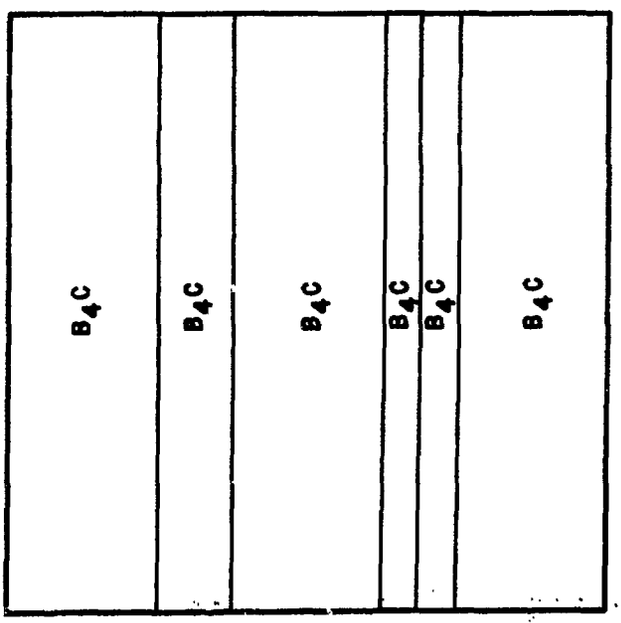

Normal ZPPR-7 Control Rod Drawer

Fig. VII.24. Designs of Drawers Used in ZPPR-7, -8, and -11 Control Rods.

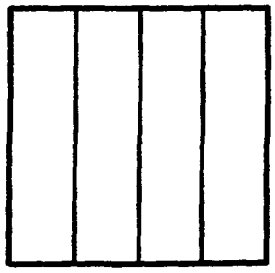

Normal Rod Drawer
for ZPPR-9

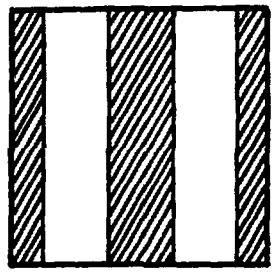

Normal Rod Drawer
for ZPPR-10

(See Fig. IV.3
for ZPPR-10 pin-
type rods)

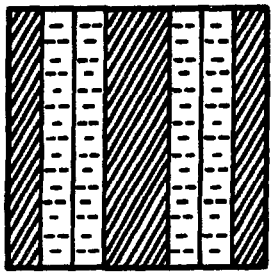

Eu_2O_3 Rod Drawer

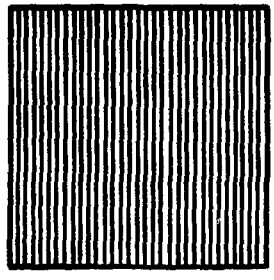

Ta Rod Drawer

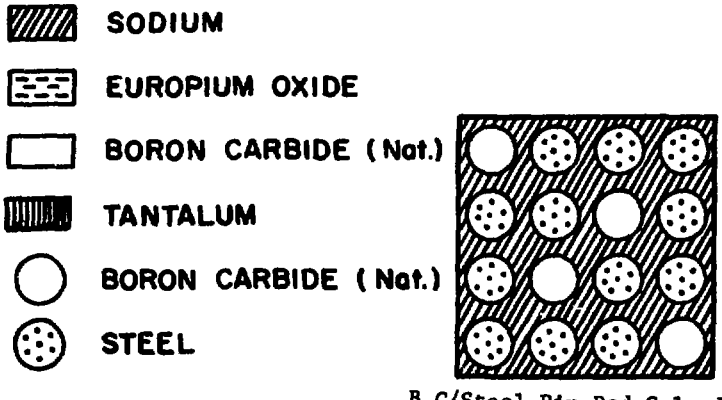

B_4C/Steel Pin Rod Calandria

Fig. VII.25. CR-Drawer Types Used in ZPPR-9.

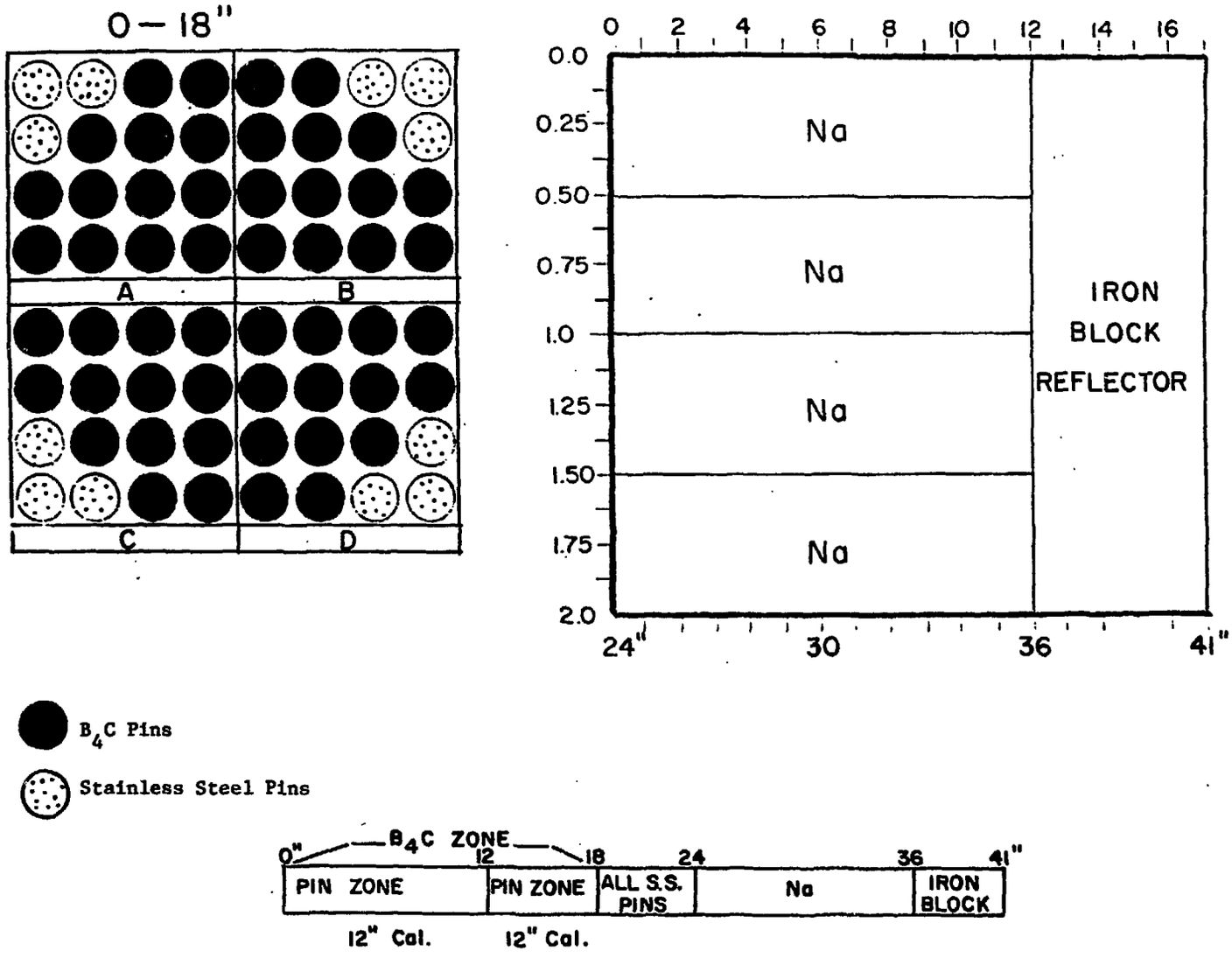

Fig. VII.26. Material Distribution in the Standard Pin Control Rod of ZPPR-11.

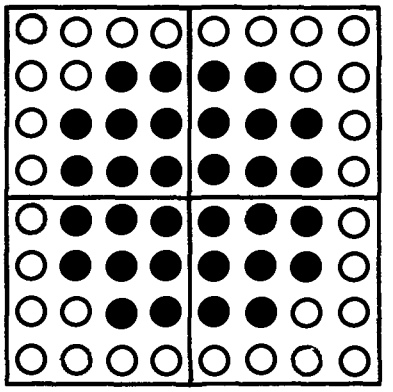

32-pin rod

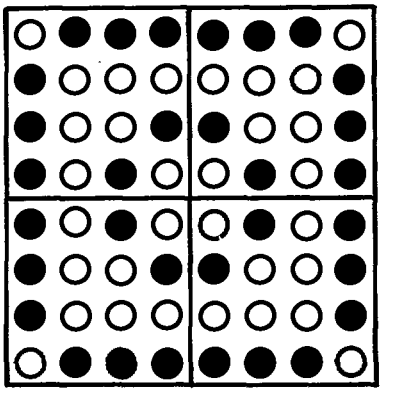

Spread out 32-pin rod

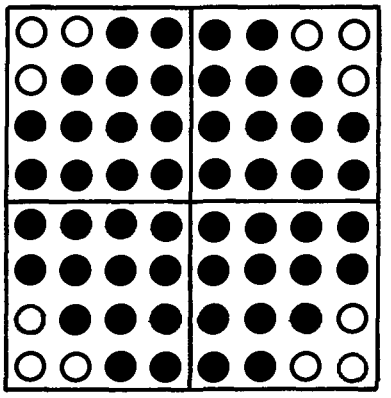

52-pin rod

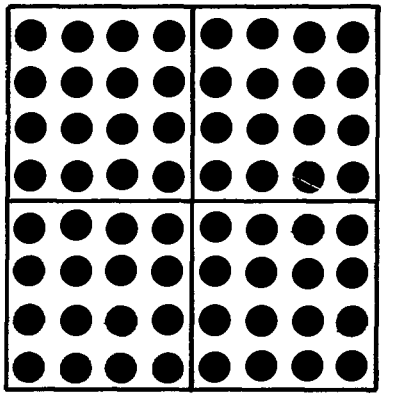

64-pin rod

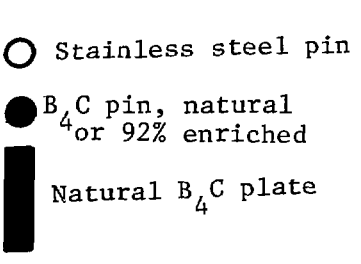

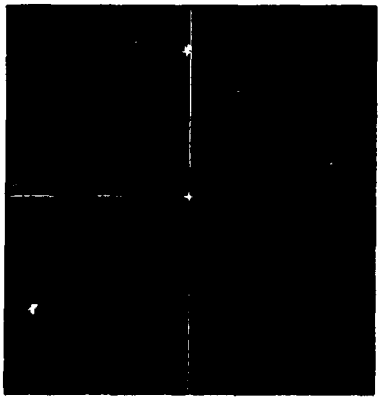

Normal plate rod

Fig. VII.27. Control Rods Used in ZPPR-11.

APPENDIX B: Other Control Rod Worth Measurements in ZPPR Assemblies 3-11

Not all control rod worth measurements in the ZPPR assemblies 3-11 could be included in the main text of this assessment. The reasons for not including data are several: (1) the experiments were not reduced in a consistent manner, (2) there were no consistent calculations, (3) the data did not fit into the topics as discussed, or (4) the data were redundant.

Additional data for control rods in ZPPR-3 are presented in Tables VII.9 through VII.11. No calculations are available to compare with these experiments, except those that were presented in Table III.5 for ZPPR-3/1B.

Table VII.12 gives additional measured control rod worths from ZPPR-4.

Table VII.13 gives the results for additional measurements in ZPPR-7B, -8F, -11B, and -11C. The measurements in ZPPR-8F, -11B, and -11C were to simulate highly-unlikely loading mistakes in the CRBR in which control rods are replaced by fresh fuel subassemblies. The effectiveness of dummy steel subassemblies in reducing the worth of the exchange was also tested.

Results of some additional control rod worth measurements in ZPPR-9 are presented in Table VII.14.

The ZPPR-11D control rod worth results are presented in Table VII.15. In Table VII.16, the effect of sodium voiding on control rod worth in ZPPR-11E is demonstrated. Results from ZPPR-11F, shown in Table VII.17, confirm those found for ZPPR-11B.

TABLE VII.9. Single Control-rod Worths Measured in ZPPR-3

Control Rod Inserted	Net Control-rod Worth[a], $, Relative to Reference Configuration					
	Phase/ 1A	1B	2	3	Sodium-Voided 3	Modified 3
A in 1	-1.50 ± 0.02	- -	- -	- -	- -	- -
A' in 1	- -	-2.13 ± 0.02	-1.94 ± 0.03	-2.18 ± 0.03	-1.95 ± 0.02	- -
B in 1	-1.68 ± 0.02	-2.48 ± 0.01	- -	- -	- -	- -
C in 1	-2.69 ± 0.05	-4.08 ± 0.03	- -	- -	- -	- -
F in 1	- -	-1.97 ± 0.02	- -	- -	- -	- -
G in 1	- -	-1.84 ± 0.02	- -	- -	- -	- -
H in 1	- -	- -	-2.14 ± 0.03	-2.41 ± 0.03	-2.24 ± 0.03	- -
I in 1	- -	-4.14 ± 0.15	-3.59 ± 0.13	-4.06 ± 0.06	-4.05 ± 0.05	- -
J in 1	- -	- -	- -	- -	- -	- -
N-1 in 1	- -	- -	- -	-3.35 ± 0.03	- -	- -
M in 1	- -	- -	- -	-4.60 ± 0.06	- -	- -
E-1 in 1	- -	- -	- -	-4.71 ± 0.05	- -	- -
E-2 in 1	- -	- -	- -	-4.72 ± 0.05	- -	- -
Ta in 1	- -	-2.75 ± 0.08	- -	- -	- -	- -
B in 2	-1.49 ± 0.02	-2.01 ± 0.02	- -	- -	- -	- -
C in 2	- -	-3.36 ± 0.02	- -	- -	- -	- -
H in 2	- -	-2.02 ± 0.01	- -	- -		-2.27 ± 0.02
Ta in 2	- -	- -	- -	- -	- -	- -
H in 5	- -	- -	-1.76 ± 0.02	-1.88 ± 0.03	-1.77 ± 0.02	- -
H in 7	- -	- -	-1.87 ± 0.02	-2.24 ± 0.03	-1.95 ± 0.02	- -
N-1 in 7	- -	- -	- -	-2.82 ± 0.05	- -	- -
M in 7	- -	- -	- -	-3.89 ± 0.04	- -	- -
C in 8	-1.51 ± 0.02	-1.93 ± 0.01	- -	- -	- -	- -
E in 8	- -	-1.87 ± 0.01	- -	- -	- -	- -
I in 8	- -	-1.94 ± 0.02	-1.87 ± 0.03	- -	- -	-1.47 ± 0.02
Ta in 8	- -	-1.35 ± 0.01	- -	- -	- -	- -
D in 9	-1.27 ± 0.01	- -	- -	- -	- -	- -
J in 9	- -	-1.97 ± 0.03	-1.78 ± 0.01	-1.85 ± 0.03	-1.82 ± 0.02	- -
Ta in 9	- -	-1.70 ± 0.02	- -	- -	- -	- -

TABLE VII.9. Single Control-rod Worths Measured in ZPPR-3 (con't)

Control Rod Inserted	Net Control-rod Worth[a], $, Relative to Reference Configuration					
	Phase/ 1A	1B	2	3	Sodium-Voided 3	Modified 3
C in 10	- -	-2.06 ± 0.02	- -	- -	- -	- -
I in 10	- -	-2.07 ± 0.02	- -	- -	- -	-1.34 ± 0.02
Ta in 10	- -	-1.47 ± 0.01	- -	- -	- -	- -
J in 11	- -	- -	-2.10 ± 0.03	-2.10 ± 0.03	-1.98 ± 0.02	- -
J in 15	- -	- -	-1.80 ± 0.01	-1.74 ± 0.02	-1.73 ± 0.02	- -
I in 16	- -	- -	-2.22 ± 0.04	- -	- -	- -
J in 17	- -	-2.16 ± 0.03	- -	- -	- -	- -
N-1 in 17	- -	- -	- -	-2.15 ± 0.02	- -	- -
M in 17	- -	- -	- -	-2.88 ± 0.03	- -	- -
E-2 in 17	- -	- -	- -	-2.95 ± 0.03	- -	- -
Ta in 17	- -	-1.88 ± 0.03	--	- -	- -	- -

[a]Statistical errors only; total uncertainty on the order of 3-5%. See Appendix A for rod and configuration descriptions.

TABLE VII.10. Multiple Control-rod Worths Measured in ZPPR-3

Number of Inserted CRs Excluding Reference CR Pattern	CR Positions Loaded with B_4C Excluding Reference CR Pattern	Net Configuration Worth[a], $, Relative to Reference Phase Configuration				
		1A	1B	2	3	Sodium Voided 3
2	2,5	-3.08 ± 0.03	-4.26 ± 0.02	- -	- -	- -
2	2,8	- -	-3.58 ± 0.02	- -	- -	- -
2	2,9	- -	-3.66 ± 0.02	- -	- -	- -
2	8,9	- -	-3.42 ± 0.02	- -	- -	- -
2	8,14	-3.47 ± 0.03	-4.24 ± 0.02	- -	- -	- -
3	2,4,6	-4.62 ± 0.05	-6.51 ± 0.04	- -	- -	- -
3	3,5,7	- -	- -	-5.76 ± 0.04	-6.54 ± 0.02	-5.71 ± 0.08
3	2,8,9	- -	-4.85 ± 0.02	- -	- -	- -
3	8,12,16	- -	- -	-7.40 ± 0.05	- -	- -
6	2,4,6,10,14,18	-9.52 ± 0.10	-14.33 ± 0.07	Ref.	- -	- -
6	8,10,12,14,16,18	-10.00 ± 0.10	-14.88 ± 0.08	- -	- -	- -
6	3,5,7,8,12,16	- -	- -	-13.88 ± 0.10	- -	- -
6	9,11,13,15,17,19	- -	- -	-13.03 ± 0.09	- -	- -
9	2,4,6,8,10,12,14,16,18	- -	-22.65 ± 0.14	- -	Ref.	Ref.
9	2,3,4,5,6,7,10,14,18	- -	-20.53 ± 0.14	- -	- -	- -
9	3,5,7,9,11,13,15,17,19	- -	- -	- -	-21.04 ± 0.07	-18.55 ± 0.26
12	2-8,10,12,14,16,18	- -	-30.12 ± 0.21	- -	- -	- -
12	8-19	-18.9 ± 0.2	-28.96 ± 0.17	- -	- -	- -
12	2,4,6,9,10,11,13,14,15,17,18,19	- -	-28.99 ± 0.20	- -	- -	- -
12	3,5,7,8,9,11,12,13,15,16,17,19	- -	- -	-27.43 ± 0.19	- -	- -
18	All except CRP-1	-30.1 ± 0.3	-44.76 ± 0.30	- -	- -	- -

[a]Statistical error only; total uncertainties on the order of 5%. See Appendix A for rod and configuration descriptions.

TABLE VII.11. Ta Control Rod Worth Measured in ZPPR-3/1B

Position Number[a]	Worth[b], $
1	2.75 ± 0.084
2	2.28 ± 0.075
8	1.35 ± 0.012
9	1.70 ± 0.019
10	1.47 ± 0.012
17	1.88 ± 0.029
8-19	20.93

[a]98 kg Ta per rod.

[b]Single rod worths measured by inverse kinetics; outer ring rod worth measured by MSM.

TABLE VII.12. Additional Single Rod Worth Measurements in ZPPR-4/1

Positions[a] with Rods Inserted	Rod Design[b]	Worth[c], $
13	A	- 1.16
13	N	- 1.71
13	I	- 2.10
13	M	- 2.28
6	N	- 2.91
14	N	- 1.32

[a]See Fig. VII.2.

[b]See Figs. VII.18 - VII.20 and Tables VII.1 and VII.2.

[c]Relative uncertianties about 1%.

TABLE VII.13. Additional Control Rod Worth Measurements in ZPPR-7B, -8F, -11B, and 11C

Assembly	CRs	Worth, $	C/E[a]
7B	8,10,12,14,16,18[b]	17.10	1.059
8F[c]	16[c]	11.43	1.125
8F	16[d,c]	7.53	1.144
8F	10[d,c]	11.95	1.145
8F	16[e,c]	8.50	1.131
8F	10[e,c]	12.57	1.138
8F	16[f,c]	10.24	1.093
11B	16	9.84[c]	1.029
11B	10	9.71[c]	1.029
11C	10	7.15[c]	1.042

[a]Refer to Section III.B for calculation descriptions for each assembly.

[b]Adjacent core subassemblies replaced by blanket subassemblies just inside the rods.

[c]Rod removed from configuration with six outer-ring corner rods inserted and replaced by fuel subassembly. Worths are positive changes in reactivity.

[d]Dummy steel subassembly replacing fuel subassembly adjacent to CR-16.

[e]Steel subassemblies adjacent to CRs-8,12,16.

[f]Steel subassemblies adjacent to CRs-8,10,12,14,16,18.

TABLE VII.14. Special Control Rod Worth Measurements in ZPPR-9

Configuration	Worth Relative to Reference, $	C/E[c]	Worth Relative to CRPs, $	C/E[c]
CRP 1, CR 2-7	16.85 ± 0.20	1.022	---	---
CRP 1; CR 9,11,13,15,17,19	19.04 ± 0.27	1.044	---	---
CRP 10	0.37 ± 0.004	1.252	---	---
CR 10	1.73 ± 0.02	1.046	1.37 ± 0.02	0.989
CR 1 (ZPPR-10 Design)	2.86 ± 0.03	1.043	2.30 ± 0.03	1.004
Stainless Steel in 1	0.78 ± 0.01	1.226	---	---
(2x3)[a] CRP 1	0.39 ± 0.004	1.200	---	---
(2x3) CR 1	2.73 ± 0.03	1.027	2.34 ± 0.03	1.010
(2x2) CRP 1	0.27 ± 0.003	1.198	---	---
(2x2) CR 1	2.16 ± 0.02	1.045	1.89 ± 0.02	1.023
(2x2) Eu_2O_3 CR 1	1.43 ± 0.02	1.074	1.16 ± 0.02	1.046
(2x2) Ta CR 1	1.67 ± 0.02	1.069	1.41 ± 0.02	1.044
(2x3) CR 13	1.41 ± 0.02	1.068	---	---
(2x2) CR 13	1.18 ± 0.01	1.077	---	---
CRP 19; Pin[b] CR 13	1.34 ± 0.02	1.193	0.59 ± 0.02	1.073
Pin CR 13, CR 19	3.08 ± 0.04	1.087	2.32 ± 0.04	1.018
Pin CR 13,19	2.02 ± 0.02	1.149	1.26 ± 0.02	1.066

[a]Cross section is 2 matrix positions by 3 matrix positions rather than the normal 3x3.

[b]Pin rod has 10% of ^{10}B content of normal ZPPR-9 rods.

[c]Refer to Table III.17, Fig. VII.25, and Table VII.5.

TABLE VII.15. Control Rod Worth Results from ZPPR-11D

Positions[a] with Rods Inserted	Measured Worth,[b] $	C/E[c]
2,4,6	6.34	0.942
9,11,13,15,17,19	14.77	0.979

[a]See Fig. VII.17 for position identification. Normal ZPPR-11 CRs; see Fig. VII.24 and Table VII.8. Six outer ring corner rods 1/3 inserted in reference configuration.

[b]Uncertainties 2.5%.

[c]9-group diffusion theory calculation in xyz geometry; 1 mesh space per drawer. β_{eff} = 0.3435% Δk.

TABLE VII.16. Control Rod Worths in ZPPR-11E, Including Variation with Sodium Void

Rod Configuration[a]	Core Sodium Condition	Measured Rod Worth[b], $
Row 7 corner rods (8,10,12,14,16,18) fully inserted	Totally flooded	16.00 ± 0.02
Fully Inserted	Two inner fuel rings voided thru Row 5)	16.23 ± 0.02
Fully Inserted	Fuel voided thru Row 7	16.24 ± 0.02
Fully Inserted	Fuel voided thru Row 8	16.15 ± 0.02
Fully Inserted	Fuel voided thru Row 9	16.02 ± 0.02
All 15 rods parked at top of core	Totally flooded	1.03 ± 0.001

[a]See Fig. VII.17 for position identification. Normal ZPPR-11 rods, see Fig. VII.24 and Table VII.8.

[b]Only statistical (relative) uncertainties are shown. There is an additional correlated uncertainty on the order of 1.5%.

TABLE VII.17. Control Rod Worth Results from ZPPR-11F

Positions[a] with Rods Inserted	Measured Worth,[b] $	C/E[c]
6	1.365 ± 0.015	0.942
16	1.693 ± 0.019	0.985
8,10,12,14,16,18	17.06 ± 0.19	0.983
	$\overline{C/E}$ = 0.970 ± 0.024	

[a]See Fig. VII.15 for position identification. Normal ZPPR-11 rods; see Fig. VII.24 and Table VII.8.

[b]Includes correlated reactivity normalization uncertainty.

[c]9-group diffusion theory calculations in xyz geometry; 1 mesh space per drawer. β_{eff} = 0.3351% Δk.

APPENDIX C: Statistical Analyses of C/E Distributions for Control Rod Worths

The C/E results that were presented in Section III.B have undergone further statistical analyses. This involved:

i. Arrangement of C/E data into 20 logical sets, involving considerable overlap between some data sets.

ii. Determination of a weighted average C/E and standard deviation for each data set.

iii. Generation of a bias factor and an uncertainty for each data set.

Table VII.18 presents a summary of the results of these analyses. Figures VII.28 - VII.47 show the individual C/E distributions. Using these results it is seen that for the range of cores in the study, biased rod worth calculations have accuracies in the range of 1-4%.

TABLE VII.18. Summary of Statistical Analyses of C/E Distributions for 20 Subsets of Data

No. of Data Points	Core Size, MWe	Core Type	Mesh, MPD	Rod Locations	$\overline{C/E}$	Bias Factor	Prediction Uncertainty, %
49	350	Hom.	4	Any	1.108±0.019	0.902	1.1
65	350	Het.	4	Any	1.030±0.034	0.966	2.8
60	350	Het.	1	Any	0.973±0.027	1.035	3.7
19	350	Hom.	1	Any	1.055±0.016	0.948	1.6
85	350	Both	4	Any	1.040±0.040	0.945	3.5
48	700-900	Hom.	1	Any	1.042±0.018	0.951	2.0
7	350	Hom.	4	Central	1.107±0.014	0.899	1.1
4	700-900	Hom.	1	Central	1.023±0.009	0.979	0.9
11	350	Hom.	4	Inner	1.101±0.030	0.913	2.3
18	350	Het.	4	Inner	0.999±0.010	1.001	0.8
9	700-900	Hom.	1	Inner	1.032±0.020	0.958	2.7
11	350	Het.	1	Inner	0.921±0.021	1.089	2.7
21	350	Hom.	4	Mixed	1.110±0.014	0.901	---
12	700-900	Hom.	1	Mixed	1.043±0.009	0.956	1.0
14	350	Het.	4	Mixed	1.043±0.031	0.958	2.7
9	350	Het.	1	Mixed	0.963±0.014	1.051	2.9
10	350	Hom.	4	Outer	1.113±0.019	0.898	1.2
34	350	Het.	4	Outer	1.057±0.024	0.949	1.8
19	700-900	Hom.	1	Outer	1.069±0.018	0.936	1.3
40	350	Het	1	Outer	0.984±0.012	1.016	2.0

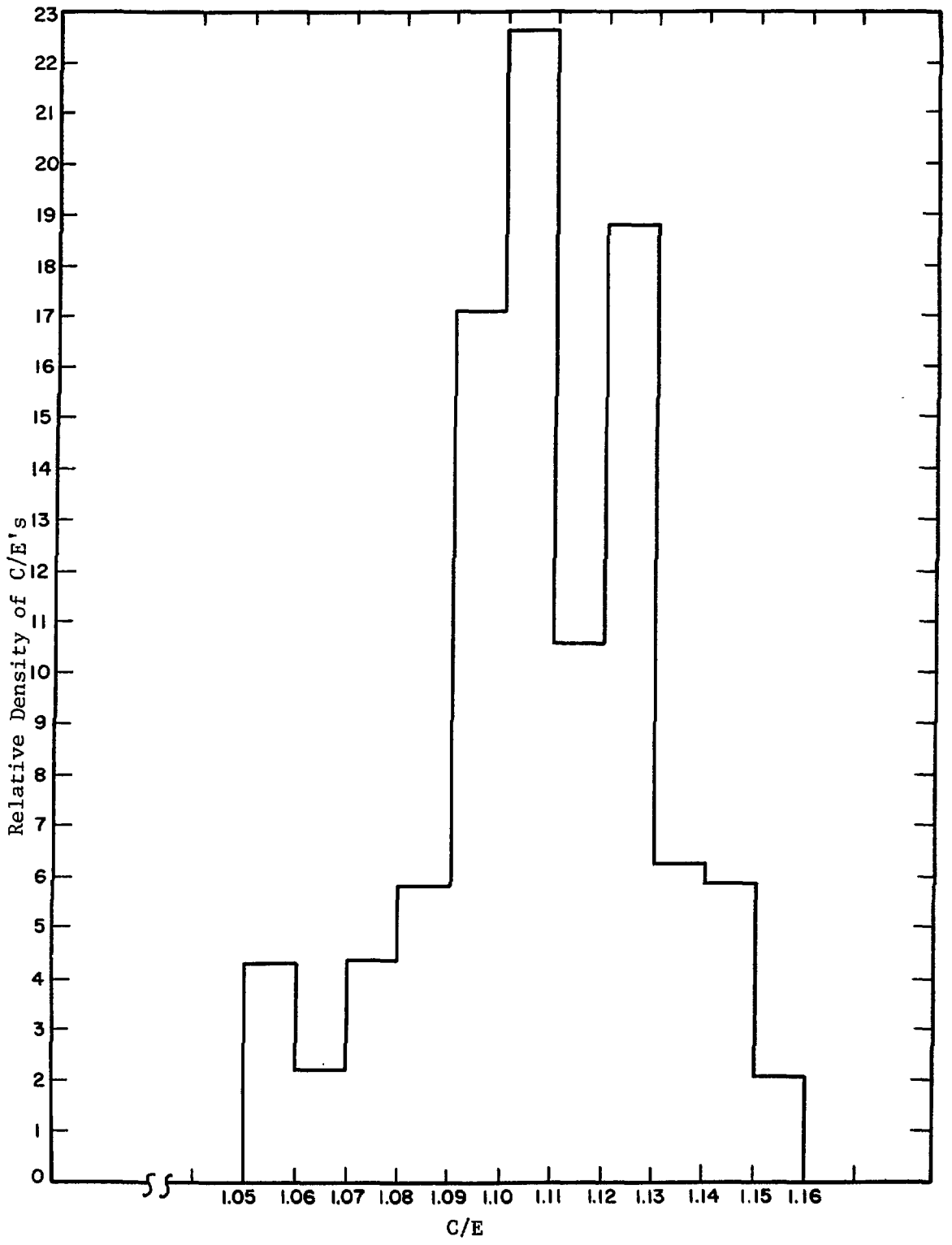

Fig. VII.28. Weighted Distribution of C/E's for 49 Control Rod Worth Measurements in 350 MWe Size Homogeneous Assemblies.

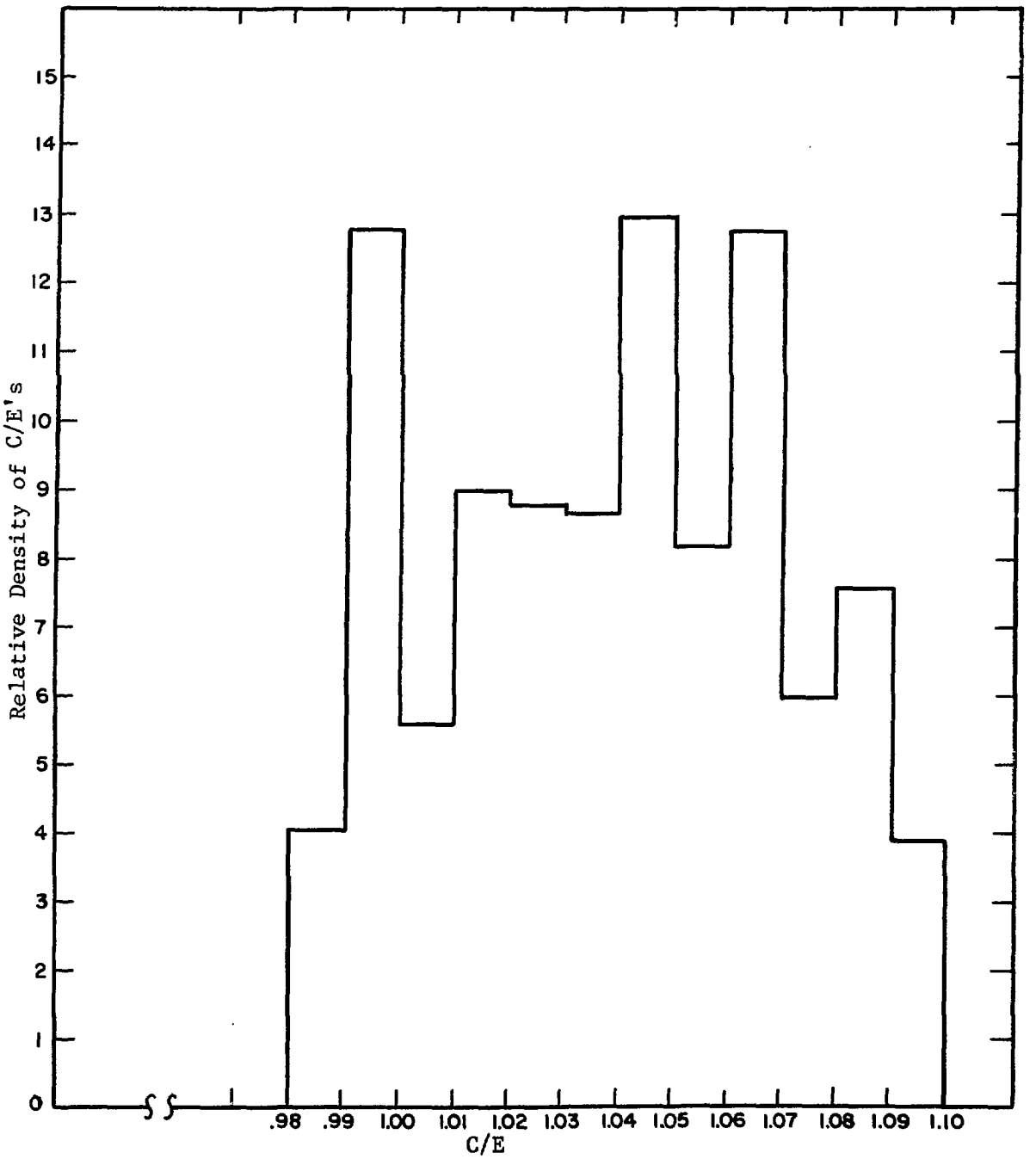

Fig. VII.29. Weighted Distribution of C/E's for 65 Control Rod Worth Measurements in 350 MWe Size Heterogeneous Assemblies.

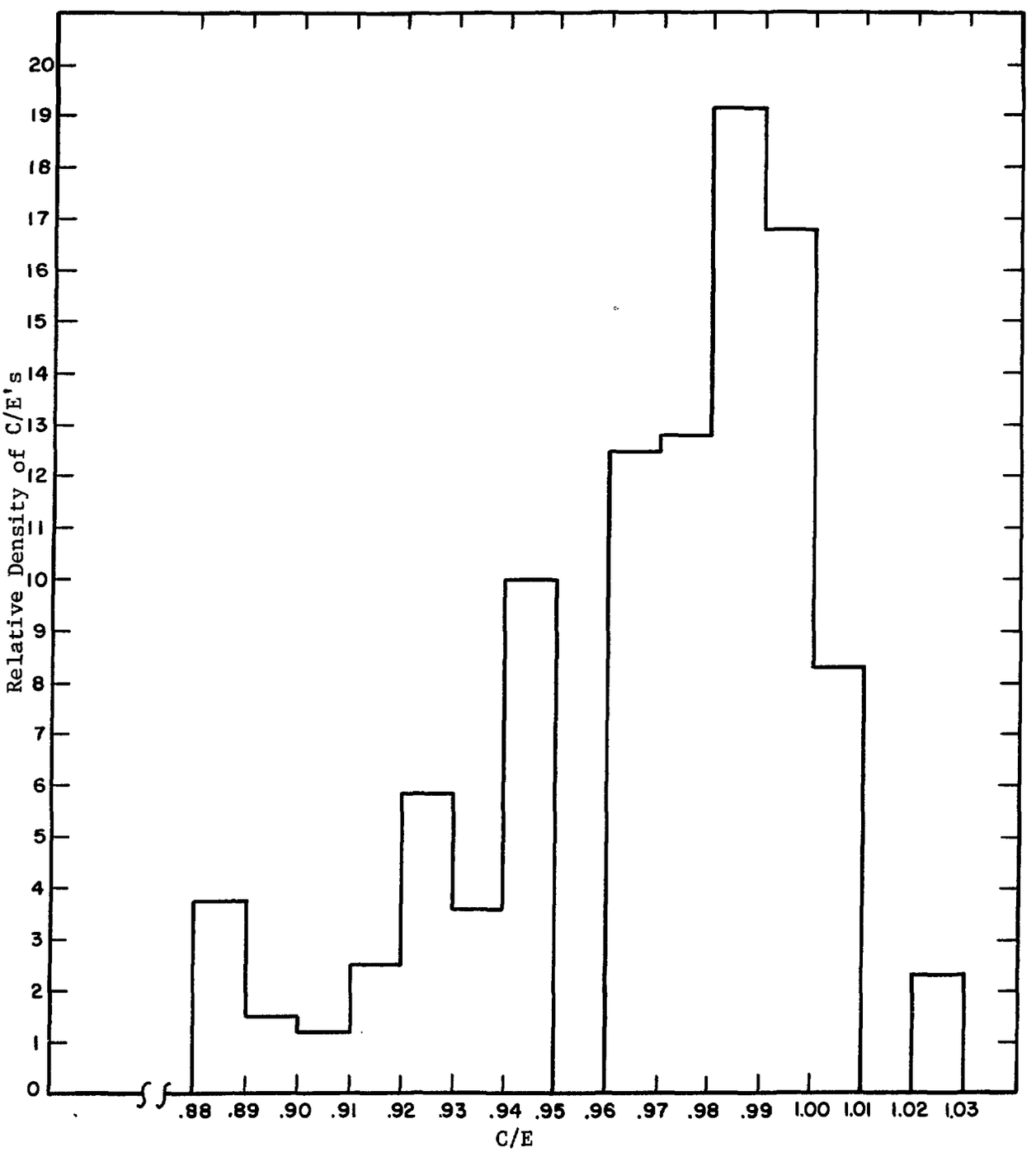

Fig. VII.30. Weighted Distribution of C/E's for 60 Control Rod Worth Measurements in 350 MWe Size Heterogeneous Cores (calculated with coarse mesh spacing).

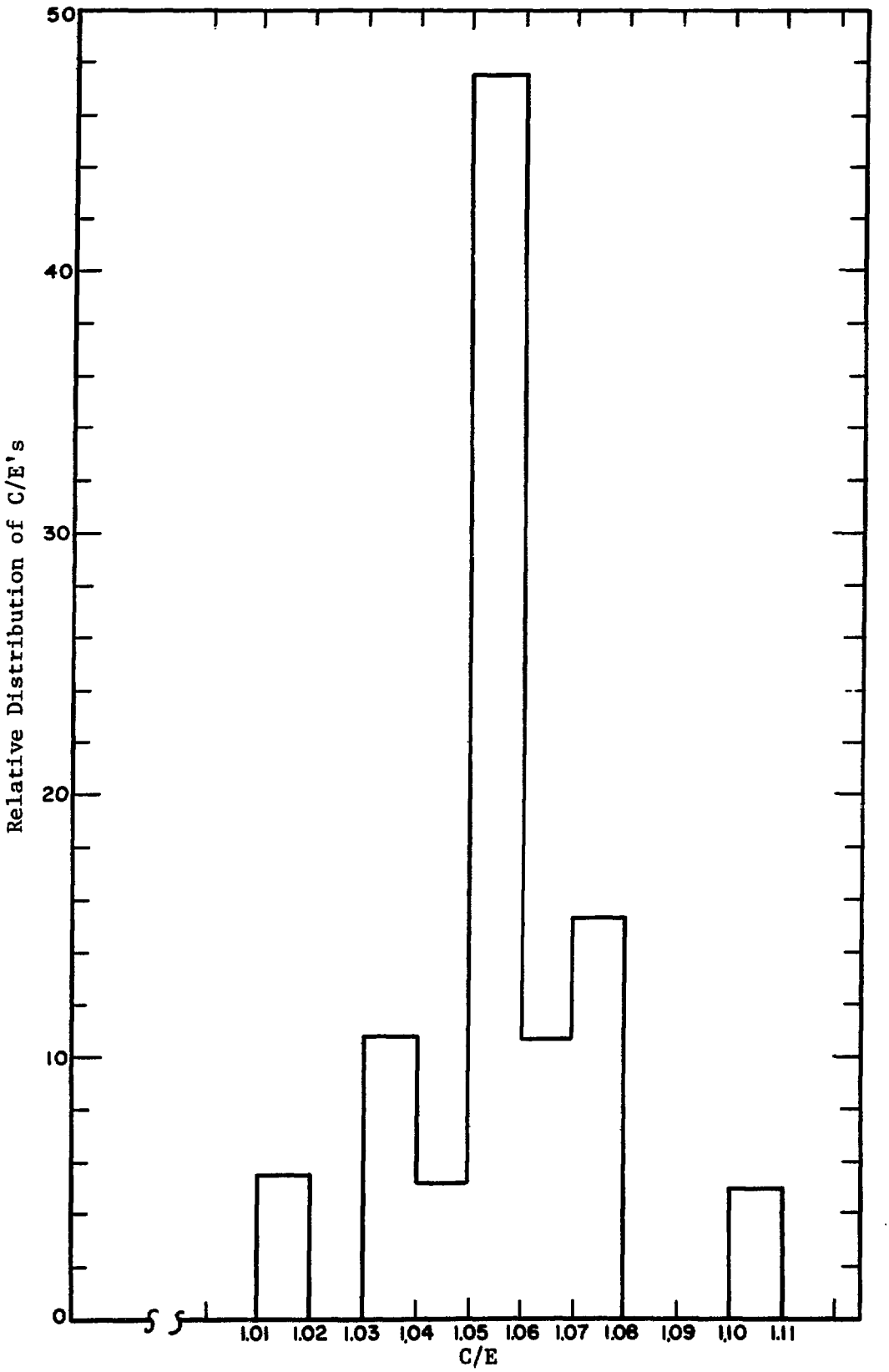

Fig. VII.31. Weighted Distribution of C/E's for 19 Control Rod Worth Measurements in a 350 MWe Homogeneous EMC (calculated with coarse mesh spacing).

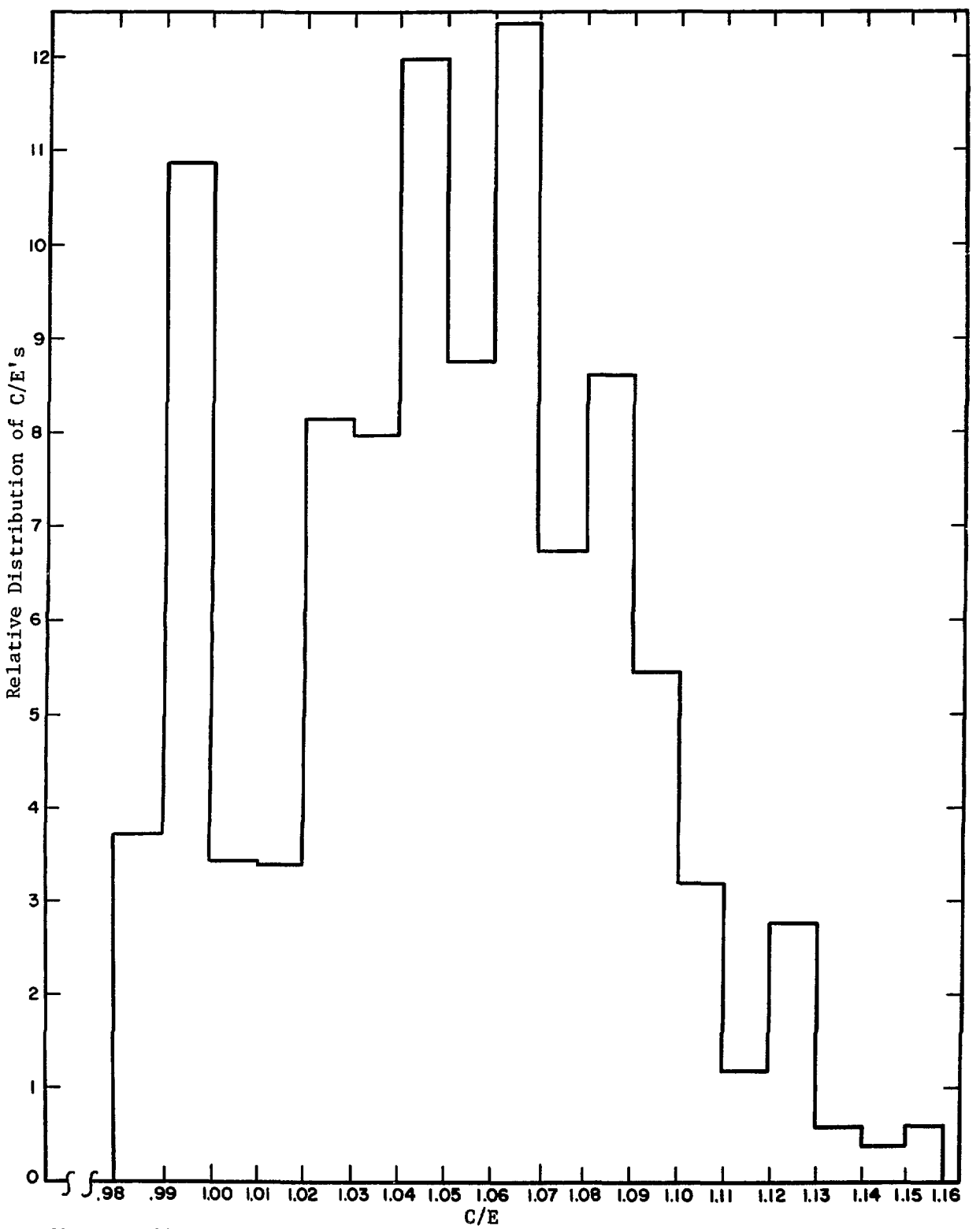

Fig. VII.32. Weighted Distribution of C/E's for 85 Control Rod Worth Measurements in 350 MWe Size Assemblies.

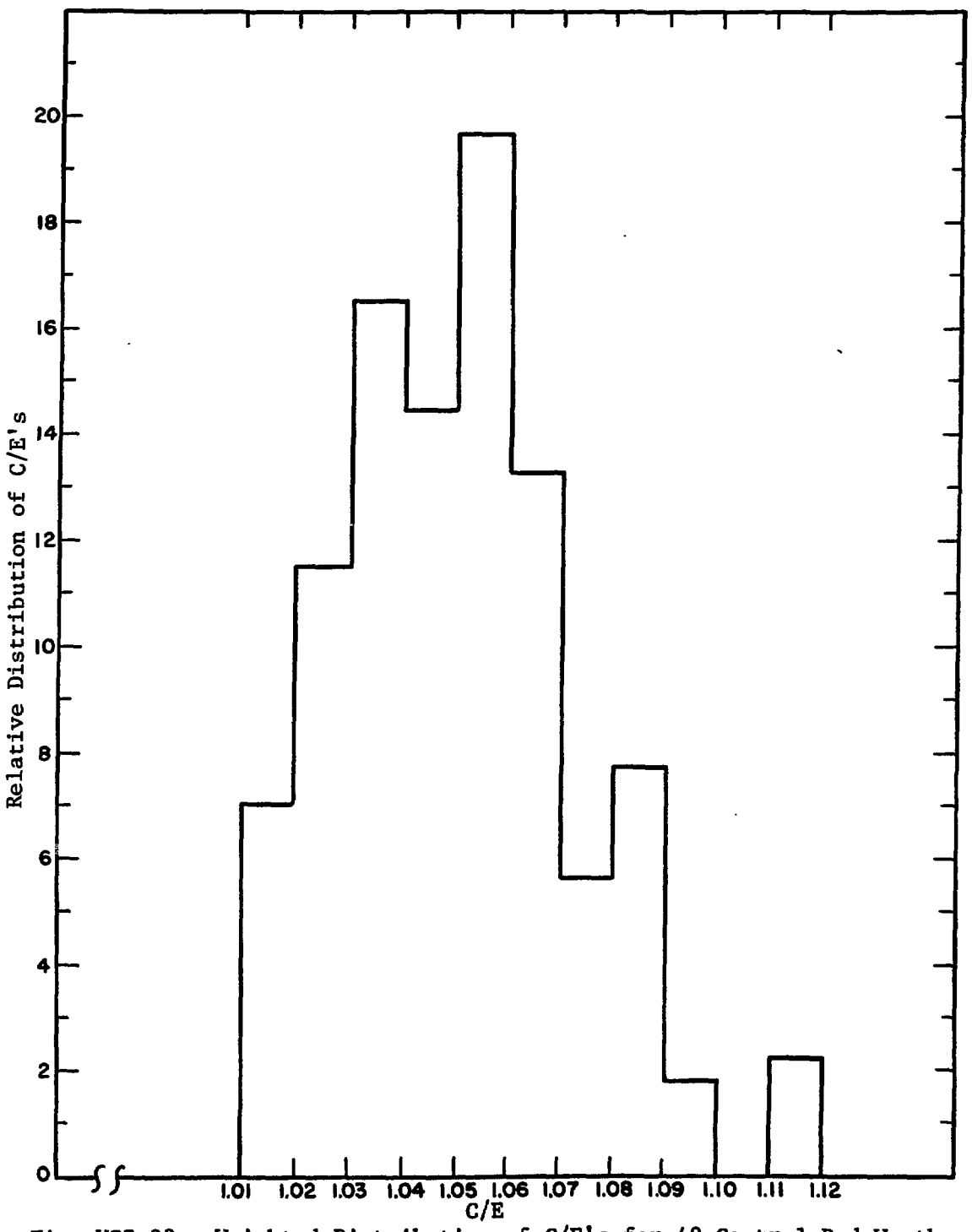

Fig. VII.33. Weighted Distribution of C/E's for 48 Control Rod Worth Measurements in 700-900 MWe Size Cores.

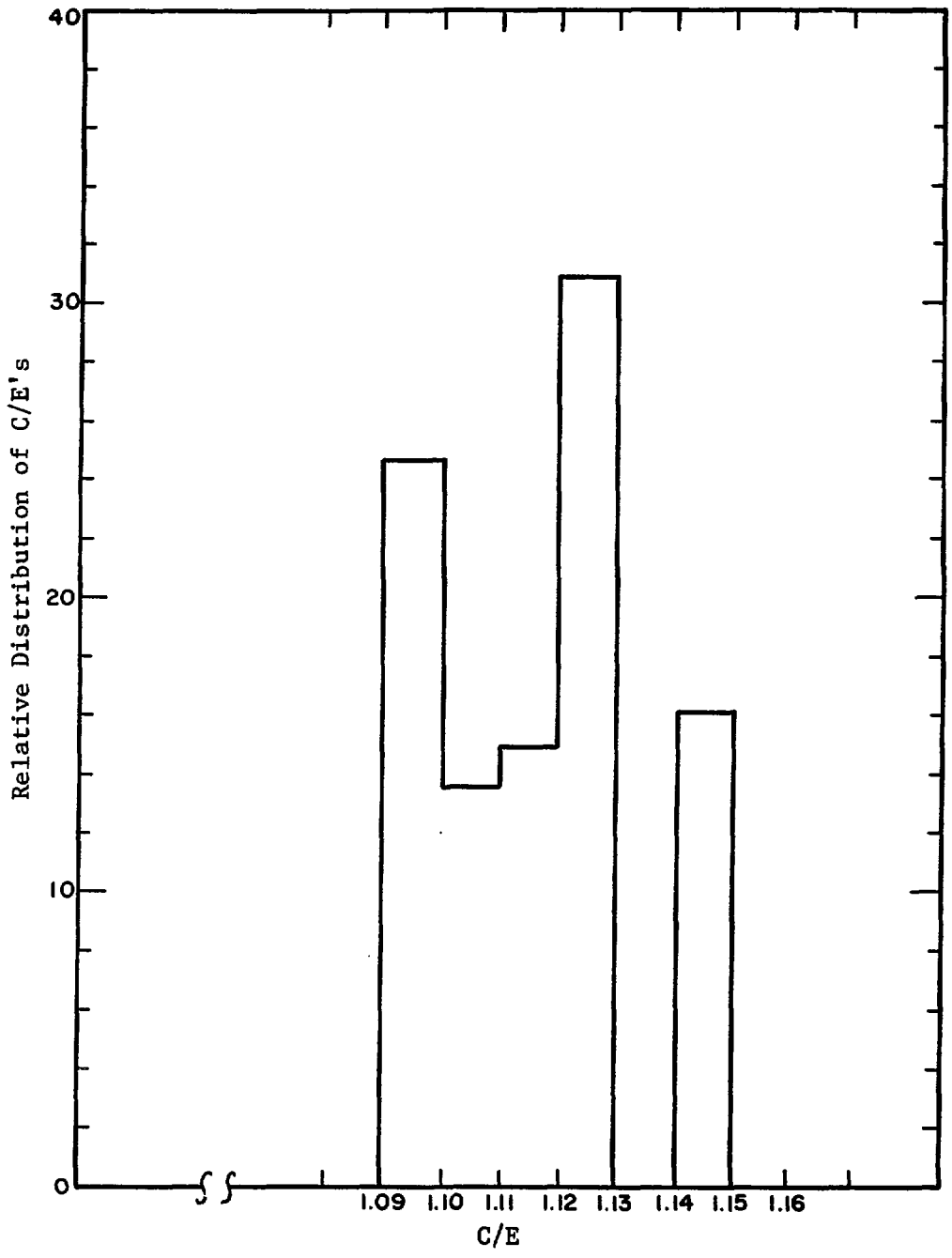

Fig. VII.34. Weighted Distribution of C/E's for 7 Central Control Rod Worth Measurements in 350 MWe Size Homogeneous Assemblies.

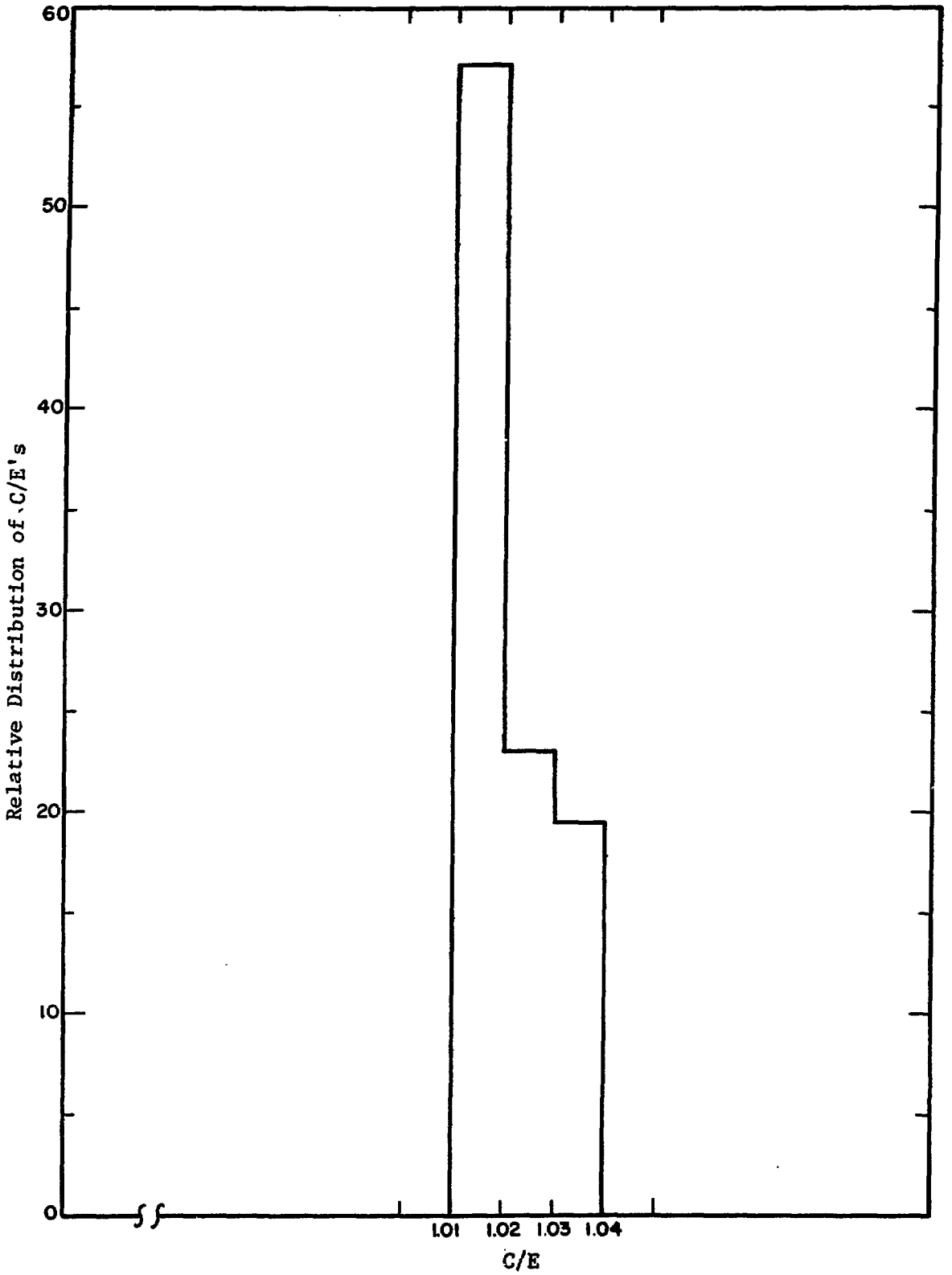

Fig. VII.35. Weighted Distribution of C/E's for Central Control Rod Worth Measurements in Four Homogeneous 700-900 MWe Size Assemblies.

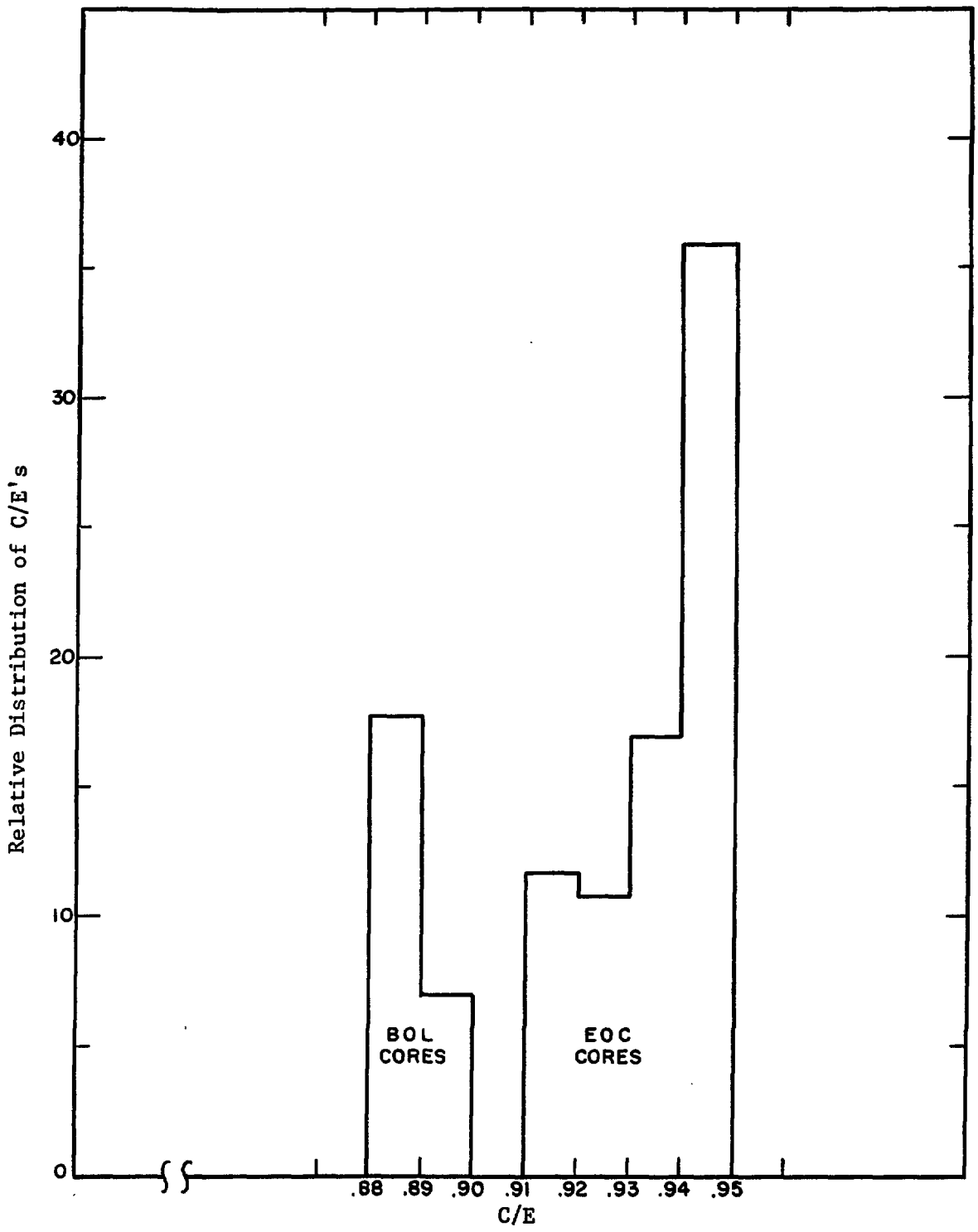

Fig. VII.36. Weighted Distribution of C/E's for 11 Measurements of Inner Ring Control Rod Worths in 350 MWe Size Heterogeneous Cores (coarse mesh spacing used in calculations).

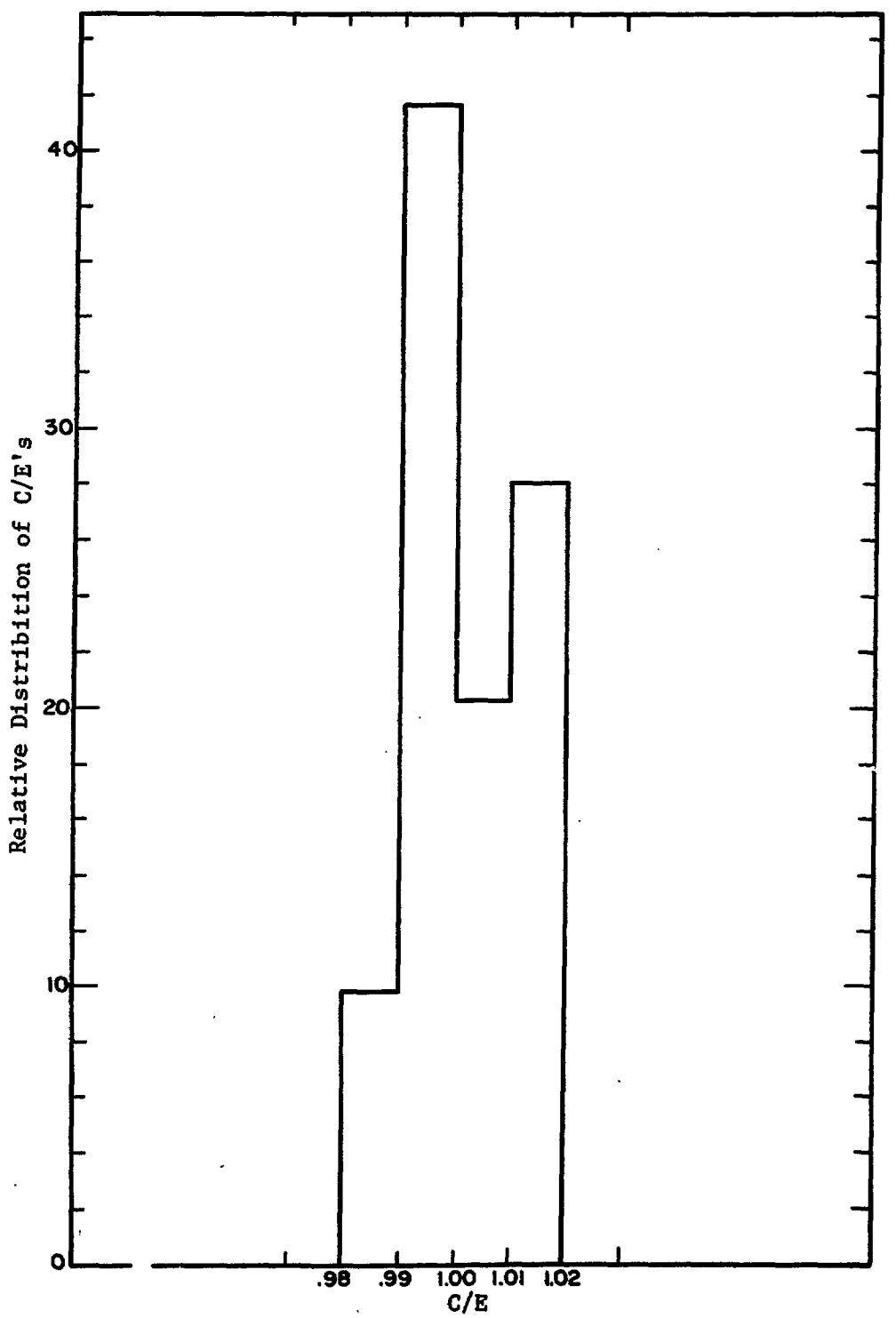

Fig. VII.37. Weighted Distribution of C/E's for 18 Measurements of Inner Ring Control Rod Worths in 350 MWe Size Heterogeneous Assemblies.

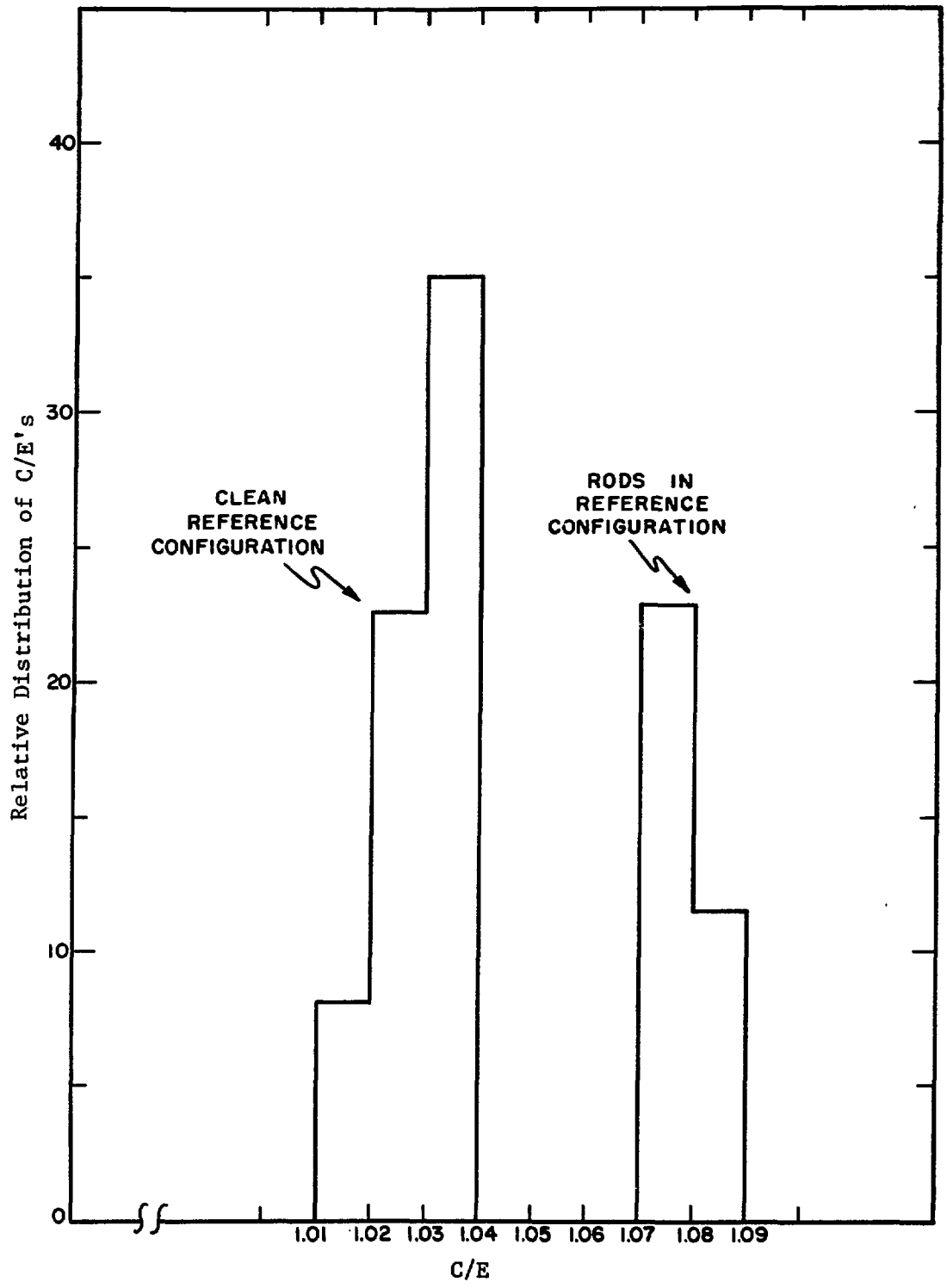

Fig. VII.38. Weighted Distribution of C/E's for 9 Measurements of Inner Ring Control Rod Worths in 700-900 MWe Size Homogeneous Assemblies.

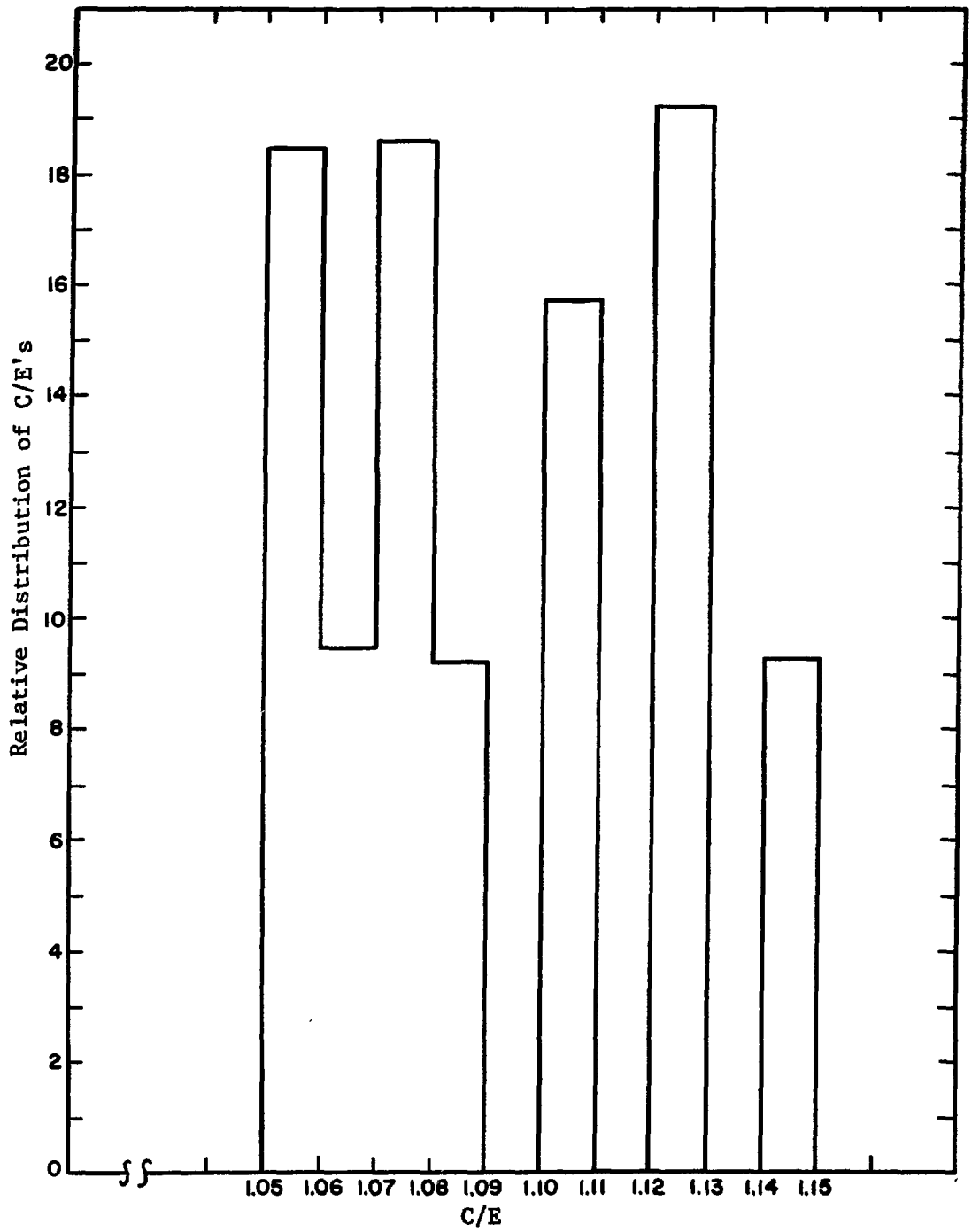

Fig. VII.39. Weighted Distribution of C/E's for 11 Measurements of Inner Ring Control Rod Worths in 350 MWe Size Homogeneous Assemblies.

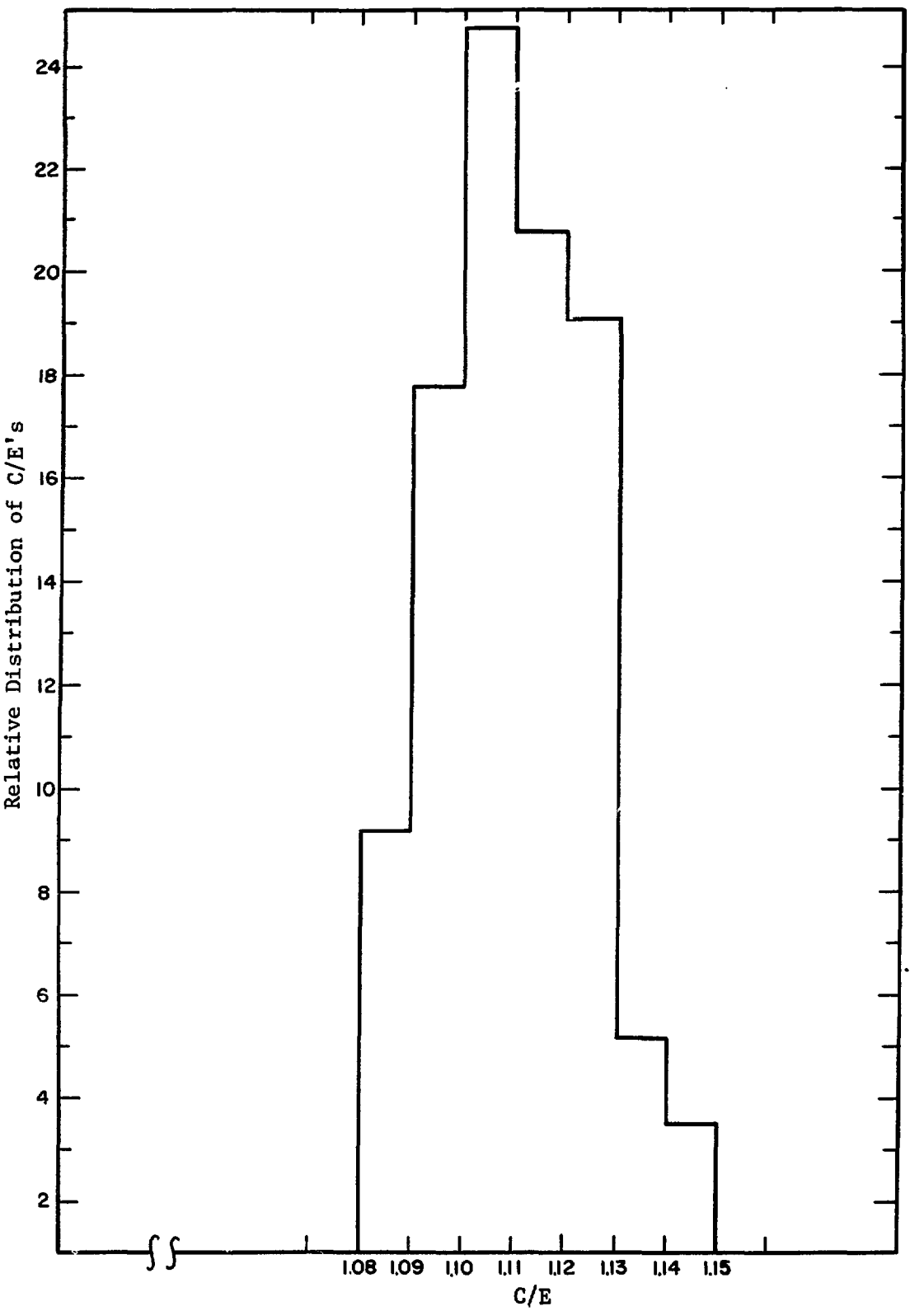

Fig. VII.40. Weighted Distribution of C/E's for 21 Measurements of Control Rod Worths in 350 MWe Size Homogeneous Assemblies (rods in more than one ring).

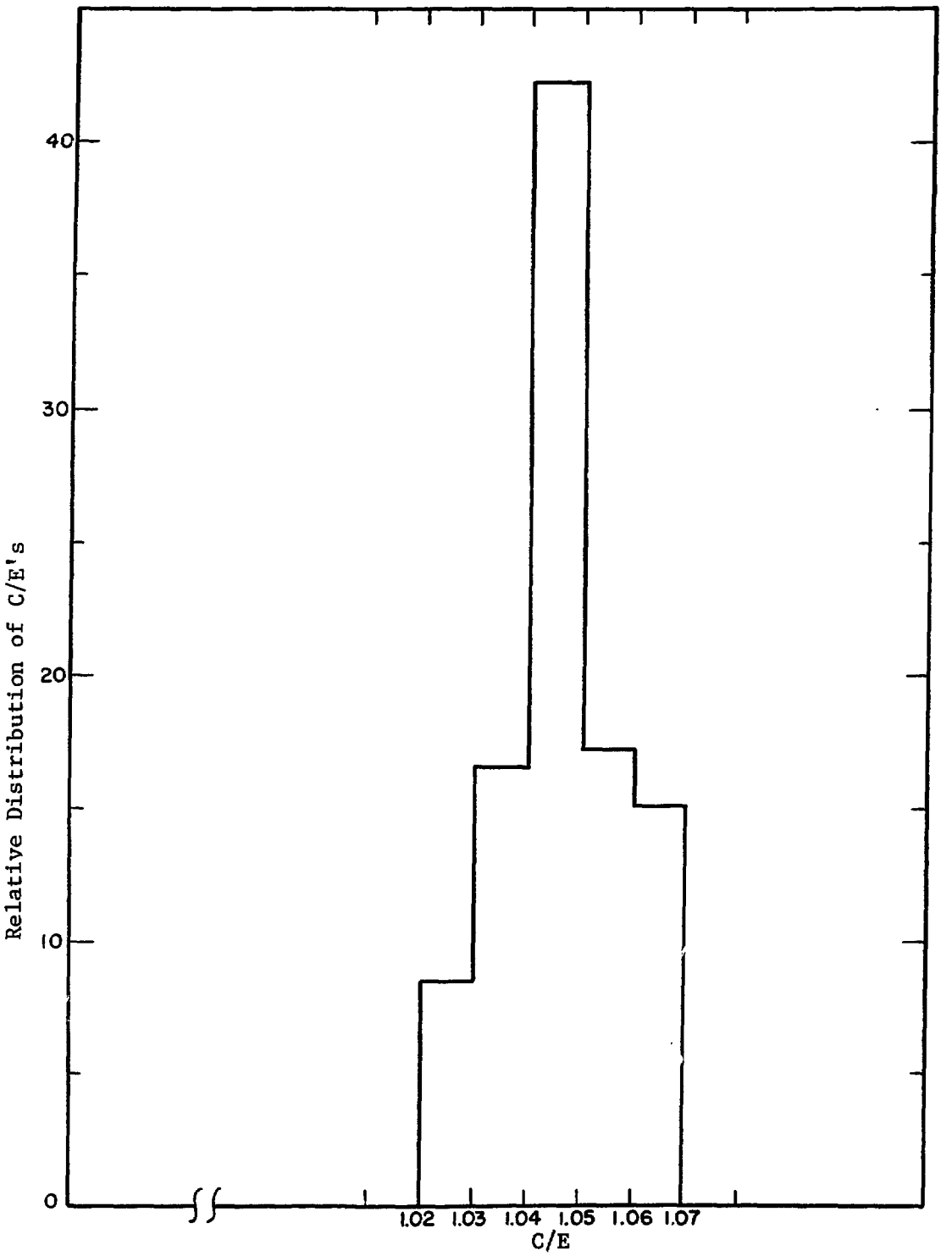

Fig. VII.41. Weighted Distribution of C/E's for 12 Measurements of Control Rod Worths in 700-900 MWe Size Homogeneous Assemblies (rods in more than one ring).

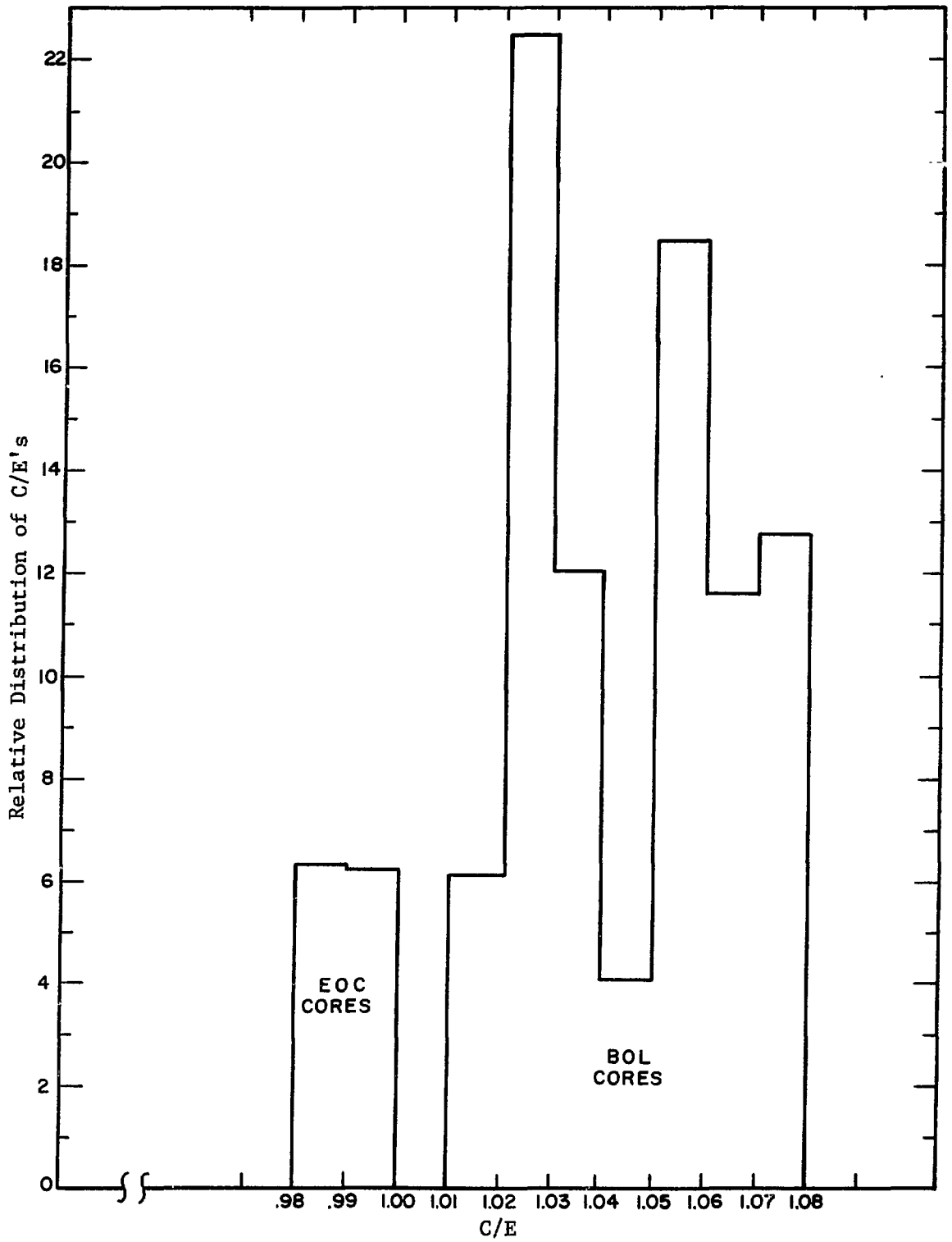

Fig. VII.42. Weighted Distribution of C/E's for 14 Measurements of Control Rod Worths in 350 MWe Size Heterogeneous Assemblies (rods in more than one ring).

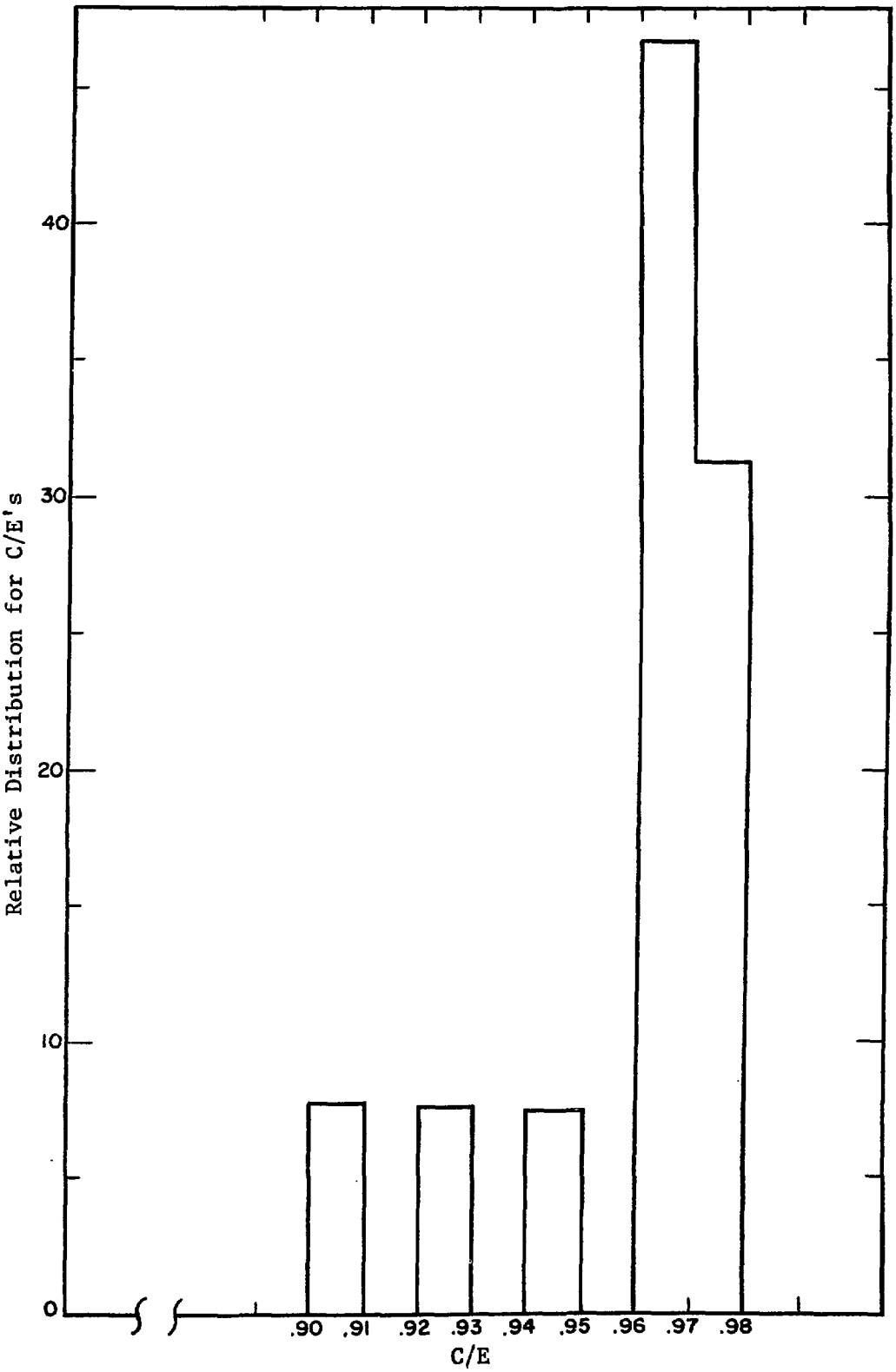

Fig. VII.43. Weighted Distribution of C/E's for 9 Measurements of Control Rod Worths in 350 MWe Size Heterogeneous Assemblies (rods in more than one ring, calculated with coarse mesh spacing).

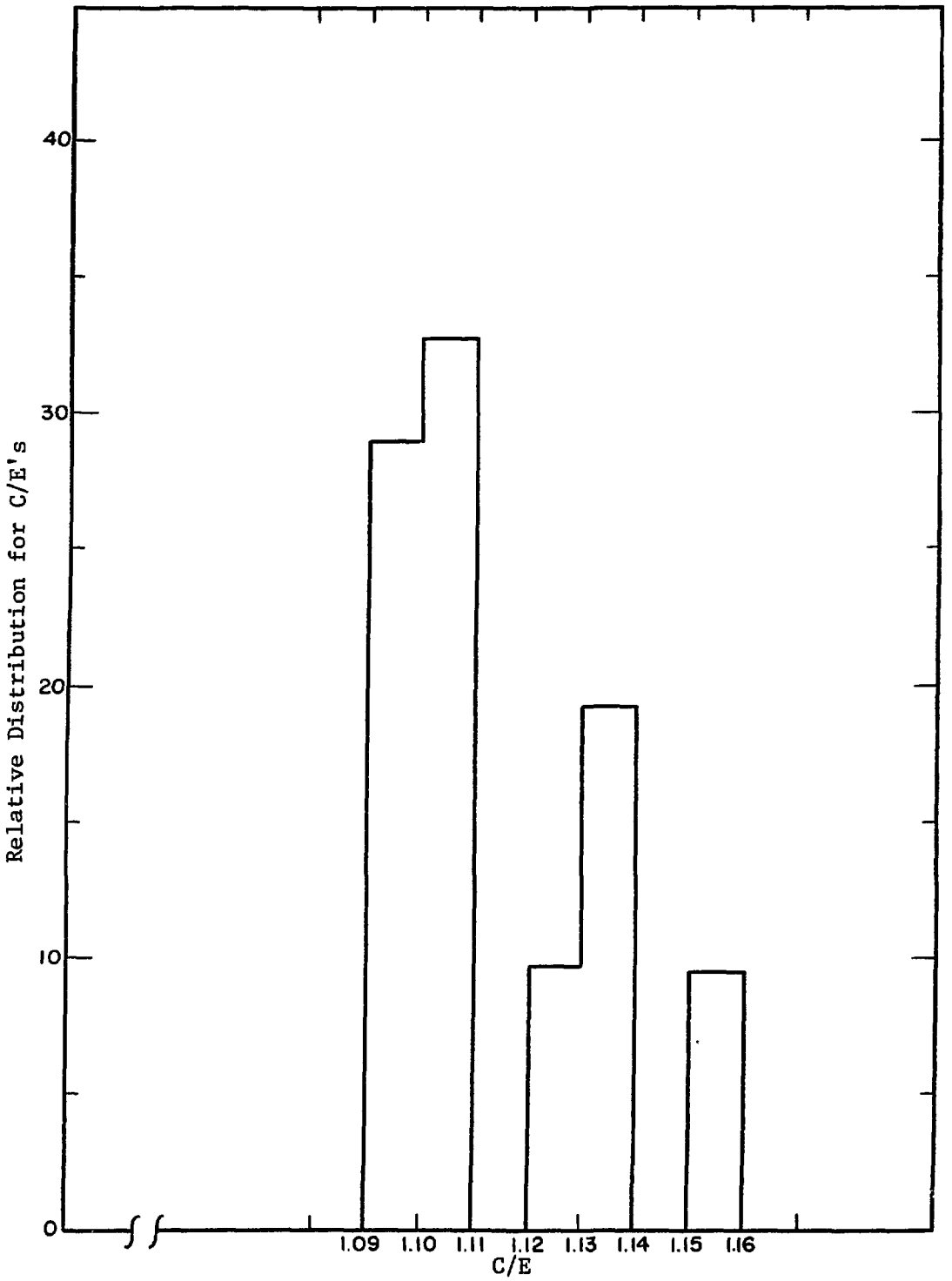

Fig. VII.44. Weighted Distribution of C/E's for 10 Measurements of Outer Ring Control Rod Worths in 350 MWe Size Homogeneous Assemblies.

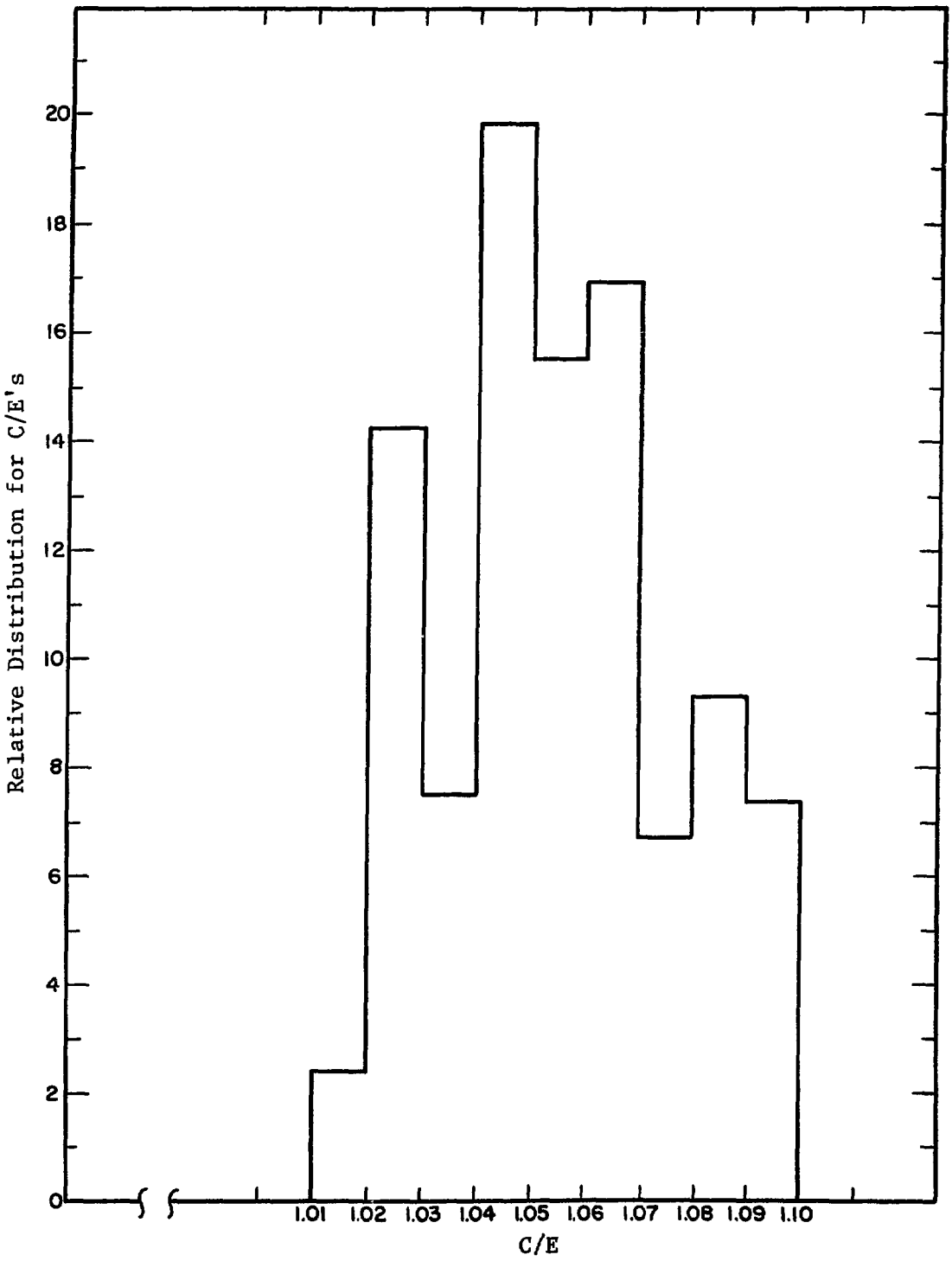

Fig. VII.45. Weighted Distribution of C/E's for 34 Measurements of Outer Ring Control Rod Worths in 350 MWe Size Heterogeneous Assemblies.

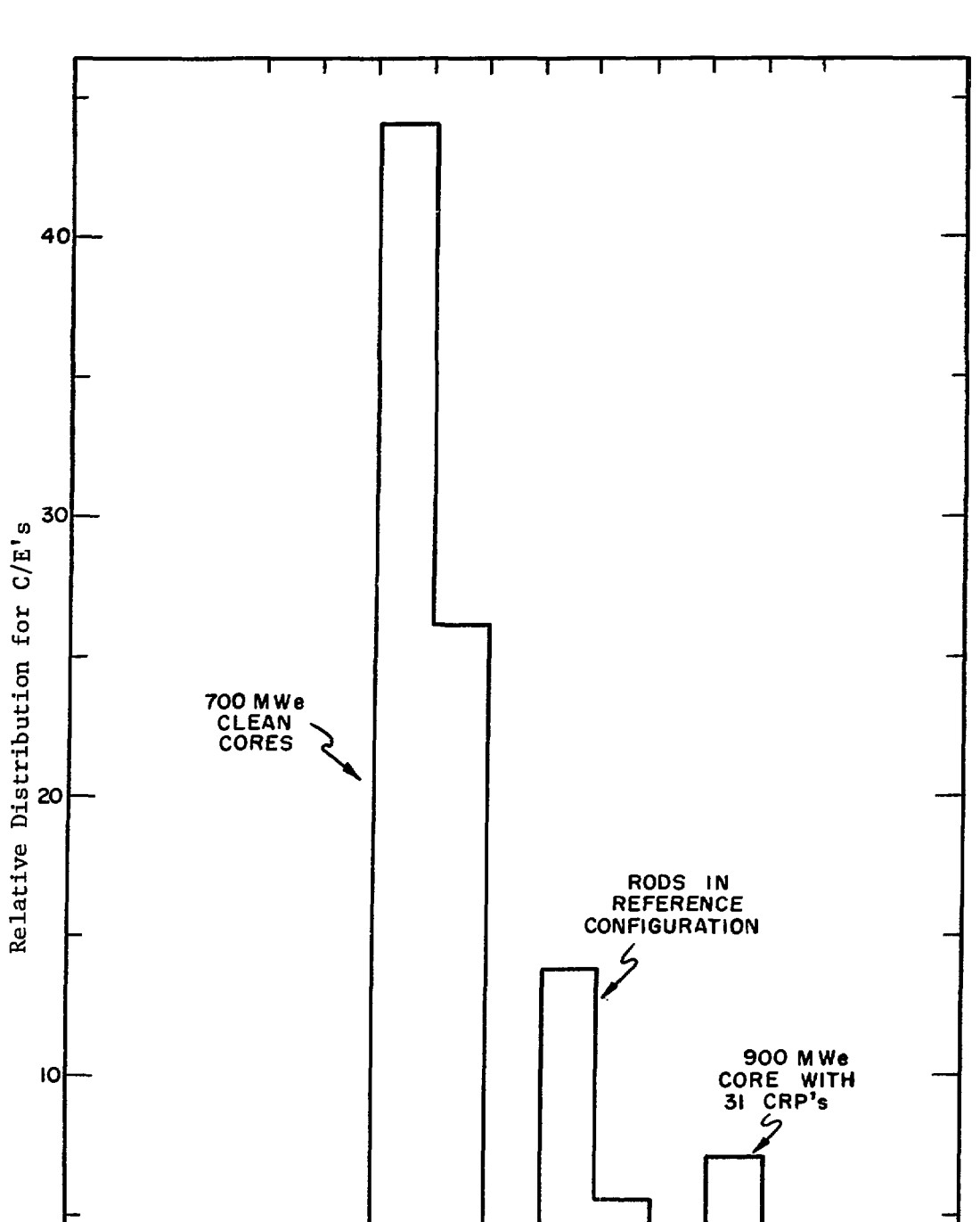

Fig. VII.46. Weighted C/E Distribution of C/E's for 19 Measurements of Outer Ring Control Rod Worths in 700-900 MWe Size Homogeneous Assemblies.

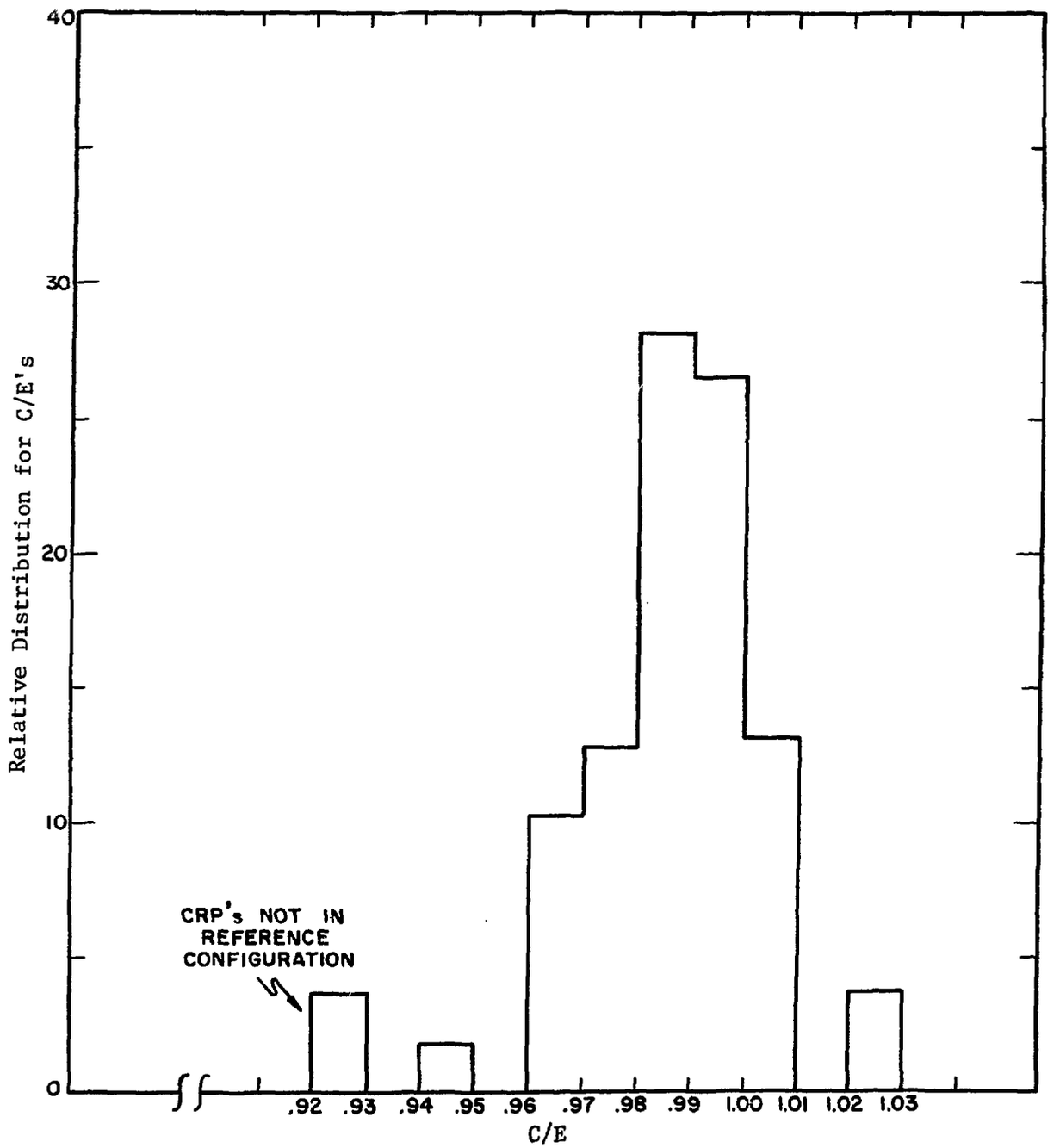

Fig. VII.47. Weighted C/E Distribution for 40 Measurements of Outer Ring Control Rod Worths in 350 MWe Size Heterogeneous Assemblies (calculated with coarse mesh spacing).

APPENDIX D: Acronymns and Critical Experiment Terminology

ANL: Argonne National Laboratory.

BFS-15: Russian fast critical facility.

BN-350: 350 MWe equivalent power reactor built near Shevchento in the Soviet Union (1000 MWt). One hundred-fifty MWe actual electrical power and 200 MWe-equivalent used for desalting.

CDS: Conceptual Design Study for a near-commercial size LMFBR design. Evolved to LDP.

C/E: Ratio of calculated to measured value.

Cell: Cross section of the smallest repeating geometry in a reactor, for example, one ZPPR matrix tube containing a drawer and columns of material.

CR: Control Rod.

CRBRP: Clinch River Breeder Reactor Plant. Proposed U.S. 350 MWe, 975 MWt demonstration fast reactor to be built on the Clinch River near Knoxville, Tennessee.

CRP: Control Rod Position.

CRP Streaming: Neutron streaming in the control rod positions.

DIF3D: One-, two-, or three-dimensional diffusion theory code with a 2D transport option.

DOT: Two-dimensional transport theory code.

DT: Diffusion theory.

EBR-II: Experimental Breeder Reactor No. 2: A 62.5 MWt metal-fueled FBR in Idaho. Used for irradiation testing, generates 18.5 MW of electricity, and produces steam for on-site use. Licensed cogeneration facility.

EMC: Engineering Mockup Critical. A critical experiment in which a specific reactor design is simulated on a critical facility, with geometry and composition matched as closely as possible. Examples are ZPPR-6 and ZPPR-11.

Engineering Benchmark: A critical experiment that generally simulates a power reactor design. Reasonable attempts are made to simulate reactor geometry, including CRPs. Composition is matched to the extent possible with simple cell types.

Fermi: Fast Power Reactor, designed for 300 MWt and 94 MWe, built in Michigan and operated from 1963-1972 at a maximum of 61 MWe.

FFTF: Fast Flux Test Facility. 400 MWt fast reactor near Hanford, Washington, to be used for breeder reactor materials testing.

FTR: Fast Test Reactor (FFTF).

G: Energy groups, e.g., 9G is nine groups.

LDP: Large Development Plant; proposed 1000 MWe LMFBR to follow CRBR.

MASURCA: French Fast Critical Facility.

Monju: Proposed Japanese demonstration fast reactor, (714 MWt and 300 MWe).

MPD: Mesh spaces per drawer, e.g. 4MPD is used for 4 mesh spaces per drawer.

MSM: Modified Source Multiplication. A technique for determining subcritical reactivity from the ratio of neutron production by fission to the neutron production from a constant source.

PFR: Prototype Fast Reactor. British fast power reactor (270 MWe and 600 MWt) built near Dounreay, Scotland.

Phenix: French demonstration fast reactor (250 MWe and 563 MWt).

Physics Benchmark: A critical experiment in which the assembly is constructed from only a few simple cell types and the reactor geometry is also simple. Such singularities as control rod positions are not included. Examples are ZPPR-2, -7, and -9.

Plate Streaming: Refers to neutron streaming in the sodium plates that are aligned in the y and z dimensions in the ZPPR critical assembly.

SEFOR: Southwest Experimental Fast Oxide Reactor. A 20 MWt reactor built in Arkansas to test the Doppler effect in mixed-oxide fuel.

SuperPhenix: Commercial-size LMFBR, 1200 MWe and 2900 MWt, under construction in France.

TOPSY: Modular code system used at ZPPR.

TWOTRAN: Two-dimensional transport theory code.

ZEBRA: British Fast Critical Facility.

ZPPR: Zero Power Plutonium Reactor. Large fast critical facility in Idaho.

ZPR: Zero Power Reactor. Any of several fast critical facilities generally identified by number. Here, ZPR could refer to ZPR-3 and ZPPR in Idaho or to ZPR-6 and ZPR-9 in Illinois, all ANL facilities.

Distribution for ANL-82-13

Internal:

C. H. Adams
P. I. Amundson
R. J. Armani
C. L. Beck
E. S. Beckjord
J. C. Beitel
E. F. Bennett
S. K. Bhattacharyya
M. M. Bretscher
H. Bigelow
S. B. Brumbach
R. G. Bucher
S. G. Carpenter
B. R. Chandler
Y. I. Chang
P. J. Collins
R. J. Cornella
T. A. Daly
J. R. Deen
K. L. Derstine
G. J. DiIorio
D. R. Ferguson
K. E. Freese
E. K. Fujita
P. J. Garner
J. M. Gasidlo
E. M. Gelbard
R. W. Goin
G. M. Greenman
G. L. Grasseschi
H. A. Harper
H. Henryson
H. H. Hummel
R. N. Hwang
R. E. Kaiser
Kalimullah
R. D. Lawrence
J. M. Larson
L. G. LeSage
J. R. Liaw
M. J. Lineberry
D. M. Maddison
D. J. Malloy
F. H. Martens
J. E. Matos
P. B. McCarthy
H. F. McFarlane (15)
R. D. McKnight
J. A. Morman
D. N. Olsen
Y. Orechwa
E. M. Pennington
P. J. Persiani
P. A. Pizzica
W. P. Poenitz
R. B. Pond
W. R. Robinson
J. R. Ross
R. W. Schaefer
J. J. Sienicki
A. B. Smith
D. M. Smith
K. S. Smith
J. L. Snelgrove
C. G. Stenberg
W. J. Sturm
S. F. Su
C. E. Till
B. J. Toppel
A. Travelli
R. B. Turski
A. J. Ulrich
D. C. Wade
W. L. Woodruff
B. S. Yarlagadda
T. J. Yule
ANL Patent Dept.
ANL Contract File
ANL Libraries (2)
TIS Files (6)

External:

DOE-TIC, for distribution per UC-79d (122)
Manager, Chicago Operations Office, DOE
Director, Technology Management, DOE-CH
Director, DOE-RRT (2)
President, Argonne Universities Association
Applied Physics Division Review Committee:
- P. W. Dickson, Jr., Clinch River Breeder Reactor Project, Oak Ridge
- K. D. Lathrop, Los Alamos National Lab.
- D. A. Meneley, Ontario Hydro
- J. E. Meyer, Massachusetts Inst. Technology
- R. Sher, Stanford U.
- C. Spight, AMAF Industries, Inc., Columbia, Md.
- D. B. Wehmeyer, Detroit Edison Co.